



ISAIAH ALLISON

TECHNO-ECONOMIC EVALUATION OF ASSOCIATED GAS USAGE FOR  
GAS TURBINE POWER GENERATION IN THE PRESENCE OF  
DEGRADATION & RESOURCE DECLINE

SCHOOL OF AEROSPACE, TRANSPORT  
AND MANUFACTURING

PHD

Academic Years: 2011 - 2014

SUPERVISOR: PROF P PILIDIS  
17 DECEMBER 2014



School of Aerospace, Transport  
and Manufacturing

Full Time PhD

Academic Years: 2011 - 2014

Isaiah Allison

Techno-Economic Evaluation of Associated Gas Usage for Gas Turbine Power  
Generation in the Presence of Degradation & Resource Decline

Supervisor: Prof P Pilidis  
17 December 2014

© Cranfield University 2014. All rights reserved. No part of this publication may  
be reproduced without the written permission of the copyright owner.



## **ABSTRACT**

This research examined the technical and economic feasibility of harnessing flare gas emissions from oil fields. The outcome would provide the basis for a substantial re-utilization of this waste energy due to the current practice of flaring and use it alternatively as energy for powering oil fields, rural electrification and desalination. Nigeria is used as a case study. Burning fossil fuels have grave environmental impact, amidst increasing global concerns over harmful emissions. This research addresses resource decline and suggests divestment as a partial cure.

The gas turbine is subject to degradation of its components as it is used. Though several methods of assessing gas turbine degradation have been developed with varying degrees of success, no one method has addressed issues pertaining to associated gas and its effects on degradation with divestment. Simulation of two single shaft, heavy duty industrial gas turbines; and three aero-derivative industrial gas turbines of the heavy medium and light capacity ranges were carried out for varying operating conditions, to ascertain the effects of degradation when run on associated gas. Thereafter, optimizations for the best power plant engine mix and the least cost of electricity were carried out.

Genetic algorithm was used to assess a population of 10,000 individuals over 500 generations; convergence was achieved for different configurations of the five study engines at discount rates of 5% and 10%, over three power ranges. The divestment pattern starts with the lightest aero-derivative industrial gas turbine; the best power plant selection was limited to the two lightest aero-derivatives in the fleet, completely ignoring the heavy engines.

A techno-economic, environmental and risk assessment model comprising performance, emission, economics and risk modules was successfully developed to assess gas turbine degradation with divestment. Using this tool, it was confirmed that associated gas usage resulted in degradation of gas turbine performance, an increase in gas collection as well as operation and maintenance

costs. Also there was increasingly higher creep life consumption during slow, medium and fast degradation scenarios for both engine sets.

The novel technical contribution of the research work therefore is the influence of degradation on the economic use of associated gas as fuel in gas turbine power generation; and the implementation of divestment in the face of fuel decline.

Keywords: *flaring, utilization, divestment, pollution and environment*

## PAPER PUBLICATIONS

1. Allison, I., Ramsden, K., Pilidis, P., and Agbadede, R. (2013), "Gas Turbine Degradation in the Techno-economic Environmental and Risk Analysis of Flare Gas Utilization in Nigeria" presented at the American Society of Mechanical Engineers (ASME) Turbo Expo 2013 at San Antonio Texas USA from 3-7 June 2013.
2. Agbadede, R., Pilidis, P., Allison, I., and Lambart, P. (2013), "Study of Wash Fluid Cleaning Effectiveness on Industrial Gas Turbine Compressor Foulants", presented at the ASME Turbo Expo 2013, San Antonio Texas USA from 3-7 June 2013.
3. Agbadede, R., Jasuja, A.K., Igie, U., Pilidis, P., Allison, I., Hameed, R., and Lambart, P., "Droplet Size Characterisation of Elliptical Fan Sprays Employed in Online Compressor Washing for Power Generation", presented at the 26<sup>th</sup> European Conference of Liquid Atomization & Spray Systems, Bremen Germany from 08-10 September, 2014.
4. Agbadede, R., Pilidis, P., and Allison, I., (2014) "Experimental and Theoretical Investigation of Liquid Injection Droplet Size Influence on Online Compressor Cleaning Effectiveness for Industrial Gas Turbines", *Journal of the Energy Institute*.





## **ACKNOWLEDGEMENTS**

I thank God Almighty, who through the agency of the Holy Spirit told me of things to come and prepared me adequately for this course of study. To Him be glory and honour for ever and ever.

I owe Dr Ken Ramsden of blessed memory a depth of gratitude for sacrificing his time and his intellect; he stirred my brains in a way unparalleled by any of my previous teachers for four decades. As my second supervisor, he effortlessly put across even the most complex technical details to me; he dissolved my doubts. His sense of humour and friendly disposition will be greatly missed. My God shall give his dear family and the Cranfield community, the fortitude to bear this great loss.

To Prof Pericles Pilidis, I am deeply indebted for his guidance, availability and financial support. He gave me the inspiration to carry on and the freehand to express my conviction that flare gas can indeed be harnessed in Nigeria. I am grateful for his personal interest in my work and for creating time out of his tight schedule to attend to my queries, and seeing me to the end of the research. My appreciation goes to Dr Stephen Ogaji of the Presidential Taskforce on Power in Nigeria, for accepting to be my Industrial Supervisor. I am delighted to mention my study visit to NLNG; and to express my sincere gratitude to Colonel MLD Saraso, the military commander in Bonny at the time, who made my visit absolutely fantastic and provided military escort to and from the NLNG plant.

Thanks to the Niger Delta Development Commission for paying my tuition for the 3 year doctoral research, my appreciation to the Bayelsa State Scholarship Board for financial assistance towards my accommodation, yet more thanks to the Chief of Army Staff for granting me study leave with pay which enabled me to feed my family through the period. To His Excellency, Admiral J Jonah, Deputy Governor of Bayelsa State, I am deeply indebted for his personal financial support.

I must acknowledge the support of my friend, Roupa Agbadede, for our nocturnal studies and his invaluable academic companionship. In the same vein, worthy of mention are my PhD housemates in Room 806 of Building 183, Atma Prakash,

Luis Sanchez De Leon and Rumugiah Ramanagiri; these are great guys! I must not fail to thank Gill Hargreaves and Nicola Datt of the School of Aerospace Transport and Manufacturing, for their wonderful administrative assistance; my appreciation also go to Alison Waters for assisting with stubborn figures and tables on the Thesis Template, and to Clare Humphries for her help with RefWorks when Write-N-Cite went haywire. A great big thank you to Dr Eric Goodger, for proofreading my work from the Abstract to Appendices; every word, every sentence, every paragraph.

Many thanks to my very own brigade - Juliet, Kelvin, Wanaemi, Tari and Bomo - for bearing with me for the long hours of study outside the home. They gave me the challenge commensurate to a husband, father and student. Special thanks to my wife, Juliet, who has had to put up with a husband thinking too much about flare gas. Thanks to Kelvin for painstakingly going through the final draft.

A million thanks to my mentor, Pastor Chris Oyakhilome PhD, who inspires me through his teachings and cultivates in me, the mind-set of excellence. Thanks also to Pastor Dipo Fisho and Pastor Patrick Ibuaku, who have continued to teach me the Word of God.

## TABLE OF CONTENTS

ABSTRACT .....	i
ACKNOWLEDGEMENTS.....	v
LIST OF FIGURES.....	xi
LIST OF TABLES .....	xiv
LIST OF EQUATIONS.....	xvi
ABBREVIATIONS AND NOTATIONS .....	xvii
CHAPTER 1: RESEARCH DEFINITION .....	1
1.1 Research Rationale .....	1
1.2 Aim & Objectives.....	2
1.3 Analysis of Associated Gas Volume .....	3
1.4 Thesis Structure.....	6
Chapter 1: Research Definition .....	6
Chapter 2: Literature Review.....	7
Chapter 3: Data Analysis & Modelling of Associated Gas.....	7
Chapter 4: Study Engines & Degradation.....	7
Chapter 5: Resource Decline Analysis.....	8
Chapter 6: Power Plant Economics & Risk Analysis .....	8
Chapter 7: Conclusions & Recommendations.....	8
CHAPTER 2: LITERATURE REVIEW.....	9
2.1 Introduction .....	9
2.2 History of Gas Flaring .....	9
2.3 Analysis of National Volume of Flare Gas.....	10
2.4 Effects of Gas Flaring .....	11
2.4.1 Greenhouse Gas Emissions.....	11
2.4.2 Air Pollution .....	12
2.4.3 Health Implications.....	12
2.4.4 Acid Rain.....	12
2.5 The Need to End Gas Flaring .....	13
2.6 Past Gas Gathering Efforts in Nigeria.....	14
2.6.1 Bonny Liquefied Natural Gas .....	15
2.6.2 Ajaokuta-Abuja Gas Pipeline Project.....	15
2.6.3 Brass Liquefied Natural Gas .....	15
2.6.4 West African Gas Pipeline.....	15
2.6.5 Olokola Liquefied Natural Gas .....	16
2.7 Chemistry of Natural Gas.....	16
2.8 Combustion of Associated Gas.....	18
2.9 Suitability of a Fuel for Gas Turbine Application .....	19
2.9.1 Gaseous Fuel Properties.....	19
2.9.2 Gaseous Fuel Impurities .....	19
2.10 Gas Turbine Degradation Types.....	20

2.11 Components' Performance Degradation.....	22
2.12 Case Studies of Associated Gas Usage .....	23
2.12.1 Case Study on Qatar.....	23
2.12.2 Case Study on Abu Dhabi.....	25
2.12.3 Case Study on Iran.....	26
2.13 Lessons Learnt from Case Studies .....	28
Onshore AG can be treated .....	28
Offshore AG can be separated.....	28
Flare Gas Recovery System is required.....	28
2.14 Significance of the Research .....	28
CHAPTER 3: SOFTWARES & DATA ANALYSIS .....	29
3.1 Introduction .....	29
3.2 Global Gas Flare Reduction Code .....	29
3.3 GasTurb Simulation Software .....	32
3.3.1 Basic Level.....	32
3.3.2 Performance Level .....	32
3.3.3 More .....	32
3.4 The TERA Framework .....	33
3.5 Field Data Analysis .....	35
3.5.1 Data Collected from DPR.....	36
3.5.2 Data Collected from PHCN .....	38
3.5.3 Data Collected from the NLNG.....	41
3.6 Creation of New Fuels on GasTurb 5.1.....	43
3.6.1 Fuel Composition Input .....	44
3.6.2 Specifying a Path to CEA and GasTurb .....	44
3.6.3 Creating the CEA Temperature Rise Input.....	44
3.6.4 First Run of CEA .....	44
3.6.5 Creating the CEA Gas Property Input .....	44
3.6.6 Second Run of CEA .....	45
3.6.7 Making the GasTurb Files .....	45
3.7 Validation of Modelled Gases Using Aspen HYSIS .....	47
3.8 Simulation Results for SS9E and DS25 .....	48
CHAPTER 4: PERFORMANCE OF STUDY ENGINES .....	49
4.1 Introduction to Performance Modelling .....	49
4.1.1 Design Point Performance .....	49
4.1.2 Off Design Point Performance.....	60
4.2 Influence of Ambient Temperature Variations.....	73
4.3 Effect of Performance Degradation Due to AG Combustion .....	74
4.3.1 Variations in the Fuel Gas Composition .....	75
4.3.2 High Temperature Corrosion Due to Trace Metal Impurities.....	76
4.3.3 Control of High Temperature Corrosion by Fuel Additives .....	76
4.3.4 Control of High Temperature Corrosion by Special Coatings.....	78

4.3.5 Control of High Temperature Corrosion by Washing.....	78
4.3.6 Control of High Temperature Corrosion by Air Filtering.....	78
CHAPTER 5: RESOURCE DECLINE AND GAS FLARING .....	81
5.1 Introduction .....	81
5.2 Reserves in Oil Fields .....	83
5.3 Decline Rate Analysis .....	84
5.4 Decline Curve Analysis .....	85
5.5 Resource Decline and Redundancy.....	90
5.6 Fuel Volume – Ultimately Recoverable Reserve.....	91
5.7 Resource Decline Implemented on GGFR Code .....	91
CHAPTER 6: OPTIMIZATION, ECONOMICS & RISK ANALYSIS.....	97
6.1 Introduction .....	97
6.2 Optimization.....	97
6.2.1 Genetic Algorithm for Optimization.....	97
6.2.2 Data and Conditions for Optimization and Divestment.....	98
6.3 Divestment Sub-Routine .....	100
6.4 Scripts for Divestment and Optimization .....	100
6.5 Penalization .....	101
6.5.1 First Simulation Run for Optimization and Divestment .....	102
6.6 Emissions and the Environment .....	106
6.6.1 Gas Turbine Pollutant Emissions .....	107
6.6.2 CO <sub>2</sub> Emissions Prediction by Hephaestus.....	107
6.6.3 Comparison of CO <sub>2</sub> Emission Cost Results .....	109
6.7 Economic Appraisal Method .....	109
6.7.1 Net Present Value .....	110
6.7.2 Internal Rate of Return.....	110
6.7.3 Pay Back Period.....	110
6.8 The Economic Model .....	110
6.8.1 Capital Costs.....	111
6.8.2 Operation and Maintenance Costs.....	111
6.8.3 Fuel Cost.....	111
6.9 Cost of Power Generation.....	112
6.9.1 Cost of Electricity .....	112
6.10 Economic Analysis.....	113
6.10.1 Assumptions and Data for Associated Gas Utilization.....	113
6.11 Risk Analysis .....	116
6.11.2 Results of Monte Carlo Analysis .....	119
CHAPTER 7: CONCLUSIONS & RECOMMENDATIONS.....	129
7.1 Conclusions .....	129
7.2 Contributions to Knowledge .....	130
7.2.1 Influence of Degradation on the Economic Use of AG .....	130
7.2.2 Resource Decline with Divestment.....	131

7.2.3 Greenhouse Gas Emissions Reduction.....	131
7.2.4 Useful Power from Flare Gas .....	131
7.2.5 Reduced Environmental Degradation.....	131
7.3 SWOT Analysis on AG Utilization .....	131
7.3.1 Strengths.....	131
7.3.2 Weaknesses.....	132
7.3.3 Opportunities.....	132
7.3.4 Threats .....	132
7.4 Recommendations for Future Work .....	133
7.4.1 Impact of Degradation on Divestment .....	133
7.4.2 Power Barges for Divestment.....	133
7.4.3 Combined Cycle/Combined Heat and Power in AG Utilization.....	133
7.4.4 Study on Harnessing Flared Shale Gas for Power .....	133
REFERENCES.....	134
APPENDICES .....	139
Appendix A : Natural Gas Production from 1999 - 2007 .....	139
Appendix B : Modelling of Associated Gases .....	140
Appendix C : Validation of Associated Gas Models .....	143
Appendix D : Performance Simulations .....	146
Appendix E : MATLAB Function for Fuel Required.....	154
Appendix F : MATLAB Script for Fitness with Divestment .....	155
Appendix G : MATLAB Script on Divestment Pattern .....	158
Appendix H : MATLAB Optimization Script.....	160
Appendix I : MATLAB Script for Penalization.....	162
Appendix J : 2 <sup>nd</sup> Simulation for Optimization and Divestment.....	163
Appendix K : 3 <sup>rd</sup> Simulation for Optimization and Divestment.....	166
Appendix L : 4 <sup>th</sup> Simulation for Optimization and Divestment .....	169
Appendix M : 5 <sup>th</sup> Simulation for Optimization and Divestment .....	172
Appendix N : 6 <sup>th</sup> Simulation for Optimization and Divestment.....	175
Appendix P : CO <sub>2</sub> Emissions by Hand Calculation.....	178
Appendix Q : TERA of the Study Engines.....	179
Appendix R : Summary of TERA on LM6K .....	187
Appendix S : Creep Life Consumption for DS25 and LM6K.....	188

## LIST OF FIGURES

Figure 1-1 Production of Natural Gas in Nigeria (Oguejiofor, 2006) .....	4
Figure 1-2 Map of Niger Delta, Nigeria (NDDC, 2011) .....	5
Figure 1-3 Gas Flaring at Kolo Creek, Nigeria (NDDC, 2011) .....	6
Figure 2-1: Nigerian Gas Flares (USAF Def Met Satellite, 2006) .....	10
Figure 2-2: Oil Production and Consumption in Nigeria, 2003-2012 (US EIA) .	11
Figure 2-3: World's Top Five Natural Gas Flaring Countries, 2011( US EIA)...	13
Figure 2-4: West African Gas Pipeline (West African Gas Pipeline Ltd).....	16
Figure 2-5: A Typical Flare Gas Recovery Unit (John Zink, 1993) .....	27
Figure 3-1: Gas Flaring Countries & GGFR Partners .....	31
Figure 3-2: Schematic of the TERA Framework .....	33
Figure 3-3: TERA of AG Utilization.....	35
Figure 3-4: Associated Gas Produced in Nigeria.....	37
Figure 3-5:Associated Gas Utilized in Nigeria .....	37
Figure 3-6: Associated Gas Flared in Nigeria.....	38
Figure 3-7: Electricity Generation Modes (PHCN, 2012) .....	40
Figure 3-8: Generation versus Unutilized Capability .....	41
Figure 3-9: Supply of Associated Gas to the NLNG .....	42
Figure 3-10: Schematic Showing the Modelling of LANatGas.....	46
Figure 3-11: Screen Shot Showing the Incorporation of the AG.....	47
Figure 4-1: The V94.3A (Siemens Website).....	49
Figure 4-2: GasTurb Representation of SS94 .....	51
Figure 4-3: The Frame 9E (GE Website).....	52
Figure 4-4: GasTurb Representation of SS9E .....	53
Figure 4-5: The LMS100 (GE Website) .....	54
Figure 4-6: GasTurb Representation of LM1H .....	55
Figure 4-7: The LM6000 (GE Website) .....	56
Figure 4-8: GasTurb Representation of LM6K.....	57
Figure 4-9: Configuration of the DS25 (GE Website) .....	58

Figure 4-10: GasTurb Representation of DS25 .....	59
Figure 4-11: Ambient Temperature Variations in the Niger Delta .....	60
Figure 4-12: Power Output versus TET for SS94 .....	62
Figure 4-13: Thermal Efficiency versus TET for SS94 .....	62
Figure 4-14: Fuel Flow versus TET for SS94 .....	63
Figure 4-15: Thermal Efficiency versus TET for LM6K.....	67
Figure 4-16: Power Output versus TET for LM6K .....	68
Figure 4-17: Fuel Flow versus TET for LM6K.....	68
Figure 4-18: Power Output versus TET for DS25.....	72
Figure 4-19: Thermal Efficiency versus TET for DS25 .....	72
Figure 4-20: Fuel Flow versus TET for DS25 .....	73
Figure 5-1: Theoretical Oil Production Curve (Robelius, 2007) .....	84
Figure 5-2: Jones Creek Giant Oil Field, Nigeria (Hook, 2009) .....	85
Figure 5-3: Historical Production of the Thistle (Hook, 2009) .....	89
Figure 5-4: Historical Production of the Thistle Plotted Differently (Hook, 2009) .....	89
Figure 5-5: Associated Gas Decline over Time .....	93
Figure 5-6: Decline in Power over Time .....	94
Figure 5-7: Resource Decline and Engine Redundancy.....	94
Figure 5-8: Resource Decline Range in Cubic Meters .....	95
Figure 5-9: Power Decline Range in MW .....	95
Figure 6-1: Best Individual, Fitness, Average Distance .....	102
Figure 6-2: Current Configuration.....	103
Figure 6-3: Divestment of Redundant Engines.....	104
Figure 6-4: Power Output .....	105
Figure 6-5: Variation of NPV with Degradation for DS25.....	115
Figure 6-6: Variation of NPV with Degradation for LM6K .....	115
Figure 6-7: Variation of Fuel/O&M Cost with Degradation for LM6K .....	116
Figure 6-9: NPV of DS25 Engine Set in Clean Condition .....	119
Figure 6-10: Cumulative Ascending Curve for DS25 in Clean Condition.....	120



Figure 6-11: NPV of DS25 Engine Set in Slow Degradation .....	121
Figure 6-12: Cumulative Ascending Curve for DS25 in Slow Degradation .....	122
Figure 6-13: NPV of DS25 Engine Set in Fast Degradation .....	123
Figure 6-14: Cumulative Ascending Curve for DS25 in Slow Degradation .....	123
Figure 6-15: NPV of LM6K Engine Set in Clean Condition .....	124
Figure 6-16: Cumulative Ascending Curve for LM6K in Clean Condition .....	125
Figure 6-17: NPV for LM6K Engine Set in Slow Degradation .....	125
Figure 6-18: Cumulative Ascending Curve for LM6K in Slow Degradation ....	126
Figure 6-19: NPV for LM6K Engine Set in Fast Degradation .....	126
Figure 6-20: Cumulative Ascending Curve for LM6K in Fast Degradation .....	127

## LIST OF TABLES

Table 1-1 Nigerian Reserves of Oil and Natural Gas (Oguejiofor, 2006).....	4
Table 3-1:Global Gas Flare Reduction Initiative Partners .....	30
Table 3-2 Natural Gas Produced, Utilized and Flared 1999-2008 .....	36
Table 3-3: National Electricity Generation (PHCN, 2012).....	39
Table 3-4: Unutilized Generation Capability Due to Gas Shortage.....	40
Table 3-5: AG Compositions from Three Locations.....	43
Table 3-6: Fuel Heating Values of the Different AG From Aspen HYSIS .....	47
Table 3-7: Results for SS9E Industrial Gas Turbine .....	48
Table 3-8: Results for DS25 Aero-derivative Gas Turbine .....	48
Table 4-1 Performance of SS94 with Ambient Temperature Variations .....	60
Table 4-2: Compressor Inputs for SS94 Degraded Performance .....	61
Table 4-3: Turbine Inputs for SS94 Degraded Performance .....	61
Table 4-4: Part Load Performance Simulation - SS94.....	64
Table 4-5: Results of Ambient Temperature Variations - SS9E.....	64
Table 4-6: Compressor Inputs for SS9E Degraded Performance.....	65
Table 4-7: Turbine Inputs for SS9E Degraded Performance .....	65
Table 4-8: Part Load Performance - SS9E .....	66
Table 4-9: Ambient Temperature Variations - LM6K .....	66
Table 4-10: Inputs for First Compressor - LM6K Degraded.....	66
Table 4-11: Inputs for First Turbine- LM6K Degraded .....	67
Table 4-12: Inputs for Second Compressor - LM6K Degraded.....	67
Table 4-13: Inputs for Second Turbine - LM6K Degraded.....	67
Table 4-14: Part Load Performance - LM6K.....	69
Table 4-15: Ambient Temperature Variations - LM1H .....	69
Table 4-16: Inputs for First Compressor – LM1H Degraded.....	69
Table 4-17: Inputs for First Turbine– LM1H Degraded .....	70
Table 4-18: Inputs for Second Compressor – LM1H Degraded.....	70
Table 4-19: Inputs for Second Turbine – LM1H Degraded.....	70

Table 4-20: Part Load Performance Simulation of – LM1H.....	70
Table 4-21: Ambient Temperature Variations - DS25.....	71
Table 4-22: Inputs for Degraded Compressor – DS25 .....	71
Table 4-23:Inputs for Degraded Compressor Turbine – DS25 .....	71
Table 4-24: Inputs for Degraded Free Power Turbine – DS25 .....	71
Table 4-25: Part Load Performance for DS25 .....	73
Table 6-1: Emission Prediction for the DS25 and LM6K Engine Sets .....	108
Table 6-2: Data & Assumptions for Economic Analysis.....	113

## LIST OF EQUATIONS

(2-1).....	19
(2-2).....	19
(5-1).....	81
(5-2).....	82
(5-3).....	82
(5-4).....	86
(6-1).....	113

## **ABBREVIATIONS AND NOTATIONS**

ADNOC:	Abu Dhabi National Oil Company
AG:	Associated Gas
BCM:	Billion Cubic Meters
BP:	British Petroleum
bpd:	Barrels per day
CEA:	Chemical Equilibrium and Application
CoE:	Cost of Electricity
DCF:	Discounted Cash Flow
DP:	Design Point
DPR:	Directorate of Petroleum Resources
EGT:	Exhaust Gas Temperature
EIA:	Energy Information Administration
EI:	Emission Index
FAR:	Fuel to Air Ratio
FCT:	Federal Capital Territory
FGRS:	Flare Gas Recovery System
FHV:	Fuel Heating Value
Gb:	Gigabarrels, equivalent to one billion barrels
GGFR:	Global Gas Flare Reduction
GT:	Gas Turbine
GTU:	Gas Treatment Unit
GTW:	Gas to Wire
GWP:	Global Warming Potential
HHV:	Higher Heating Value
HI:	Heat Input
HPT:	High Pressure Turbine
ICAO:	International Civil Aviation Organization
IEA:	International Energy Agency

IGT:	Industrial Gas Turbine
IRR:	Internal Rate of Return
ISA:	International Standard Atmosphere
ISO:	International Standards Organization
Kg:	Kilogram
LANatGas:	Lean Associated Natural Gas
LHV:	Lower Heating Value
LNG:	Liquefied Natural Gas
LPG:	Liquefied Petroleum Gas
MANatGas:	Medium Associated Natural Gas
MATLAB	Matrix Laboratory
MCS:	Monte Carlo Simulation
MDEA:	Methyl Diethanolamin
MSCFD:	Million Standard Cubic Feet per Day
MW:	Mega Watts
MYTO:	Multi-Year Tariff Order
NASA:	National Aeronautics and Space Administration
NERC:	Nigerian Electricity Regulatory Commission
n:	Project's life in years
NDDC:	Niger Delta Development Commission
NDT:	Non Destruct Test
NG:	Natural Gas
NGC:	Nigerian Gas Company
NGL:	Natural Gas Liquid
NNPC:	Nigerian National Petroleum Corporation
NPV:	Net Present Value
OD:	Off Design

OEM:	Original Equipment Manufacturer
O&M:	Operation and Maintenance
OIP:	Oil In Place
PBP:	Pay Back Period
PHCN:	Power Holding Company of Nigeria
PR:	Pressure Ratio
RANatGas:	Rich Associated Natural Gas
SFC:	Specific Fuel Consumption
SPDC:	Shell Petroleum Development Company
SPE:	Society of Petroleum Engineers
TERA:	Techno-economic Environmental and Risk Analysis
TET:	Turbine Entry Temperature
USD:	United States Dollars
UHC:	Un-burnt Hydro Carbons
URR:	Ultimate Recoverable Resources
WI:	Wobbe Index
WAGP:	West African Gas Pipeline
ZADCO:	Zakum Development Company

## **Chemical Formulae**

CH <sub>4</sub> :	Methane
C <sub>2</sub> H <sub>6</sub> :	Ethane
C <sub>3</sub> H <sub>8</sub> :	Butane
C <sub>4</sub> H <sub>10</sub> :	Propane
C <sub>5</sub> H <sub>12</sub> :	Pentane
C <sub>6</sub> H <sub>14</sub> :	Hexane
CO:	Carbon Monoxide
CO <sub>2</sub> :	Carbon Dioxide
H <sub>2</sub> S:	Hydrogen Sulphide

H <sub>2</sub> O:	Water
N <sub>2</sub> :	Nitrogen
NO <sub>2</sub> :	Nitrogen Dioxide
NO <sub>x</sub> :	Oxides of Nitrogen
SO <sub>2</sub> :	Sulphur Dioxide

## Notations

$\eta$ :	Efficiency
$\infty$ :	Infinity
$\beta$	Shape parameter
$q(t)$	Production rate at time t
$Q(t)$	Cumulative Production at time t
$Q_0$	Initial Cumulative Production
$t_{cut}$	Time that production stops when the economic limit is reached
$V_{rec}$	Technically Recoverable Volume
$\lambda$	Decline rate
$r_0$	Initial rate of production
$t_0$	Time at which decline in production starts
$T_{amb}$ :	Ambient Temperature



## **CHAPTER 1: RESEARCH DEFINITION**

### **1.1 Research Rationale**

Energy is of paramount importance to growth and development of societies. The rapid growth of population and extensive urbanization results in an ever increasing demand for energy. That is, the demand of electricity is increasing consistently even as usage patterns are changing. However, there has been a rapid increase in the extraction of fossil fuels as technologies get sophisticated and more advanced. Conventional energy resources such as petroleum and natural gas are on the decline. Oil is the dominant source of energy, but future supply is unsure or expected to decrease.

This growing electricity demand at the global stage calls for an improvement in power generation techniques as well as an upgrade of generation processes and equipment. Storage of electricity is cumbersome, necessitating the development of economically efficient generating systems that will not have a negative impact on availability and reliability.

Global energy demand has increased greatly in the last ten years, thanks to increased economic activity and the development of downstream industries. For instance, in Nigeria there is an increase in the gas requirement for power generation to satisfy the needs of the population, which is about 170 million people. Most of the energy requirement is yet to be met, but the country has an overwhelming capacity to generate electricity by exploiting the potentials that exist in her abundant natural resources.

A critical volume of natural gas is being wasted to flaring, hence a vital aspect of this quest for energy will involve the recovery of associated gas (AG) from onshore and offshore fields. AG is natural gas that comes in conjunction with crude oil. AG is the dissolved gas contained in an oil reservoir at high pressure; it is the gas produced as oil is being extracted from the well. Increased oil exploration/exploitation results in more AG emissions. Harnessing AG would greatly reduce greenhouse gas emissions, and generation of useful power, although it requires a relatively high investment and running cost. The presence

of contaminants in AG results in degradation of gas turbine (GT) components which translates to an increase in maintenance cost and reduced creep life.

This work is meant to encourage the gas turbine user in countries still practising gas flaring, to harness AG for power generation. It also explores ways of eliminating the emission of greenhouse gases and environmental degradation that result from gas flaring. Nigeria is the second highest gas flaring country in the world, second only to Russia (Juez et al., 2010). Global Warming Potential (GWP) is a way of comparing global warming of a given mass of a particular greenhouse gas to an equivalent mass of carbon dioxide (CO<sub>2</sub>). Regrettably, communities where gas flaring occur in the Niger Delta are bedevilled by erratic power supply or the sheer absence of electricity in some coastal communities.

AG is a future source of energy that can be used to generate electricity, provide energy for desalination plants, while excess energy can be fed into the national grid. Harnessing AG would result in additional energy for sustainable growth, reduced greenhouse gas emissions with minimized environmental impact. Oil and gas producers, governments and power companies are working to evolve efficient ways and means to stop flaring with a view to harnessing its inherent energy. However, uncertainties such as production decline introduces technical and economic constraints, hence the need for this techno-economic assessment in the face of decline, while analysing the risks.

## **1.2 Aim & Objectives**

The aim of this research is to assess the technical and economic feasibility of harnessing AG with a view to using it for power generation, while considering degradation of the GT and decline of AG. In this light, emphasis is on the development of a tool for optimizing power output from a combination of GTs of different capacities and configurations that would use AG as fuel.

The specific objectives of the research are to:

- Evaluate AG production quantities by carrying out a Decline Curve Analysis

- Simulate engine performance by modelling a fleet of study engines, at varying operating conditions for the purpose of developing an economic model
- Employ Hephaestus for the prediction of CO<sub>2</sub> emissions for the economic model, and the use of Palisade's @RISK software for risk analysis
- Carry out optimization in order to select the best plant, the least cost of electricity (CoE), and specify the time to divest redundant engines due to AG decline

### **1.3 Analysis of Associated Gas Volume**

This section discusses the Niger Delta Region, the hub of oil exploration activities in Nigeria vis-à-vis environmental degradation, lack of infrastructure, health challenges and absence of electricity.

Geology reveals that some of the richest deposits of oil sit together with deposits of natural gas. Crude oil production results in the release of dissolved natural gas; and when the gas cannot be conserved, it is flared. Statistics show that over 100 billion standard cubic meters (BSCM) of gas is flared annually worldwide, equivalent to 200 million tons of CO<sub>2</sub> emissions (Abdulkareem and Odigure, 2010).

Nigeria has vast quantities of oil and gas resources. Erinne classifies the Nigerian reserves of oil and natural gas (NG) as presented in Table 1-1, showing over 200 and 30 years of proven reserves of NG and oil respectively. Nigeria is considered more of a gas than an oil region (Oguejiofor, 2006). The information is further illustrated in Figure 1-1.

**Table 1-1 Nigerian Reserves of Oil and Natural Gas (Oguejiofor, 2006)**

	Oil (Million Barrels)	Natural Gas (BCM)
Ultimate Reserves	31400	8500
Proven Reserves	20000	4250
Annual Production	663	21
Depletion	30 years	202 years

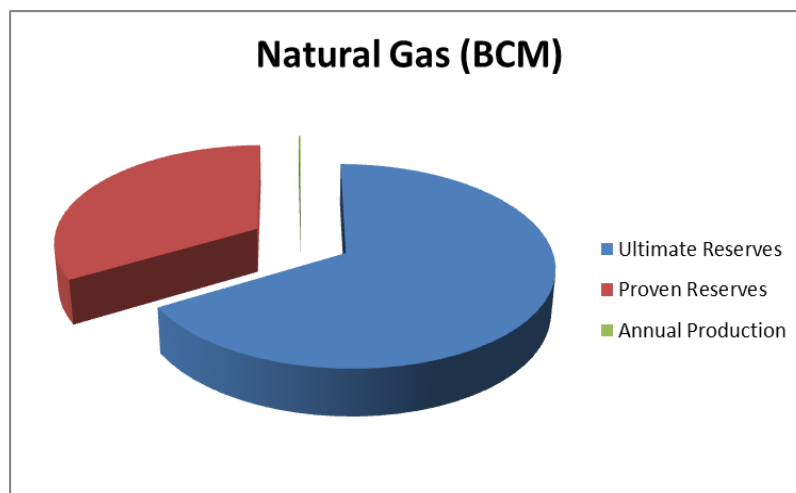


**Figure 1-1 Production of Natural Gas in Nigeria (Oguejiofor, 2006)**

Figure 1-2 reveals the rivers and the tributaries in the oil-rich region at close range. The Niger Delta is a geologic province in West Africa called Akata-Agbada which contained about 34.5 billion barrels of recoverable oil and 94 trillion cubic feet of NG at the onset (Tuttle, Charpentier & Brownfield, 1999, The Niger Delta Petroleum System).

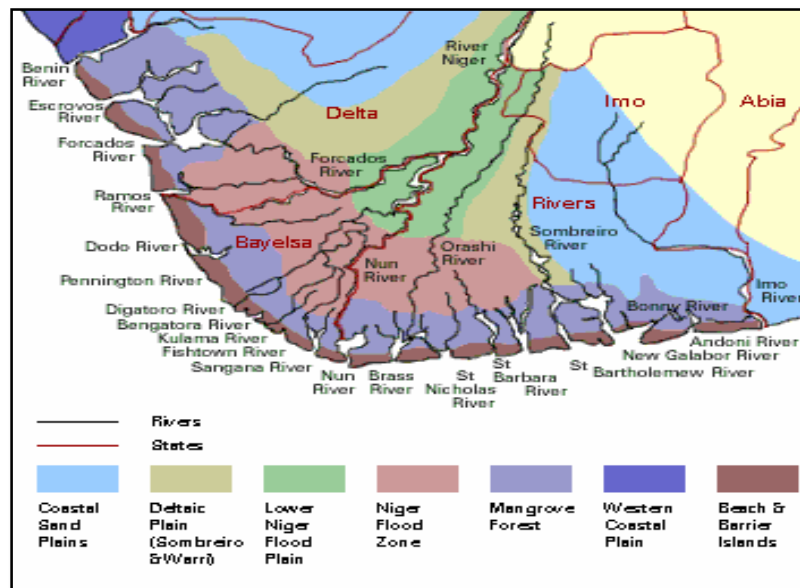


**Figure 1-2 Map of Niger Delta, Nigeria (NDDC, 2011)**

Through extensive literature review, the feasibility and economic viability of using AG to generate electricity for rural electrification has been ascertained. A gas-to-wire (GTW) system of 5MSCFD gas supply was found to be capable of generating 14.4MW of electricity (Osaghae, 2003). Also, in Indonesia a country with many small islands near fields, GTW seems promising. Studies show that even AG flare as small as 0.7MSCFD could fire a 3MW generator and supply about 7500 Indonesian households (Khalilpour and Karimi, 2009). From the foregoing, there is every reason to explore ways of harnessing flare gas in Nigeria whose hydrocarbon is characterised 'sweet', that is, sulphur-free (Nwasike et al., 2000).

Emissions from the combustion of AG in an open, uncontrolled manner as shown in Figure 1-3, results in an outpouring of particulates, combustion by-products, carcinogenic substances and unburned fuel components. These constitute health hazards, contribute to global warming and are a colossal wastage of energy.



**Figure 1-3 Gas Flaring at Kolo Creek, Nigeria (NDDC, 2011)**

The heat produced as a result of flaring has adverse effects on the environment. A World Bank mission in 1993 reported that Nigeria's gas flaring takes place at 1300-1400°C (Abdulkareem et al., 2009), from the centre of the flame. Areas close to the flare stations have their vegetation scorched and the ground near the flare is devoid of vegetation. Plants play an important role in absorbing the CO<sub>2</sub> released into the atmosphere, but since they are destroyed by the heat from the flare, the ecosystem becomes disturbed. This devastation results from a resource that ordinarily is a good source of electricity.

The first oil field in Nigeria was found at Oloibiri in 1956 and the first export was made in 1958 (Ndubuisi and Amanetu, 2003); so flaring of gas mixed with crude oil began almost six decades ago.

## **1.4 Thesis Structure**

The Thesis is organized as follows:

### **Chapter 1: Research Definition**

Chapter 1 entails a background to the study of AG utilization. It states the aim and objectives of the research, captures an analysis of the volume of AG flared

and spells out the contributions to knowledge. The chapter ends with the thesis structure.

## **Chapter 2: Literature Review**

Chapter 2 provides an insight into the constituents of fuel gas, and their effects on GT components. It looks at GT degradation broadly and components' performance degradation. The chapter expounds the concepts of fouling, corrosion, oxidation, creep and erosion. Chapter 2 is essentially a literature survey that logically leads to the conclusion that component efficiency and flow capacity are the important changes on which performance simulations will be based. After discussing the history and effects of gas flaring in Nigeria and examining a few case studies, the significance of the research is brought to the fore and the knowledge gap revealed.

## **Chapter 3: Data Analysis & Modelling of Associated Gas**

Chapter 3 introduces simulation softwares and codes employed in the research. GasTurb was used to simulate three compositions of AG (LANatGas, MANatGas and RANatGas). The chapter also presents data collected from the Niger Delta region of Nigeria; an analysis of data from Power Holding Company of Nigeria (PHCN), Directorate of Petroleum Resources (DPR), and Nigeria Liquefied Natural Gas (NLNG). It brings out gas flaring trends, the national power requirement, the current production capacity, power deficiency due to gas shortages and emphasizes the need to harness AG currently being flared. The Chapter crystallizes the Fuel Heating Value (FHV) calculations as well as power and efficiency variations from simulations run.

## **Chapter 4: Study Engines & Degradation**

Chapter 4 explores the performance of the study engine fleet made up of two single shaft, heavy duty IGTs and three multiple shaft aero-derivative GTs ranging from light to heavy categories. Using TurboMatch, degradation was implemented in three scenarios: fast, medium and slow. The relationship between degradation and maintenance of power plants and creep life were brought to the fore.

## **Chapter 5: Resource Decline Analysis**

Chapter 5 discusses the concept of resource decline and carries out a decline curve analysis. As GT power plants are operated on AG drawn from reserves, depletion is inevitable. As crude oil depletes, the AG depletes as well. Resource decline analysis was done with a view to applying it to the power plant economics. Also a risk analysis of the Ultimately Recoverable Resource (URR) volume estimation was covered.

## **Chapter 6: Power Plant Economics & Risk Analysis**

Chapter 6 centres on power plant economics, drawing from the Techno-economic Environmental and Risk Analysis (TERA), Global Gas Flare Reduction (GGFR), Resource Decline with Divestment. Also covered is optimization for the best power plant configuration and the most appropriate time to divest redundant engines. The genetic algorithm embedded in MATLAB was used in the optimization, while the software @RISK was employed to assess the risk factors.

## **Chapter 7: Conclusions & Recommendations**

Chapter 7 draws conclusions on work done, and presents a summary of the results obtained while succinctly stating the gap in knowledge that has been bridged. The chapter ends with recommendations for future work.



## **CHAPTER 2: LITERATURE REVIEW**

### **2.1 Introduction**

This chapter traces the history of gas flaring in Nigeria and makes an effort to assess the national volume of gas flare with a mention of the effects. That leads logically into the need to end gas flaring while stating past gas gathering efforts.

GTs burn NG, whether clean or impure, to produce power. Impurities have effects and cause the LHV of one fuel to differ from that of another. The impurities initiate the process of degradation of the GT or components along the hot gas path. This chapter will also examine the chemistry of NG, specifically looking at the constituents of AG, while assessing the suitability of its use as fuel. Also the combustion and properties of AG are surveyed, before the degradation of the hot gas path of the GT is scrutinized with specific reference to oxidation, corrosion and creep; and the performance degradation of the components.

A few case studies where AG has successfully been harnessed were examined, with a view to drawing lessons from them.

### **2.2 History of Gas Flaring**

Gas flares are open air fires that burn the NG that is released when oil is extracted from the ground. In other words, gas flaring is the practice of burning off NG when it is brought to the surface in places where there is no infrastructure to utilize it. Gas flares are used to eliminate AG which is deemed un-economical for use. It is sometimes used as a safety system for non-waste gas and released through a pressure relief valve. The size and brightness of the resulting flame depend on how much flammable material is released. The practice endangers human health, upsets the ecosystem, emits large amounts of greenhouse gases, and wastes vast quantities of energy.

When Nigeria's oil and gas industry was hatched; the utilization of the AG was not given much thought, since the demand for its usage was low. Hence, most of the AG was being flared. The current production of about 2.5 million barrels of oil per day has resulted in the production of large quantities of AG. Until 2005, over

90% of this gas was flared (Abdulkareem et al., 2009). This is not unconnected with the fact that at the onset of oil exploration in Nigeria, there was neither market for NG nor AG. Little was known also about the consequences of gas flaring, hence hardly anything was done to end gas flaring, neither were there facilities constructed to collect AG. Oguejiofor submits that on the average, Nigeria flares about 86% of her NG production (Oguejiofor, 2006).

### 2.3 Analysis of National Volume of Flare Gas

When crude oil is extracted, it comes with AG which must be separated from the crude to produce export quality oil. In Nigeria, this is mostly done by the burning of AG, a practice that has gone on for almost six decades.

According to satellite research, 168 BCM of NG is flared yearly worldwide (equivalent to about 400 million tons of carbon dioxide). Nigeria accounts for 23 BCM, the biggest after Russia; about 13% of global flaring is attributed to originate from Nigeria (Anosike, 2010). Figure 2-1 is a colour composite of the night-time flares obtained from data acquired by the US Air Force Defence Meteorological Satellite Program, showing the amount of AG unleashed into the environment.

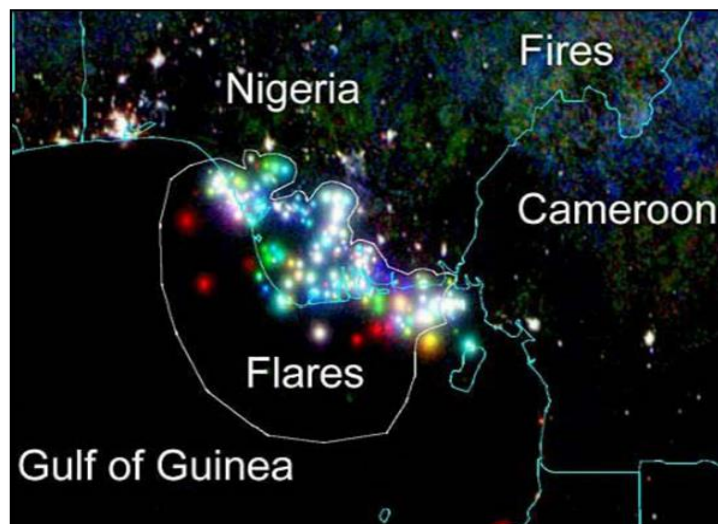
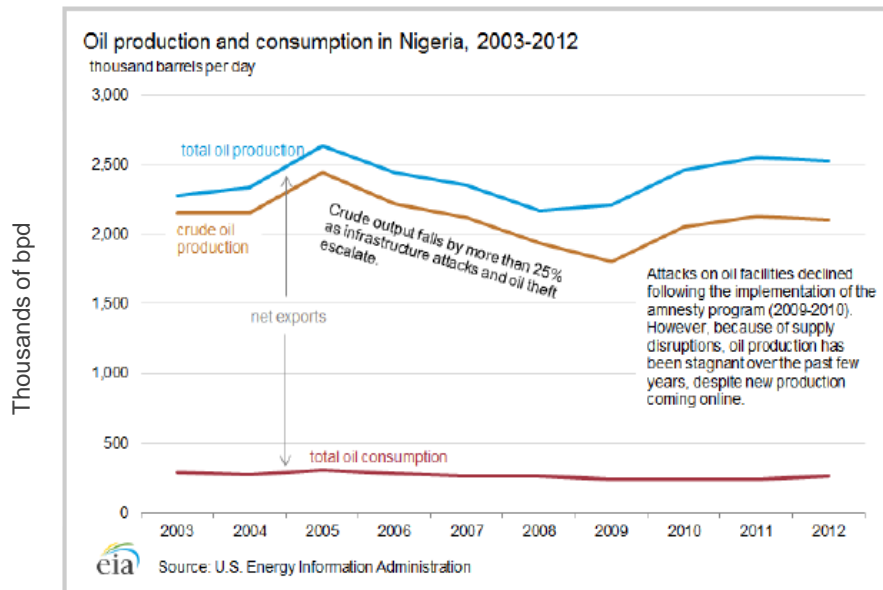


Figure 2-1: Nigerian Gas Flares (USAF Def Met Satellite, 2006)

Oil production and consumption in Nigeria is as shown in Figure 2-2.



**Figure 2-2: Oil Production and Consumption in Nigeria, 2003-2012 (US EIA)**

By using the gas for energy, instead of flaring, much of the acute power needs in Nigeria would be fulfilled. The scale of flaring is a reflection of the years of oil and AG production as shown by the flaring data. About 1000 standard cubic feet (SCF) of AG is produced in Nigeria with each barrel of oil. Hence oil production of 2.5 million bpd amounts to about 2.5 billion SCF of AG produced daily (Igbatayo, 2007). This amounts to an annual financial loss of about \$2.5 billion (Ogbe et al., 2011).

Nigeria's oil sector provides about 95% of its foreign exchange earnings and about 63% of government revenue, (Ndubuisi and Amanetu, 2003). This means that oil exploration is crucial to the economy. The massive amount of NG flared annually is an enormous economic waste and gives off greenhouse gas emissions, causes air pollution, have health implications and results in acid rain.

## 2.4 Effects of Gas Flaring

### 2.4.1 Greenhouse Gas Emissions

The burning of fossil fuel results in greenhouse gases which leads to global warming. The Kyoto Protocol of 1997 imposed legally binding emission cuts on member countries. Carbon dioxide emissions from flaring have high global

warming potential and contribute to climate change. Flaring also contributes significantly to emissions of carbon monoxide (CO) and oxides of nitrogen (NO<sub>x</sub>), gases that are instrumental to the formation of tropospheric ozone (another greenhouse gas). In the stratosphere, methane is a greenhouse gas; while in the troposphere (ground level), methane is one of the reactants in the photochemical process of forming ground level ozone and smog (Riti Singh, 2010).

#### **2.4.2 Air Pollution**

Ambient air is chemically a gaseous mixture consisting of 78% Nitrogen, 21% Oxygen, 0.04% Carbon dioxide in addition to water vapour and rare gases such as Argon and Helium. When the concentration of the components change, ambient air no longer exists and the air is polluted. Gas flaring constitutes one of the major causes of air pollution. About 15 million tonnes reduction of CO<sub>2</sub> is expected to come from ending continuous flaring at oil production facilities, especially in Nigeria (Veerkamp and Heidug, 2006).

#### **2.4.3 Health Implications**

The flares contain a cocktail of toxins that affect the health and livelihood of locals. Scientific studies, according to the US Environmental Protection Agency, have linked breathing particulate matter to health problems such as asthma, respiratory disorders, coughing, painful breathing, chronic bronchitis, decreased lung function and premature death.

#### **2.4.4 Acid Rain**

The chemicals released from gas flares are H<sub>2</sub>S, SO<sub>2</sub>, CO<sub>2</sub> and volatile organic compounds such as Benzene, Xylene, and Toluene. The release of these gases results in acid rain. Rain water chemically combines with oxides of sulphur and nitrogen to form sulphuric and nitric acids respectively. Figure 2-3 shows the world's top 5 gas flaring countries in percentages.

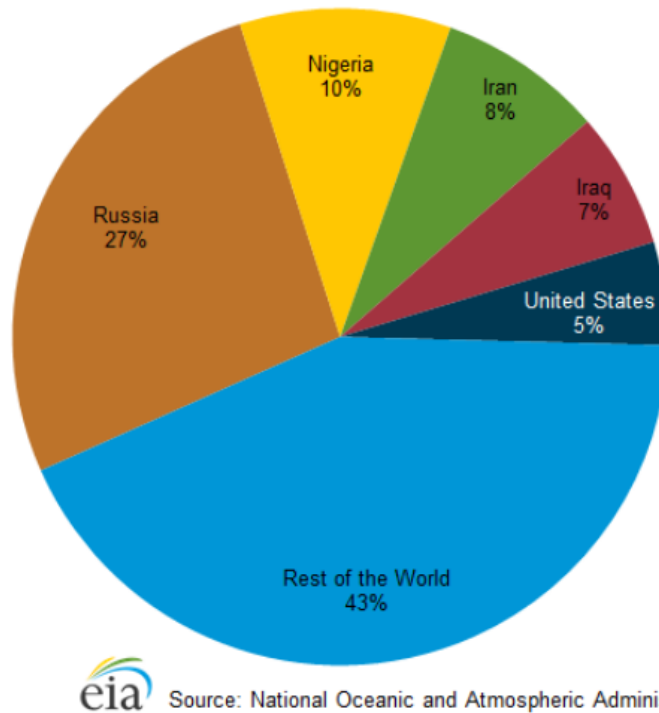


**Figure 2-3: World’s Top Five Natural Gas Flaring Countries, 2011( US EIA)**

Sonibare and Akeredolu showed that, of the total NG production in Nigeria, about 17% is re-injected, 33% used commercially and 50% flared (equivalent to about 75% of total AG produced, Akeredolu and Sonibare, 2007).

A 2004 World Bank report stated, “In accordance with the Associated Natural Gas Reinjection Act 1979, a fee is charged for flaring. This was first set at 50 Kobo per million cubic feet; but effective January 1998, the fee became 10 Naira (\$0.06) per million cubic feet. A study carried out for the Bureau of Public Enterprises of Nigeria estimated that each year the country loses between US\$500 million and US\$2.5 billion to gas flaring.” The difference in figures between the fee charged and the amount lost is astronomical.

## **2.5 The Need to End Gas Flaring**

The oil exploration and exploitation companies have a responsibility to operate in an environmental way. It is worthy to note that despite the fact that the price of gas has gone up, and transportation techniques have been developed, the gas is still mostly flared. Experts believe Nigeria is burning billions of Dollars from its

oil wells and letting potential profits go up in flames. Nigeria is in need of extra power generation and the gas that is being burned could go a long way towards providing the electricity that the country so desperately needs.

With a rise in crude oil production, there will be a corresponding increase in the amounts of AG. Communities that live near the over 1000 onshore well heads are blighted by gas plumes daily (Adewale and Ogunrinde, 2010). The gas flares produce considerable heat, and the noise that emanates from the flares is a continuous roar. The living conditions in the Niger Delta will be improved by a shift from gas flaring to gathering for electricity generation. This will not go without great technical and cost implication, though.

Worldwide, the practice has been reduced mainly because companies have realized the potential of the hitherto wasted gas. This brings to the fore the need to utilize AG in Nigeria.

Nigeria has an estimated proven natural gas reserve of about 183 trillion cubic feet, ranking as the 7<sup>th</sup> largest NG reserve holder and the 6<sup>th</sup> highest oil exporter worldwide (Adewale and Ogunrinde, 2010). A 1996 report from Shell Petroleum Development Company (SPDC) confirms that about 2 billion standard cubic feet per day of gas was flared by Nigeria, and this calls for flare reduction schemes for Nigeria.

## **2.6 Past Gas Gathering Efforts in Nigeria**

NG is an important component of the world's energy supply, being one of the safest and most useful sources; it is clean burning, produces less harmful fumes, and is used as feedstock for petrochemicals and fertilizers. The Nigeria Gas Company (NGC) was established in 1988 as a subsidiary of the Nigerian National Petroleum Company (NNPC) with the responsibility to transmit and market gas in Nigeria and West Africa. Several efforts have been made and are still in progress to gather AG as will be discussed in succeeding paragraphs.

### **2.6.1 Bonny Liquefied Natural Gas**

The Liquefied Natural Gas (LNG) plant located in Bonny Rivers State is supposedly SPDC's main flares-out programme. Nigeria Liquefied Natural Gas (NLNG) Limited was established in 1989, 49% owned by NNPC, 25.6% by SPDC, 15% by Total and 10% by Agip. In the arrangement, one strategy for eliminating flaring is to replace non-AG with AG. Nigeria exported her first LNG cargo from Bonny to Italy in August 1999.

### **2.6.2 Ajaokuta-Abuja Gas Pipeline Project**

Proposed to be the bedrock of the Abuja 450MW thermal plant, the project involves a 460Km pipeline from Ajaokuta to Abuja and then Kaduna with a pipeline meant to carry 450MSCFD. It is meant to cater for industrial, residential and commercial needs of gas in the Federal Capital Territory (FCT) and industries in Kaduna and Kano.

### **2.6.3 Brass Liquefied Natural Gas**

The contract has been awarded for the construction of its LNG trains in Bayelsa State, to Bechtel LNG Contractors Limited, USA. Brass LNG is owned by a consortium of oil companies consisting of Eni, ConocoPhillips, Total and NNPC.

### **2.6.4 West African Gas Pipeline**

In November 2004, the World Bank approved \$125 million USD in guarantees in support of the construction of a 678Km gas pipeline to transport NG from Nigeria to Benin, Ghana and Togo; as shown in Figure 2-4. The West African Gas Pipeline (WAGP) was to be built, and operated by the WAGP Company owned by Chevron (36.7%), NNPC (25%) SPDC (18%), Ghana (16.3%), Benin Republic (2%) and Republic of Togo (2%). The major positive environmental impact of WAGP was to be the development and use of AG currently flared in Nigeria.



**Figure 2-4: West African Gas Pipeline (West African Gas Pipeline Ltd)**

### **2.6.5 Olokola Liquefied Natural Gas**

Olokola LNG was established in 2005 and is owned by a consortium of oil companies comprising Chevron, SPDC, BP and NNPC as well as the Ogun and Ondo State governments. When completed, it is expected to process 2 billion cubic feet of gas per day.

### **2.7 Chemistry of Natural Gas**

The main bonded elements available for energy generation in fuels comprise hydrogen and carbon, the combining powers of the atoms inherent in their valency. The simplest hydrocarbon molecule is methane CH<sub>4</sub>. The sizes of hydrocarbon compounds indicate their physical states; that is gas, vapour, liquid or solid and therefore their volatility and flammability. High hydrogen content indicates high specific energy, and clean, active burning; while high carbon content indicates radiant flames with a propensity to reduce engine life as well as potential soot formation (Goodger & Ogaji, 2011).

Deposits of natural gas worldwide, range in composition from near pure methane (99.4% Ravenna, Italy), through ‘wet’ gases containing higher hydrocarbon condensate (27.8% Kuwait) to the high Nitrogen content gases with relatively low



energy density (14.3% N<sub>2</sub> and 29MJ/m<sup>3</sup>, Groningen Netherlands) to high Carbon dioxide content (44% CO<sub>2</sub>, Kapuri, New Zealand) to the sour gases containing Hydrogen sulphide (15% H<sub>2</sub>S, Lacq, France).

NG consist mainly of methane CH<sub>4</sub>, though having evolved from organic matter contain higher hydrocarbons such as ethane C<sub>2</sub>H<sub>6</sub>, propane C<sub>3</sub>H<sub>8</sub>, butane C<sub>4</sub>H<sub>10</sub>, pentane C<sub>5</sub>H<sub>12</sub> and hexane C<sub>6</sub>H<sub>14</sub> plus traces of inert Nitrogen N<sub>2</sub>, Carbon dioxide CO<sub>2</sub>, hydrogen sulphide H<sub>2</sub>S and water H<sub>2</sub>O (Melvin, 1988) . The presence of these additional components increases the density by 8% and reduces its specific energy by 4% while increasing its energy density by 4% ( Goodger & Ogaji, 2011).

In contemplating the use of AG as fuel, it is worthy to note that impurities within GT may come from the air, fuel gas, fuel oil and water. Excessive concentration of these could become detrimental to gas turbine components such as compressors, turbine aerofoils, burners, coatings and cooling channels. The chemistry of gas turbine power plants is dominated by the combustion behaviour of the fuel or by the corrosion and scaling properties of the gas in the hot gas path.

Treatment of NG involves the separation of the higher hydrocarbon condensates and water at the well head, followed by refrigeration to give appropriate dew points. CO<sub>2</sub> and/or H<sub>2</sub>S are then removed by alkaline scrubbing or adsorption. Liquefaction of CH<sub>4</sub> is not possible by compression at ambient temperature as its critical temperature is as low as -82°C (Goodger & Ogaji, 2011).

Crude oils are described 'sweet' if sulphur concentrations are below 0.5%, and 'sour' if above 0.5%. NG treatment would therefore comprise the removal or sweetening of the sulphur-bearing compounds such as H<sub>2</sub>S with a view to eliminating the potential for corrosion.

Untreated gaseous fuels contain some hydrocarbon components along with contaminants that may be incombustible such as CO<sub>2</sub> and N<sub>2</sub>; or combustible but corrosive components such as SO<sub>2</sub> or H<sub>2</sub>S. Treatment can be by selective

absorption in chemical reagents, by physical adsorption and desorption in chromatographic column, or by infrared adsorption (Goodger & Ogaji, 2011).

## **2.8 Combustion of Associated Gas**

Combustion is a chemical reaction accompanied by the release of heat and light. Efficient combustion should be a controlled generation of maximum combustion heat with minimal emissions. A stoichiometric, or chemically correct, equation defines the exact proportions of fuel and oxidant that, on completion of the reaction, leaves no excess or deficiency in fuel or oxidant.

Combustion products include fully burnt components, CO<sub>2</sub> and H<sub>2</sub>O, and partially burnt products CO, H<sub>2</sub>, O<sub>2</sub> and inert N<sub>2</sub>, and unburnt hydrocarbons (UHC), oxides of Nitrogen (NO<sub>x</sub>) and oxides of sulphur (SO<sub>x</sub>). Thermal NO<sub>x</sub> is produced by conversion of atmospheric Nitrogen in the flame via the Zeldovich Mechanism, while fuel-bound NO<sub>x</sub> is formed by the conversion of a fraction of the chemically-bound nitrogen within the fuel (Lefebvre, 1984).

Calorific value is the energy released on complete combustion of fuel with oxygen. From thermodynamic considerations, the combination of constant pressure and steady flow, the energy of combustion of a fuel is released as heat only, thus gaseous fuels are tested under these conditions.

The blades on a gas turbine disc operate continuously in a high temperature environment, and are subjected to centrifugal stresses. Typically, about 28% of the chamber air is used for combustion in the primary zone which gives a flame temperature of about 2300K, while introducing the remaining air progressively downstream. The secondary air reduces the temperature of the combustion products to about 1700K to offset the effects of dissociation. It also acts as dilution air to bring down the firing temperature to about 1350K depending on the amount of cooling employed (Goodger & Ogaji, 2011).

## 2.9 Suitability of a Fuel for Gas Turbine Application

GTs with annular or can combustors often require gaseous fuels or liquid distillate fuels. Colombo and Ruetschi use the following parameters to evaluate the suitability of a fuel for GT application:

### 2.9.1 Gaseous Fuel Properties

- Range of Lower Heating Value
- Range of net Wobbe Index
- Gas pressure fluctuations
- Gas temperature
- Hydrogen sulphide content
- Hydrogen content
- Higher hydrocarbons (C<sub>2+</sub>) content

### 2.9.2 Gaseous Fuel Impurities

- Dust content
- Particle size
- Lube oil content
- Relative humidity

Typically the levels of higher hydrocarbons, methane and inerts are used by Original Equipment Manufacturers (OEMs) to specify fuel composition. Fuels are also specified using the Wobbe Index (WI), defined as:

$$WI = \text{Volumetric Heating Value}/(\text{Fuel Relative Density})^{0.5} \quad (2-1)$$

The calorific value of a fuel forms the basis for its evaluation. This is the energy released on complete combustion of fuel with oxygen. Calorific value, in a gravimetric sense, is the specific energy of a fuel expressed in MJ/kg. In a volumetric sense, the energy density measured in MJ/m<sup>3</sup>, is defined thus:

$$\text{Energy Density} = \text{Specific Energy} \times \text{Density} \quad (2-2)$$

The heat energy liberated per unit mass of fuel combusted at constant pressure with the water products of the combustion mixture in a liquid phase is called the Higher Heating Value (HHV). Should the water in the combustion products be in vapour state, the energy released, called the Lower Heating Value (LHV) is considered.

## 2.10 Gas Turbine Degradation Types

Degradation can be broadly categorised into recoverable and non-recoverable degradation. Degradation that can be salvaged or reversed by compressor cleaning is regarded as recoverable. Degradation caused by fouling is usually reversed or partially reversed by compressor cleaning while degradation that requires repair, replacement of engine component or complete engine overhaul is regarded as non-recoverable (Diakunchak, 1991).

A GT will in its lifetime show the effects of degradation, though the environment within which an engine operates determines the extent of degradation it will suffer from. The degradation of an engine will no doubt have an adverse effect on the engine's overall performance, thus it is important to predict the effects of degradation on the performance of an engine and the attendant economic implications.

Engine component degradation results in performance deterioration, which requires the engine to run hotter in order to meet the required power output. Engine performance is inseparable from the economics as performance measures such as fuel burn, life and maintenance requirements are driven by the performance parameters. Degradation could be due to foreign object ingestion, or simply associated with the natural ageing of the engine or due to other factors such as fouling, erosion, corrosion and oxidation. The occurrence of corrosion, erosion and foreign object damage is difficult to predict owing to the influence of external factors. On the other hand, creep and oxidation lead to damage due to the nature of the operating conditions. These mechanisms are briefly discussed below.

Oxidation is the formation of an oxide layer on the surface of the metal part. Turbine blades oxidise at high temperatures by forming an oxide layer. Corrosion is caused by contaminants in the inlet air and/or contaminants derived from the fuel and combustion. The fusion of particles onto hot surfaces cause blocking of cooling passages, altering the surface shape and interfering with heat transfer.

With erosion, particles impinge on flow surfaces and remove materials from the flow path by abrasion. It occurs in aerofoils when foreign particles are ingested into the engine. Ingestion of particles can cause the engine to stall, and erode seals or blade materials. Erosion of the blade can lead to excessive blade metal temperatures and premature failures due to changes in the profile of the cooling holes, which affects the effectiveness of cooling the blade (Naeem, 1999).

Creep is the time-dependent deformation of components under the application of load at high temperatures, causing plastic deformation; it is time sensitive and thermally enhances material deformation under stress. Fouling is the adherence of particles on the surface of aerofoils in the presence of oil or water, resulting in a reduced flow area; an increased surface roughness and changes in the aerofoil shape which influences its aerodynamic behaviour (Leusden, C.P., Sorgenfrey, C. and Dummel, L., 2004).

Fouling could lead to a reduction in power output, efficiency drop and increased fuel consumption depending on its operation. Compressor fouling is the most common cause of engine degradation and can lead to increases in turbine temperatures up to 15°C, flow reductions of up to 8% and efficiency reductions of 1% (Little, 1994). Regular offline washing in conjunction with online washing mitigates the effects of fouling (Kurz, R., Brun, K., 2007). The turbine will suffer similar effects from fouling as does the compressor. Particles may clog the turbine blade cooling holes and promote damage due to overheating. The decrease in engine performance requires higher Turbine Entry Temperatures (TET) and speeds to maintain the required power output.

Due to high temperatures, ingested particles are melted in combustors and these accumulate on turbine surfaces, reducing air flow capacity and adversely affecting turbine efficiency. Molten impurities in the hot gas stream could stick to turbine surfaces as temperature and pressure drop. Results of such material deposition in turbines are increased Specific Fuel Consumption (SFC), decreased efficiency, increased flow capacity, and fall in power.

Hot Corrosion is the loss or deterioration of material from components in the flow path due to chemical reactions with contaminants such as salts, mineral acids or

reactive gases. Scaling occurs when the products of these reactions adhere to the components. Chemical reactions also occur between the metal atoms and oxygen found in the surrounding hot gases, causing high temperature oxidation (Kurz R., 2001).

Carbon could stick to the turbine blade and erode the metal, gumming the injector and causing a heat shield. Also, sulphur introduced into engine components could cause corrosive reactions. Though the combustion efficiency would not usually decrease, deterioration could lead to a variation in the combustor exit temperature profile; which could damage the turbine section, increase secondary flow activities thereby reducing turbine efficiency; the measured temperature turns out to be different from the true thermodynamic average temperature.

Having examined the aforementioned degradation mechanisms; it has become obvious that fuel composition has a prominent role in the degradation and life consumption of the GT, as efforts are made to improve efficiency, fuel burn and power output.

## **2.11 Components' Performance Degradation**

Changes in compressor and combustor performance give rise to changes in turbine entry conditions. Changes in the combustor effect changes in the temperature profile at the entry of the turbine, resulting in elevated local temperatures. The efficiency and life of the turbine suffer from thermal distortions; the combustor also suffers from thermal distortion resulting in premature component failure and increased life cycle costs (Little, 1994; Naeem, 1999).

The performance characteristics of an engine component are determined by the following performance parameters: compressor efficiency and flow capacity, combustor efficiency, turbine efficiency, areas of nozzle guide vanes and the exhaust nozzle. Performance characteristics change with degradation and are dependent on the following engine design parameters: fuel flow, power, temperatures, pressures and rotational speeds. When an engine degrades, it seeks a different steady operating point in relation to that of a clean engine. The

variation in the engine's steady operating point causes changes in the SFC and/or fuel flow (Naeem, 1999) (Kurz, R., Brun, K., 2007).

Compressor degradation affects the compressor pressure ratio, efficiency and flow capacity. An engine with reduced compressor flow capacity or increased clearances will exhibit power degradation. An engine with a degraded turbine nozzle due to erosion or corrosion experiences a turbine pressure ratio and efficiency drop, leading to a reduction in engine speed.

Performance degradation mechanisms associated with compressors reduce flow capacity and efficiency whereas those associated with the turbines largely increase flow capacity and reduce efficiency. Degradation increases turbine flow capacity, loss of turbine efficiency and life reduction of hot section components which in turn results in expensive maintenance.

## **2.12 Case Studies of Associated Gas Usage**

In the past, flaring the world over was used to routinely dispose of flammable gases that were either unusable or uneconomical to recover. However, modern technology has introduced ways and means of harnessing AG for very productive uses. Countries such as Saudi Arabia have drastically reduced its gas flaring, from 38 BCM in 1980 to less than 1 BCM of gas per year, in recent times (Abdulkareem and Odigure, 2010). Other countries that have successfully harnessed AG are highlighted hereunder.

### **2.12.1 Case Study on Qatar**

In Qatar, NG which was once produced from wells or oil degassing stations and flared had to be processed and used or exported. Qatar therefore makes a good test case to refer to, as reported by Ferdrin (Ferdrin, 1985).

Towards the end of the 1950s, the Qatar government started exploring the possibility of supplying AG to consumers in Doha and by 1962, the first trans-peninsular gas pipeline was completed. It supplied high pressure separator gas from Khatiyah degassing station to Doha. By 1963, the Ras Abu Aboud Power

and Desalination facilities were commissioned, plants which used gas/crude oil to fire their turbines.

Between 1965 and 1970, the realisation to exploit AG as a clean burning energy source to fuel industries came to the fore. Gas was supplied from Jaleha to a cement plant near Dukhan, and a gas based fertilizer plant was set up at Umm Said.

From 1970-1980, gas supply and utilization saw the recovery and export of liquefiable gas products C<sub>3</sub>, C<sub>4</sub>, and C<sub>5+</sub> condensate. Also the use of lighter gas components to produce fertilizer, petrochemicals and steel began. The provision of gas supply, to power and water desalination plants commenced as well. Before long, onshore AG was transported to Umm Said and Doha from separation centres in the North to areas in the South.

Recovery of Natural Gas Liquids (NGLs) from onshore AG also began when an NGL plant was commissioned in 1974. A new pipeline was laid connecting each degassing station to deliver gas to an NGL liquefaction plant. Propane, Butane and natural gasoline were separated and exported.

Gas was separated from crude oil at three offshore production platforms, compressed, dehydrated and fed onshore. The gas liquids formed at the compression platform were also gathered and pumped onshore. The stripped methane-rich gas produced was set aside for industrial consumers while the LPG and C<sub>5+</sub> condensate were exported.

A fertilizer plant utilizing offshore stripped AG was commissioned; a petrochemical plant meant to produce Ethylene from Ethane rich gas commenced production; and a steel plant was also set up at Umm Said to meet the growing energy demand.

As at 1980, the basic infrastructure for gas production and utilisation had been established in Qatar. After the methane rich gas stripping stage, the raw NGL is stabilised in a second stage. AG received at the stripping plant from the onshore field gas gathering stations is compressed prior to entering the chilling train for stripping of methane rich gas and condensing the NGL products.



### **2.12.2 Case Study on Abu Dhabi**

Achievements made by Zakum Development Company (ZADCO) towards meeting the zero flaring strategic objective of Abu Dhabi National Oil Company (ADNOC) were outlined by Misellati and Ghassnawi (Misellati and Amari, 2006).

Initially, sour gas recovery project at ZADCO flared a predominantly acid gas stream considered to be harmful to the environment and human health. A sour gas recovery project was instituted, which involved the design of a compression system that prevented reduced oil production at facilities and removed the need for flaring through export of the sour gas to a sulphur recovery unit. The compression system was designed to have two operating scenarios: a low pressure compression and a high pressure operating mode.

ZADCO operated in such a way that oil production from offshore fields were sent to Zirku through a subsea pipeline for stabilization. Large amounts of gases were flared in the 1970s but recent policies adopted by the Company were to target zero flaring. An amine unit was therefore used to treat the low pressure gas, such that some amounts of sweet gases were recovered.

In the early 1990s, regulations were introduced to reduce environmental pollution and to recover the gas flared. A study to identify the most feasible techno-economic method of achieving this objective was launched and a recovery compressor was installed, which greatly improved the flaring situation.

The installation of an acid gas recovery compressor to recover the 2MSCFD of gas was made. In addition, a stand-by export compressor was also used for continued production during shutdown of the main export compressor.

ADNOC announced its first real “zero flaring” system in operation, with a 90% reduction of the field’s total daily flaring from about 2.8MSCFD to 0.3MSCFD (Wasfi, 2004). According to the report, using a pilot plant for zero flaring facilities, ADNOC achieved a total recovery of hydrocarbon vapours and eliminated flaring completely under normal operating conditions.

The zero flaring system requirements in terms of equipment are:

- A vapour recovery compressor
- High integrity quick opening valve with zero leakage
- High integrity ignition system
- N<sub>2</sub> purge gas facility for continuous supply
- New flare tip to suit the new operating conditions
- Control and monitoring system.

The system was designed to operate normally in zero flaring mode. If upsets occurred, then it would automatically go on minimized flaring mode. The flare stack was continuously purged with nitrogen downstream of the quick operating valve to avoid air ingress during normal operation. High H<sub>2</sub>S content makes it mandatory to ensure the system design integrity and safety of personnel by minimizing or eliminating the risk of potential cold gas venting to the atmosphere.

### **2.12.3 Case Study on Iran**

(Mokhatab et al., 2010) posit that a Flare Gas Recovery System (FGRS) reduces flaring noise, thermal radiation, operating and maintenance costs, air pollution and emissions. They discussed the installation of an FGRS at the Khangiran Gas Refinery in Iran and how the system was used in reducing, recovery and reuse of flare gases.

In time past, large amounts of gases were flared in the Khangiran Gas Refinery to the tune of 21000m<sup>3</sup>/hr, thus the operating conditions were investigated particularly in the units that produced flare gases. Data collected were analysed and it was found that the methyl diethanolamin (MDEA) flash drum, MDEA regenerator column and MDEA regenerator reflux drum, residue gas filter and inlet separator into the Gas Treatment Unit (GTU) were most critical in harnessing flare gas.

The FGRS, located downstream of the knockout drum where flare gases from various units in the refinery converge, was able to handle varying gas loads and compositions. It consists of compressors that take suction from the flare gas header upstream of the liquid seal drum, compress the gas and cool it for reuse

in the refinery fuel gas system. Factors that needed to be taken into consideration while compressing the flare gas were:

- The amount of gas which is not constant
- The composition of the gas which varies
- The gas which contains components that condense during compression
- The gas which contains corrosive components

The compressed gas is passed on to the amine treatment system for H<sub>2</sub>S removal, while condensing some hydrocarbon vapour for discharge into the separator.

This hitherto waste gas put into use as fuel was found to have greatly reduced the plant's emissions such as NO<sub>x</sub>, SO<sub>x</sub>, H<sub>2</sub>S, CO, CO<sub>2</sub> and other hazardous air pollutants. By installing an FGRS at the Khangiran gas refinery, gas emissions were reportedly reduced by 90%. Figure 2-5 shows a typical FGRS.

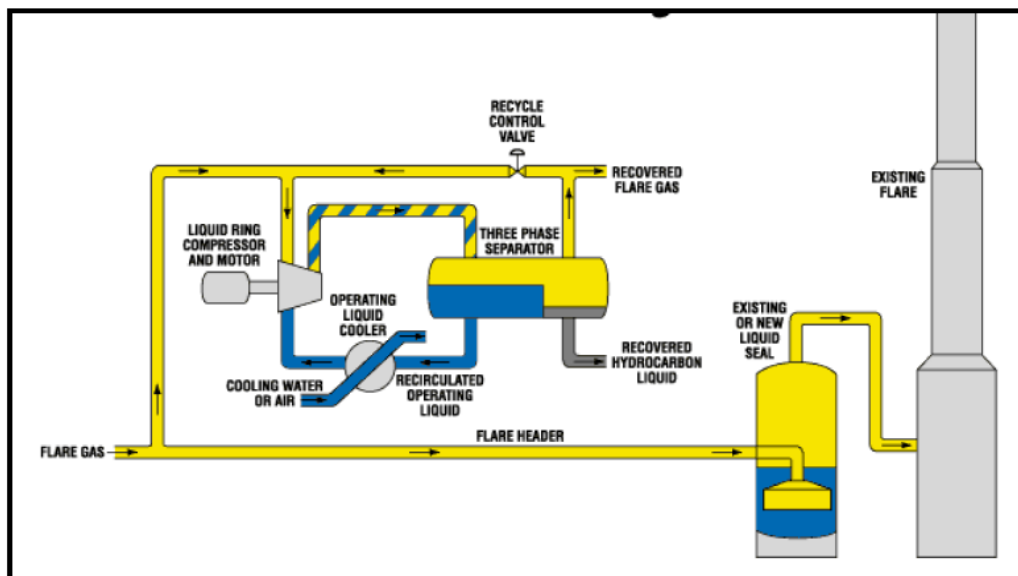


Figure 2-5: A Typical Flare Gas Recovery Unit (John Zink, 1993)

While investigating the thermal radiation from the flame at Khangiran Gas Refinery, the radiation fluxes that vary with distance from the flame were measured. It was

discovered that installing an FGRS not only reduced gas flaring but also decreased the harmful impacts of flaring due to thermal radiation.

## **2.13 Lessons Learnt from Case Studies**

### **Onshore AG can be treated**

- Separated at degassing stations
- Gas is collected from separators
- Compressed at compressor stations
- Flows to stripping plant

### **Offshore AG can be separated**

- Separated from crude oil at the offshore production platforms
- From oil production, AG is produced lean (methane-rich) after condensation and the removal of NGL is effected at the stripping plant

### **Flare Gas Recovery System is required**

FGRS is required, having been successfully applied in the past.

## **2.14 Significance of the Research**

In all the aforementioned case studies, nothing was said about the degradation that the gas turbine was subjected to as a result of AG combustion, neither was the life consumption of the hot gas components quantified, nor the inevitable decline in fuel taken into consideration, nor the economic implications spelt out in terms of investments and revenue.

This research underscores reducing energy wastage by harnessing AG currently being flared in several places around the world; it explores cost effective power generation vis-à-vis degraded performance of a fleet of engines under various conditions, and employs discounting techniques to assess the economic gain of the proposed investment. The work delves into the possibility of divesting engines that become redundant as a result of resource decline, as a way of improving the return on investment.

## **CHAPTER 3: SOFTWARES & DATA ANALYSIS**

### **3.1 Introduction**

This section introduces the softwares and codes that were employed in the studies. It details aspects of the GGFR code developed by a team of specialists/experts at the World Bank that was useful and relevant to this study. The *GasTurb* software was also described and its use to model the three compositions of AG: LANatGas, MANatGas and RANatGas. *TurboMatch* which is a Cranfield-developed GT simulation software was used to simulate the performance of the fleet of study engines (SS94, SS9E, LM1H, LM6K and DS25) and the results were used in creep life estimation and the economic analysis; and *Hephaestus* was employed to predict the CO<sub>2</sub> emission. Palisade's @RISK, the risk analysis tool employed in the research was also briefly described. The entire analysis was tied up and coordinated by the TERA framework which brings in MATLAB's Genetic Algorithm as the optimizer.

### **3.2 Global Gas Flare Reduction Code**

The Global Gas Flare Reduction (GGFR) partnership launched at the World Summit on Sustainable Development in August 2002 is a World Bank-led initiative that aims to support and facilitate efforts to use currently flared gas by promoting regulatory frameworks and tackling the constraints on gas utilization.

The GGFR partnership supports national governments and petroleum industries in their efforts to reduce flaring and venting of AG. The World Bank-led Global Gas Flare Reduction initiative is a public-private partnership that includes countries, companies and multilateral organizations aimed at utilizing AG. See Table 3-1 for the GGFR partners while Figure 3-1 shows the partners on a world map.

**Table 3-1: Global Gas Flare Reduction Initiative Partners**

Countries	Oil Companies	Organizations
Algeria	BP (UK)	European Bank for Reconstruction and Development,  European Union,  Wartsila,  World Bank
Angola	Chevron (US)	
Azerbaijan	ConocoPhillips (US)	
Cameroon	Eni (Italy)	
France	ExxonMobil (US)	
Gabon	Kuwait Oil Co	
Indonesia	Marathon Oil (US)	
Iraq	Maersk Oil&Gas (Denmark)	
Kazakhstan	NNPC (Nigeria)	
Khanty-Mansiysk (Russian Fed)	Pemex (Mexico)	
Kuwait	PetroEcuador	
Mexico	Pertamina (Indonesia)	
Nigeria	Shell (UK, Netherlands)	
Norway	Sonatrach (Algeria)	
Republic of Congo	Sonangol (Angola)	
Qatar	SOCAR (Azerbaijan)	
USA	SNH (Cameroon)	
Uzbekistan	Statoil (Norway)	
	Total (France)	
	Qatar Petroleum	

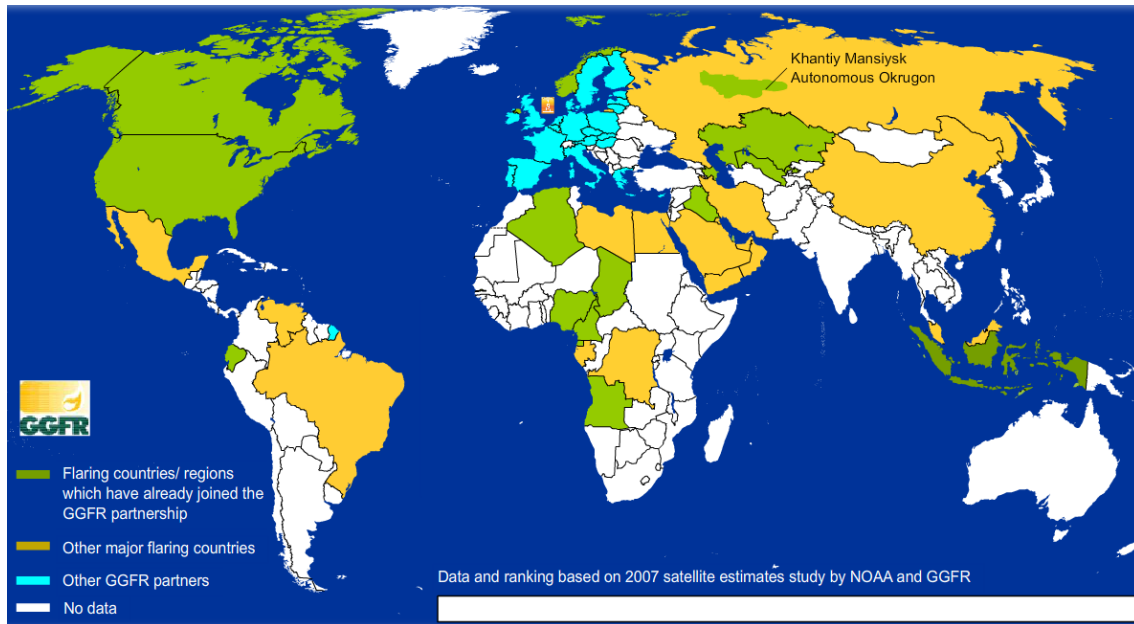


**Figure 3-1: Gas Flaring Countries & GGFR Partners**

The GGFR research team developed a financial model capable of evaluating costs and benefits of using AG for power production, industrial gas use and LPG production.

To use the tool for evaluation of a specific project, data on a number of subjects need to be inserted by the user. Data inputs include unit investment costs, operation and maintenance costs, CO<sub>2</sub> emission costs, discount rates, amounts and quality of AG, demand for energy, cost of electricity. Other inputs include daily flow of AG, equivalent required power at the oil field, required power for compression of the gas at the well head, cost of fuel, gas demand by power plant, maximum grid absorption capacity, and distance to plant. The tool's predictions include cost of gas compression, cost of gas based power generating plant, cost of power transmission, operating cost, maintenance cost, cost of fuel, CO<sub>2</sub> emission tax, construction and installation cost as well as contingency fund.

The GGFR is developing concepts on how local communities close to flaring sites can use NG that is being wasted through flaring. The GGFR partners have endorsed a global standard for significant gas flare reduction by finding commercial uses for the AG through increased collaboration between countries.

The Excel based code was employed in Chapter 5 which deals with resource decline and gas flaring.

### **3.3 GasTurb Simulation Software**

Developed by Dr Joachim Kurze, Gasturb is a GT performance program which uses pre-defined engine configurations to evaluate the thermodynamic cycle of the most common GT architectures, both for design and off-design performance. Three levels of simulation details are offered by the software, as explained hereunder.

#### **3.3.1 Basic Level**

Basic gas turbine cycle analysis in which the input data is limited to properties such as pressure ratios, burner inlet temperature and component efficiencies. Sophisticated details are set to default values and are hidden.

#### **3.3.2 Performance Level**

This level adds the details required for professional GT performance simulations. More data input options such as simulation of internal air systems and turbine cooling are included. The performance level was employed for this research work, details of which are presented in Chapter 6.

#### **3.3.3 More**

This level is adopted when the aim is to go a bit more than the professional. The flow area at all the thermodynamic stations will be calculated during the cycle design, from which the static quantities are determined, during design and off-design simulations.

An overwhelming attribute of the GasTurb 11, is the incorporation of the tool GasTurb Details 5.1 which has the capability to model new fuels for the software. GasTurb Details 5.1 was used to model the different compositions of AG gotten from the field study. The steps taken to create the new fuels (LANatGas, MANatGas and RANatGas) are explained in Section 3.6



### 3.4 The TERA Framework

Techno-economic Environmental and Risk Analysis (TERA) which is a framework developed in Cranfield University provides a pattern of assessing turbo-machinery based on specific technical, economic, environmental and risk factors.

TERA can be used to make a useful contribution to complex decisions and increase confidence that research investments and power plants selection are made in a systematic and consistent manner. It is an adaptable decision support tool for preliminary analysis which can assess mechanical systems and guide design decision, by identifying the best design configuration and provide optimum values of relevant parameters.

TERA for power generation consists of four modules: performance, emissions, lifing and economic modules. The core module is the performance, which simulates the design point and off-design operations of the GT. It provides the performance parameters of the thermodynamic cycles under investigation in off-design conditions. On the whole, the TERA framework shown in Figure 3-2, is a philosophy meant to achieve the required generation with minimum cost and least degradation to the environment.

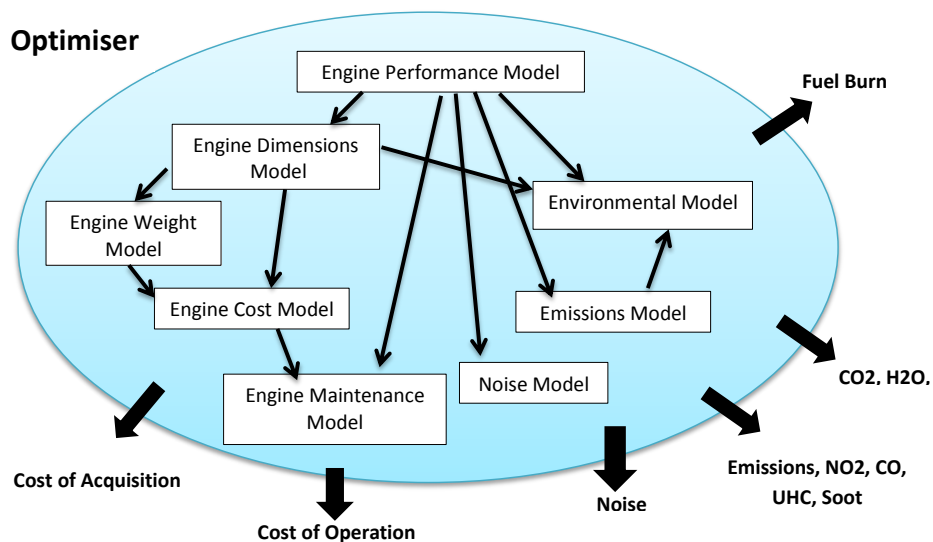
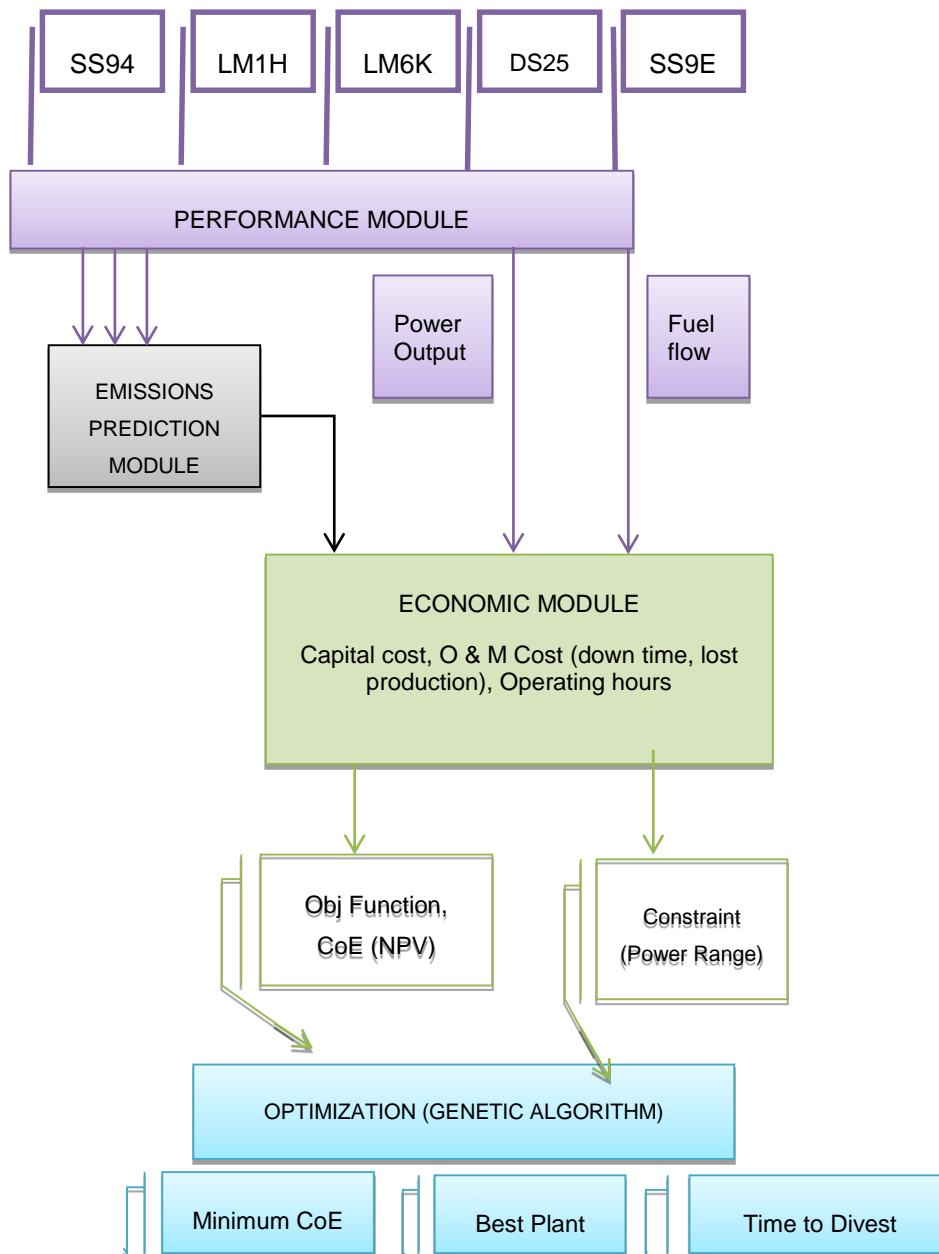


Figure 3-2: Schematic of the TERA Framework

Data from the GT performance module is extracted and fed into the economic module; the fuel consumption is used to calculate annual fuel cost, capital, operation and maintenance cost, emissions predicted with Hephaestus for CO<sub>2</sub>, are inputs for the economic module. The framework ends with the optimization. Outputs from the economic model are NPV and CoE. The TERA framework was built and integrated using MATLAB as shown in Figure 3-3. Details of the performance, economics, emissions and risk analysis are presented in Chapters 5 and 6.



**Figure 3-3: TERA of AG Utilization**

### 3.5 Field Data Analysis

The essence of this section is to correlate the actual situation in the Niger Delta to the research, necessitating an analysis of data obtained from the field. Data on AG usage was collected from three places in Nigeria, namely Directorate of

Petroleum Resources (DPR); data on power generation was gathered from the Power Holding Company of Nigeria (PHCN); and data on AG composition came from the Nigeria Liquefied Natural Gas (NLNG).

### 3.5.1 Data Collected from DPR

Data items collected from DPR, spanning from 1999 to 2008, are:

- Gas quantity in BSCM produced from oil exploitation activities
- Gas quantity utilized
- Gas quantity flared

Details are in Table 3-2, and the analyses are presented in Figures 3-4 to 3-6.

**Table 3-2 Natural Gas Produced, Utilized and Flared 1999-2008**

Year	Production (BSCM)	Gas Used (BSCM)	% Used	Gas Flared (BSCM)	% Flared
1999	39.05	14.57	37.32	24.48	62.68
2000	48.73	22.39	45.96	26.33	54.04
2001	55.04	27.27	49.54	22.26	50.50
2002	49.59	26.21	52.85	23.38	47.15
2003	53.90	31.20	57.89	22.70	42.11
2004	59.75	35.64	59.64	24.12	40.36
2005	60.47	37.66	62.28	22.81	37.72
2006	64.84	41.61	64.17	23.23	35.83
2007	73.82	53.41	72.35	23.12	31.33
2008	72.27	53.42	73.91	18.85	26.09

Gas usage above refers to its use as fuel, re-injection for Enhanced Oil Recovery (EOR), for domestic sales, processing of Natural Gas Liquid (NGL), Liquid Petroleum Gas (LPG) or Liquefied Natural Gas (LNG).

AG produced over the period by the 3 big multi-national oil companies are shown by the trend in Figure 3-4. Details are at Appendix A.

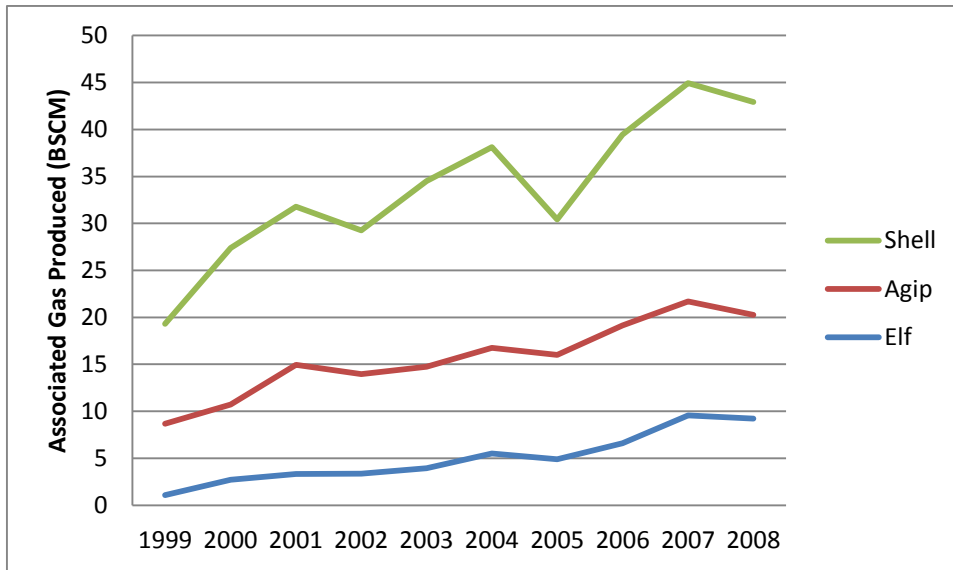


**Figure 3-4: Associated Gas Produced in Nigeria**

Almost the same pattern is adopted by these companies in the utilization of AG, as depicted in Figure 3-5.

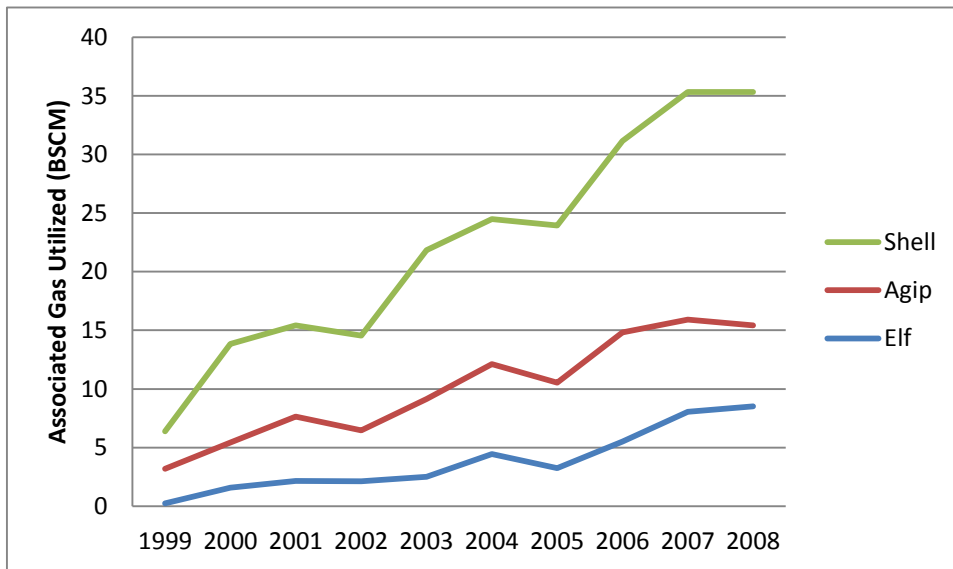


**Figure 3-5: Associated Gas Utilized in Nigeria**

The flare volumes per company are reportedly decreasing as shown in Figure 3-6.

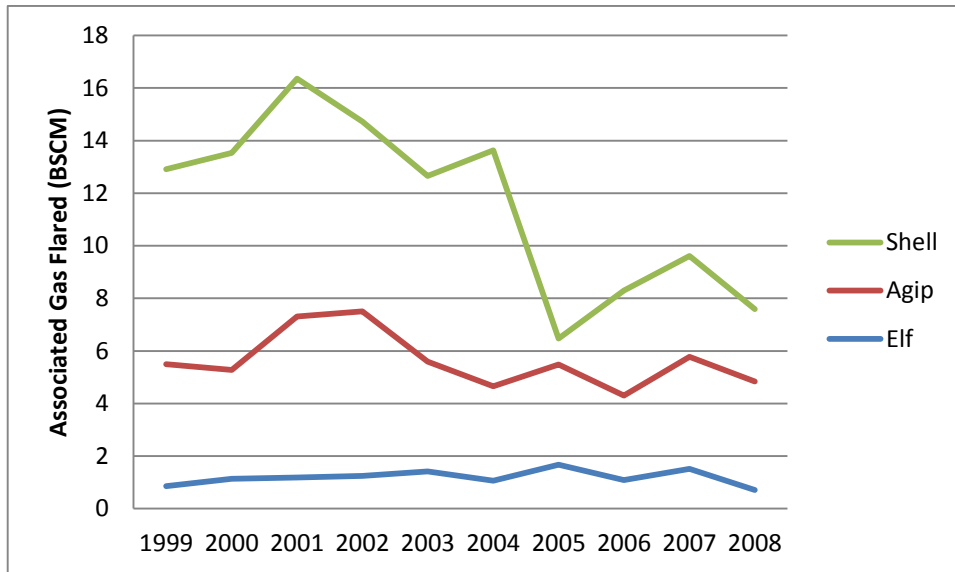


**Figure 3-6: Associated Gas Flared in Nigeria**

Though the aforementioned values were collected from the DPR, the authenticity of the figures cannot be wholly ascertained as they negate the situation on the ground. Consequently, a factor of safety will be built in and a risk analysis carried out with a view to modelling uncertainties associated with the data collected.

### 3.5.2 Data Collected from PHCN

Data items collected from PHCN, for 2012 are:

- Capacity of selected electricity generating power stations of the study country
- Electricity generation modes in the study country
- Data on generation capability as against actual generation of specific power plants

The peak energy demand forecast for Nigeria is 10200 MW, but the current generation capability is 5157 MW. The highest generation recorded as at April 2012 stood at 3462 MW while the lowest generation recorded was 2444 MW (PHCN, 2012).

The national peak electricity generation was computed considering hydro, steam and gas stations across the entire country. The dominant mode of power

generation in Nigeria is gas, as shown in Table 3-3 and illustrated in the bar chart at Figure 3-7.

**Table 3-3: National Electricity Generation (PHCN, 2012)**

Power Station	Mode	Generation (MW)
Kainji	Hydro	206
Jebba	Hydro	177
Shiroro	Hydro	255
Egbin	Steam	877
A.E.S.	Gas	243.2
Sapele	Steam	76
Sapele NIPP	Gas	112.6
Okpai	Gas	346
Afam Iv-V	Gas	61
Afam VI	Gas	532
Delta	Gas	140
Geregu	Gas	199
Omoku	Gas	46.6
Omosho	Gas	50.8
Olorunsogo Phase 1	Gas	40.9
Olorunsogo Phase 2	Gas	98.5
Total		3461.6

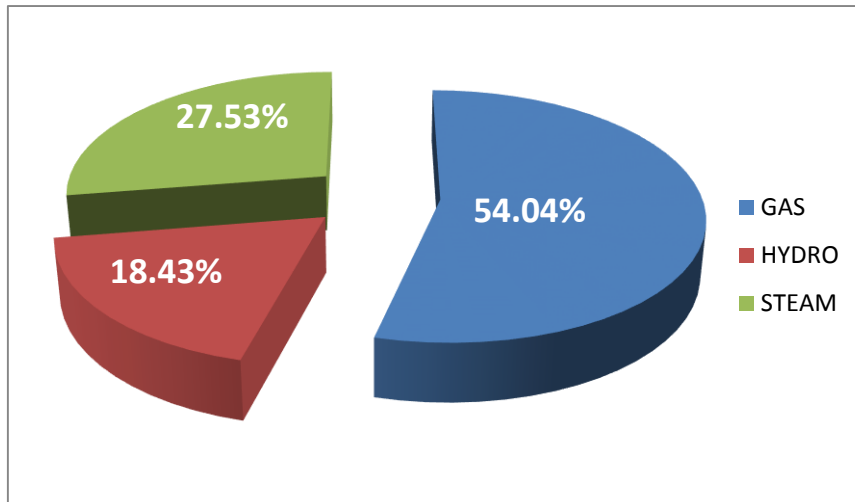


**Figure 3-7: Electricity Generation Modes (PHCN, 2012)**

For the purpose of this work, emphasis will be on generation from gas stations. Table 3-4 below summarizes the unutilized electricity generation capability of existing gas stations as a result of gas shortages. Figure 3-8 graphically depicts the actual generation capability as against the unutilized generation, at the level of individual stations and a combined case.

**Table 3-4: Unutilized Generation Capability Due to Gas Shortage**

Power Station	Actual Generation Capability (MW)	Unutilized Generation Capability (MW)
Sapele NIPP	240	126.3
Olorunsogo I	192	150.9
Olorunsogo II	480	389.1
Geregu	277	0
Trans Amadi	20	20
Total		686.3



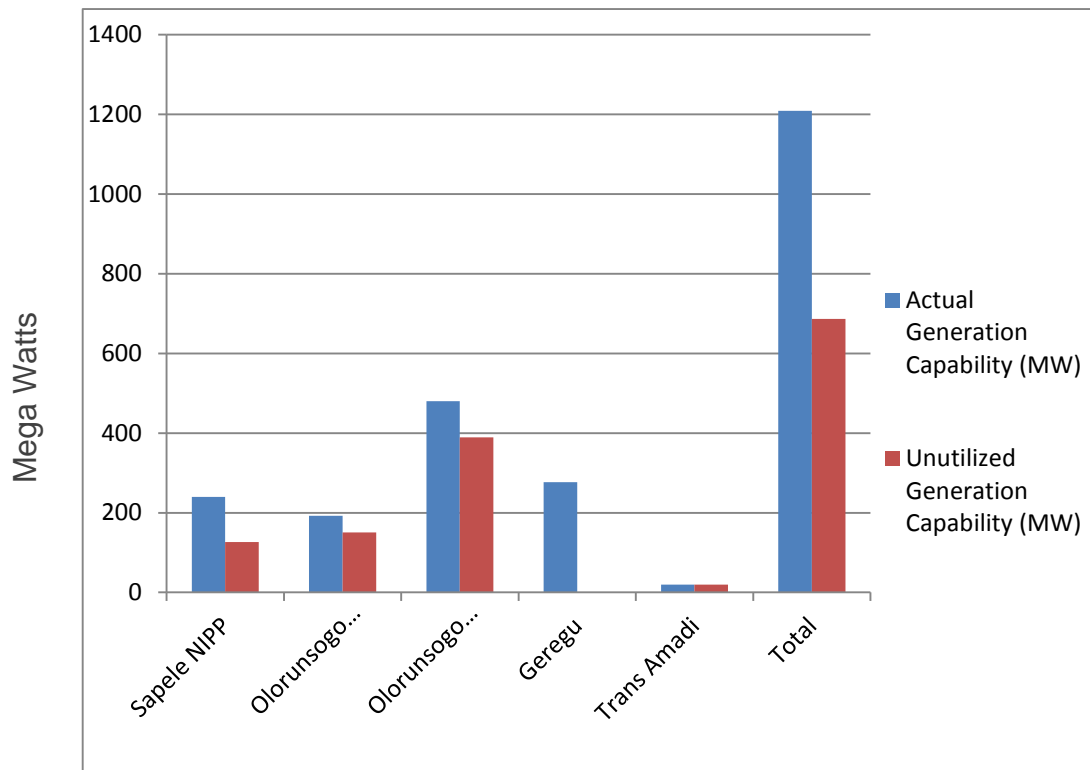


**Figure 3-8: Generation versus Unutilized Capability**

The histogram shows that though the generation capability is much more than the actual generation; unutilized generation capability is almost equal to the actual generation. This underscores the need for efforts to harness AG so as to achieve the full generation capability.

### 3.5.3 Data Collected from the NLNG

Data items collected from NLNG cover the compositions of three compositions of AG, designated as:

- Lean Associated Natural Gas (LANatGas)
- Medium Associated Natural Gas (MANatGas)
- Rich Associated Natural Gas (RANatGas)

The NLNG is currently processing, shipping and marketing Nigeria's gas resources and aims to stop flaring AG, with a view to diversifying the economy and minimising the environmental impact. For the NLNG Plant at Bonny, AG is collected from onshore concession areas in the Niger Delta and from offshore pipelines and transported to the plant. The gas is supplied by three production ventures, NNPC/Agip, NNPC/Elf and NNPC/ Shell, at three transfer points from dedicated gas fields in Rivers State namely Obiafu, Obite and Soku respectively as shown in Figure 3-9.

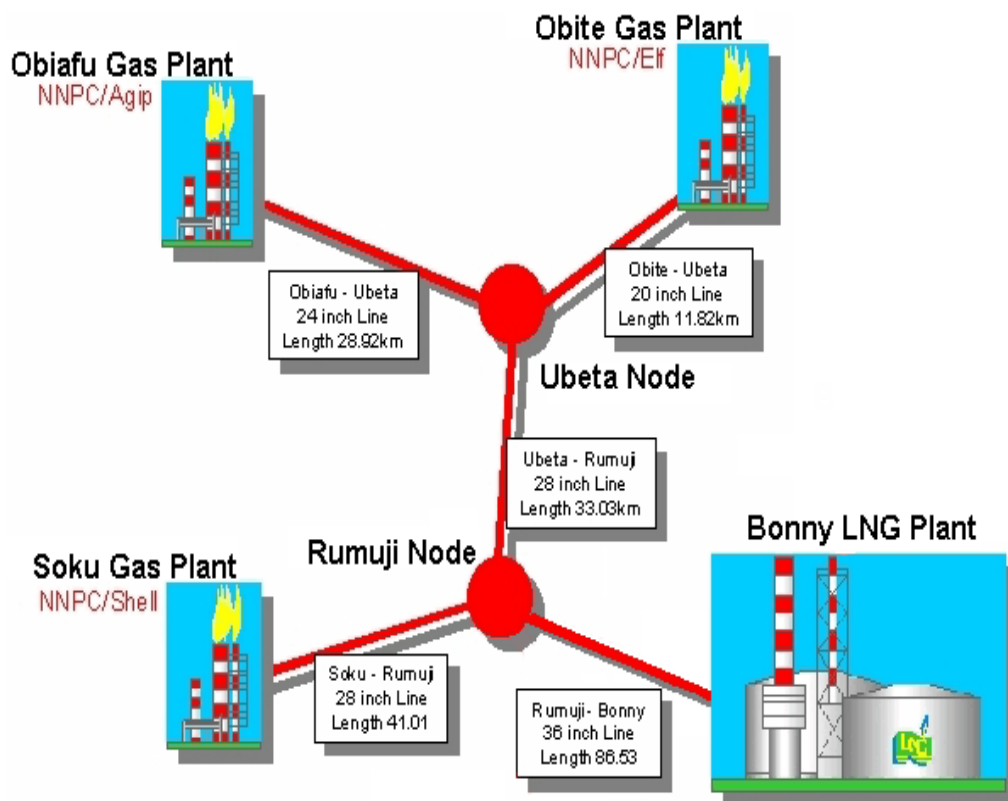


**Figure 3-9: Supply of Associated Gas to the NLNG**

The compositions for the trunk line fluid can be identified as Lean Associated Natural Gas (LANatGas), Medium Associated Natural Gas (MANatGas) and Rich Associated Natural Gas (RANatGas), each of which represents different degree of gas quality. The different compositions of AG collected during the tour to the Niger Delta are as shown in Table 3-5.

**Table 3-5: AG Compositions from Three Locations**

Constituents	LANatGas	MANatGas	RANatGas
Methane, CH <sub>4</sub>	0.88748	0.84734	0.82483
Ethane, C <sub>2</sub> H <sub>6</sub>	0.04402	0.06300	0.07026
Propane, C <sub>3</sub> H <sub>8</sub>	0.02572	0.04185	0.04819
iso-Butane, C <sub>4</sub> H <sub>10</sub>	0.00553	0.01158	0.01332
n-Butane, C <sub>4</sub> H <sub>10</sub>	0.00843	0.01161	0.01332
iso-Pentane, C <sub>5</sub> H <sub>12</sub>	0.00265	0.00335	0.00405
n-Pentane, C <sub>5</sub> H <sub>12</sub>	0.00195	0.00336	0.00405
Hexane, C <sub>6</sub> H <sub>14</sub>	0.00174	0.00182	0.00224
Heptane+, C <sub>7</sub> H <sub>16</sub>	0.00178	0.00198	0.00233
Carbondioxide, CO <sub>2</sub>	0.01957	0.01297	0.01579
Nitrogen, N <sub>2</sub>	0.00113	0.00114	0.00163
Total	1	1	1

### 3.6 Creation of New Fuels on GasTurb 5.1

In order to model the three compositions of AG on GasTurb Details 5.1, two input data sets were created for the program FCEA2.exe, that is, temperature rise due to combustion and the gas properties of air and combustion gases. After running these two input data sets on FCEA2.exe, GasTurb Details 5.1 reads the two output files with extension *.plt* and combined them into a single file with extension *.prp*. The new names were then added to the Fuels.gtb file. Details of the steps used for creating the new fuel are as follows:

### **3.6.1 Fuel Composition Input**

The fuel composition was worked out by selecting the reactants from the file thermo.inp offered by the NASA website. The fuel composition was defined by entering mole fractions, the sum of which equal 1.

### **3.6.2 Specifying a Path to CEA and GasTurb**

GasTurb Details 5.1 needed to know the path to the directory where FCEA2.exe resides so as to store the input files for FCEA2.exe and to read the output created by the code. Also, the final new gas property data sets created in the last step was stored in the directory specified for GasTurb.

### **3.6.3 Creating the CEA Temperature Rise Input**

After defining the fuel composition, the first input file for the FCEA2.exe program *LANatGas\_DT.inp* was created in the directory specified as path to FCEA2.exe. This input created results with the equilibrium burner exit temperature as a function of inlet air temperature, injected fuel-air-ratio and pressure.

### **3.6.4 First Run of CEA**

From where the FCEA2.exe resides, the first run of the CEA was executed. Into the DOS box which opened, *LANatGas\_DT* was entered to start the FCEA2.exe program. The two files *LANatGas\_DT.out* and *LANatGas\_DT.plt* were thus created and stored where the FCEA2.exe resides.

### **3.6.5 Creating the CEA Gas Property Input**

After creating the chemical equilibrium temperature information, the second input file for the FCEA2.exe program was then prepared. GasTurb Details 5.1 read the temperature rise output file from the FCEA2 program and set the fuel-air-ratio in the gas property input file to a suitable number, lower than the stoichiometric value. By the click of a button, the gas property input file *LANatGas\_GP.inp* was created and stored in the directory specified as path to CEA.

### 3.6.6 Second Run of CEA

At the directory where FCEA2.exe resides, the program is executed. An input of *LANatGas\_GP* is made in the DOS interface. Two files *LANatGas\_GP.out* and *LANatGas\_GP.plt* were created in the directory.

### 3.6.7 Making the GasTurb Files

After running the two input data sets with FCEA2.exe, GasTurb Details 5.1 read the two files *LANatGas\_DT.plt* and *LANatGas\_GP.plt* and combined them to the single file *LANatGas.prp*, which was added to the file *Fuels.gtb*. This was done by searching the directory where gasturb11.exe resides for the *Fuels.gtb*, which is a pure text file, and the name of the new fuels added. Thereafter, the newly created *.prp* file is copied to the GasTurb11 directory, which then reflects in the list of fuels.

Figure 3-10 is a schematic showing the steps described above for LANatGas, while Figure 3-11 is a screen shot showing the incorporation of all three AG compositions into the software. Further details are at Appendix B.

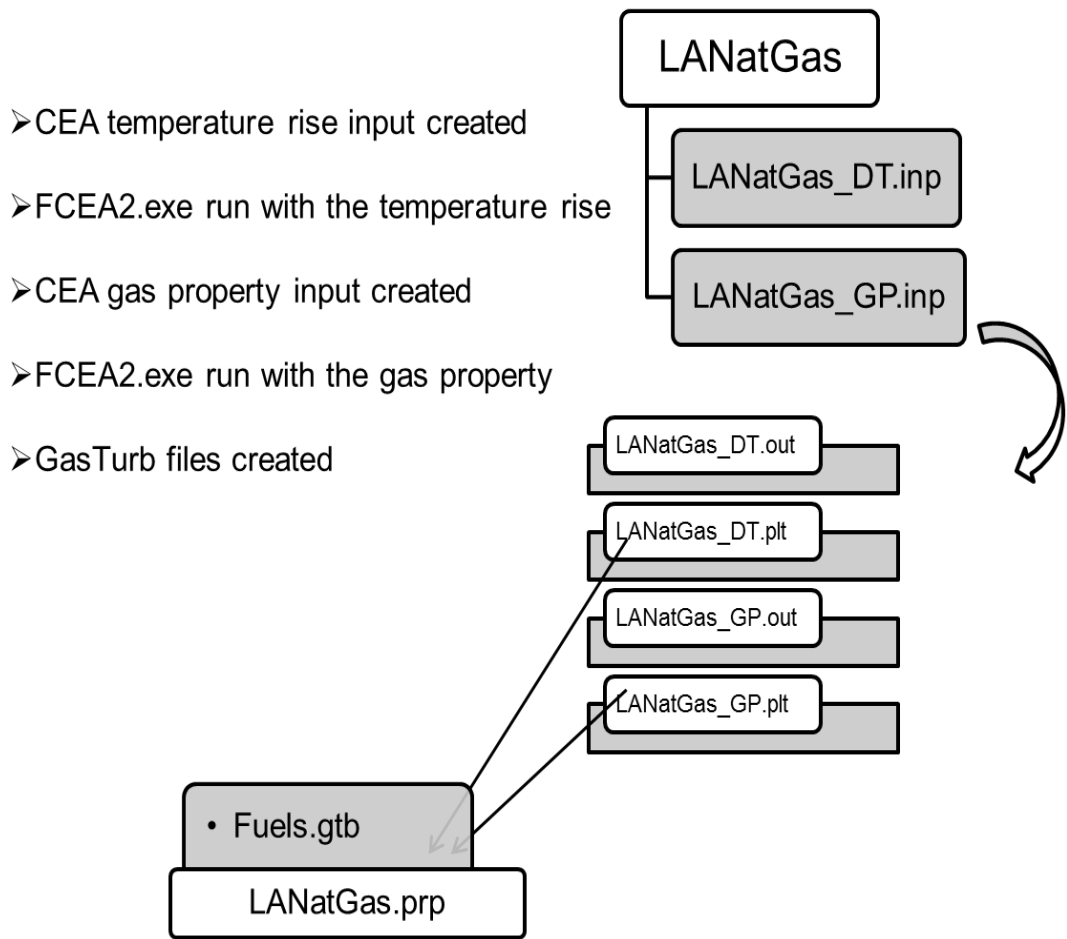


**Figure 3-10: Schematic Showing the Modelling of LANatGas**

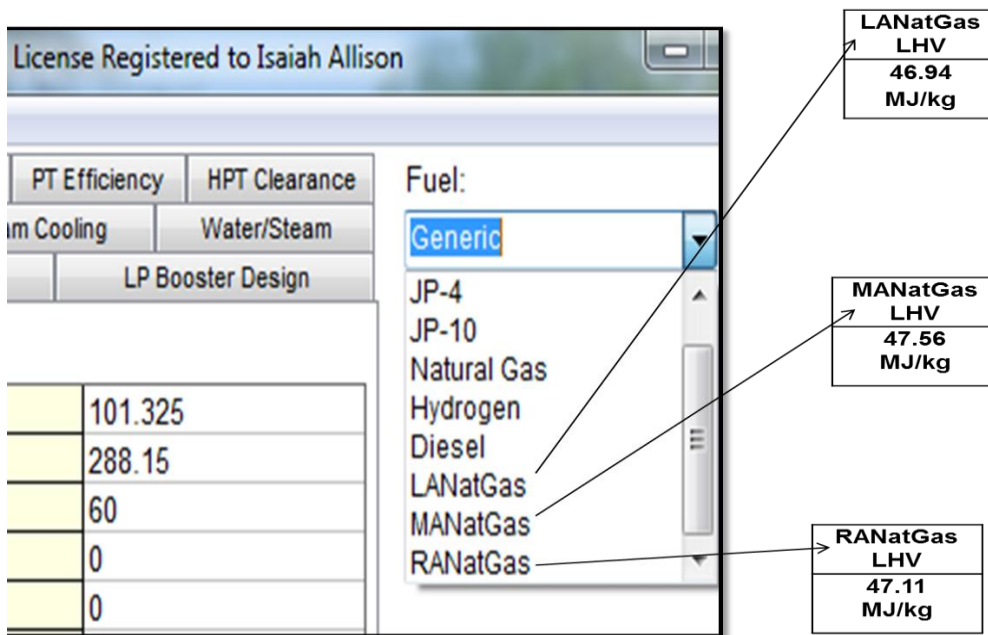


**Figure 3-11: Screen Shot Showing the Incorporation of the AG**

### 3.7 Validation of Modelled Gases Using Aspen HYSIS

Using Aspen HYSIS Version 7.3, the AG streams whose compositions are given in Table 3-5 were modelled. The results for LANatGas, MANatGas and RANatGas are presented at Appendix C. Table 3-6 gives a summary of the FHV from the gas streams modelled; these figures agree closely with the results from GasTurb.

**Table 3-6: Fuel Heating Values of the Different AG From Aspen HYSIS**

Fuel Heating Values	LANatGas	MANatGas	RANatGas
LHV (MJ/kg)	46.94	47.46	47.053

### 3.8 Simulation Results for SS9E and DS25

To ascertain the variation in the performance as a result of the difference in compositions, SS9E and DS25 were modelled using GasTurb 11 for the Design Point, for the varying compositions of LANatGas, MANatGas and RANatGas embedded in the software. The tables below reveal that the differences in power output and efficiency from using the different fuel gases are quite negligible. Details of the results for LANatGas, MANatGas and RANatGas are shown at Appendix D.

**Table 3-7: Results for SS9E Industrial Gas Turbine**

	LANatGas	MANatGas	RANatGas
Power (MW)	120.185	120.003	119.925
Efficiency (%)	32.37	32.36	32.34

**Table 3-8: Results for DS25 Aero-derivative Gas Turbine**

	LANatGas	MANatGas	RANatGas
Power (MW)	25.159	25.107	25.091
Efficiency (%)	35.29	35.26	35.24

Considering the corroboration of the figures, the reliability of the software is confirmed but the reliability of data collected from NLNG is in doubt. The difference between clean NG and the AG LHV is marginal, which casts some doubts on the authenticity of the data on fuel composition in the first place. Consequently, I am compelled to adopt the LHV figure of the GGFR team of experts that proposed 41MJ/Kg as against 47MJ/Kg that was generated.



## CHAPTER 4: PERFORMANCE OF STUDY ENGINES

### 4.1 Introduction to Performance Modelling

GasTurb was used to simulate thermodynamic models of the engines under investigation. The design points were obtained by varying the component efficiencies, bleeds and the Turbine Entry Temperatures (TET) to arrive at values comparable to those in the open domain. Any movement away from design point, due to internal alterations such as component degradation or external alterations such as changes in ambient conditions, give the off-design performance.

A fleet of five study engines were selected; these are the SS94, SS9E, LM1H, LM6K and DS25. They are inspired from the V.94A, Frame 9E, LMS100, LM6000 and LM2500 respectively.

#### 4.1.1 Design Point Performance

##### 4.1.1.1 The SS94 Gas Turbine

The V94.3A, shown at Figure 4-1, is a single shaft, heavy duty industrial gas turbine designed for operating with NG.



Figure 4-1: The V94.3A (Siemens Website)

The V94.3A properties, courtesy Siemens, are as follows:

- Efficiency, 36 %
- Power, 226MW
- Heat Rate 9114KJ/kWh
- Exhaust Gas Temperature, 853K
- Exhaust Flow, 688kg/s
- Pressure Ratio, 17

The fuel flow is calculated thus,

$$\begin{aligned}W_{ff} &= \text{Heat Rate} \cdot \text{Power} / \text{FHV} \\ &= 9114 \cdot 226 / (49 \cdot 3600) \\ &= 11.68 \text{kg/s}\end{aligned}$$

$$\text{Inlet Mass Flow} = 688 - 11.68 = 676.32 \text{kg/s}$$

The aforementioned parameters were used to model the study engine designated SS94, the design point performance results of which are shown in Figure 4-2.

**DESIGN POINT RUN FOR HEAVY DUTY GAS TURBINE - SS94**

Station	kg/s	K	kPa	kg/s	PWSD	=	226445.6 kW
1	675.204	288.15	101.325		PSFC	=	0.2082 kg/(kW*h)
2	675.204	288.15	101.325	676.500	Heat Rate=		10356.0 kJ/(kW*h)
3	675.204	692.15	1722.525	61.675	Therm Eff=		0.3476
31	600.932	692.15	1722.525		WF	=	13.09725 kg/s
4	614.029	1530.00	1670.849	86.640			
41	647.789	1490.91	1670.849	90.191	s NOx	=	0.44897
49	647.789	854.90	106.495		incidence=		0.00000 °
5	681.549	847.33	106.495	1121.944	XM8	=	0.2109
6	681.549	847.33	104.365		A8	=	13.6826 m <sup>2</sup>
8	681.549	847.33	104.365	1144.841	P8/Ps8	=	1.03000
Bleed	6.752	692.15	1722.521		WBld/W2	=	0.01000
Ps0-P2=	0.000	Ps8-Ps0=	0.000		Ps8	=	101.325 kPa
Efficiencies:	isent	polytr	RNI	P/P	W_NGV/W2	=	0.05000
Compressor	0.8600	0.9024	1.000	17.000	WCL/W2	=	0.05000
Burner	0.9990			0.970	Loading	=	100.00 %
Turbine	0.8900	0.8512	2.417	15.690	e45 th	=	0.87158

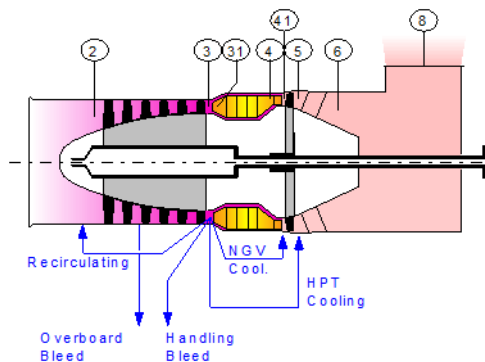


**Figure 4-2: GasTurb Representation of SS94**

#### 4.1.1.2 The SS9E Gas Turbine

The Frame 9E shown at Figure 4-3, is a single shaft IGT designed for high ambient temperature performance.

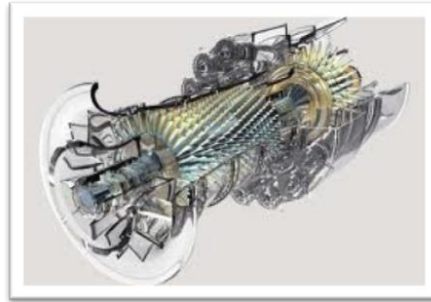


**Figure 4-3: The Frame 9E (GE Website)**

Its properties, courtesy General Electric, are as follows:

- Efficiency, 34%
- Power, 120MW
- Heat Rate 10880KJ/kWh
- Exhaust Temperature, 850.15K
- Exhaust Flow, 358kg/s
- Pressure Ratio, 12.3

The fuel flow is calculated thus,

$$\begin{aligned}W_f &= \text{Heat Rate} \cdot \text{Power} / \text{FHV} \\ &= 10880 \cdot 120 / (49 \cdot 3600) \\ &= 7.4 \text{ kg/s}\end{aligned}$$

$$\text{Inlet Mass Flow} = 358 - 7.4 = 350.6 \text{ kg/s}$$

Using the aforementioned parameters, the SS9E shown in Figure 4-4 was modelled. The design point performance is also displayed therein.

**DESIGN POINT RUN FOR HEAVY DUTY GAS TURBINE - SS9E**

	W	T	P	WRstd		
Station	kg/s	K	kPa	kg/s	PWSD	= 120631.1 kW
1	350.328	288.15	101.325		PSFC	= 0.2146 kg/(kW*h)
2	350.328	288.15	101.325	351.000	Heat Rate=	10673.4 kJ/(kW*h)
3	350.328	626.46	1246.297	42.076	Therm Eff=	0.3373
31	311.792	626.46	1246.297		WF	= 7.19091 kg/s
4	318.982	1520.00	1208.909	62.032		
41	336.499	1478.66	1208.909	64.514	s NOx	= 0.28134
49	336.499	898.66	106.495		incidence=	0.00000 °
5	354.015	886.10	106.495	596.197	XM8	= 0.2112
6	354.015	886.10	104.365		A8	= 7.2715 m <sup>2</sup>
8	354.015	886.10	104.365	608.364	P8/Ps8	= 1.03000
Bleed	3.503	626.45	1246.287		WBld/W2	= 0.01000
Ps0-P2=	0.000	Ps8-Ps0=	0.000		Ps8	= 101.325 kPa
Efficiencies:	isent	polytr	RNI	P/P	W_NGV/W2	= 0.05000
Compressor	0.8700	0.9061	1.000	12.300	WCL/W2	= 0.05000
Burner	0.9990			0.970	Loading	= 100.00 %
Turbine	0.9000	0.8693	1.765	11.352	e45 th	= 0.88340

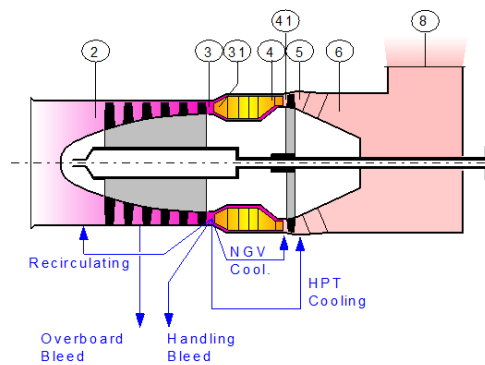


**Figure 4-4: GasTurb Representation of SS9E**

#### 4.1.1.3 The LM1H Gas Turbine

The LMS100, shown at Figure 4-5, is a multiple shaft aero-derivative gas turbine designed for operating with NG.



Figure 4-5: The LMS100 (GE Website)

Its properties are:

- Efficiency, 44%
- Power, 100.2MW
- Heat Rate, 8240KJ/kWh
- Exhaust Temperature, 679.15K
- Exhaust Flow, 222kg/s
- Pressure Ratio, 42

The fuel flow is calculated thus,

$$\begin{aligned}W_{ff} &= \text{Heat Rate} * \text{Power} / \text{FHV} \\ &= 8240 * 100 / (49 * 3600) \\ &= 4.67 \text{kg/s}\end{aligned}$$

$$\text{Inlet Mass Flow} = 222 - 4.67 = 217.33 \text{kg/s}$$

Using these parameters, the LM1H (Figure 4-6) was modelled and the performance results are shown hereunder.

**DESIGN POINT RUN FOR AERODERIVATIVE GAS TURBINE - LM1H**

Station	kg/s	K	kPa	kg/s	PWSD	=	100193.8 kW
1	219.579	288.15	101.325		PSFC	=	0.1646 kg/(kW*h)
2	219.579	288.15	101.325	220.000	Therm Eff=		0.43969
24	219.579	409.49	303.975	87.421	Heat Rate=		8187.7 kJ/(kW*h)
25	219.579	288.15	285.980	77.948	P2/P1	=	1.0000
3	214.089	650.29	4003.716	8.155	P25/P24	=	0.9408
31	203.110	650.29	4003.716		P3/P2	=	39.51
35	189.935	747.11	3923.641	7.913	P35/P3	=	0.98000
4	194.517	1650.00	3766.696	12.654	WF	=	4.58167 kg/s
41	207.692	1599.01	3766.696	13.293	Loading	=	100.00 %
42	207.692	1293.95	1300.731		s NOx	=	0.82796
43	216.475	1270.38	1300.731				
44	216.475	1270.38	1300.731	35.750			
45	217.573	1266.96	1300.731	35.882	P45/P43	=	1.00000
49	217.573	777.02	123.622				
5	224.160	770.95	123.622	303.355			
6	224.160	770.95	121.149		P6/P5	=	0.98000
8	224.160	687.88	111.458	317.819	P7/P6	=	0.92000
Bleed	0.000	650.29	4003.725		WBld/W2	=	0.00000
Ps0-P2=	0.000	Ps8-Ps0=	0.000		Ps8	=	101.325 kPa
Efficiencies:	isent	polytr	RNI	P/P	A8	=	2.22982 m <sup>2</sup>
Booster	0.8700	0.8882	1.000	3.000	driven by PT		
Compressor	0.8700	0.9074	2.822	14.000	TRQ	=	100.0 %
Burner	0.9995			0.960			
HP Turbine	0.8900	0.8774	5.025	2.896			
LP Turbine	0.8900	0.8569	2.266	10.522	eta t-s	=	0.66366

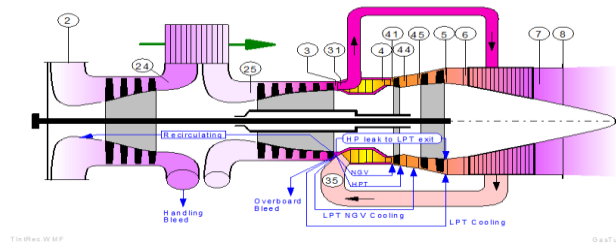


**Figure 4-6: GasTurb Representation of LM1H**

#### 4.1.1.4 The LM6K Gas Turbine

The LM6000, shown at Figure 4-7, is a multiple shaft aero-derivative gas turbine designed for operating with NG.



**Figure 4-7: The LM6000 (GE Website)**

Its properties are:

- Efficiency, 40 %
- Power, 41MW
- Heat Rate 9496KJ/kWh
- Exhaust Gas Temperature, 727K
- Exhaust Flow, 128kg/s
- Pressure Ratio, 31.1

The fuel flow is given by,

$$\begin{aligned}W_{ff} &= \text{Heat Rate} \cdot \text{Power} / \text{FHV} \\ &= 9496 \cdot 41 / (49 \cdot 3600) \\ &= 2.2 \text{kg/s}\end{aligned}$$

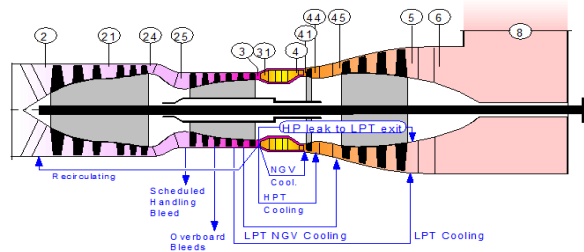
$$\text{Inlet Mass Flow} = 128 - 2 = 125.8 \text{kg/s}$$

Using these parameters, the LM6K (Figure 4-8) was modelled and the design point performance is as presented below.



**DESIGN POINT RUN FOR AERODERIVATIVE GAS TURBINE - LM6K**

	W	T	P	WRstd	PWSD	=	40752.9 kW
amb		288.15	101.325				
1	126.357	288.15	101.325		SFC	=	0.1909 kg/(kW*h)
2	126.357	288.15	101.325	126.600			
21	126.357	319.22	138.815	97.263			
24	126.357	391.32	260.973	57.281	P25/P24	=	0.98000
25	126.357	391.32	255.753	58.450	P3/P2	=	30.29
3	123.830	828.20	3069.039	6.944			
31	109.931	828.20	3069.039		Heat Rate=		9495.5 kJ/(kW*h)
4	112.092	1567.00	2976.968	8.977	WF	=	2.16122 kg/s
41	119.674	1524.38	2976.968	9.448	Loading	=	100.00 %
43	119.674	1138.70	704.052		s NOx	=	1.1389
44	124.728	1127.01	704.052		Therm Eff=		0.37913
45	124.728	1127.01	689.971	36.523	P45/P44	=	0.98000
49	124.728	756.01	106.495		P6/P5	=	0.98000
5	127.255	754.16	106.495	197.466			
6	127.255	754.16	104.365		A8	=	2.43270 m <sup>2</sup>
8	128.519	754.87	104.365	203.579	P8/Pamb	=	1.03000
Bleed	0.000	828.20	3069.027		WBld/W2	=	0.00000
Ps0-P2=	0.000	Ps8-Ps0=	0.000		Ps8	=	101.325 kPa
Efficiencies:	isent	polytr	RNI	P/P			
LP Booster	0.8700	0.8757	1.000	1.370	driven by PT		
HP Booster	0.8700	0.8810	1.213	1.880			
Compressor	0.8700	0.9049	1.753	12.000	WHc1/W2	=	0.04000
Burner	0.9950			0.970	WLc1/W2	=	0.02000
HP Turbine	0.8900	0.8719	4.199	4.228	e444 th	=	0.87168
LP Turbine	0.8900	0.8641	1.375	6.479	eta t-s	=	0.66172



82T801.WMF

GasTurb

**Figure 4-8: GasTurb Representation of LM6K**

#### 4.1.1.5 The DS25 Gas Turbine

The LM2500, shown at Figure 4-9, is a double shaft aero-derivative gas turbine.



**Figure 4-9: Configuration of the DS25 (GE Website)**

Its properties are:

Efficiency, 36 %

Power, 25MW

Heat Rate 9705KJ/kWh

Exhaust Gas Temperature, 839K

Exhaust Flow, 70.5kg/s

Pressure Ratio, 18

The fuel flow is calculated thus,

$$\begin{aligned}W_{ff} &= \text{Heat Rate} \cdot \text{Power} / \text{FHV} \\ &= 9705 \cdot 25 / (49 \cdot 3600) \\ &= 1.38 \text{kg/s}\end{aligned}$$

$$\text{Inlet Mass Flow} = 70.5 - 1.38 = 69.12 \text{kg/s}$$

Using these parameters, the DS25 was modelled and the design point performance calculated with the GasTurb software. See details at Figure 4-10.

**DESIGN POINT RUN FOR AERODERIVATIVE GAS TURBINE - DS25**

Station	kg/s	K	kPa	kg/s	PWSD	=	25102.5 kW
amb		288.15	101.325				
1	68.868	288.15	101.325		PSFC	=	0.1973 kg/(kW*h)
2	68.868	288.15	101.325	69.000	Heat Rate	=	9814.9 kJ/(kW*h)
3	68.179	703.58	1823.850	5.930	V0	=	0.00 m/s
31	64.391	703.58	1823.850		FN res	=	8.41 kN
4	65.767	1525.00	1769.135	8.749	WF	=	1.37602 kg/s
41	65.767	1525.00	1769.135	8.749	s NOx	=	0.48717
43	65.767	1170.98	475.720		Therm Eff	=	0.36679
44	69.211	1149.70	475.720		P45/P44	=	0.97500
45	69.211	1149.70	463.827	30.479			
49	69.211	841.83	106.495		Incidence	=	0.00000 °
5	69.900	839.09	106.495	114.526	P6/P5	=	0.98000
6	69.900	839.09	104.365		PWX	=	0 kW
8	69.900	839.09	104.365	116.863	P8/Pamb	=	1.03000
Bleed	0.344	703.58	1823.856		WBld/W2	=	0.00500
-----							
					A8	=	1.39676 m <sup>2</sup>
Efficiencies:	isent	polytr	RNI	P/P	TRQ	=	100.0 %
Compressor	0.8600	0.9030	1.000	18.000	P2/P1	=	1.00000
Burner	0.9990			0.970	Loading	=	100.00 %
HP Turbine	0.8900	0.8738	2.493	3.719	e444 th	=	0.86948
LP Turbine	0.8900	0.8705	0.903	4.355	WHc1/W2	=	0.05000

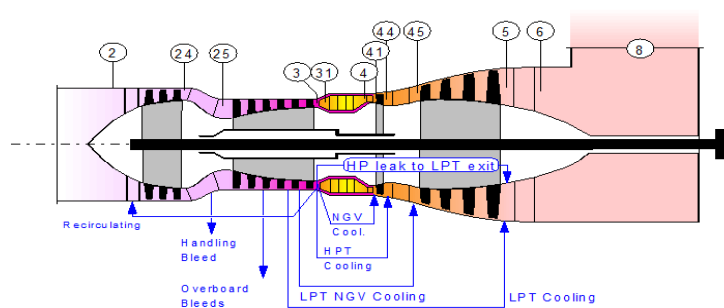


**Figure 4-10: GasTurb Representation of DS25**

## 4.1.2 Off Design Point Performance

### 4.1.2.1 Effects of Ambient Temperature Variations - SS94

Ambient temperature variations were investigated to cover typical values from the Niger Delta as depicted in Figure 4-11.

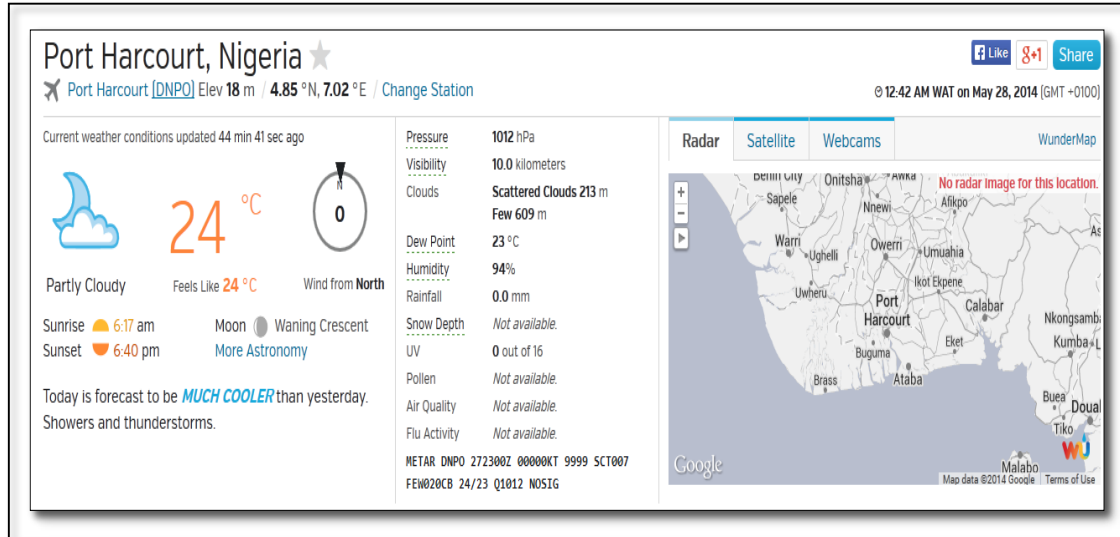


**Figure 4-11: Ambient Temperature Variations in the Niger Delta**

Source: <http://www.wunderground.com/history/airport/> (Assessed 28 May 2014)

Ambient temperature variations were taken from 283.15K, in steps of 5K to 308K. The results are shown in Table 4-1.

**Table 4-1 Performance of SS94 with Ambient Temperature Variations**

T <sub>amb</sub> (K)	283.15	288.15	293.15	298.15	303.15	308.15
Power (kW)	233093	226446	220040	213898	208020	202443
Efficiency	0.3509	0.3476	0.3443	0.3408	0.3372	0.3335
EGT (K)	846	847	848	850	851	852

As air temperature increases, density decreases. Hence for constant volume flow rate, the mass flow rate into the gas turbine decreases with a corresponding effect on performance. That is, a decrease in the density of inlet air means a reduction in mass flow into the turbine; hence more work is required to compress a unit mass of the warm air. In other words, when ambient temperature increases, more work is done per unit mass during compression, but the work done during

expansion remains constant. The useful work therefore decreases. Thermal efficiency falls as useful work falls.

#### 4.1.2.2 Degradation Simulations for SS94

Moderate degradation of gas turbines can be represented by a 3% loss in flow capacity and 1% loss in component efficiency (Razak, 2007) . In this study therefore, moderate degradation by 3% loss in flow, 1% loss in component efficiency were implemented; while variations from these values represent an optimistic or pessimistic scenario. To simulate the effects of degradation that would result from AG usage in gas turbines, typical degradation values of compressor and turbine isentropic efficiency and flow capacities from open literature, were implanted.

The SS94 is a heavy duty single shaft engine which has a single turbine and a compressor. The degraded compressor and turbine inputs are as presented in Tables 4-2 and Table 4-3 respectively.

**Table 4-2: Compressor Inputs for SS94 Degraded Performance**

Flow capacity	Isentropic Efficiency	Remarks
-2	-0.7	1st Degradation
-3	-1	2nd Degradation
-4	-2	3rd Degradation

**Table 4-3: Turbine Inputs for SS94 Degraded Performance**

Flow capacity	Isentropic Efficiency	Remarks
2	-0.5	1st Degradation
3	-1	2nd Degradation
4	-2	3rd Degradation

Using GasTurb, degradation was implemented by adjusting the modifiers for compressor and turbine flow and isentropic efficiency respectively, while fixing the TET. Figures 4-12 to 4-14 show the engine performance plots of power output, thermal efficiency and fuel flow against TET.

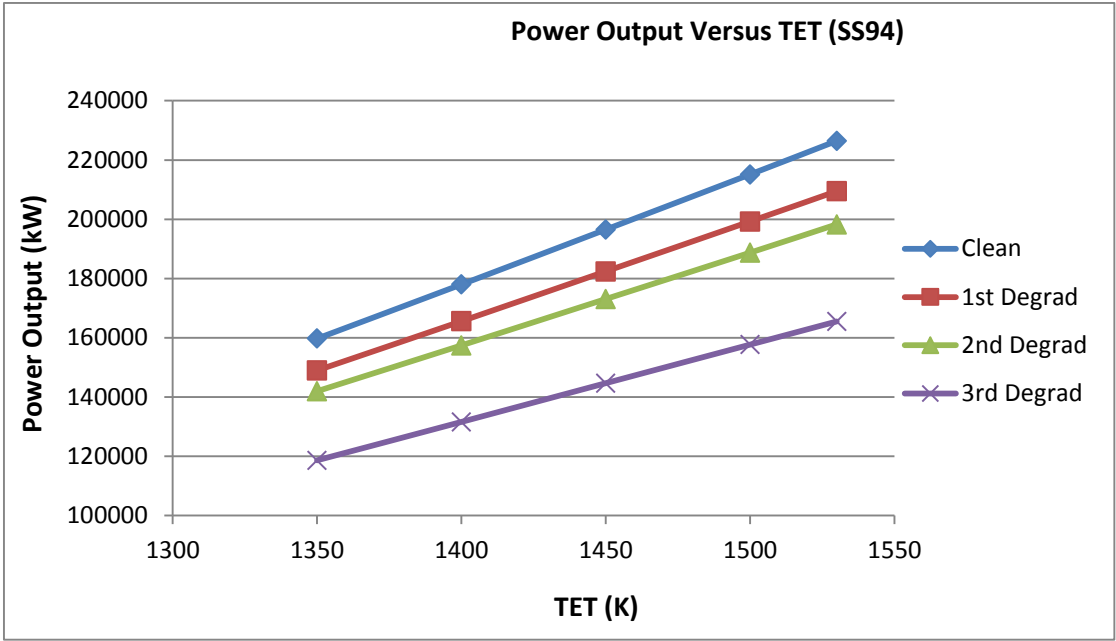


Figure 4-12: Power Output versus TET for SS94

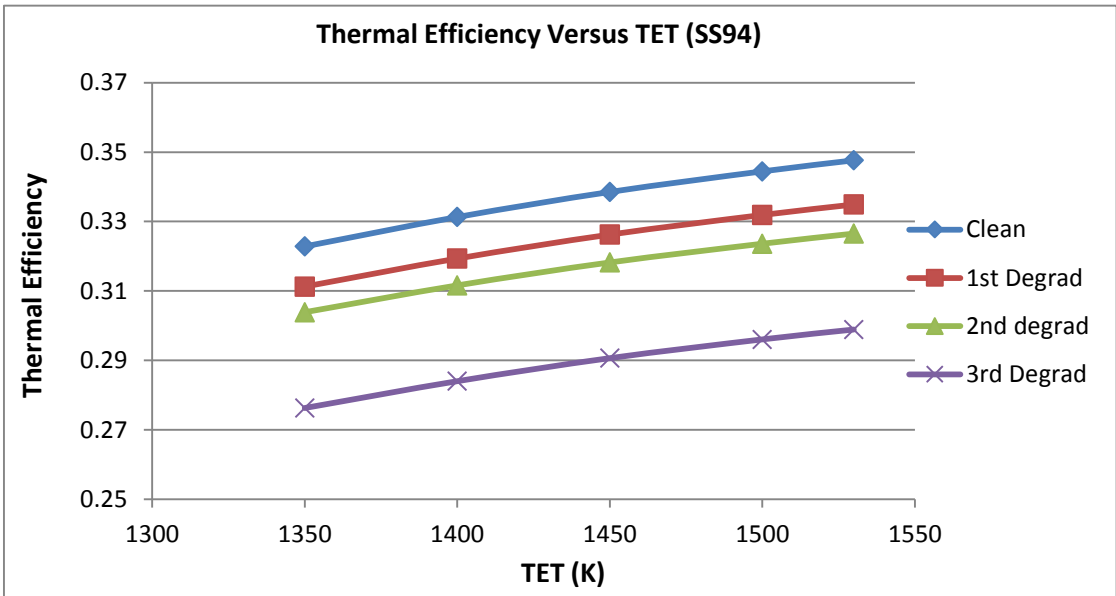
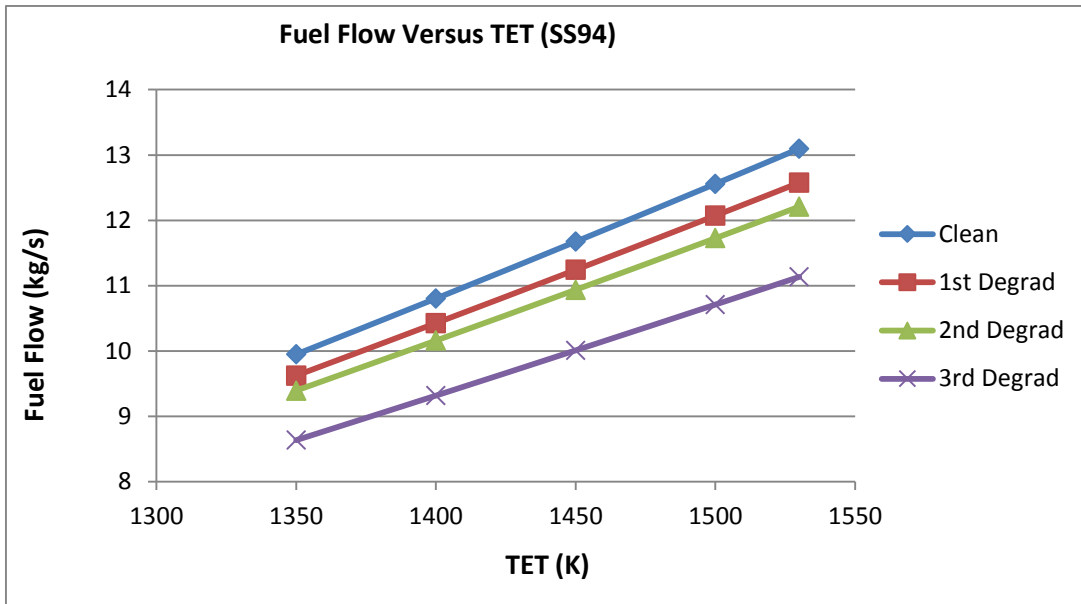


Figure 4-13: Thermal Efficiency versus TET for SS94



**Figure 4-14: Fuel Flow versus TET for SS94**

For power generation GT, the burner exit temperature range is typically from 1200-1600K at base load operations (Kurzke, 2011). The parameters varied in the simulations were isentropic efficiency changes and flow capacity changes.

Degradation was implemented in the 3 scenarios against a baseline clean NG. In the simulations, which are meant to give an understanding of degradation, the trends show that the fuel flow dropped with degradation from the clean case and worsened as the rate of degradation increased.

The trend shows that the effects of degradation can be alleviated by increasing TET. However, increasing TET to reduce the effects of degradation would shorten the life of the turbine blades.

From the results, it is obvious that the power output increases linearly with TET, as is the case with efficiency. As can be seen, the trend indicates a power loss in the degraded case. In like manner, power dropped with degradation from the clean case and worsened as the rate of degradation increased.

A greater measure of fuel flow decrease implies much less work done and even lowers power output with a much lower efficiency. To counteract this effect would

mean raising TET much more which is tantamount to higher life consumption and translates to more maintenance cost.

#### 4.1.2.3 Part Load Performance Simulation SS94

Also, Part Load performance was simulated and the results presented in Table 4-4. Power outputs were observed at varying TET from 1300K, in steps of 50K. Cognisance was taken of the fact that part load operations of gas turbine engines are expected to run at a minimum of 40-60% engine capacity (Razak, 2007).

**Table 4-4: Part Load Performance Simulation - SS94**

TET (K)	1300	1350	1400	1450	1500	1530
Power (Kw)	141511	159729	178004	196534	215141	226446
Efficiency	0.3124	0.3228	0.3313	0.3385	0.3444	0.3476
EGT (K)	711.97	740.94	770.17	799.99	829.40	847.33
Fuel Flow	9.109	9.948	10.80	11.67	12.56	13.10

#### 4.1.2.4 Effects of Ambient Temperature Variations - SS9E

Ambient temperature variations were investigated, with typical values from the Niger Delta of Nigeria, and the results as shown in Table 4-5.

**Table 4-5: Results of Ambient Temperature Variations - SS9E**

T <sub>amb</sub> (K)	283.15	288.15	293.15	298.15	303.15	308.15
Power (kW)	123697	120631	117676	114839	112125	109550
Efficiency	0.3398	0.3373	0.3347	0.3321	0.3294	0.3266
EGT (K)	885	886	887	888	889	891

At low values of ambient temperature of say -30°C, the engine is working near its maximum power rating. Thus at low ambient temperature, increasing firing temperature produces only marginal improvement in cycle efficiency. For ambient temperature of say 30°C, the efficiency is relatively low for small values of firing temperature. Thus for higher ambient temperature, increasing firing temperature



produces noticeable improvement in cycle efficiency. Power increases linearly with increase in firing temperature for all ambient temperatures.

#### 4.1.2.5 Degradation Simulations for SS9E

The SS9E is a heavy duty, single shaft engine which has a turbine and compressor. The degraded compressor and turbine inputs are as presented in Tables 4-6 and Table 4-7 respectively.

**Table 4-6: Compressor Inputs for SS9E Degraded Performance**

Flow capacity	Isentropic Efficiency	Remarks
-2	-0.7	1st Degradation
-3	-1	2nd Degradation
-4	-2	3rd Degradation

**Table 4-7: Turbine Inputs for SS9E Degraded Performance**

Flow capacity	Isentropic Efficiency	Remarks
2	-0.5	1st Degradation
3	-1	2nd Degradation
4	-2	3rd Degradation

Using GasTurb, degradation was implemented by changing the modifiers for compressor and turbine flow and efficiency respectively, while fixing the TET. The results follow the same pattern with the SS94.

#### 4.1.2.6 : Part Load Performance Simulation of SS9E

Power outputs were observed at varying TET from 1300K, in steps of 50K, and the results are in Table 4-8.

**Table 4-8: Part Load Performance - SS9E**

TET (K)	1300	1350	1400	1450	1500	1520
Power ( Kw)	81803	90523	99268	108133	117029	120631
Efficiency	0.3161	0.3226	0.3279	0.3324	0.3360	0.3373
EGT (K)	749.5	780.4	811.2	842.2	873.4	886.1
Fuel Flow (kg/s)	5.2	5.64	6.09	6.54	7	7.19

**4.1.2.7 Ambient Temperature Variations - LM6K**

Results for ambient temperature variations for the LM6K are presented in Table 4-9.

**Table 4-9: Ambient Temperature Variations - LM6K**

T <sub>amb</sub> (K)	283.15	288.15	293.15	303.15	308.15
Power (kW)	42227	40753	39330	36658	35417
Efficiency	0.3838	0.3791	0.3743	0.3644	0.3592
EGT (K)	753.7	754.9	756.2	759.3	761.2
Fuel Flow (kg/s)	2.21	2.16	2.11	2.02	1.98

**4.1.2.8 Degradation Simulations - LM6K**

The LM6K is a double shaft, aero-derivative engines that has two compressors and two turbines. Degradation was therefore implemented as shown in Tables 4-10 to 4-13, while plots of the simulation results are shown in Figures 4-15 to 4-17.

**Table 4-10: Inputs for First Compressor - LM6K Degraded**

Flow capacity	Isentropic Efficiency	Remarks
-2	-0.7	1st Degradation
-3	-1	2nd Degradation
-4	-2	3rd Degradation

**Table 4-11: Inputs for First Turbine- LM6K Degraded**

Flow capacity	Isentropic Efficiency	Remarks
2	-0.7	1 <sup>st</sup> Degradation
3	-1	2 <sup>nd</sup> Degradation
4	-2	3 <sup>rd</sup> Degradation

**Table 4-12: Inputs for Second Compressor - LM6K Degraded**

Flow capacity	Isentropic Efficiency	Remarks
-1.5	-0.5	1 <sup>st</sup> Degradation
-2	-0.7	2 <sup>nd</sup> Degradation
-3	-1	3 <sup>rd</sup> Degradation

**Table 4-13: Inputs for Second Turbine - LM6K Degraded**

Flow capacity	Isentropic Efficiency	Remarks
1.5	-0.5	1 <sup>st</sup> Degradation
2	-0.7	2 <sup>nd</sup> Degradation
3	-1	3 <sup>rd</sup> Degradation

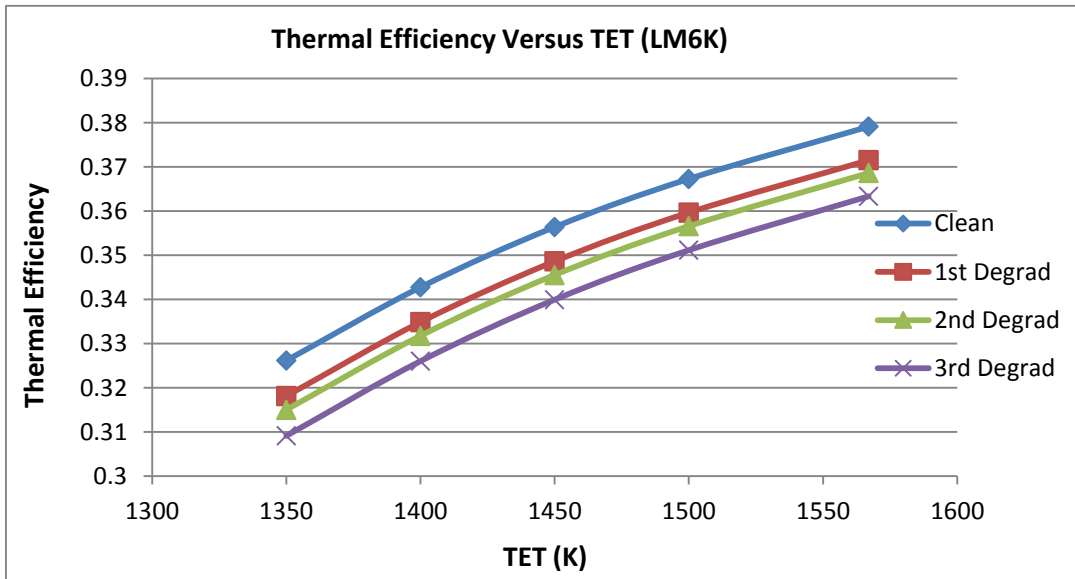


**Figure 4-15: Thermal Efficiency versus TET for LM6K**

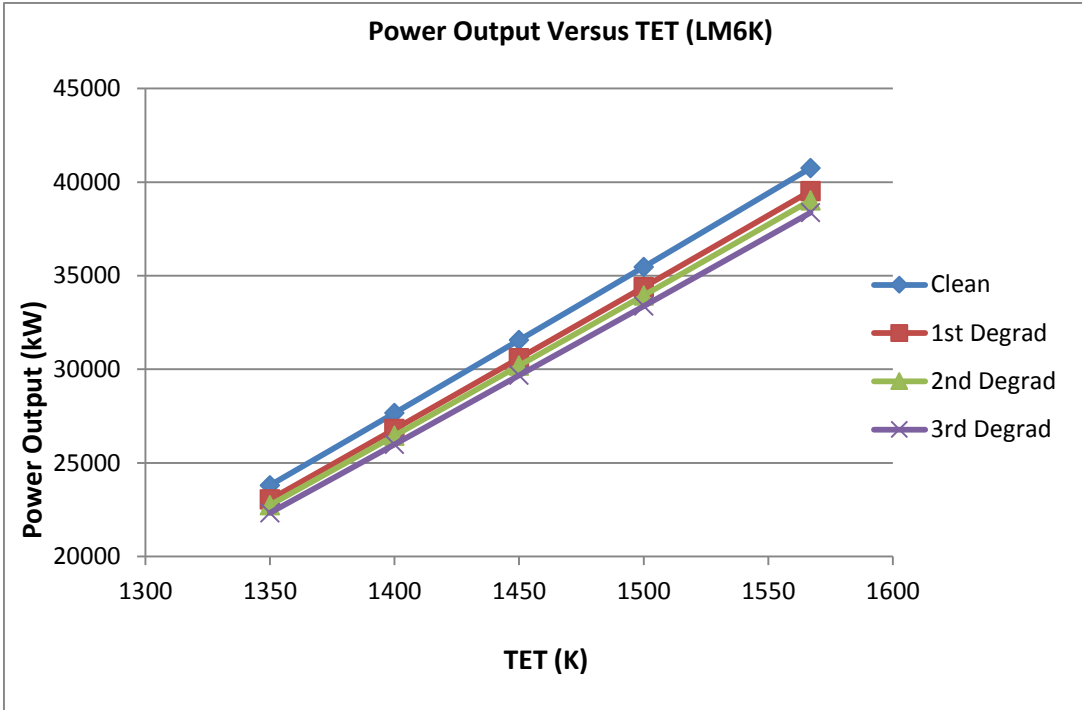


Figure 4-16: Power Output versus TET for LM6K

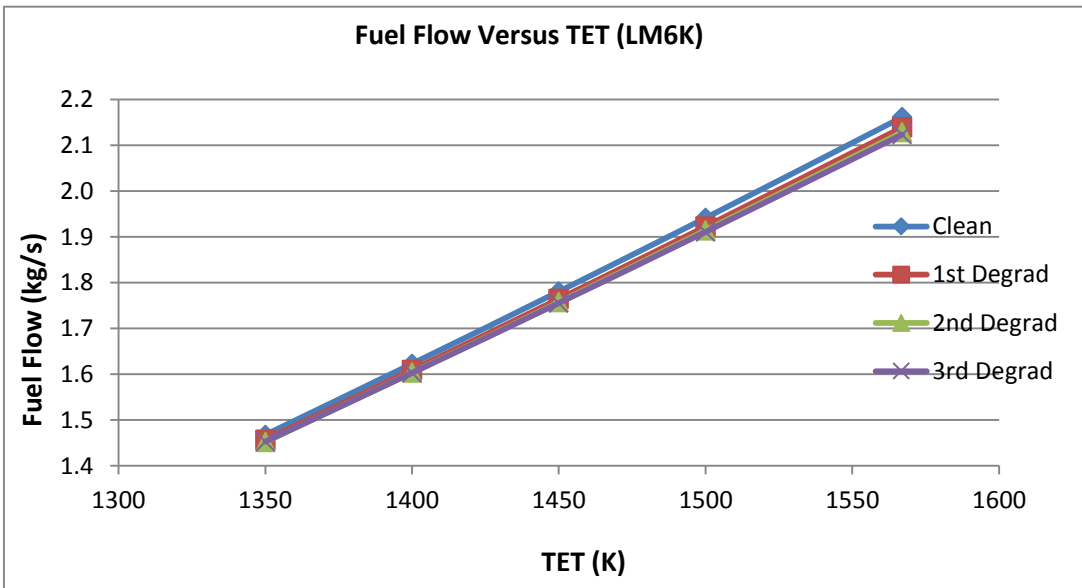


Figure 4-17: Fuel Flow versus TET for LM6K

#### 4.1.2.9 Part Load Performance Simulation - LM6K

Part Load performance at varying TET from 1350K, in steps of 50K, is presented in Table 4-14

**Table 4-14: Part Load Performance - LM6K**

TET (K)	1350	1400	1450	1500	1567
Power (Kw)	23808	27664	31562	35464	40753
Efficiency	0.3262	0.343	0.356	0.3673	0.3791
EGT (K)	644.3	669.2	694.7	720.1	754.9
Fuel Flow (kg/s)	1.468	1.623	1.781	1.941	2.161

#### 4.1.2.10 Ambient Temperature Variations - LM1H

The results for ambient temperature variations are presented in Table 4-15

**Table 4-15: Ambient Temperature Variations - LM1H**

T <sub>amb</sub> (K)	283.15	288.15	293.15	298.15	303.15	308.15
Power (kW)	101402	100194	99057	98001	97035	96174
Efficiency	0.4416	0.4397	0.4378	0.4361	0.4343	0.4327
Fuel Flow (kg/s)	4.65	4.58	4.55	4.52	4.49	4.47

#### 4.1.2.11 Degradation Simulations for LM1H

The LM1H is a double shaft, aero-derivative engines that has two compressors and two turbines. Degradation was implemented as shown in Tables 4-16 to 4-19. Plots of the results assume the same pattern with those of LM6K.

**Table 4-16: Inputs for First Compressor – LM1H Degraded**

Flow capacity	Isentropic Efficiency	Remarks
-2	-0.7	1 <sup>st</sup> Degradation
-3	-1	2 <sup>nd</sup> Degradation
-4	-2	3 <sup>rd</sup> Degradation

**Table 4-17: Inputs for First Turbine– LM1H Degraded**

Flow capacity	Isentropic Efficiency	Remarks
2	-0.7	1 <sup>st</sup> Degradation
3	-1	2 <sup>nd</sup> Degradation
4	-2	3 <sup>rd</sup> Degradation

**Table 4-18: Inputs for Second Compressor – LM1H Degraded**

Flow capacity	Isentropic Efficiency	Remarks
-1.5	-0.5	1 <sup>st</sup> Degradation
-2	-0.7	2 <sup>nd</sup> Degradation
-3	-1	3 <sup>rd</sup> Degradation

**Table 4-19: Inputs for Second Turbine – LM1H Degraded**

Flow capacity	Isentropic Efficiency	Remarks
1.5	-0.5	1 <sup>st</sup> Degradation
2	-0.7	2 <sup>nd</sup> Degradation
3	-1	3 <sup>rd</sup> Degradation

#### **4.1.2.12 Part Load Performance Simulation for LM1H**

Part Load performance for the LM1H at varying TET from 1450K, in steps of 50K, is presented in Table 4-20.

**Table 4-20: Part Load Performance Simulation of – LM1H**

TET (K)	1450	1500	1550	1600	1650
Power (kW)	72578	79407	86306	93218	100194
Efficiency	0.3822	0.399	0.414	0.4273	0.4397
EGT (K)	655.2	663.1	671.1	679.3	687.9
Fuel Flow kg/s	3.8	4.0	4.2	4.4	4.6

#### 4.1.2.13 Ambient Temperature Variations for DS25

Ambient temperature variation results are shown in Table 4-21.

**Table 4-21: Ambient Temperature Variations - DS25**

T <sub>amb</sub> (K)	283.15	288.15	293.15	298.15	303.15	308.15
Power (kW)	25815	25103	24415	23754	23121	22518
Efficiency	0.3697	0.3668	0.3637	0.3605	0.3571	0.3537
Fuel Flow (kg/s)	1.404	1.376	1.35	1.325	1.302	1.28

#### 4.1.2.14 Degradation Simulations for DS25

The DS25 is a double shaft engine which has a compressor, a compressor turbine and a free power turbine. Inputs for degrading the compressor and turbines are as shown in Tables 4-22 to 4-24, while the result plots are in Figures 4-18 to 4-20.

**Table 4-22: Inputs for Degraded Compressor – DS25**

Flow capacity	Isentropic Efficiency	Remarks
-2	-0.7	1 <sup>st</sup> Degradation
-3	-1	2 <sup>nd</sup> Degradation
-4	-2	3 <sup>rd</sup> Degradation

**Table 4-23: Inputs for Degraded Compressor Turbine – DS25**

Flow capacity	Isentropic Efficiency	Remarks
2	-0.7	1 <sup>st</sup> Degradation
3	-1	2 <sup>nd</sup> Degradation
4	-2	3 <sup>rd</sup> Degradation

**Table 4-24: Inputs for Degraded Free Power Turbine – DS25**

Flow capacity	Isentropic Efficiency	Remarks
1.5	-0.5	1 <sup>st</sup> Degradation
2	-0.7	2 <sup>nd</sup> Degradation
3	-1	3 <sup>rd</sup> Degradation

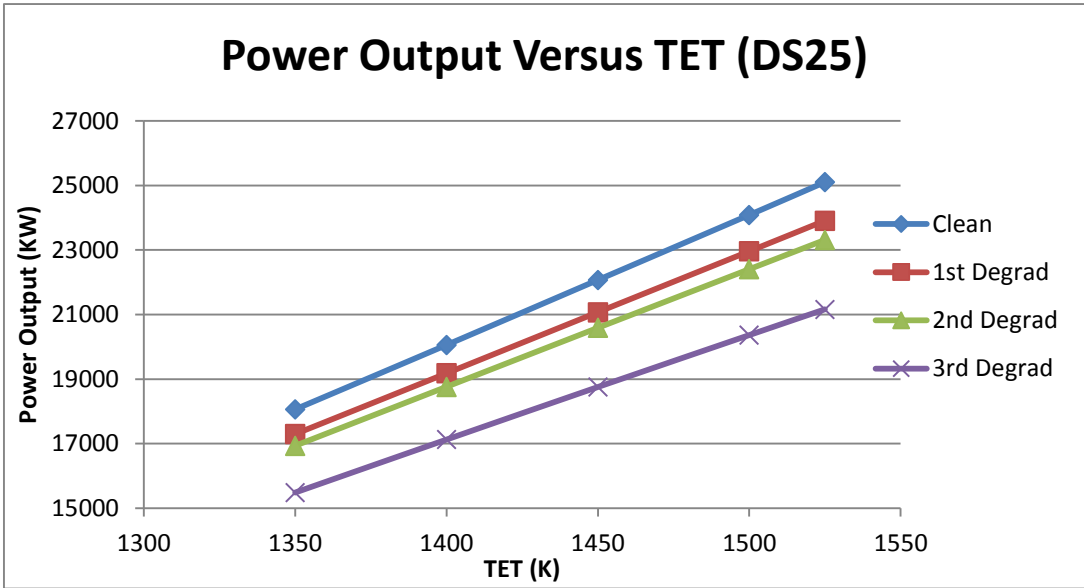


**Figure 4-18: Power Output versus TET for DS25**

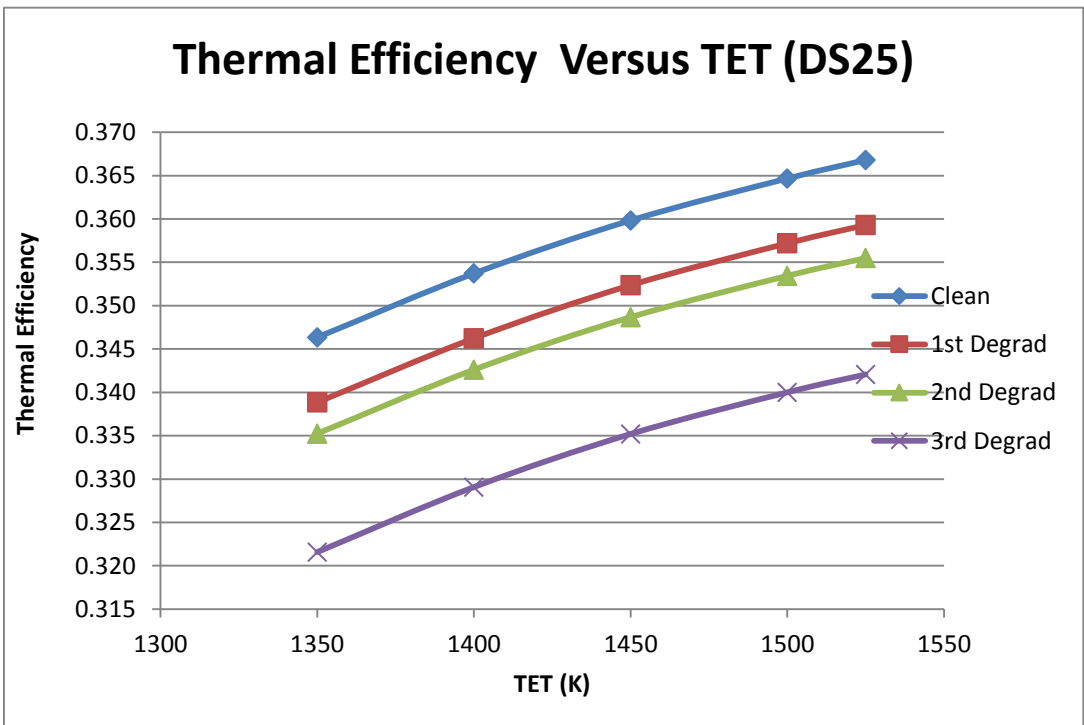


**Figure 4-19: Thermal Efficiency versus TET for DS25**



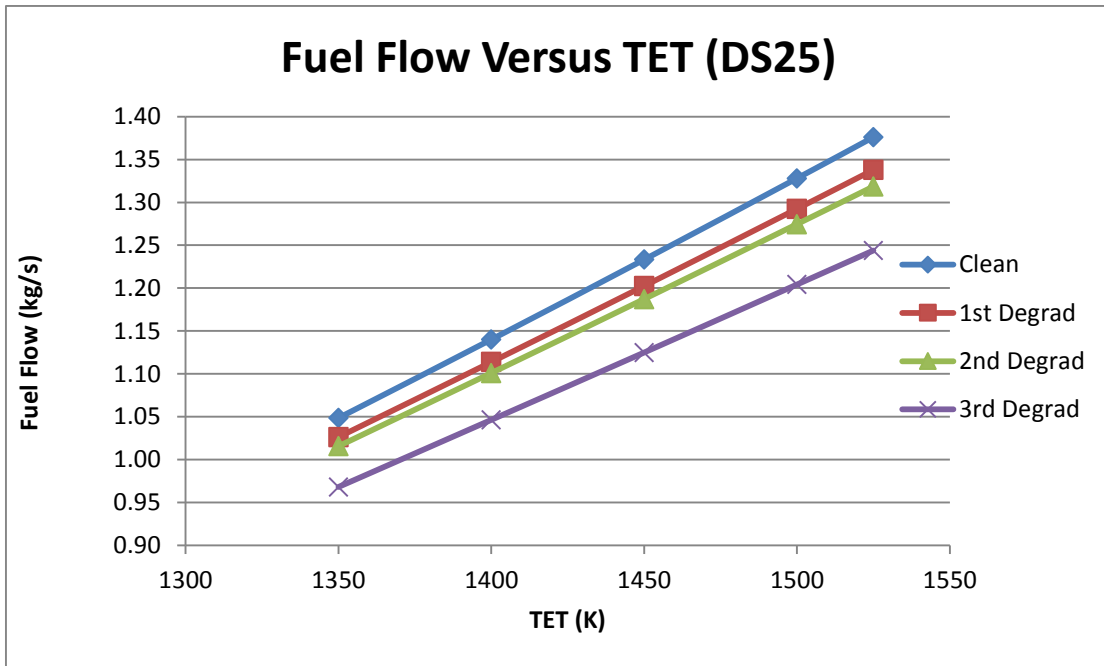


**Figure 4-20: Fuel Flow versus TET for DS25**

#### 4.1.2.15 Part Load Performance of DS25

Part Load performance for DS25 was simulated and the results presented in Table 4-25. Power outputs were observed at varying TET from 1350K, in steps of 50K.

**Table 4-25: Part Load Performance for DS25**

TET (K)	1350	1400	1450	1500	1525
Power (Kw)	18063	20057	22071	24085	25103
Efficiency	0.3463	0.3537	0.3598	0.3647	0.3668
Fuel Flow (kg/s)	1.0486	1.1401	1.233	1.328	1.376

## 4.2 Influence of Ambient Temperature Variations

Ambient temperature impacts significantly on GT performance. The price of fuel and CoE show seasonal and/or daily trends, hence fuel cost, CoE and

maintenance costs are major considerations for operational planning of power plants.

Changes in the mass flow rate of air entering the GT alter its performance; factors affecting air density include pressure, temperature and humidity. An increase in the height above sea level causes the air pressure and temperature to decrease, resulting in a decrease in air density. GT performance and efficiency decreases on hot days due to reduced air density, reduced mass flow, reduced pressure ratio, increased specific fuel consumption

Higher ambient temperatures decrease efficiency of electricity production by increasing fuel consumption per unit of electricity produced. Increased  $T_{amb}$  decreases fuel consumption at constant TET, due to the reduction in power output. A higher TET will be required to maintain power output at an elevated  $T_{amb}$ . Higher fuel consumption results in higher operating costs. Running GTs at peak load for prolonged periods consumes the life of hot end components. Higher power output associated with peak loads comes with additional maintenance costs.

There is an expected increase in maintenance cost when a GT runs beyond its rated TET, due to frequent replacement of HPT blades and lower creep life. There is also tremendous impact of higher TET on the turbine thermal efficiency.

### **4.3 Effect of Performance Degradation Due to AG Combustion**

Deviation of NG from typical pipeline gas quality would not only result in low thermodynamic performance, but will initiate degradation of the hot gas path of the GT from contaminants (Eliaz et al., 2002). Decreased service life is expected from degradation and an increased cost of maintenance as a result of short time between overhauls.

Compositions of AG vary widely, though the high content of methane makes it attractive for power generation. Variation in composition of gas can affect its heat content; for instance a high mass composition of Nitrogen can reduce the heating value of the gas, much as the Hydrogen content of the fuel affects the flame

speed which could distort the uniformity of heat released in the combustor (Jaber et al., 1998).

#### **4.3.1 Variations in the Fuel Gas Composition**

Variations in the fuel gas composition tend to affect the mass flow through the turbine, the enthalpy of the products of combustion, thermodynamic changes in turbine components and associated turbine control systems (Walsh, P.P. and Fletcher, P., 2008). Consequently, each GT would perform differently due to changes in gas composition, depending on the design.

Turbine blade problems associated with use of heavy-fuel concentrations of contaminants depend mainly on relative levels of ash melting point and blade metal temperatures. This is because solid ash particles tend to pass through turbine discs; also liquid droplets deposit on the blades by impact and could result in corrosion. Emphasis therefore is on removal of the potentially harmful contaminants via fuel treatment.

Sulphur burns to sulphur dioxide, then to sulphur trioxide and when in contact with water, to sulphuric acid which is corrosive when condensed onto cool metal surfaces. Sulphur also forms sulphides with Chromium and Nickel in the blades, offering no protection to the underlying metal. These would have a direct bearing on the creep life of the turbine blade and by extension, the life of the GT.

A major concern about gaseous fuels is the condensable content. Swells of hydrocarbon condensates may cause overheating of the burner. Condensed water can cause corrosion in the fuel distribution system. If the corrosion products reach the combustor, hard deposits of the molten oxides will be deposited on the turbine. If the fuel gas contains high levels of sulphur, deposits are formed by reaction with water and condensed hydrocarbons in the fuel gas. In order to avoid condensation, the fuel gas has to be pre-heated to at least 20K above the dew point (Colombo, M. and Ruetschi, R.,2000).

In the combustion chamber, alkali metal impurities in the fuel react with the sulphur of the fuel to form sodium and potassium sulphates, which condense on the surfaces of the turbine and hot gas path. At temperature ranges of 700 –

900°C, the alkali sulphates on the turbine are molten and react with the metal, causing sulphidation due to hot corrosion (Colombo, M. and Ruetschi, R., 2000).

#### **4.3.2 High Temperature Corrosion Due to Trace Metal Impurities**

Corrosion mechanisms can occur, attributable to the formation of low melting point ash deposits originating from certain trace metal impurities in GT fuels. Crude oils and residual-grade fuel oils typically contain small quantities of vanadium as a naturally-occurring component of petroleum. Liquid fuels are not the only source of ash-forming impurities. Sodium salts and other contaminants can also enter gas turbines via the compressor inlet air, and also from water and steam that may be injected for NO<sub>x</sub> control or power augmentation. Thus, the risk of contamination from non-fuel sources must also be considered in gas-fired applications.

During combustion, these types of fuels create ash deposits composed mainly of vanadium pentoxide, and with a low melting point of about 675°C (TurboTech 2014). At typical GT operating temperatures the vanadic ash deposits are molten, and thereby accelerate the surface oxidation rate of blades. Other trace metal impurities such as lead and zinc will also initiate high temperature corrosion by similar mechanisms. Crude oil could contain sodium and potassium salts, originating from both oilfield and refinery sources. The presence of these alkali metal impurities could lead to sulphidation attack which involves the formation of sodium sulphates, through reaction with fuel sulphur, causing pitting of hot section components. In situations where both vanadium and sodium impurities are present, even lower melting point ash deposits can form and increase the risk of high temperature corrosion.

#### **4.3.3 Control of High Temperature Corrosion by Fuel Additives**

Burning of heavy fuels in gas turbines requires the use of additives to prevent hot corrosion of hot gas path components. The cause and nature of this type of corrosion is due to vanadium, or vanadium and sodium contaminants in heavy fuels such as crude oils, residual oils and blended residual oils. These metals have the effect of destroying the protective oxide films on hot gas path parts

where the heavy fuel oils are being burned. Most crude oils contain relatively high levels of vanadium requiring the use of a corrosion inhibition additive. Magnesium particles greater than 2 microns are known to have a detrimental effect on GT performance and routine maintenance intervals (Bell Performance, 2012).

Sodium and potassium salts are water soluble, and can be removed by on-site treatment processes. However, Vanadium and other oil-soluble trace metals cannot be removed by fuel washing, necessitating corrosion inhibition through the use of chemical additives. Additive formulations are based on active components in various combinations and concentrations of Magnesium, Chromium and Silicon.

Magnesium is used primarily to control vanadic oxidation and function by modifying ash composition and increasing ash melting point. Through combination with  $V_2O_5$  at an appropriate Magnesium-Vanadium treatment ratio, magnesium orthovanadate with a high melting point of about 1243°C is formed as a new ash component. Corrosion is thus controlled by ensuring that the combustion ash does not melt, and that it remains in a solid state on gas turbine blades and vanes. Through reaction with fuel sulphur, the magnesium inhibition mechanism also generates magnesium sulphate as an additional ash component. This compound is water-soluble and therefore facilitates the removal of combustion ash via periodic water wash of the hot gas path.

Chromium additives inhibit sulphidation corrosion promoted by alkali metal contaminants such as sodium and potassium. Chromium reduces ash fouling, and the mechanism is believed to involve the formation of volatile compounds which pass through the turbine without depositing. Silicon is used to provide added corrosion protection in specific applications.

Fuel additive properties are also extremely important, and can significantly influence the reliability and effectiveness of a treatment. Additive quality is considered to be top priority, but depends on site handling and dosing procedures. Problems such as the plugging of filters and fuel nozzles could be alleviated by the use of appropriate fuel additives.

Excellent solubility and low viscosity properties of additives ensure rapid mixing and uniform distribution in the fuel, which improves reaction efficiency in the combustion zone.

The basic requirements for an inhibitor additive is that it forms a high melting point, non-corrosive ash by combining with the harmful trace metal contaminants in the fuel. Another requirement is for the hot gas path deposits from the ash should not cause excessive maintenance of the turbine.

#### **4.3.4 Control of High Temperature Corrosion by Special Coatings**

The resistance of superalloys against hot corrosion is related to the chemical composition of the alloy and its thermo-mechanical history. Tungsten, vanadium and molybdenum are excellent in improving the mechanical properties, though there is usually a trade-off in material selection and protective coatings chosen for corrosion resistance. Chromium is the most effective alloying element for improving the hot corrosion resistance of superalloys.

High temperature coatings are in three categories: diffusion, overlay and thermal barrier coatings. Diffusion coatings are formed by the surface enrichment of an alloy with aluminium, chromium or silicon. Overlay coatings are corrosion-resistant alloys (nickel, cobalt or a combination of both) designed for high-temperature surface protection. Thermal barrier coatings are designed to insulate the substrate from the heat of the gas flow, consisting of an outer ceramic coating overlaid on an oxidation-resistant bond coat.

#### **4.3.5 Control of High Temperature Corrosion by Washing**

A good way of minimizing hot corrosion is washing of hot parts using plain water, which allows for dissolving of salts and contaminants from the part, thereby preventing the initiation of hot corrosion.

#### **4.3.6 Control of High Temperature Corrosion by Air Filtering**

High temperature corrosion would be prevented by air filtration. A minimum level of 0.008 ppm by weight is suggested for the content of sodium in the air below which hot corrosion will not exist. Hence secondary corrosion may be

prevented by installing high efficiency pair filters.





## CHAPTER 5: RESOURCE DECLINE AND GAS FLARING

### 5.1 Introduction

Fossil fuels are the dominant source of energy and over the years, improved technology has led to increased extraction. No doubt, the main source of energy in the foreseeable future will still be fossils. Energy is key to growth and development of societies and its availability is driven by the speed of extraction.

Crude oil is formed as a result of geological processes; oil and gas reservoirs are the basic units of production. An oil field is made up of one or more subsurface reservoirs where hydrocarbons are located. These hydrocarbons reside in microscopic pores in rocks, with a tight and impermeable layer called the cap rock, which traps the fuel. In the absence of a suitable reservoir rock, hydrocarbons cannot gather to form a commercially extractable quantity.

All oil and gas fields represent a limited geological structure; hence they have a maximum amount of hydrocarbons they contain. The size of the reservoir, defined by geological and geophysical means, gives an estimate of the potential volume of oil in the field before the commencement of drilling. The total amount of oil in a field is termed Oil in Place (OIP), equivalent to the total quantity in the pores of one or more reservoirs making up the field (Robelius, 2007). Not all the OIP can be recovered from a field, the recoverable amount being classified as the reserve. Reserve volume is expressed mathematically in Equation 5-1 thus

$$\text{Reserve} = \text{Recovery Factor} \times \text{OIP} \quad (5-1)$$

Where Recovery Factor is the estimated percentage of the total OIP volume that can be recovered, which can vary from less than 10% to over 80% depending on the reservoir properties and recovery methods. Also, recovery will be limited by the natural laws governing reservoir flows, saturation levels, and porosity.

The rate of formation of oil and gas as against extraction is necessary for proper forecasts to be made. With advances in technology, the extraction process has become faster than the formation process, thus fossil fuels are categorized non-renewables and therefore subject to depletion. Reservoirs and their intrinsic

properties are therefore fundamental for oil and gas production. Two fundamental concepts worth examining are decline and depletion of reserves.

Decline curve analysis is a reliable tool for oil production forecasts from individual wells or an oilfield. Depletion has an active role in the extraction of finite resources and is a major consideration for oil flows in a reservoir. Depletion rate is also a useful tool for forecasting crude oil production as it can be connected to decline curves analysis. Drawing from comprehensive databases with reserve and production data for hundreds of fields, it was possible to identify typical behaviours and properties of oil fields; and a thorough analysis of all factors affecting future oil production was investigated and used to provide a realistic forecast. Giant oil fields were found to be the most important contributors to world oil supply. Data from over 300 giant fields were used to work out decline and depletion rates; revealing the fact that high extraction rate of recoverable volumes will result in rapid decline (Höök et al., 2009) .

An important component of oil production modelling and hydrocarbon extraction forecasting is an in-depth study of mathematical models that express the physical behaviour of the production processes. Depletion-driven decline occurs when the recoverable resources become exhausted and the production flow is reduced due to the physical limitations of the reservoir.

Boyle's Law in Equations 5-2 and 5-3 spell out the inverse proportionality of the pressure and volume of a gas, if the temperature is constant. This is applicable to gas reservoirs as they are reasonably isolated and in thermal equilibrium with the surrounding bedrock

$$\text{Pressure} \times \text{Volume} = \text{Constant} \quad (5-2)$$

$$P_1V_1 = P_2V_2 \quad (5-3)$$

Where  $p_1$ ,  $p_2$  are pressure of gas at state 1 and 2 respectively; while  $v_1$ ,  $v_2$  are the specific volumes of the gas at states 1 and 2 respectively.

This shows that, extraction removes mass without changing the volume in the different states; consequently, pressure drops in order to maintain the balance. It

follows therefore that decreasing pressure leads to decreased flow rates, all other things being equal. Thus extraction of gas from a reservoir will result in declining production with time.

From the foregoing, there is a compelling need to be mindful of the fact that extraction of hydrocarbons from a reservoir will ultimately lead to a decline of this resource.

## **5.2 Reserves in Oil Fields**

Decline curve analysis is a veritable tool for future outlook into production from oil wells and useful for forecasting crude oil production (Höök et al., 2009). Giant oil fields are fields with more than 0.5 Gb of Ultimately Recoverable Resources (URR) or a production of more than 100 000 barrels per day (bpd) for over a year. Crude oil from smaller fields that are not large enough to be classified as Giants, are called Dwarf oil fields (Robelius, 2007) .

Though Giant oil fields are only a small fraction of the total number of oil fields in the world, they are the most important contributors to world oil supply. Over 50% of the world oil production came from Giants as at 2005 and over half of the world's ultimate reserves are found in Giants.

Giant oil fields go into decline faster than Dwarfs, the average decline rate of all Giant fields being -13.4%. When weighted against the peak production of every individual field, the decline rate goes even further to -13.8%. The high decline rates have a tremendous effect on the total oil production due to the huge contribution from Giant oil fields. The typical decline rate of a giant oil field is -13% (Höök and Aleklett, 2008) .

According to Robelius, the production of an oil field tends to pass through the stages shown at Figure 5-1. It begins with the discovery of the well, its appraisal and the first oil production which marks the beginning of the build-up phase. Then the field enters a plateau phase, where the full installed extraction capacity is used, before getting to the onset of decline, which ends in abandonment at the economic limit. Small fields have very short plateau phases, but large fields stay several decades at the plateau phase as is the case with giants.

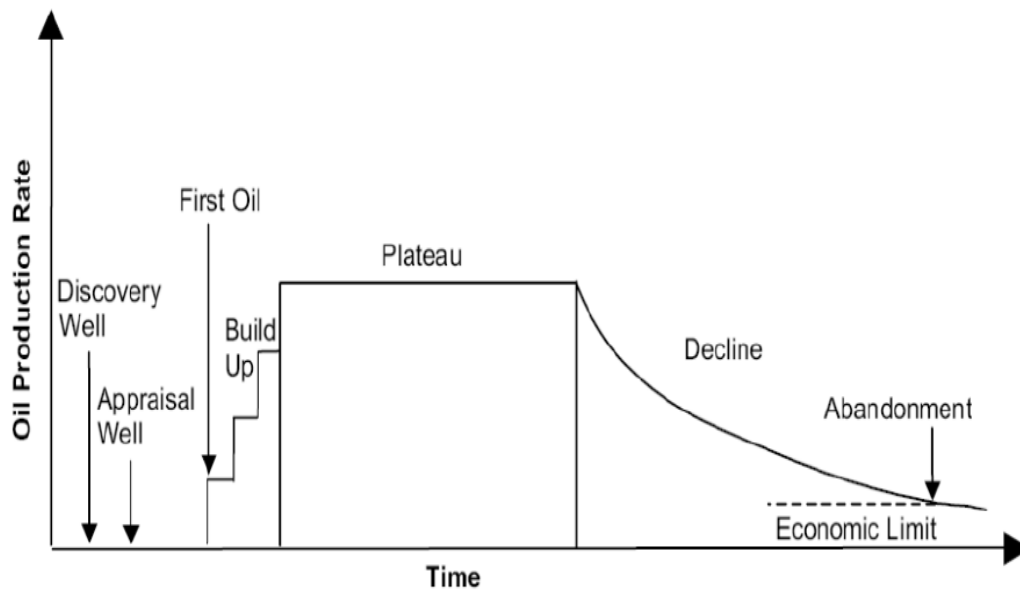


**Figure 5-1: Theoretical Oil Production Curve (Robelius, 2007)**

### **5.3 Decline Rate Analysis**

Decline rate refers to the decrease in petroleum extraction over time, usually calculated annually, giving the change in produced volume from one year to another.

Decline could be caused by politics, sabotage, depletion or malfunctions. There may also be economics-driven decline where lack of payments, services, modernization and investments have reduced the production level. Depletion-driven decline occurs when the recoverable resources become exhausted and the production flow is reduced. This research concerns itself with depletion-driven resource decline.

In order to isolate politics and economics from physical factors affecting decline rates, a real life scenario based on sample exponential decline functions is presented hereunder.

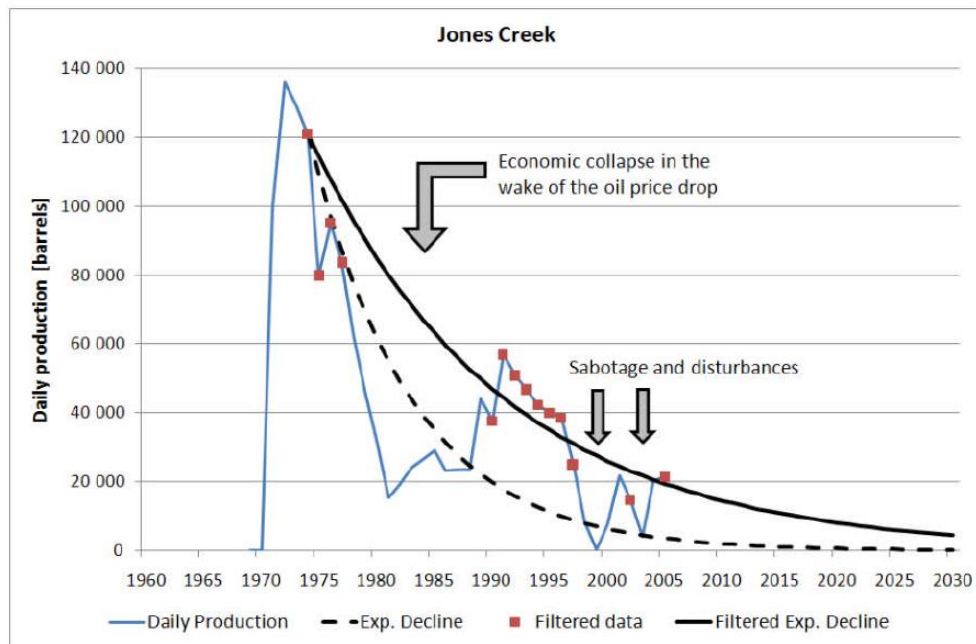


**Figure 5-2: Jones Creek Giant Oil Field, Nigeria (Hook, 2009)**

The Giant oil field Jones Creek shows several production disturbances caused by collapse of the economy in the wake of the oil price drop in the 1980s, caused in part by sabotage and militant activities. In order to obtain a good fit, drops in production due to such socio-economic factors were filtered to produce an exponential decline curve, as shown in Figure 5-2.

#### 5.4 Decline Curve Analysis

(Hook, 2009) reports that Arps (1945) laid the foundation of decline curve analysis by proposing simple mathematical curves (exponential, harmonic or hyperbolic) for estimating the production of an oil well at the onset of decline.

The Arps decline curves are used to obtain expressions that could be utilized in a simple manner. Assuming that the decline in production starts at time  $t_o$ , with an initial production rate of  $r_o$  and an initial cumulative production  $Q_o$ .

The production rate at  $t \geq t_0$  is denoted by  $q(t)$ , and the corresponding cumulative production is given by,

$$Q(t) = \int q(t)dt. \text{ from } t_0 \text{ to } t \quad (5-4)$$

The three important parameters of decline curves are:

Initial rate of production  $r_0 > 0$ ,

Decline rate  $\lambda > 0$

Shape parameter,  $\beta$

If the production continues till infinity, the integral  $Q(t) = \int q(t)dt$  converges as  $t_0$  tends to infinity ( $\infty$ )

Normally, production stops when the economic limit is reached at time  $t_{cut}$ . This cut-off point is  $r_c < r_0$  and is calculated by solving  $q(t) = r_c$  with respect to  $t$  and the solution occurs at  $t_{cut}$ . By substituting  $t_{cut}$  as the upper limit for  $Q(t)$ , the technically recoverable volume  $v_{rec}$  can be calculated.

The equations defining Exponential, Harmonic and Hyperbolic curves are presented in Tables 5-1 to 5-3.

**Table 5-1: Key Properties of Arps Exponential Decline Curve**

	<b>Exponential</b>
$\beta$	$\beta = 0$
$q(t)$	$r_0 \exp(-\lambda(t - t_0))$
$Q(t)$	$Q_0 + \frac{r_0}{\lambda} (1 - \exp(-\lambda(t - t_0)))$
URR	$Q_0 + \frac{r_0}{\lambda}$
$t_{cut}$	$t_0 + \frac{1}{\lambda} \ln\left(\frac{r_0}{r_c}\right)$
$V_{rec}$	$Q_0 + \frac{r_0 - r_c}{\lambda}$

**Table 5-2: Key Properties of Arps Harmonic Decline Curve**

	<b>Harmonic</b>
$\beta$	$\beta = 1$
$q(t)$	$r_0 [\exp(-\lambda(t - t_0))]^{-1}$
$Q(t)$	$Q_0 + \frac{r_0}{\lambda} \ln(1 + \lambda(t - t_0))$
URR	Not defined
$t_{cut}$	$t_0 + \frac{1}{\lambda} \left[ \frac{r_0}{r_c} - 1 \right]$
$V_{rec}$	$Q_0 + \frac{r_0}{\lambda} \ln\left(\frac{r_0}{r_c}\right)$

**Table 5-3: Key Properties of Arps Generalized Hyperbolic Decline Curve**

	<b>Hyperbolic</b>
$\beta$	$\beta \in [0,1]$
$q(t)$	$r_0[1 + \lambda\beta(t - t_0)]^{-\frac{1}{\beta}}$
$Q(t)$	$Q_0 + \frac{r_0}{\lambda(1 - \beta)} \left[ 1 - \left( 1 + \lambda\beta(t - t_0) \right)^{1 - \frac{1}{\beta}} \right]$
URR	$Q_0 + \frac{r_0}{\lambda(1 - \beta)}$
$t_{cut}$	$t_0 + \frac{1}{\lambda\beta} \left[ \left( \frac{r_0}{r_c} \right)^\beta - 1 \right]$
$V_{rec}$	$Q_0 + \frac{r_0}{\lambda(\beta - 1)} \left[ \left( \left( \frac{r_0}{r_c} \right)^{\beta - 1} - 1 \right) \right]$

Hyperbolic and Harmonic Decline Curves involve complicated functions, hence are more cumbersome to apply. Exponential Decline Curve is the most convenient and agrees well with field data, hence will be the reference for this study.

A good example of the application of decline curves was made from the UK offshore Giant field Thistle shown in Figure 5-3. The field peaked at a production of about 123,000 bpd in 1982 and has since been on the decline. At present, the daily output is a few thousand barrels only, even when there has not been any major disturbance to production from inception (Hook, 2009).



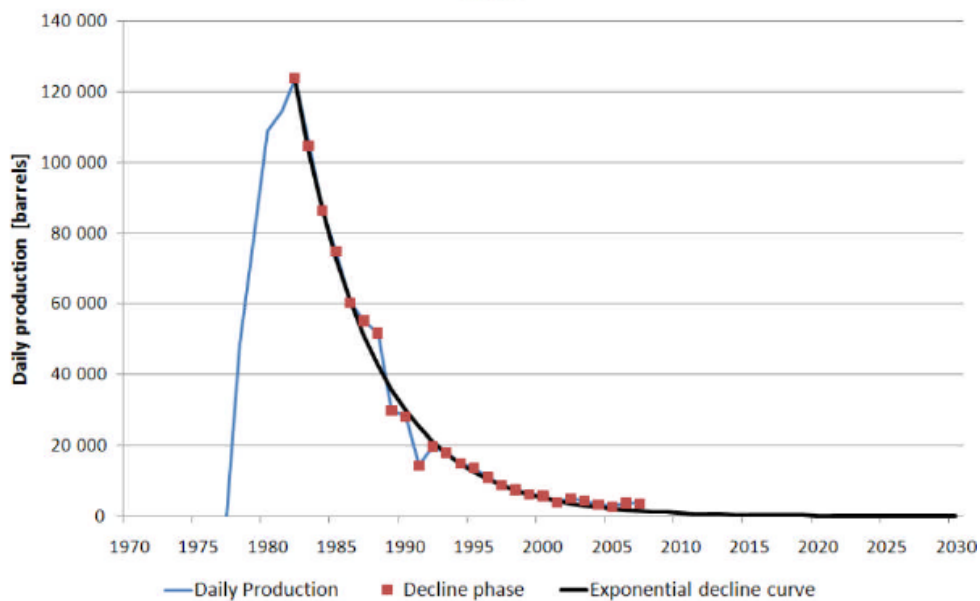


**Figure 5-3: Historical Production of the Thistle (Hook, 2009)**

The historical production of Thistle in Figure 5-4 is here fitted with an exponential decline curve, showing good agreement with minimal scatter.

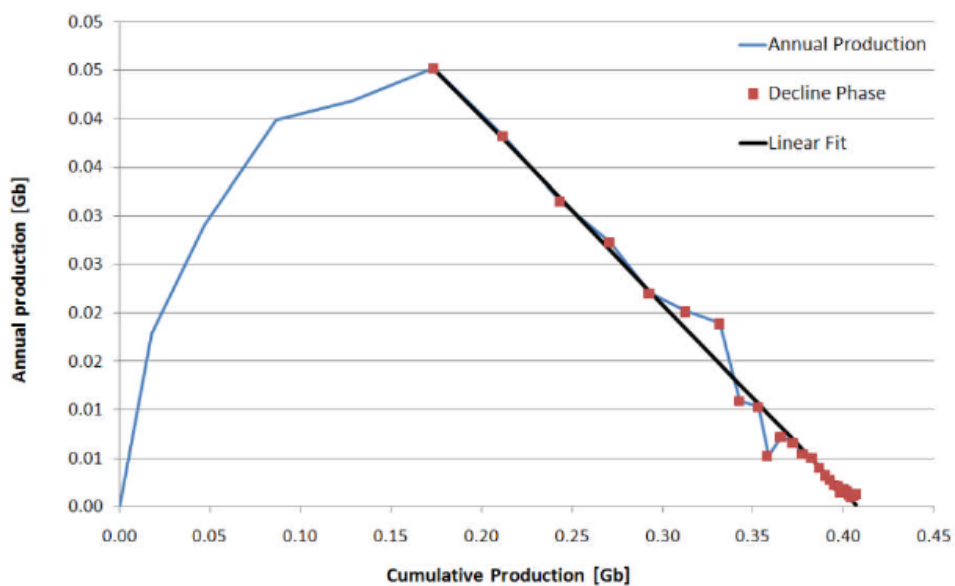


**Figure 5-4: Historical Production of the Thistle Plotted Differently (Hook, 2009)**

Often times, by plotting annual production against cumulative production, a linear trend is found in the decline phase and extrapolated to give an idea of future oil production. This way, decline curves could be used to validate official reserve estimates based on geological methods. This can also be used to estimate the

URR of a field where only production data is available. The major advantage of decline curve analysis is that it is independent of the size and shape of the reservoir (Doublet et al., 1994), thus avoiding the need for detailed reservoir volume. Decline curve analysis is applied, however, only to fields that have reached the onset of decline.

Land and offshore fields enter the decline phase when about 40% of the URR have been produced, but offshore fields tend to extract the oil at a higher rate than land based fields (Hook, 2009). This is why the average lifetimes of offshore fields are shorter than those of land based fields and why they decline faster.

The Kaji-Semoga oil field has an on-site LPG facility that recovers AG. Upon decline, its production in 2004 was 15,800 MSCFD but with a projected daily production of about 3000 MSCFD in 2014. This means the plant should be shutting down as a result of the AG depletion far below its designed capacity. As can be inferred from above, the decline within only ten years went from 15,800 to 3000 MSCFD, in a real life situation.

## **5.5 Resource Decline and Redundancy**

Reservoir production history show that the rate of oil and gas production declines as a function of time. It is almost impossible to extract all the resources within a reservoir, but higher gas mobility ensures more recoverability of about 80% for gas and 40% in the case of oil (Alekklett and Campbell, 2003) .

In line with the law of conservation of mass and energy at steady state, Lawal et al. (Lawal et al., 2006) opines that any of the following could occur:

- Oil production decline could lead to gas production increase
- Oil production decline could result in exactly the same gas production decline
- Oil production decline could be different from gas production decline
- Oil production could decline while gas production remains constant

For the present research, the second possibility will be adopted; that is, as crude oil declines, the AG obtained from it also declines. That will result in a

corresponding reduction in the available power from GTs used for power generation with AG.

## 5.6 Fuel Volume – Ultimately Recoverable Reserve

The annual global AG flaring is estimated at about 150 BCM. The sizes of reserves are often reported as proven reserves, probable reserves or possible reserves (Capen, 2001) which portray speculations and uncertainty.

In 2002, the World Bank organized a Summit for Sustainable Development in Johannesburg South Africa and launched the Global Gas Flaring Reduction (GGFR) Initiative, principally to tackle the problem of global gas flaring. In this research, a decline rate of -13% is applied over the 20-year period of power plant life, beginning from Year 2015. The plant is deemed to be operating for 8000 hours per year, utilizing AG as fuel (with the LHV of 41MJ/Kg kept constant), and a URR of 40,000m<sup>3</sup>/day per well as suggested by the team of World Bank experts.

Figures 5-5 to 5-7 show the expected trends as power available falls with reduced fuel availability, resulting in increased redundant engines and by extension redundant power.

## 5.7 Resource Decline Implemented on GGFR Code

Number of oil wells	One
Operating hours per year	8000
Year in which the first AG will be used	2015
Resource Decline implemented for 20 years	-13% per year

Year	2015	2016	2017	2018	2019
AG Quantity (m <sup>3</sup> /day)	40,000	34,800	30,276	26,340	22,916
AG Quantity (MMSCFD)	1.4	1.22	1.06	0.92	0.8
LHV of AG (MJ/kg)	41	41	41	41	41
Power(MW)	19.2	16.7	14.5	12.7	11
Power Loss (MW)	0	2.5	2.2	1.8	1.7
Redundant Power(MW)	0	2.5	4.7	6.5	8.2

Year	2020	2021	2022	2023	2024
AG Quantity (m <sup>3</sup> /day)	19,937	17,345	15,090	13,128	11,421
AG Quantity (MMSCFD)	0.7	0.61	0.53	0.46	0.4
LHV of AG (MJ/kg)	41	41	41	41	41
Power(MW)	9.6	8.3	7.2	6.3	5.5
Power Loss (MW)	1.4	1.3	1.1	0.9	0.8
Redundant Power(MW)	9.6	10.9	12	12.9	13.7

Year	2025	2026	2027	2028	2029
AG Quantity (m <sup>3</sup> /day)	9936	8645	7521	6543	5692
AG Quantity (MMSCFD)	0.35	0.3	0.26	0.23	0.2
LHV of AG (MJ/kg)	41	41	41	41	41
Power(MW)	4.8	4.2	3.6	3.1	2.7
Power Loss (MW)	0.7	0.6	0.6	0.5	0.4
Redundant Power(MW)	14.4	15	15.6	16.1	16.5

Year	2030	2031	2032	2033	2034
AG Quantity (m <sup>3</sup> /day)	4952	4309	3749	3261	2837
AG Quantity (MMSCFD)	0.17	0.15	0.13	0.11	0.1
LHV of AG (MJ/kg)	41	41	41	41	41
Power(MW)	2.4	2.1	1.8	1.6	1.4
Power Loss (MW)	0.3	0.3	0.3	0.2	0.2
Redundant Power(MW)	16.8	17.1	17.4	17.6	17.8

As crude oil declines, the AG obtained from it also declines. That will result in a corresponding reduction in the available power from gas turbines used for power generation with AG. Figure 5-5 shows the expected trend as power available falls with reduced fuel availability, resulting in increase in redundant engines and by extension redundant power.

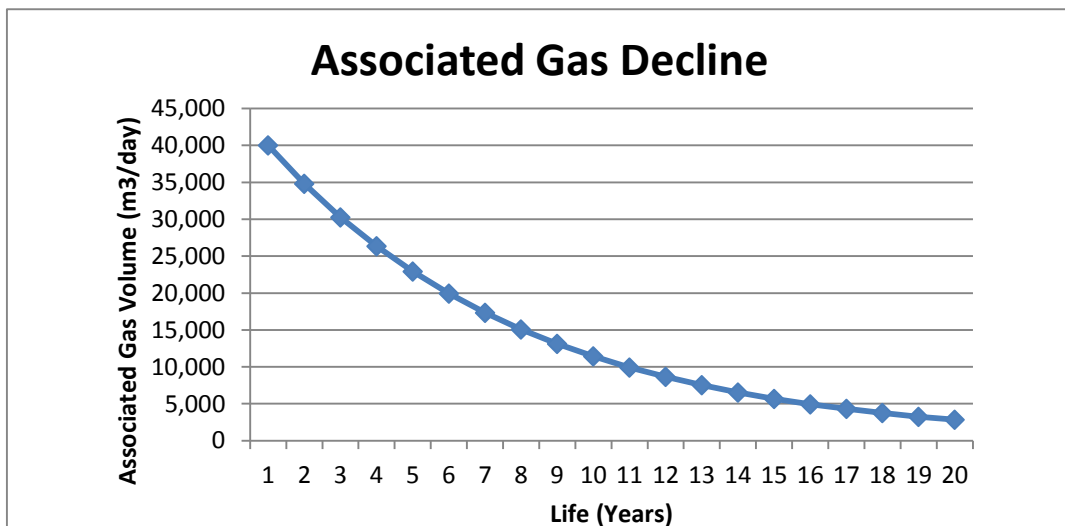


Figure 5-5: Associated Gas Decline over Time

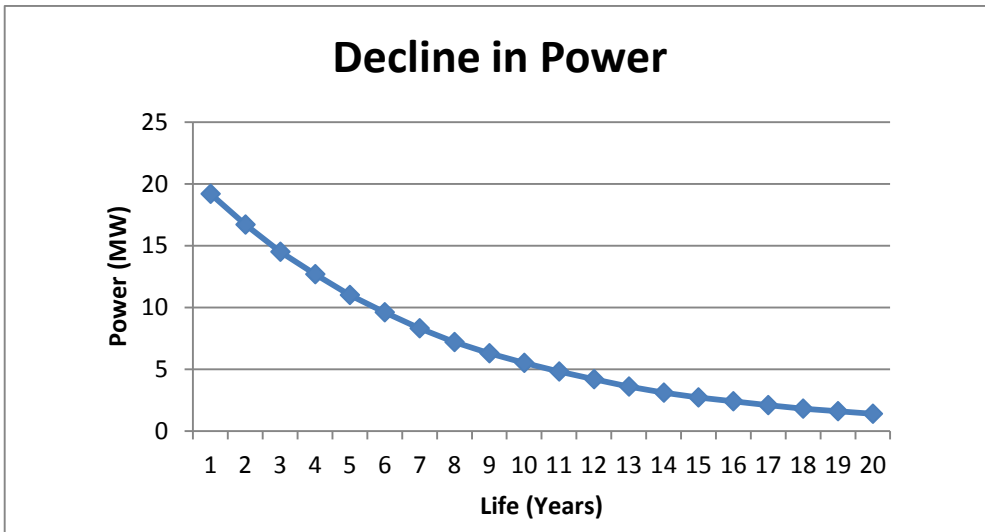


Figure 5-6: Decline in Power over Time

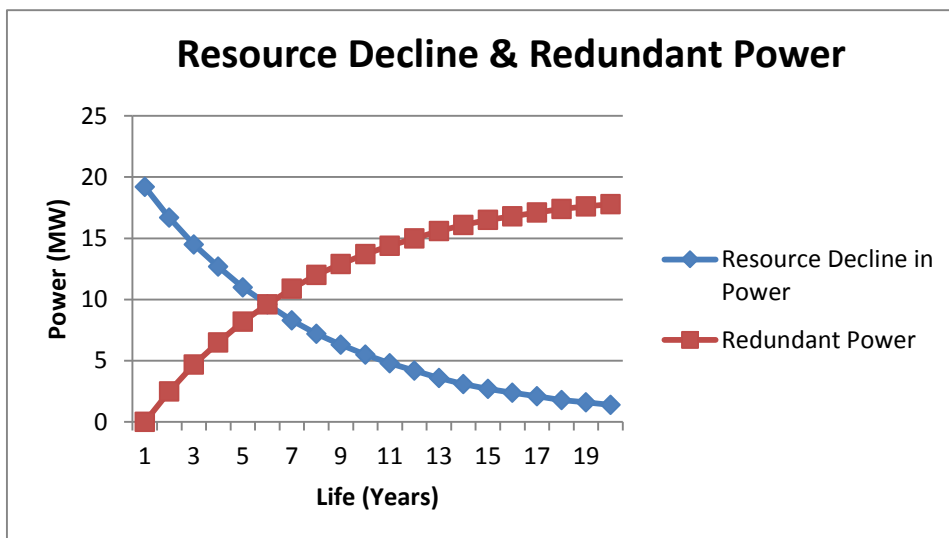


Figure 5-7: Resource Decline and Engine Redundancy

In the next section, a genetic algorithm will be used for divesting the redundant engines as a way of improving the overall return on investment in a power plant utilizing AG.

### 5.9 Uncertainties in the Ultimately Recoverable Resource

In exploring uncertainties with the URR, MCS was carried out using Palisade's @RISK software. A deterministic value of 40,000m<sup>3</sup> was inputted as most likely, with a lower limit of 20,000m<sup>3</sup> and an upper limit of 60,000m<sup>3</sup> on a Pert Distribution. The results presented in Figures 5-8 and 5-9, show an 89%

probability of the URR dropping from 34,800m<sup>3</sup> to 2,837m<sup>3</sup> while the power derivable could fall from 16.7MW to 1.4MW over the 20-year period.

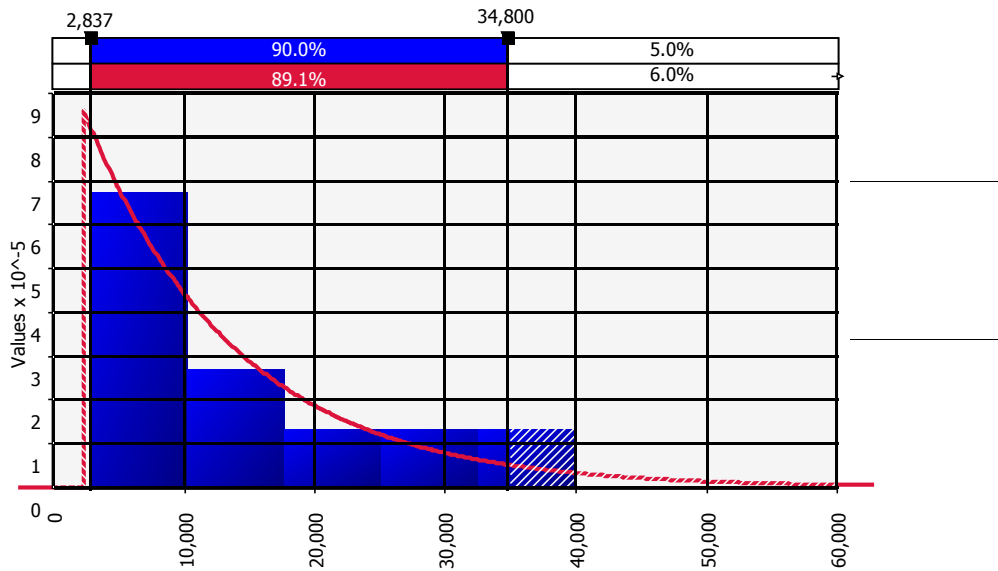


Figure 5-8: Resource Decline Range in Cubic Meters

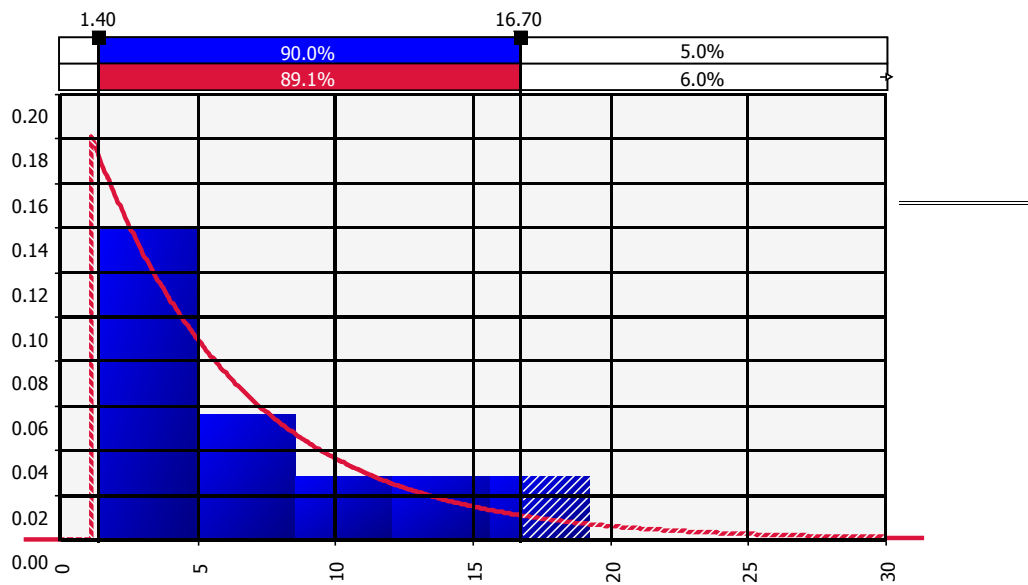


Figure 5-9: Power Decline Range in MW





## **CHAPTER 6: OPTIMIZATION, ECONOMICS & RISK ANALYSIS**

### **6.1 Introduction**

Before undertaking an investment, its cost effectiveness needs to be ascertained. It is difficult to predict specific values for capital, O&M and other costs; hence assumptions have to be made, thereby increasing the level of uncertainty. Even prevailing costs cannot be adequately captured by deterministic values, except by building in a factor of safety to compensate for volatility of prices. Uncertainties beset future costs, particularly as new technologies are introduced and fuel prices change. To tackle this problem, Monte Carlo Simulation would be used to model uncertainties.

In order to set the stage for a thorough economic model, there is need to decide on the appropriate engine mix by carrying out the optimization using MATLAB genetic algorithm (GA).

### **6.2 Optimization**

#### **6.2.1 Genetic Algorithm for Optimization**

GA is based on the mechanics of natural selection. It transforms a population of individual objects each with a fitness value, into a new generation of population, using Darwin's principle of survival of the fittest. It also uses analogues of naturally occurring genetic operations such as crossover and mutation.

GA uses encoded parameters, and searches for solutions from a population, not just from a point; it uses stochastic rather than deterministic parameters. When employed as part of an optimization routine, each possible point in the search space of a problem is encoded. The GA then attempts to find the best solution by genetically breeding a population of individuals over a number of generations. GA is suitable for optimizing power plants as it would often times define the properties of the most cost effective equipment to guide purchase decisions; and help determine the minimum life cycle costs. The aim of this section is to optimize a fleet of GT engines for power generation, based on specified load ranges.

The plant consists of 5 GTs of varying sizes and outputs. The central focus of the optimization is to minimize the electricity cost, meet the required load, select the engines to run the plant efficiently, and stipulate the time to divest engines that become redundant due to fuel shortage. The definition of the GA problem was done by first specifying the number of variables, domain boundaries and assumptions.

The optimization employed mutation and/or crossover. MATLAB's global optimisation toolbox makes use of inputs from the Performance, Emissions and Economic Module.

### **6.2.2 Data and Conditions for Optimization and Divestment**

The fleet of engines is made up of two heavy duty single shaft GTs of capacities 226MW and 120MW respectively, three aero-derivative multiple shaft GTs with capacities of 100MW, 41MW and 25MW respectively. Five variables were thus used in the optimization designated as SS94, SS9E, LM1H, LM6K and DS25.

The design space is specified by the domain boundaries. This was done by considering the least number and the maximum number of each engine that can possibly be used to satisfy the power requirement. The boundaries were thereby set as [0, 4], [0, 8], [0,10], [0, 20] and [0, 38] for the SS94, SS9E, LM1H, LM6K and DS25 respectively.

The plot options selected are good for convergence; a population size of 10,000 for better exploration and wider design space coverage; a generation of 500 for the solver to have enough time for simulation.

From the URR, the various engines in the fleet would consume the amount of fuel required in a year as specified by the fuel flow and the number of each engine type in the plant. Yearly Fuel Consumption per engine is given by:

- SS94\_YearlyConsumption = 448,100,241 kg
- SS9E\_YearlyConsumption = 255,451,142kg
- LM1H\_YearlyConsumption = 157,865,639kg
- LM6K\_YearlyConsumption = 74,394,217 kg
- DS25\_YearlyConsumption = 47,467,952kg

The total weight of fuel for the fleet of engines is rounded off to 1,000,000,000kg (about 120.9MMSCFD). Consequently, 1e9 was set as the URR to be fed into the GA. The composition of the engine fleet must not be changed, but the number of individual engines making up the plant could be changed by the GA.

The following conditions were assumed and encoded:

- Fuel declines at 13% per annum; over a 20 year life span
- Calculation of the number of engines starved of fuel, hence needing to divest
- Time't' to divest engine(s) from the fleet to be calculated
- Engines with smaller capacities to be divested first, as fuel declines
- As much power as possible should be gotten out of the plant at any time within the range of 450-500; 501-700; 701-950MW; while providing an opportunity for the best combination of heterogeneous engine mix.
- Need to cater for revenue from divested engines
- There shall be no divestment in the first year, when initialization is implemented
- The best power plant is the one with the most economical engine mix
- Availability of fuel determines the progression to the next year

It is an established fact that matter is neither created nor destroyed. Thus by sheer energy balance, it is obvious that CO<sub>2</sub> that would have been emitted at flare site would still be emitted via the exhaust gas even after harnessing AG for power generation in a GT.

The solver which minimizes the CoE for each power demand finds the minimum value of the objective function, subject to the constraints imposed. Using MATLAB Optimization Toolbox, the objective function was entered, constraints specified and initial conditions stated. The search population comprises a combination of engines, various configurations of plants, the purpose of the search being to get the most cost-effective plant.

### **6.3 Divestment Sub-Routine**

A divestment sub-routine was created to cater for fuel decline and divestment of redundant engines. Divestment of engines as fuel resource decline is shown and the time to divest is calculated by the optimizer. For a high degree of accuracy, the population size was increased to ensure that it runs long enough to achieve good convergence: 10,000 individuals with a 500 generation limit.

A script that spells out the divestment pattern was written with the aim of divesting smaller GT units in the order DS25, LM6K, LM1H, SS9E and SS94. The sub-routine works with fuel quantity in the current year for the present engine configuration.

In order to bring out the divestment pattern, which depends on the commencement of decline, an initial fuel quantity that is just enough to serve the engine mix is used. Using the MATLAB Script at Appendix E, the fuel requirement is calculated and rounded up to 1,000,000,000 kg/year (3424658m<sup>3</sup>/day or 120.9MMSCFD). This value was therefore adopted for all scenarios.

For the purpose of selecting the best engine mix in a utopian setting that portrays the true life situation in Nigeria, where AG is currently being flared, two important assumptions are made. One, the flare gas when collected for use as fuel is free of charge. Two, emissions tax is currently not being levied in Nigeria for flaring; hence emission tax is set at zero. These two assumptions are strictly for the purpose of simulations to get the best engine mix. In the economic analysis, gas collection costs and emission tax will be considered. The script for Fitness with Divestment is at Appendix F. The variable definition items per engine that were entered include power output, fuel cost, maintenance cost, and capital cost.

### **6.4 Scripts for Divestment and Optimization**

A script to specify the fitness function for possible yearly divestment was developed. Fitness was defined to cater for resource decline per year, for a particular plant configuration. The aim is to divest the smaller engines, depending on fuel availability. The MATLAB function for the divestment pattern at Appendix G is a repetitive subroutine; that is, it runs itself as many times as needed, making

the check for fuel availability, divesting one engine at a time, re-checking and re-divesting more engines if need be. This it did for the entire 20 years. The optimization was implemented by the script at Appendix H which sort of brings everything together, considering the various individual engines, the power ranges and specified boundaries. It employs the *gaoptimset* as spelt out in the script.

## **6.5 Penalization**

The fitness was programmed to be penalized if it goes outside the specified power range. A penalizing factor was therefore introduced to discard a potential individual that falls outside the power requirement. See Appendix I for the Penalization Script. Results of the GA optimisation are presented hereunder.

## 6.5.1 First Simulation Run for Optimization and Divestment

### Simulation at Discount Rate of 5%

- a. Range: 450-500MW
- b. Fuel: 1e9
- c. Decline: 13%
- d. Life: 20 Years
- e. Hours: 8000
- f. Population 10,000; Generation 500

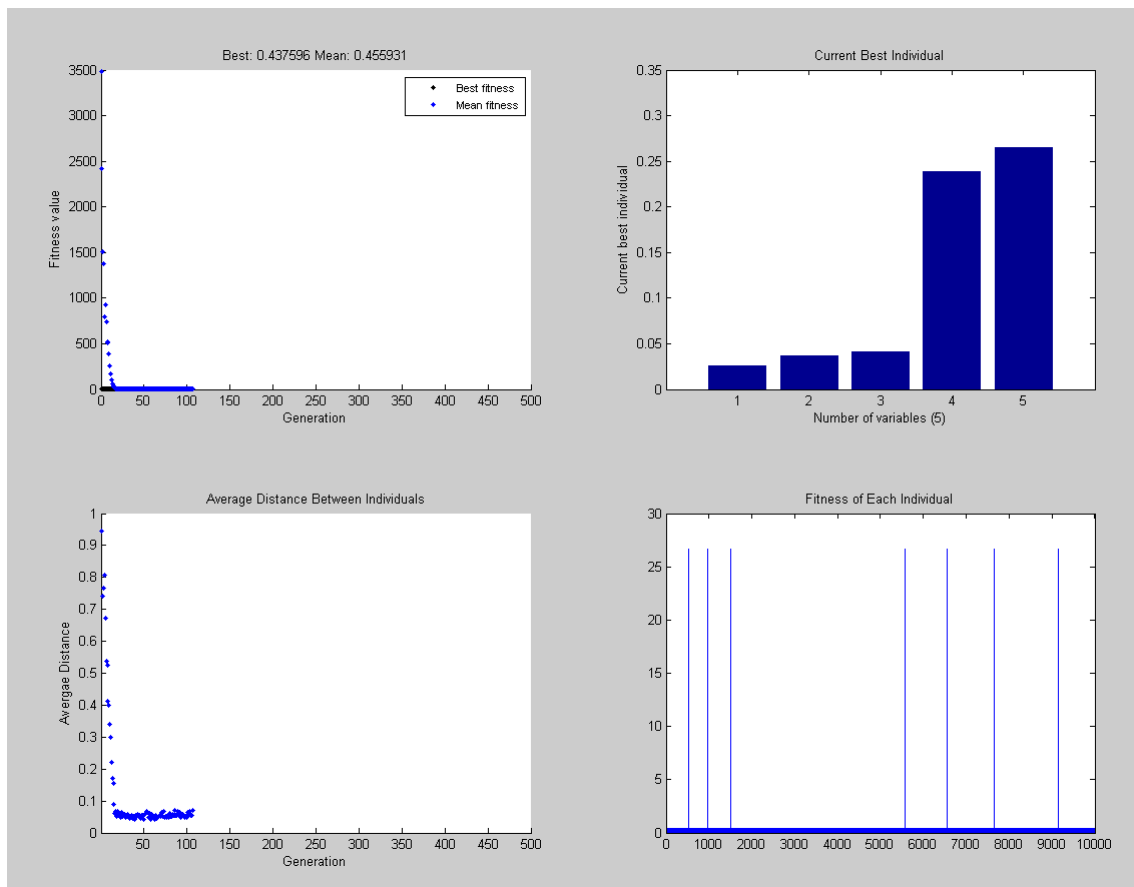


**Figure 6-1: Best Individual, Fitness, Average Distance**

The pictorial representation of the results in Figure 6-1 show the current best individual, the fitness value, the average distance between individuals over the generation, and the fitness of each individual out of the 10,000 considered.

Top right, the histogram shows the selection of the best plant in the order: Engine 1 (SS94), Engine 2 (SS9E), Engine 3 (LM1H), Engine 4 (LM6K) and Engine 5

(DS25). The solver selects the highest number of DS25, followed by LM6K as can be seen in the detailed result.

The histogram top left shows the fitness value of the CoE presented as Best Fitness and Mean Fitness, from relatively high values which were refined from generation to generation as the simulation progressed. Good convergence was achieved from about Generation 20 which became consistent up till the stall limit at Generation 100. The result is particularly good as convergence was achieved within 20% of the available 500 generations in the design space.

Bottom left, shows the average distance between individuals as the simulation progressed. Here again, very good convergence was achieved at the 100<sup>th</sup> generation.

Bottom right represents the fitness of each individual. Out of a total of 10,000 individuals, the plot shows very few individuals that are not in line numbering about 7 scatters only, which is such a small number that the simulation can be adjudged very accurate.

	1	2	3	4	5	6	7	8	9	10
1	0	0	0	5	10					
2	0	0	0	5	10					
3	0	0	0	5	10					
4	0	0	0	5	8					
5	0	0	0	5	6					
6	0	0	0	5	4					
7	0	0	0	5	2					
8	0	0	0	5	1					
9	0	0	0	5	0					
10	0	0	0	4	0					
11	0	0	0	3	0					
12	0	0	0	3	0					
13	0	0	0	2	0					
14	0	0	0	2	0					
15	0	0	0	2	0					
16	0	0	0	1	0					
17	0	0	0	1	0					
18	0	0	0	1	0					
19	0	0	0	1	0					
20	0	0	0	1	0					
21	0	0	0	0	0					

**Figure 6-2: Current Configuration**

The screen shot at Figure 6-2 shows a matrix presenting the current configuration of the plant, and how redundant engines are divested progressively over time. The first column shows the years from 1 to 21; that is, from commission to the full 20 year lifespan. The first row shows the number of each engine type at the commencement of operations. The best configuration of power plant is given by [0, 0, 0, 5, 10], that is 5 units of LM6K and 10 units of DS25.

Subsequent rows show the progression with time and the reduction in numbers of each type of engine. A beautiful thing about this matrix is that it helps to specify the year in which the divestment takes place and the number of engines as well as the type of engines. This clearly shown in Figure 6-3.

	1	2	3	4	5	6	7	8	9	10
1	0	0	0	0	0					
2	0	0	0	0	0					
3	0	0	0	0	0					
4	0	0	0	0	2					
5	0	0	0	0	2					
6	0	0	0	0	2					
7	0	0	0	0	2					
8	0	0	0	0	1					
9	0	0	0	0	1					
10	0	0	0	1	0					
11	0	0	0	1	0					
12	0	0	0	0	0					
13	0	0	0	1	0					
14	0	0	0	0	0					
15	0	0	0	0	0					
16	0	0	0	1	0					
17	0	0	0	0	0					
18	0	0	0	0	0					
19	0	0	0	0	0					
20	0	0	0	0	0					
21	0	0	0	1	0					

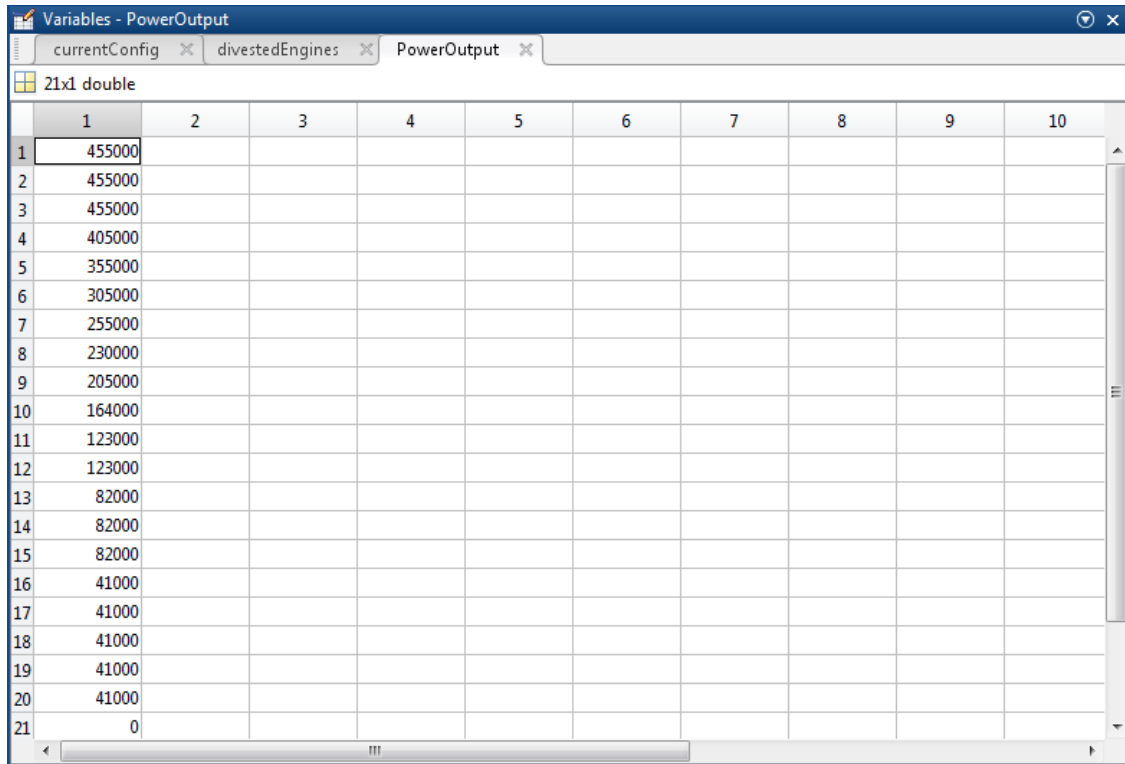
**Figure 6-3: Divestment of Redundant Engines**

The screen shot shows a matrix presenting the number of engines of each type divested and in what year the divestment is expected to take place. The divestment pattern is as shown in the matrix above. Divestment begins in the 3<sup>rd</sup> year of operation with 2 units of DS25, for 4 consecutive years; then 1 unit of DS25 divested in the 7<sup>th</sup> and 8<sup>th</sup> year ; thereafter, 1 unit each of LM6K divested in the 9<sup>th</sup>, 10<sup>th</sup>, 12<sup>th</sup> and 16<sup>th</sup> years. The last unit of LM6K will be divested in the 20<sup>th</sup> year.



## Power Output

The power churned out over the 20 year period is as shown by the matrix in Figure 6-4 below.



	1	2	3	4	5	6	7	8	9	10
1	455000									
2	455000									
3	455000									
4	405000									
5	355000									
6	305000									
7	255000									
8	230000									
9	205000									
10	164000									
11	123000									
12	123000									
13	82000									
14	82000									
15	82000									
16	41000									
17	41000									
18	41000									
19	41000									
20	41000									
21	0									

**Figure 6-4: Power Output**

The screen shot above gives the year-by-year power output from the plant. It is worth mentioning here that, since engines are being divested over time, power output is reduced through the years. In order to calculate a realistic CoE, the average power output for the whole plant is used. Consequently, the Power Average is calculated as can be seen on the workspace summary on previous screen shots.

Other power ranges and discount rates were also simulated and the results are presented in Appendices J - N. The explanation follow the same pattern as the preceding results of the first simulation run.

## Deductions from Optimization

In all scenarios, the simulation underscored the fact that the fitness for each individual out of 10,000 was accurate as only a few scattered ones were noticed; corroborating good convergence as evidenced by the distance between individuals.

Out of a generation of 500 that was set, the simulations stalled at the 100<sup>th</sup> generation after consistent convergence for almost the whole stretch, attesting to a stable fitness value.

The current best individuals for all scenarios were adjudged to be DS25 and LM6K from all 5 variables. Irrespective of the discount rate that was used, the engine mix for optimum results was the same for each power range. The number of LM6K for all three power ranges remained at 5. However, the solver picked different figures for the DS25 as shown in the table below.

**Table 6-: Best Engine Mix for Power Plant Per Range**

Power Range	450-500MW	501-750MW	751-950MW
LM6K	5	5	5
DS25	10	12	22

For the purpose of a detailed economic analysis, only the first category will be considered, that is 5 units of LM6K and 10 units of DS25. However, there is need to work out the emissions before going into the economic analysis.

## 6.6 Emissions and the Environment

The difficulty encountered in trying to store electricity, underscores the need for production to meet demand. This results in start-up and shut-down of generating units, hence the continued production of emissions. Fossil fuels constitute the major source of air pollution, acid rains and global warming. Reduced fossil fuel consumption by power plants would result in reduced emissions, but there is an

overriding need to increase power generation as world population soars and industrialization grows.

There are concerns about increased methane emissions resulting from drilling for oil and natural gas, with conflicting estimates about how much methane is produced. AG is methane rich and that makes it a resource capable of bringing in millions of Dollars from electricity generated. Methane as a powerful greenhouse gas released by landfills and leaks from oil and gas production is 21 times more potent a greenhouse gas than CO<sub>2</sub> on a molecule-to-molecule basis (Steed Jr and Hashimoto, 1994). In Nigeria, huge amounts of methane and other gases are flared during oil production, wasting millions of Dollars and contributing to air pollution and global warming.

### **6.6.1 Gas Turbine Pollutant Emissions**

Meeting low pollutant emissions targets is highly dependent on the design of both the engine cycle and the type of combustor which are in turn influenced by the type of fuel used (Singh, 2001). The main components of GT exhaust gases are CO<sub>2</sub>, CO from partial combustion; NO<sub>x</sub>, from high temperatures; SO<sub>x</sub>, usually from fuel bound sulphur; unburnt hydrocarbons (UHCs) and solid particulates. NO<sub>x</sub> increases exponentially with combustor firing temperature (though NO<sub>x</sub> emissions can be curtailed by lowering firing temperatures, which would lead to an increased production of CO<sub>2</sub> and UHCs).

### **6.6.2 CO<sub>2</sub> Emissions Prediction by Hephaestus**

Cycle efficiency, combustor geometry and fuel type affect the amount of emissions produced. Assuming complete combustion, CO<sub>2</sub> emission will depend on the type, quality and quantity of fuel used. To calculate CO<sub>2</sub> emission, the simplest basic combustor geometry, fuel type, residence time, and combustion efficiency are used. The output of the performance module provides information on the operating conditions— combustor exit temperature and pressure ( $T_3$ ,  $P_3$ ), LHV of the fuel, and the proportion of air in the primary zone.

This section employs Hephaestus, a code developed in Cranfield University to predict the CO<sub>2</sub> emissions. Chemical reaction in the combustor of a gas turbine requires O<sub>2</sub> from the air and fuel, to produce CO<sub>2</sub> and H<sub>2</sub>O. N<sub>2</sub> from the air combines with O<sub>2</sub> to produce NO<sub>x</sub> while Carbon in the fuel mixes with Oxygen to form CO<sub>2</sub>, and CO from incomplete combustion.

Hephaestus utilizes the temperature, pressure, airflow, fraction of air in flame front, fraction in the primary zone, intermediate zone, fraction in the dilution zone, and fuel flow. The software calculates the chemical reaction at each level: flame front, combustion as well as the dilution zone, and combines all the emissions that come out of the reaction. The executable file that is created within Hephaestus is utilized in the NASA CEA code and the results are displayed in the output file.

Following are the results of emissions predicted for the fleet of engines under consideration.

**Table 6-1: Emission Prediction for the DS25 and LM6K Engine Sets**

Natural Gas		
EICO <sub>2</sub>	EINO <sub>x</sub>	Power(MW)
2821.605	12.80678	25.02
2821.805	12.40885	23.79
2821.392	11.27294	23.61

Natural Gas		
EICO <sub>2</sub>	EINO <sub>x</sub>	Power(MW)
2825.617	21.28929	40.8
2826.069	20.44163	38.6
2825.662	18.43123	38.2

Associated Gas	
EICO <sub>2</sub>	EINO <sub>x</sub>
2833.715	12.79896
2833.915	12.40125
2833.502	11.26606

Associated Gas	
EICO <sub>2</sub>	EINO <sub>x</sub>
2837.723	21.2758
2838.175	20.42868
2837.769	18.41961

### **6.6.3 Comparison of CO<sub>2</sub> Emission Cost Results**

When compared with the hand calculation at Appendix P, the results are within acceptable limits for the study engines and are therefore deemed correct. The results also show that there is a higher amount of CO<sub>2</sub> emission with the AG than NG.

## **6.7 Economic Appraisal Method**

The appraisal method that used to enhance the decision making process is the Discounted Cash Flow (DCF). DCF considers the time dependent value of money, while predicting cash inflows and outflows over the life of the project. That is, cash inflows and outflows that happen in future are discounted back to their present values (Arnold, 2008). Financial investments are usually evaluated in terms of Net Present Value (NPV), Internal Rate of Return (IRR) and Pay Back Period (PBP).

The best estimates are calculated for each input variable based on information in the open domain, though actual cash flows could differ considerably from forecasts. Thereafter, the economic analysis is carried out on a yearly basis using the DCF model and the performance indices are quantified to see the merits and demerits of the investment.

Among the key variables capable of significantly affecting the economic performance are the capital cost, fuel price and CO<sub>2</sub> emission tax. Fuel cost contributes the highest figure and is usually accounted for separately. Ideally, the annual tax comprises two parts: tax on the profit and levy on emitted CO<sub>2</sub>. The carbon tax is proportional to the mass of CO<sub>2</sub> emissions, while the revenue of a power station comes from the electricity generated and sold to the grid.

Risk variables would be identified, a probability distribution specified for each, and different input values would be selected therefrom. These probabilistic and deterministic values would be used in the model to assess the project's performance. As iterations are repeated and converge, a probability distribution with the best solution is predicted. The output distribution set up as the key

outcome parameters is NPV. The NPV and other economic appraisal techniques are explained below.

### **6.7.1 Net Present Value**

NPV is a discounting technique used to ascertain how profitable an investment is. It is calculated by discounting future cash-flows, using an interest rate and adding the discounted cash flows to the initial capital investment cost. The bigger the NPV, the greater the profit and the more attractive the project is.

### **6.7.2 Internal Rate of Return**

The IRR is the value of the discount rate that equals the cost of an investment with the subsequent net cash-flow over a number of years that result from the investment. It is the discount rate at which NPV is equal to zero; that is, the discount rate that gives the cash flow for a project, a zero NPV. A project is acceptable if its IRR exceeds the required rate of return for the project.

### **6.7.3 Pay Back Period**

The PBP is the period that must elapse for a project to recover its investment cost. This is a measure of the time required to recover the initial investment, a measure of the liquidity warranted by the investment as it gives the analyst an idea of the duration that the invested cash is at risk.

## **6.8 The Economic Model**

One very important factor affecting the selection of a thermal system design is the cost of the final product (Bejan and Moran, 1996). Costs can be fixed or variable. Fixed costs do not depend on production schedule, e.g. depreciation, taxes, rent. Variable costs, on the other hand, change as production volume changes, e.g. cost of materials, fuel and labour.

Cost elements under consideration are capital investment, operating and maintenance cost and other subsidiary costs. The resultant value of these costs determines the final cost of electricity, which gives an idea of the viability of the project. The cost elements are explained briefly below.

### **6.8.1 Capital Costs**

Capital cost encompasses equipment, installation and project costs. The prime mover, heat recovery system, exhaust gas system, fuel supply control, interconnection with the electric utility, piping, ventilation and combustion air systems, shipping charges and taxes make up the equipment cost. The specific capital cost from the open domain is \$973/kWh (US EIA 2013).

### **6.8.2 Operation and Maintenance Costs**

As the name implies, O&M costs consist of operation and maintenance costs which include cost due to downtime and cost of components for replacement. O&M is often times considered as a percentage of the capital cost, for both the fixed and variable components, a simplification that is used as a first estimate.

The non-fuel O&M cost comprises a fixed and variable component as well as major maintenance cost. Fixed O&M costs are expenses incurred at a power plant that do not vary significantly with generation, for example routine preventive and predictive maintenance or staffing and monthly fees. Variable O&M costs are production related costs that vary with electrical generation, examples of which are the acquisition and supplies of consumables, lubricants and chemicals. Major maintenance expenses generally require extended outages, typically undertaken once a year, such as scheduled major overhaul.

### **6.8.3 Fuel Cost**

Fuel cost which is the major operating cost for thermal power plants is a function of the fuel quality and tariff structure. Natural gas prices are a function of market supply and demand. Due to limited alternatives for natural gas consumption or production, changes in supply or demand over a short period often result in large price movements to bring supply and demand back to equilibrium.

In Nigeria, the domestic price of NG has been increased to \$1.5 per 1,000 standard cubic feet (SCF) with a view to ensuring an efficient supply of NG to thermal power stations nationwide. Power producers account for about 80% of the domestic gas consumption. These prices are, however, below the

international market price for gas, which is about \$3 per 1,000 SCF (Chuks Isiwu, 28 January 2014, Sweet Crude, Lagos). Fuel cost is not considered in this work because flare gas, which is currently being wasted would be utilized free of charge. However, there are gas collection costs to account for the Flare Gas Recovery System that would be employed or procured.

## **6.9 Cost of Power Generation**

The initial capital cost is usually the highest expenditure. The greatest operational cost would normally be fuel burn. Future incomes could be under conditions different from the ones perceived during the project evaluation. Costs such as gas collection costs are deemed to be part of the cost of acquisition of machinery.

In the course of the project life, there will be two financial streams: the cost stream (capital and operational costs) and benefits stream; the cost stream being an outward flow of cash. The life cycle costs of a project depend mainly on the capital investment cost, O&M cost and the discount rate used.

### **6.9.1 Cost of Electricity**

Levelized Cost of Electricity (LCOE) is frequently used in evaluating electricity produced by GT systems such that if every unit of electricity produced were sold at the LCOE, the project would break even and the NPV would be zero. LCOE operates on the assumption that the interest rate used for discounting costs and revenue does not change throughout. Also, that electricity price does not vary throughout the life of the project. LCOE, widely used for comparing the costs of different power generation technologies; considers capital cost, fuel cost, O&M cost and emission cost.

Levelized costing is adopted in the present research due to its simplicity and the ease with which varying costs over the lifespan of the project are made constant. An annuity factor is applied on the capital, O&M, emission and the fuel costs to give the levelized cost of electricity, as shown in Equation 6-1. Levelized costing uses the time-value of money to normalize a number of varying quantities over a specified time period.



$$LCOE \left( \frac{\$}{kWh} \right) \tag{6-1}$$

$$= \frac{CapCost + \sum_{i=1}^n \frac{FuelCost}{(1+r)^i} + \sum_{i=1}^n \frac{MaintCost}{(1+r)^i} + \sum_{i=1}^n \frac{EmissionsCost}{(1+r)^i}}{Total\ Power * Operating\ Hours}$$

The annual cash flow for the entire life of the plant was computed where degraded performance data generated from TurboMatch served as inputs. Three levels of degradation (slow, medium and fast) were implemented, and the resulting model is capable of calculating the revenue generated and the cost of electricity over a 20-year lifespan, at a discount rate of 10%.

## 6.10 Economic Analysis

An economic code developed on Microsoft Excel was used to carry out the calculations for slow, medium and fast degradation scenarios. Some parameters used for the economic analysis are as specified in Table 6-1; details are at Appendices Q and R. A Creep Life Estimation Code was equally used to assess the life consumption as a result of degradation due to AG usage in slow, medium and fast scenarios; details are at Appendix S.

**Table 6-2: Data & Assumptions for Economic Analysis**

Parameter	Figure	Unit
Power Range	450-500	MW
Capital Cost	973	\$/kW
Electricity Price	0.09	\$/kWh
Discount Rate	10	%
Capacity Factor	8000	Hours/year
Plant Life	20	Years
Electricity Price Escalation	5	%
O&M Cost Escalation	3	%

### 6.10.1 Assumptions and Data for Associated Gas Utilization

- Decline curve analysis discussed in Chapter 5 reveals the likely onset of resource shortage which compels the plant to operate below its rated

power output. An increase in the cost of electricity will be a consequence of the production decline from reduced fuel.

- Performance simulation on TurboMatch of the fleet of study engines furnishes inputs for the economic analysis.
- The economic module calculates the cost of electricity expressed as NPV.
- Multiple engine units of different capacities and configurations are considered so that redundant units can be retired and/or divested
- Carbon Emission Index is 2.75KgCO<sub>2</sub>/Kg fuel, (AMY Razak, Industrial Gas Turbines: Performance & Operability, 2007).
- Exponential Decline of Crude Oil from Giant Fields occurs at -13%. This was adopted from the collaborative studies that were based on cost data provided from over 130 power plants. The calculations took the levelized lifetime cost approach, using generic assumptions for the main technical and economic parameters as agreed upon by an ad hoc group of experts from the World Bank.

Results from the economic analysis will be presented separately for the DS25 and LM6K engine sets. For the DS25 engine set, the NPV falls steadily from DP to slow degradation, to medium, to fast degradation, the maintenance cost increased from the beginning. The major maintenance cost increased progressively with degradation. For the fast degradation scenario, major maintenance cost is more than doubled the value for each of the other cases. The emissions tax in all cases was almost constant.

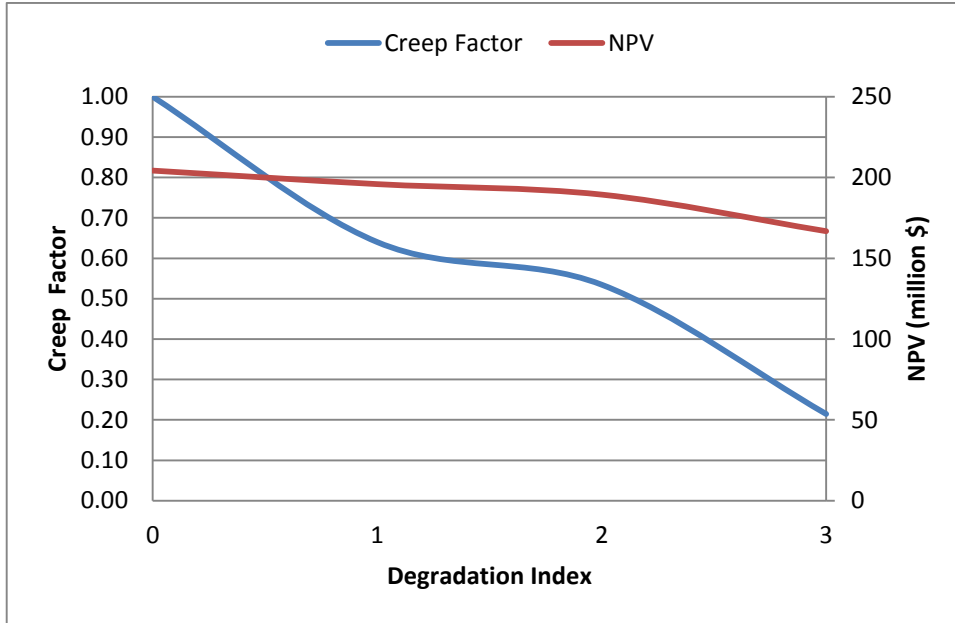


**Figure 6-5: Variation of NPV with Degradation for DS25**

As degradation increases, the creep life falls and the NPV decreases as well (Figure 6-5).

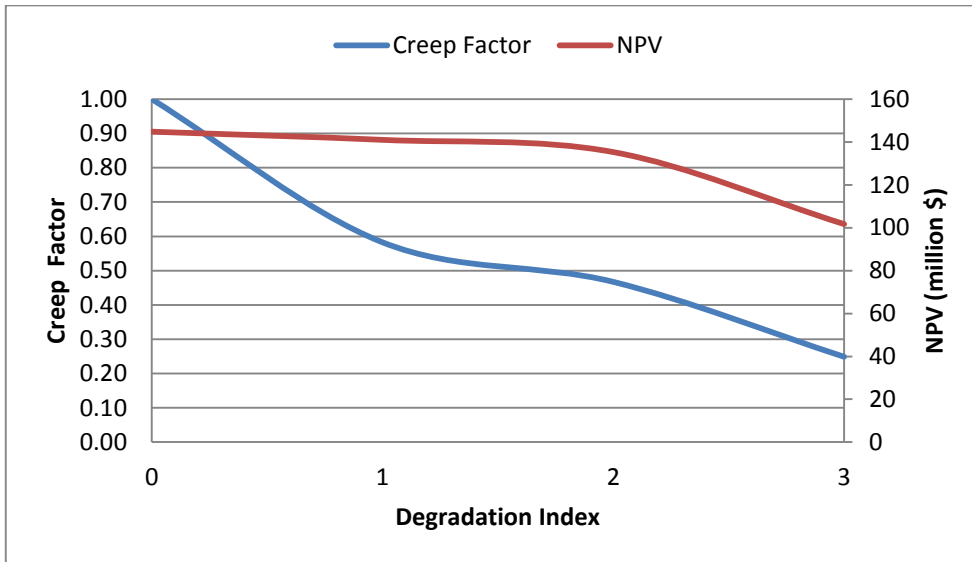


**Figure 6-6: Variation of NPV with Degradation for LM6K**

For the LM6K engine set, as degradation rate increased, the creep life falls and the NPV falls (Figure 6-6).

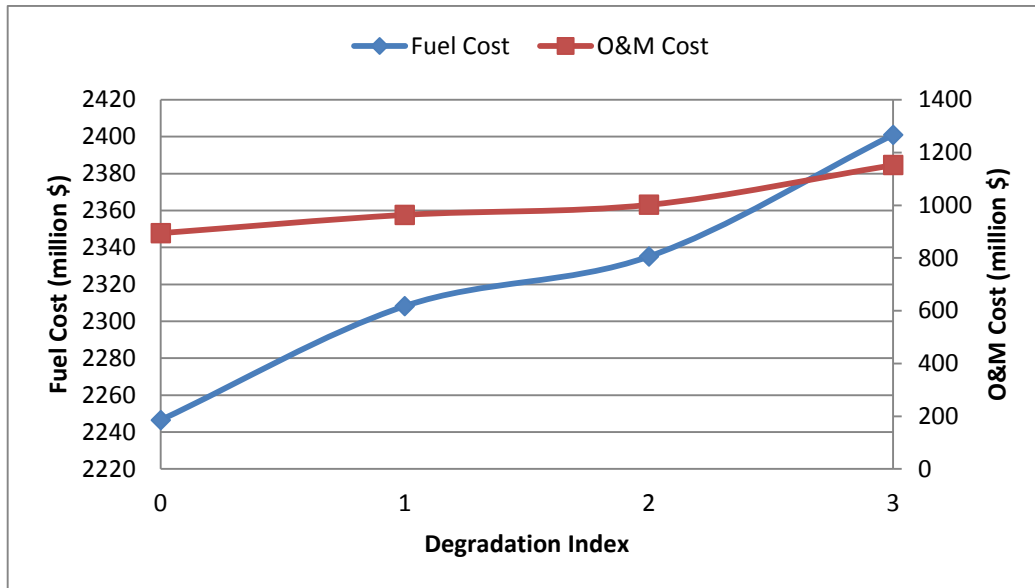


**Figure 6-7: Variation of Fuel/O&M Cost with Degradation for LM6K**

Gas collection cost increases with increase in degradation, much as the O&M Costs increases (Figure 6-7).

## 6.11 Risk Analysis

Risk is viewed in the sense that the future is uncertain; hence there is no guarantee of a particular return on investment. Returns can be quantified in terms of cash, but risk is a measure of uncertainty and volatility of returns. It is the probability that a project does or does not achieve its objectives of cost (profit, performance and schedule).

Risk management involves the plan, identification, analysis, monitoring and control of the risks in a project; it encompasses the processes involved in maximizing the probabilities and consequences of opportunities and minimizing the probabilities and consequence of adverse events. Risk can be expressed in a measurable way such as down time, availability, reliability, cost; and is usually given a numeric value for the purposes of comparison. These are often times point estimates which may not be accurate. Risk analysis in this research is done using the software @RISK.

Rather than use deterministic estimates, @RISK uses a range of possible values to reduce the errors that might arise from uncertainties. The software also has the capacity to capture correlations between input variables. That way, investment decisions can be made with uncertainty in mind, such that the decision maker is better prepared for unexpected exigencies. One understands what could happen and can predict how likely it is. It operates with 3 point estimates and takes samples from the selected distribution into the model to generate a range of results that could be in the form of:

- Probability distribution of cost.
- Probability distribution of revenue.
- Probability distribution of duration.
- Probability distribution of rates.

The necessary steps are to determine the uncertain components, then convert them to ranges using probability distribution. Thereafter, the simulation is run to generate thousands of scenarios for each uncertain input. @RISK employs computational Monte Carlo Simulations (MCS) as a way of modelling uncertainty and revealing its potential consequences. MCS stores results in designated output cells as the simulation runs, then reports them in various graphical and tabular formats. It is a sampling technique meant to estimate the probability of key performance outcome variables that depend on uncertain input variables. @RISK uses the following in its analysis:

- The most likely input
- The optimistic scenario by incorporating future parameters that are more favourable than they seem at the time of evaluation
- The pessimistic scenario that expects that future events will be less favourable than they appear today

Three factors that determine the feasibility of a project are: the investment required, operational cost, and discount rate. Uncertainty in this work emanates principally from forecast of AG quantity that can be recovered, capital investment and O&M cost estimations as well as the price of electricity. AG quantity forecast has already been covered in Chapter 5.

#### **6.11.1.1 Capital Costs Modelling**

A triangular probability distribution was used to reflect forecasts of the capital costs, which are input parameters. The deterministic value obtained from the open domain is taken as most likely, that is \$973/kWh.

#### **6.11.1.2 O&M Costs Modelling**

O&M Cost was simulated using a triangular distribution with a view to reproducing the range of values found in the literature. With the level of degradation expected as a result of flare gas usage, there is likely to be more maintenance and component replacements, hence the escalation rate is assumed to be up to 3%. O&M cost is made up of three components: fixed O&M cost, variable O&M cost and major maintenance cost.

#### **6.11.1.3 Discount Rate Modelling**

Discount rate was simulated using a triangular distribution. An optimistic figure of 5% and a pessimistic figure of 15% were used, the most likely discount rate being 10%.

#### **6.11.1.4 Electricity Price**

The prices of electricity typically vary depending on location, as well as customer type. In Nigeria, which is the case study for this research, prices were raised from a range of N11.94 (\$0.07) to N15.57 (\$0.09) per kilowatt/hour (KWh) to a range of N13.21 (\$0.08) to N17 (\$0.10) this year. In Abuja, electricity price was raised from N13.25 (\$0.08) to N14.70 (\$0.09). (Oxford Business Group, 25 Jun 2014). The price of electricity in Abuja \$0.09/kWh is adopted for this work, as the deterministic value.

In all, a sufficiently large number of samples and wide design space is necessary to achieve good results. Variations in the values of the output parameters stabilises as the number of iterations increase. Consequently, 5000 iterations were chosen, and the results are presented hereunder.

### 6.11.2 Results of Monte Carlo Analysis

The performances of the plant under investigation was analysed by considering one engine set at a time. The plant is made up of 10 units of DS25, making up the DS25 engine set; and 5 units of LM6K, making up the LM6K engine set.

#### Results of Clean Condition for the DS25 Engine Set

For 10 clean DS25 engines, the histogram in Figure 6-9 and the curve at Figure 6-10 both show that there is a 5% chance that the profit will not be less than \$53 million and could go up to a maximum of \$454 million. However, one is only 5% confident that the value would exceed \$454 million and 5% sure that it would be less than \$53 million.

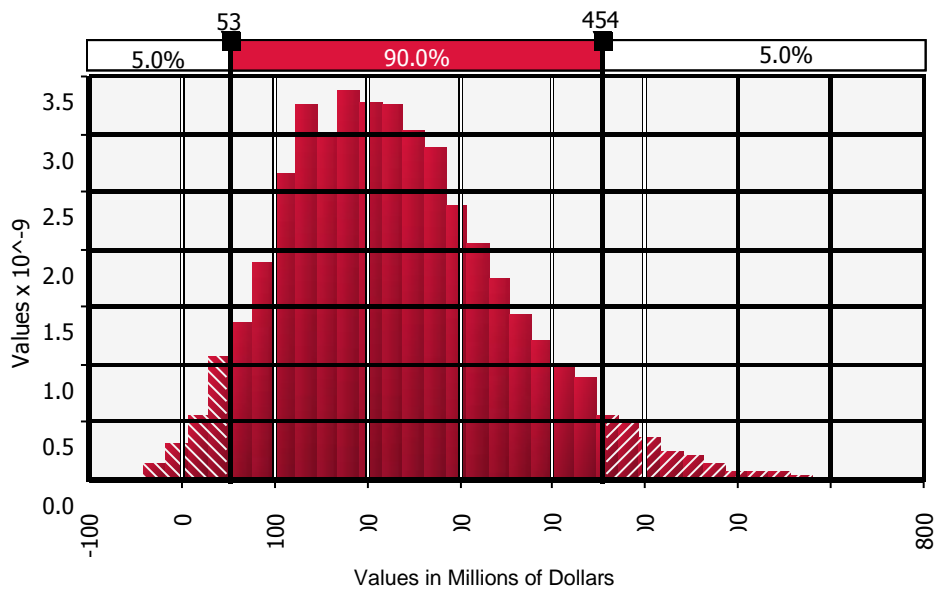
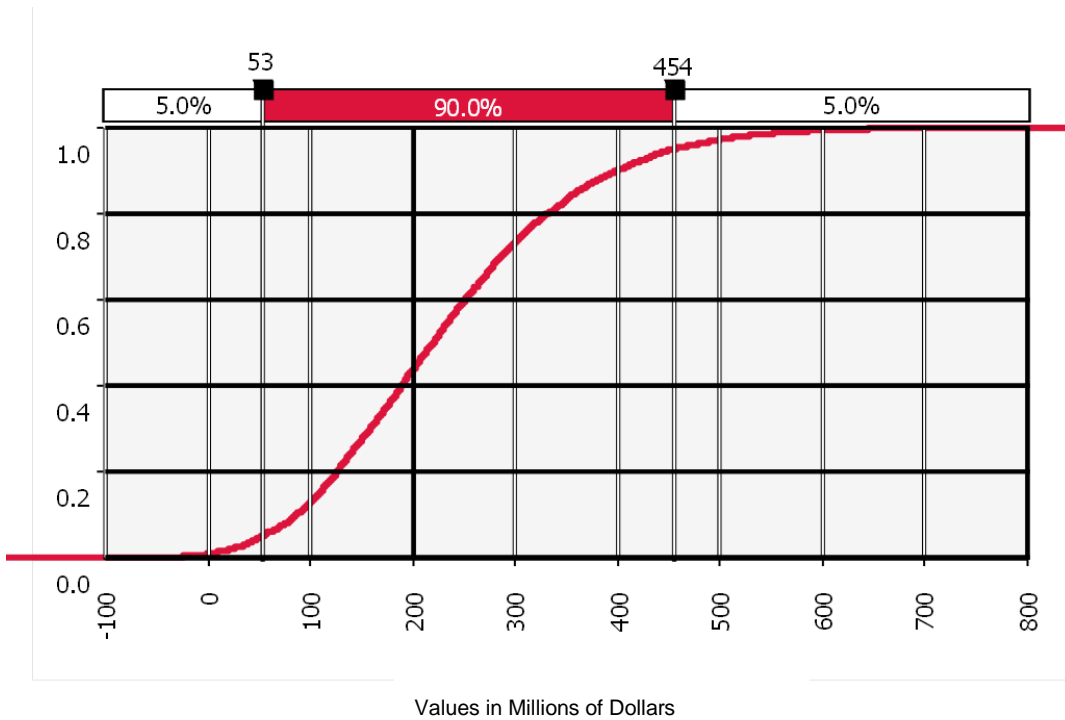


Figure 6-8: NPV of DS25 Engine Set in Clean Condition



**Figure 6-9: Cumulative Ascending Curve for DS25 in Clean Condition**



### Results of Slow Degradation for the DS25 Engine Set

For the DS25 engine set during slow degradation, Figures 6-11 and 6-12 show that there is a 5% chance that the profit will not be less than \$55 million and could go up to a maximum of \$445 million.

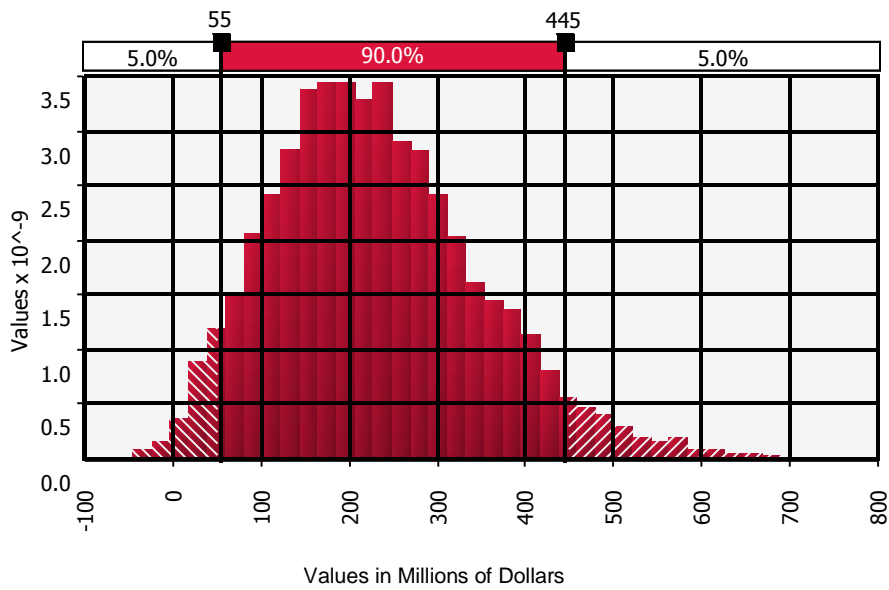


**Figure 6-10: NPV of DS25 Engine Set in Slow Degradation**

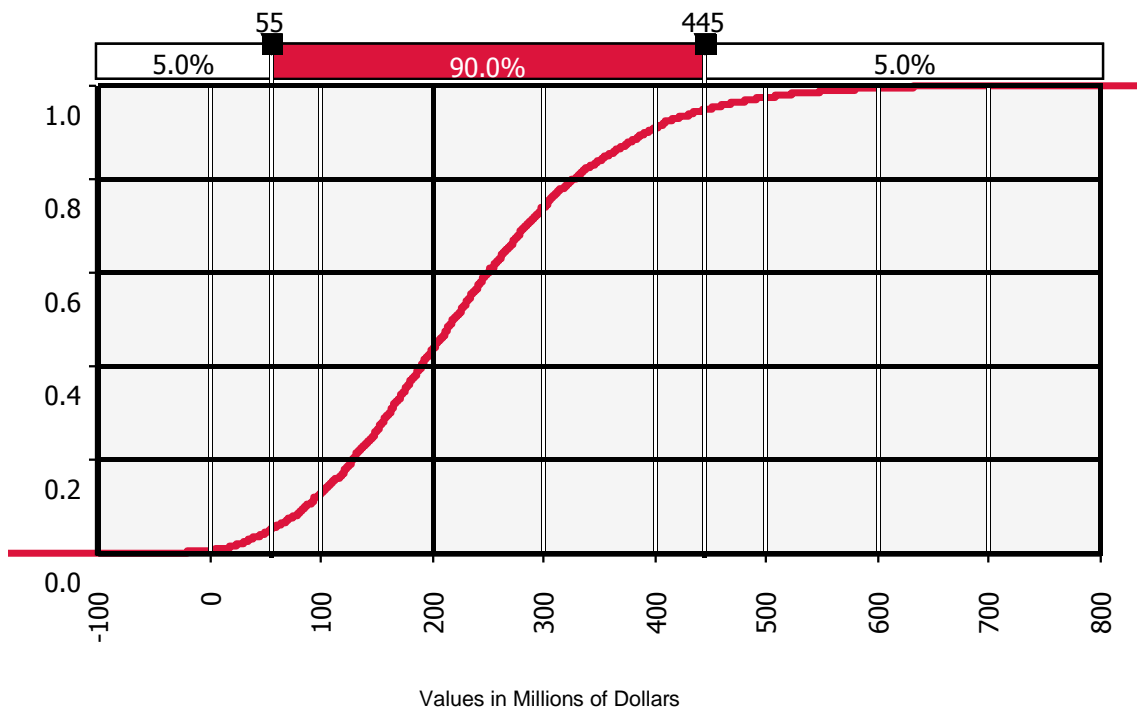


**Figure 6-11: Cumulative Ascending Curve for DS25 in Slow Degradation**

### **Results of Fast Degradation for the DS25 Engine Set**

For the DS25 engine set, during fast degradation, the histogram at Figure 6-13 and the cumulative ascending curve at Figure 6-14 show a 5% chance that the profit will be \$24 million and above, up to a maximum of \$408 million.

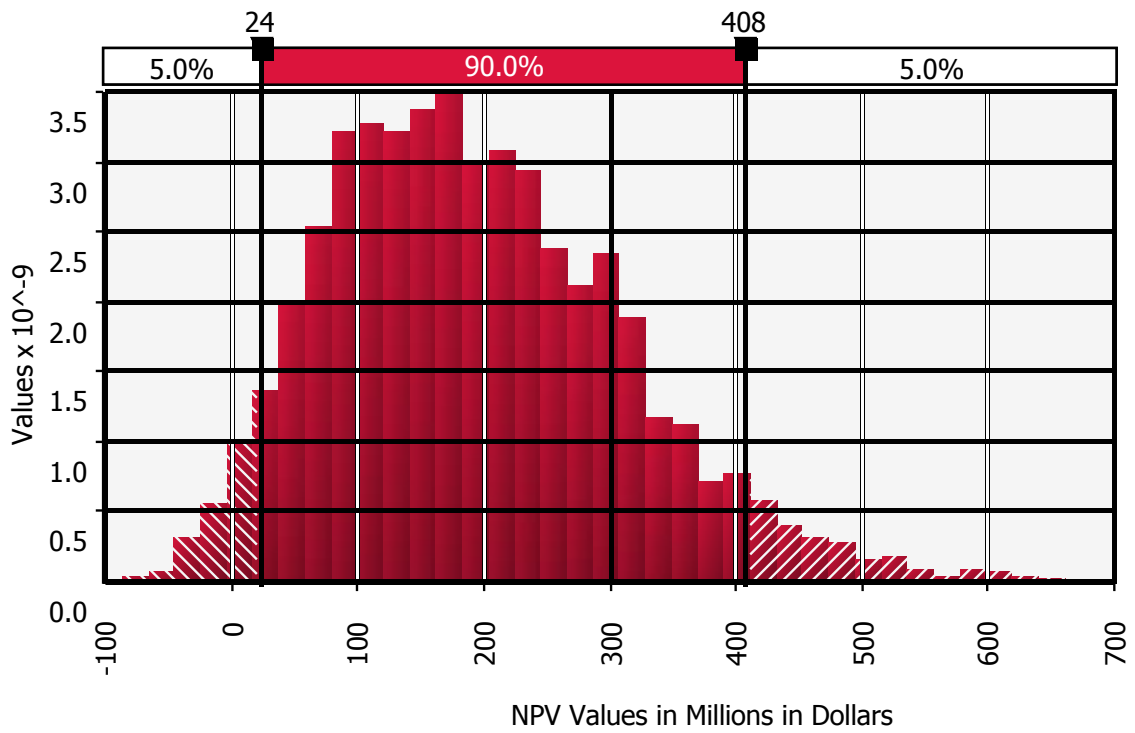


Figure 6-12: NPV of DS25 Engine Set in Fast Degradation

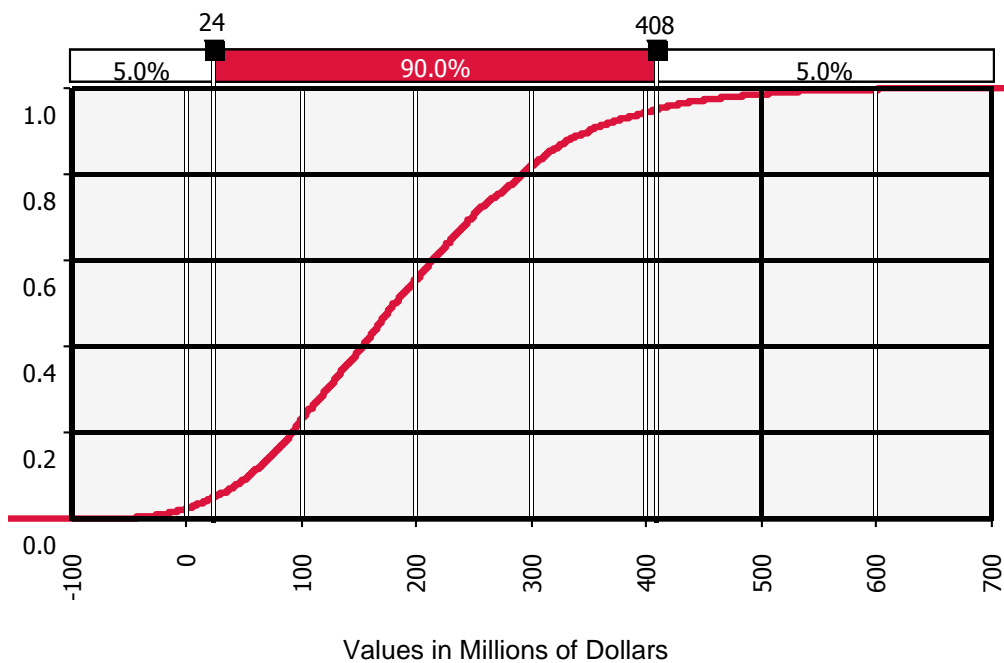
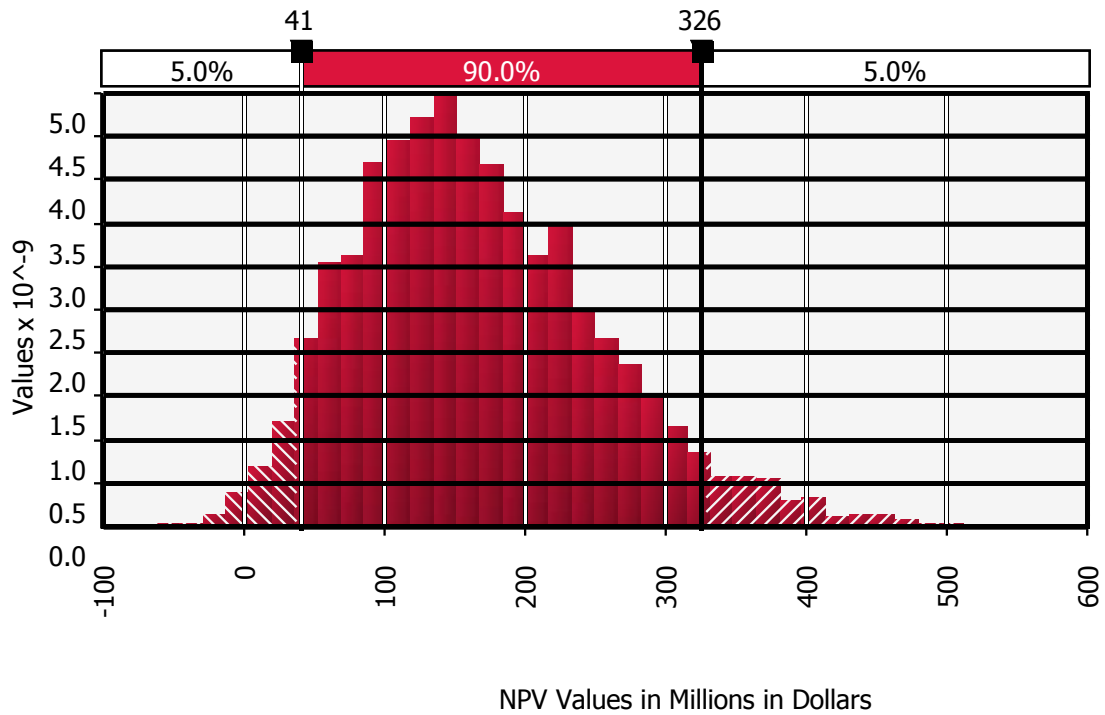


Figure 6-13: Cumulative Ascending Curve for DS25 in Slow Degradation

### Results of Clean Condition for the LM6K Engine Set

For 5 clean LM6K engines, the graphs at Figure 6-15 and Figure 6-16 show that there is a 5% chance that the profit will not be less than \$41 million and could go up to a maximum of \$326 million.



**Figure 6-14: NPV of LM6K Engine Set in Clean Condition**

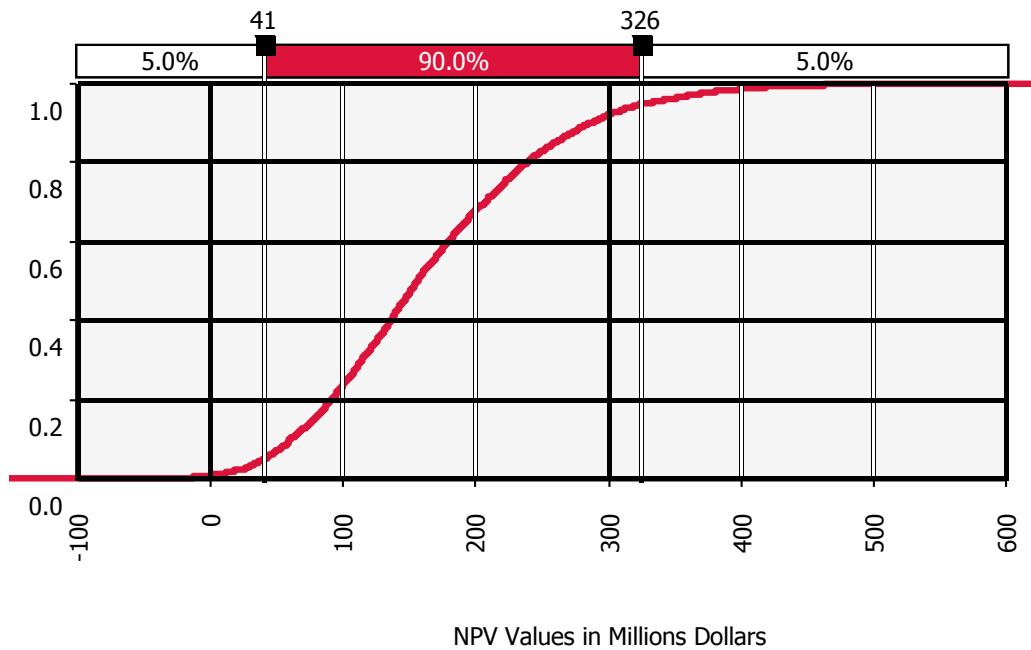


**Figure 6-15: Cumulative Ascending Curve for LM6K in Clean Condition**

**Results of Slow Degradation for the LM6K Engine Set**

The LM6K engine set during slow degradation, Figure 6-17 and Figure 6-18 show a 5% chance that the profit will not be less than \$35 million and could go up to a maximum of \$322 million.

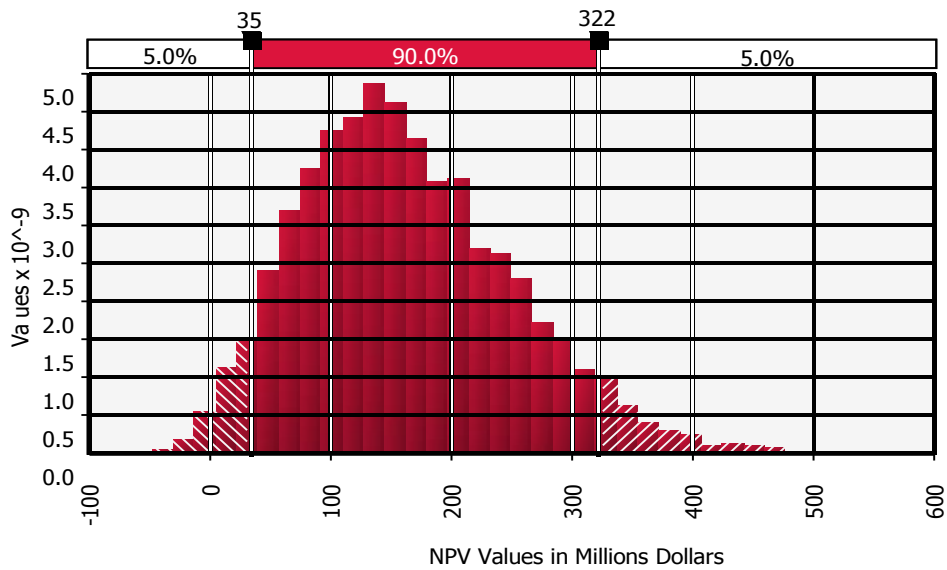


**Figure 6-16: NPV for LM6K Engine Set in Slow Degradation**

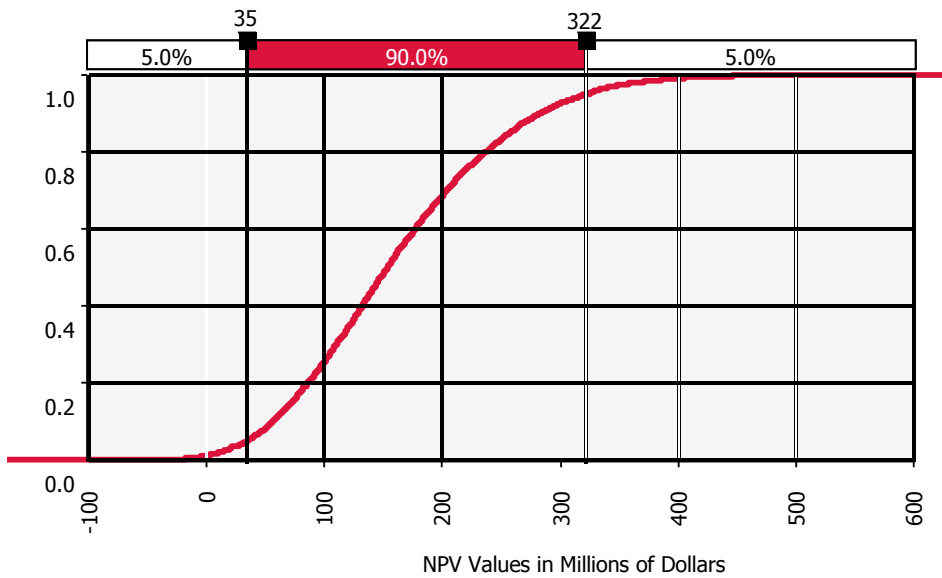


**Figure 6-17: Cumulative Ascending Curve for LM6K in Slow Degradation**

**Results of Fast Degradation for the LM6K Engine Set**

For the LM6K engine set during fast degradation, Figure 6-19 and Figure 6-20 show a 5% chance that the profit will not be less than \$2 million and could go up to a maximum of \$276 million.

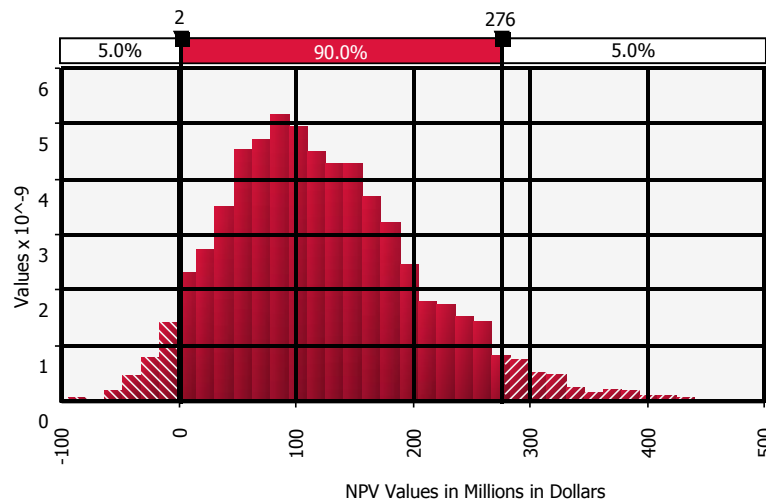


**Figure 6-18: NPV for LM6K Engine Set in Fast Degradation**

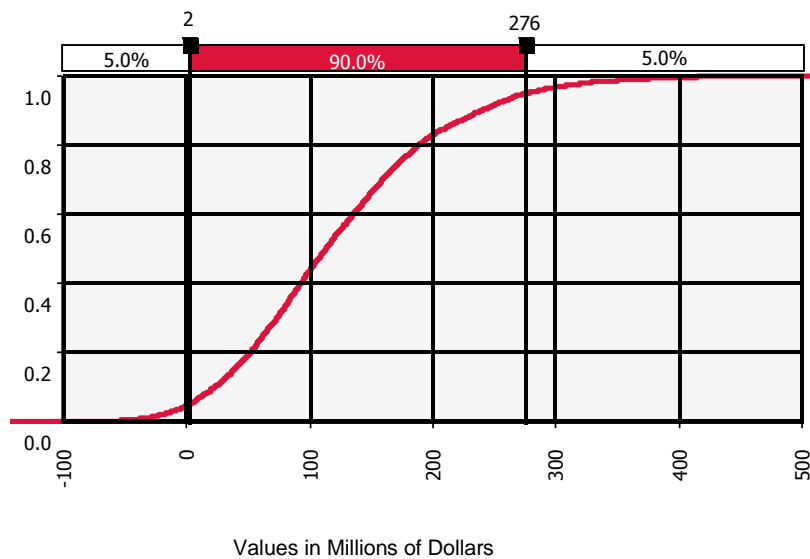


**Figure 6-19: Cumulative Ascending Curve for LM6K in Fast Degradation**

### Comparing LM6K and DS25 Engine Sets

The NPV is better for the DS25 cluster of engines than the LM6K cluster, when assessed separately. This is attributable to the capacity gradient of the two engines, and the revenue that comes from successive divestment of the DS25 engines that become redundant over time.

In all three cases and all three conditions, the standard deviation of the variable O&M cost is higher than that of the capital cost and this indicates that the uncertainty associated with Variable O&M cost exceeds the uncertainty associated with capital cost.

In all three cases, the sensitivity analyses indicate higher uncertainty associated with discount rate than electricity tariff.





## CHAPTER 7: CONCLUSIONS & RECOMMENDATIONS

### 7.1 Conclusions

The feasibility of harnessing flare gas from oil fields for productive uses was assessed, while looking into ways of curtailing the negative outcomes of gas flaring. Analysis of data from PHCN, DPR, and NLNG revealed gas flaring trends, national power requirement, current production capacity and power deficiency due to gas shortages, underscoring the need to harness AG currently being flared.

Five study engines of different configurations/capacities were modelled and performance simulations carried out. Degradation was implanted to simulate the build-up of deposits, erosion and corrosion that could result due to impurities in the AG; that is slow, medium and fast degradation scenarios. The relationship between degradation, maintenance and creep life were brought out.

Optimization was carried out using MATLAB's genetic algorithm which assessed a population of 10,000 individuals over 500 generations; during which convergence was achieved for different configurations of the study engines at discount rates of 5% and 10%. Three outcomes are worth mentioning: for the 450-500MW range, the best configuration was [0 0 0 5 10]; for the 501-750MW range, the best configuration was [0 0 0 5 12]; while for the 751-950MW range, the best configuration was [0 0 0 5 22]. The divestment pattern starts with DS25, followed by LM6K; and the best power plant selection was limited to 10 or 12 or 22 units of DS25 and 5 units of LM6K only in all three cases, completely ignoring the heavier engines. The outcome thus favoured small capacity aero-derivative gas turbines deployed at the onset in large numbers, and divested as fuel declined. The GA also specified the time to divest engines that become redundant due to fuel decline.

This tool was developed to figure out the most economic plant by calculating the least cost of electricity derived through the LCOE, taking into consideration the effects of degradation, fuel decline, increased operations and maintenance cost,

CO<sub>2</sub> emissions and the attendant tax levy. The techno-economic, environmental and risk assessment tool comprises performance, emission, economics and risk modules. The level of degradation manifested as an increase in O&M and increasingly higher creep life consumption during slow, medium and fast degradation scenarios for both engine sets.

The fuel decline was quantified by first carrying out Decline Curve Analysis of a Giant Oil Field which implied that depletion is inevitable. As crude oil depletes, the AG depletes as well. For better economic profit, divestment of GTs as second hand machines or parts was effected as engines became redundant due to fuel depletion.

Hephaestus was used to predict the CO<sub>2</sub> emissions that would result from the utilization of AG for power, and this was incorporated into the economic module. The economic assessment was based on levelized costing which considered cash flows from capital cost, operation and maintenance cost and the prevailing cost of electricity.

@RISK was employed to assess the risk factors. Uncertainties as they relate to URR, discount rate and capital as well as O&M costs were catered for by replacing deterministic figures with a range of values. Using the @RISK, thousands of scenarios were simulated to determine the viability of the project, as a wide range of outcomes were generated to give a much bigger picture. The results show a high influence of discount rate, electricity tariff and variable O&M cost on the overall CoE.

## **7.2 Contributions to Knowledge**

The novel technical contribution of the research work therefore is the influence of degradation on the economic use of associated gas as fuel in gas turbine power generation; and the implementation of divestment in the presence of fuel decline.

### **7.2.1 Influence of Degradation on the Economic Use of AG**

The composition of flare gas varies from field to field; as does the calorific value depending on its composition. Some of the components are heavy hydrocarbons and metal oxides which have a high propensity to condense. The research

unveiled how AG degrades the performance of the gas turbine and the economic implications of its use as fuel.

### **7.2.2 Resource Decline with Divestment**

Researchers are yet to come to terms with the reality that as crude oil is continually being exploited, it declines and so does the AG that it generates. As the quantity of AG being used as fuel drops, the available power output will also drop. This research explored AG resource decline and proffered divestment of redundant engines as a partial remedy. The divestment sub-routine of the optimization ensures that redundant engines are sold to improve on the return on investment.

### **7.2.3 Greenhouse Gas Emissions Reduction**

The high volume of methane when burnt for power generation, would consume the highly potent greenhouse gas, CH<sub>4</sub>, and the emission of the less potent CO<sub>2</sub>. Plants consume CO<sub>2</sub> and in turn give off O<sub>2</sub>.

### **7.2.4 Useful Power from Flare Gas**

Useful power so harnessed could be used for powering oil fields and/or desalination of the abundant salt water in the Niger Delta.

### **7.2.5 Reduced Environmental Degradation**

Harnessing flare gas would no doubt reduce environmental degradation from oil spills, scorched earth and noise pollution.

## **7.3 SWOT Analysis on AG Utilization**

Harnessing AG for power generation presents challenges as well as benefits. SWOT - Strengths, Weaknesses, Opportunities and Threats – analysis on AG utilization drawn from the research findings is summarized below.

### **7.3.1 Strengths**

- Reduced environmental degradation
- Additional useful energy supply (derived from hitherto wasted resource)

- Job creation and poverty alleviation

### **7.3.2 Weaknesses**

- CO<sub>2</sub> emissions will still be given off through the GT exhaust
- Not economically attractive in terms of capital cost

### **7.3.3 Opportunities**

- Greenhouse gas emission would be drastically curtailed
- Power barges for mobile power could be deployed to coastal communities
- Desalination of salt water for consumption in coastal communities
- In situ energy generation to power oil and gas facilities

### **7.3.4 Threats**

- Possibility of rejection by government due to large capital costs
- Possibility of rejection by oil and gas operators

In the coastal communities where gas flaring not only damages the eco-system but also constitutes health hazards and represents a colossal loss of over \$2.5 Billion USD of gas resources, power requirement is high. It would be ultimately more profitable to make this investment as a way of giving back to a region from which much oil wealth is generated.

## **7.4 Recommendations for Future Work**

The following are recommended as future work in this field:

### **7.4.1 Impact of Degradation on Divestment**

This work has demonstrated the influence of degradation on the economic use of AG as well as the onset of resource decline and the palliative divestment protocol. However, there is need for another researcher to explore the impact of degradation on divestment.

### **7.4.2 Power Barges for Divestment**

In order to fully benefit from investments made on harnessing flare gas, it is necessary for another researcher to explore the installation of redundant gas turbines on floating barges, which could have the flexibility to meet varying power requirements at onshore support facilities, or mobile production facilities that are self-supportive in coastal environments.

### **7.4.3 Combined Cycle/Combined Heat and Power in AG Utilization**

Future researchers could consider the employment of CCGT in harnessing AG with the added advantage of improved efficiency on the one hand; or Combined Heat and Power for the purpose of harvesting the exhaust heat, on the other hand.

### **7.4.4 Study on Harnessing Flared Shale Gas for Power**

The boom of shale gas has caused crude oil prices to plummet and put the US as the highest producer of NG. However, with shale gas comes a huge amount of flaring, necessitating future researchers to collect data on compositions of shale gas currently flared from different parts of the world, with a view to carrying out a techno-economic assessment to curtail the ongoing wastage.

## REFERENCES

- Abdulkareem, A. S. and Odigure, J. O. (2010), "Economic Benefit of Natural Gas Utilization in Nigeria: A Case Study of the Food Processing industry", *Energy Sources, Part B: Economics, Planning and Policy*, vol. 5, no. 1, pp. 106-144.
- Abdulkareem, A. S., Odigure, J. O. and Abenege, S. (2009), "Predictive model for pollutant dispersion from gas flaring: A case study of oil producing area of Nigeria", *Energy Sources, Part A: Recovery, Utilization and Environmental Effects*, vol. 31, no. 12, pp. 1004-1015.
- Adewale, D. and Ogunrinde, J. O. (2010), "An economic approach to gas flare-down in a selected field in Nigeria", Vol. 2, pp. 922.
- Akeredolu, F. A. and Sonibare, J. A. (2007), "Safety implications of bridging the energy supply/demand gap in Nigeria through associated natural gas utilization", *Energy and Environment*, vol. 18, no. 3-4, pp. 363-372.
- Aleklett, K. and Campbell, C. J. (2003), "The peak and decline of world oil and gas production", *Minerals and Energy-Raw Materials Report*, vol. 18, no. 1, pp. 5-20.
- Anosike, C. R. (2010), "Unhealthy Effects of Gas Flaring and Wayforward to Actualize the Stopping of Gas Flaring in Nigeria", *Nigeria Annual International Conference and Exhibition, 01/01/2010*, Society of Petroleum Engineers, Tinapa - Calabar, Nigeria, .
- Arnold, G. (2008), *Corporate financial management*, Pearson Education.
- Bejan, A. and Moran, M. J. (1996), *Thermal design and optimization*, John Wiley & Sons.
- Capen, E. (2001), "Probabilistic reserves! Here at last?", *SPE Reservoir Evaluation & Engineering*, vol. 4, no. 05, pp. 387-394.
- Colombo, M. and Ruetschi, R. *Chemistry and Corrosion Aspects in Gas Turbine Power Plants*, , Alstom, Baden.
- Diakunchak, I. S. (1991), "Performance Degradation in Industrial Gas Turbines", *Transactions of the ASME, Journal of Engineering for Gas Turbines and Power*, , no. ASMEpp91-GT-228.
- Doublet, L. E., Pande, P. K., McCollom, T. J. and Blasingame, T. A. (1994), "Decline Curve Analysis Using Type Curves: Analysis of Oil Well Production Data Using Material Balance Time: Application to Field Cases", *Society of Petroleum Engineers Paper Presented at the International*

*Petroleum Conference and Exhibition of Mexico, 10-13 October 1994, Veracruz, Mexico.*

- Eliaz, N., Shemesh, G. and Latanision, R. (2002), "Hot corrosion in gas turbine components", *Engineering Failure Analysis*, vol. 9, no. 1, pp. 31-43.
- Ferdrin, J. P. (1985), "Utilization of Gas Resources in Qatar: A Decade of Planned Development and Integration", *Middle East Oil Technical Conference and Exhibition*, 01/01/1985, 1985 Copyright 1985, Society of Petroleum Engineers, Bahrain.
- Goodger, E. M. and Ogaji, S. O. T. (2011), *Fuel and Combustion in Heat Engines*, First Edition, Cranfield University Press, Cranfield.
- Hook, M. (2009), *Depletion and Decline Curve Analysis in Crude Oil Production* (PhD thesis), Uppsala University.
- Höök, M. and Aleklett, K. (2008), "A decline rate study of Norwegian oil production", *Energy Policy*, vol. 36, no. 11, pp. 4262-4271.
- Höök, M., Söderbergh, B., Jakobsson, K. and Aleklett, K. (2009), "The evolution of giant oil field production behavior", *Natural Resources Research*, vol. 18, no. 1, pp. 39-56.
- Igbatayo, S. A. (2007), "Achieving Nigeria's Gas Flares-Out Target: Challenges and Implications for Environmental Sustainability and Global Climate Change", *Nigeria Annual International Conference and Exhibition*, 01/01/2007, Society of Petroleum Engineers, Abuja, Nigeria.
- Jaber, J., Probert, S. and Williams, P. (1998), "Gaseous fuels (derived from oil shale) for heavy-duty gas turbines and combined-cycle power generators", *Applied Energy*, vol. 60, no. 1, pp. 1-20.
- John Zink (1993), *Safe Flare System Design*.
- Juez, J. M., MacKinnon, J., Giron, E. and Sanchez-Luengo, A. B. (2010), "Successfully Leveraging Gas Flaring Reduction through the CDM – Overcoming Methodological Barriers", *SPE International Conference on Health, Safety and Environment in Oil and Gas Exploration and Production*, 01/01/2010, Society of Petroleum Engineers, Rio de Janeiro, Brazil.
- Khalilpour, R. and Karimi, I. A. (2009), "Evaluation of LNG, CNG, GTL and NGH for Monetization of Stranded Associated Gas with the Incentive of Carbon Credit", *International Petroleum Technology Conference*, 01/01/2009, 2009, International Petroleum Technology Conference, Doha, Qatar.
- Kurz R., B. K. (2001), "Degradation in gas turbine systems", *Journal of Engineering for Gas Turbines and Power*, vol. 123, no. 1, pp. 70-77.

- Kurz, R., Brun, K. (2007), "Gas Turbine Tutorial - Maintenance and Operating Practices, Effects on Degradation and Life", *Proceedings from the 36<sup>th</sup> Turbo machinery Symposium* .
- Kurzke, J. (2011), "GasTurb 11".
- Lawal, K. A., Uwaga, A. O. and Osoro, O. F. (2006), "A Systematic Methodology for Extrapolating Gas-Oil Ratio During Declining Oil Production", *Nigeria Annual International Conference and Exhibition*, Society of Petroleum Engineers.
- Lefebvre, A. H. (1984), "Fuel Effects on Gas Turbine Combustions-Liner Temperature Pattern Factors and Pollutant Emissions", *AIAA Journal of Aircraft*, vol. 21, no. No 11, pp. 887-898.
- Leusden, C.P., Sorgenfrey, C. and Dummel, L. (2004), "Performance Benefits Using Siemens Advanced Compressor Cleaning System ", *Journal of Engineering for Gas Turbines and Power*, vol. Vol 126, no. no. 4, pp. pp. 763-769.
- Little, P. D. (1994), *The Effects of Gas Turbine Engine Degradation on Life Usage* (MSc thesis), Cranfield University, Cranfield.
- Melvin, A. (1988), *Natural Gas: Basic Science and Technology*, Grosvenor Press Ltd, Portsmouth.
- Misellati, M. and Amari, J. A. A. (2006), "The Path to Zero Flaring in ZADCO", *SPE International Health, Safety & Environment Conference*, 01/01/2006, Society of Petroleum Engineers, Abu Dhabi, UAE.
- Mokhatab, S. and Poe, W., ( 2012), *Handbook of Natural Gas Transmission and Processing*.
- Mokhatab, S., Vatani, A. and Zadakhari, O. (2010), "Gas refineries can benefit from installing a flare gas recovery system", *Hydrocarbon Processing*, vol. 89, no. 8.
- Naeem, M. (1999), *Implication of Aero-Engine Deterioration for a Military Aircraft's Performance* (PhD thesis), Cranfield University.
- Ndubuisi, E. N. and Amanetu, M. C. (2003), "The Emerging Role of Natural Gas on the African Economy: The Case Study of the Nigerian Gas Industry", *Canadian International Petroleum Conference*, 01/01/2003, Petroleum Society of Canada, Calgary, Alberta.
- Nwasike, O. T., Okwukenye, C. N. and Nwagwu, N. H. (2000), "Process Technologies and Considerations for Gathering Associated Gas: Experiences from the Niger Delta, West Africa", 01/01/2000.



- Ogbe, E., Ogbe, D. O. and Iledare, O. (2011), "Optimization of Strategies for Natural Gas Utilization: Niger Delta Case Study", *Nigeria Annual International Conference and Exhibition*, 01/01/2011, Society of Petroleum Engineers, Abuja, Nigeria.
- Oguejiofor, G. C. (2006), "Gas flaring in Nigeria: Some aspects for accelerated development of SasolChevron GTL plant at Escravos", *Energy Sources, Part A: Recovery, Utilization and Environmental Effects*, vol. 28, no. 15, pp. 1365-1376.
- Osaghae, E. O. (2003), "Economic Model for Gas-to-Power Project Capitalization in Developing Economy", *SPE Hydrocarbon Economics and Evaluation Symposium*, 01/01/2003, Society of Petroleum Engineers, Dallas, Texas.
- Razak, A. (2007), *Industrial gas turbines: performance and operability*, Elsevier.
- Riti Singh. (2010), *Gas Turbine Combustion* (unpublished Cranfield University Short Course Notes).
- Robelius, F. (2007), *Giant Oil Fields - The Highway to Oil: Giant Oil Fields and their Importance for Future Oil Production* (PhD thesis), Uppsala University.
- Singh, R. (2001), "An Overview: Gas Turbine Generated Pollutants and the Emerging Technology Solutions", *lecture notes of course in gas turbine performance, June*, , pp. 11-15.
- Steed Jr, J. and Hashimoto, A. G. (1994), "Methane emissions from typical manure management systems", *Bioresource technology*, vol. 50, no. 2, pp. 123-130.
- Veerkamp, W. and Heidug, W. K. (2006), "A Strategy for the Reduction of Greenhouse Gas Emissions", *SPE International Health, Safety & Environment Conference*, 01/01/2006, Society of Petroleum Engineers, Abu Dhabi, UAE.
- Walsh, P.P. and Fletcher, P. (2008), *Gas Turbine Performance*, 2nd Edition ed, Oxford Blackwell Publishing.
- Wasfi, A. K. (2004), "The First Real Zero Gas Flaring Project in the Middle East and Gulf Region", *Abu Dhabi International Conference and Exhibition*, 01/01/2004, Society of Petroleum Engineers, Abu Dhabi, United Arab Emirates.



## APPENDICES

### Appendix A : Natural Gas Production from 1999 - 2007

	1999			2000			2001		
	Gas Produced	Gas Utilized	Gas Flared	Gas Produced	Gas Utilized	Gas Flared	Gas Produced	Gas Utilized	Gas Flared
	BSCM	BSCM	BSCM	BSCM	BSCM	BSCM	BSCM	BSCM	BSCM
Elf	1.08	0.23	0.85	2.72	1.58	1.14	3.32	2.14	1.18
Agip	7.60	2.95	4.65	7.99	3.84	4.14	11.63	5.50	6.13
Shell	10.62	3.21	7.41	16.67	8.41	8.25	16.83	7.79	9.05
	2002			2003			2004		
	Gas Produced	Gas Utilized	Gas Flared	Gas Produced	Gas Utilized	Gas Flared	Gas Produced	Gas Utilized	Gas Flared
	BSCM	BSCM	BSCM	BSCM	BSCM	BSCM	BSCM	BSCM	BSCM
Elf	3.37	2.12	1.25	3.93	2.52	1.41	5.52	4.45	1.06
Agip	10.60	4.35	6.26	10.81	6.63	4.18	11.25	7.66	3.59
Shell	15.30	8.08	7.22	19.77	12.69	7.07	21.36	12.39	8.98
	2005			2006			2007		
	Gas Produced	Gas Utilized	Gas Flared	Gas Produced	Gas Utilized	Gas Flared	Gas Produced	Gas Utilized	Gas Flared
	BSCM	BSCM	BSCM	BSCM	BSCM	BSCM	BSCM	BSCM	BSCM
Elf	4.91	3.25	1.67	6.60	5.51	1.09	9.55	8.04	1.51
Agip	11.09	7.28	3.81	12.53	9.32	3.21	12.13	7.86	4.26
Shell	14.41	13.42	0.99	20.31	16.31	4.00	23.26	19.42	3.84

# Appendix B : Modelling of Associated Gases

## Appendix B.1 - Modelling of LANatGas

Path to CEA: C:\CEA.exec

Path to GasTurb Details or to GasTurb: C:\Program Files (x86)\GasTurb\Details5

Name of the new fuel: LANatGas

Maximum Fuel-Air-Ratio: 0.08

Reactant	in Lib	Formula	Ass Enth	Molec W	Mole Frac	Mass Frac
CH4	yes	C1H4	-74.6	16.0425	0.88748	0.780499
C2H6	yes	C2H6	-83.8515	30.069	0.04402	0.0725623
C3H8	yes	C3H8	-104.68	44.0956	0.02572	0.0621739
C4H10, isobutane	yes	C4H10	-134.99	58.1222	0.00553	0.0176201
C4H10, n-butane	yes	C4H10	-125.79	58.1222	0.00843	0
C5H12, iso-pentane	no	C5H12	-153.70	72.1498	0.00265	0.0104815
C5H12, n-pentane	no	C5H12	-146.76	72.1498	0.00195	0.00771271
C6H14	yes	C6H14	-166.92	94	0.00174	0
C7H16	yes	C7H16	-187.78	100	0.00178	0
CO2	yes	C1O2	-393.51	44.0095	0.01957	0.0472149
N2	yes	N2	0	28.0134	0.00113	0.0017353
				Sum	1	1

**Fuels available:**

- Generic
- JP-4
- JP-10
- Natural Gas
- Hydrogen
- Diesel
- LANatGas

**How to proceed:**

- 1 - Enter a name for the new fuel
- 2 - Enter the fuel composition
- 3 - Enter the path to FCEA2.exe
- 4 - Enter the path to GasTurb
- 5 - Create CEA temp rise input
- 6 - Run FCEA2 with that input
- 7 - Create CEA gas prop input
- 8 - Run FCEA2 with that input
- 9 - Make GasTurb files

**More CEA input data:**

Fuel Temperature [K]: 298.15

Water Temperature [K]: 298.15 | Water-Fuel-Ratio: 1

Steam Temperature [K]: 0 | Steam-Fuel-Ratio: 1

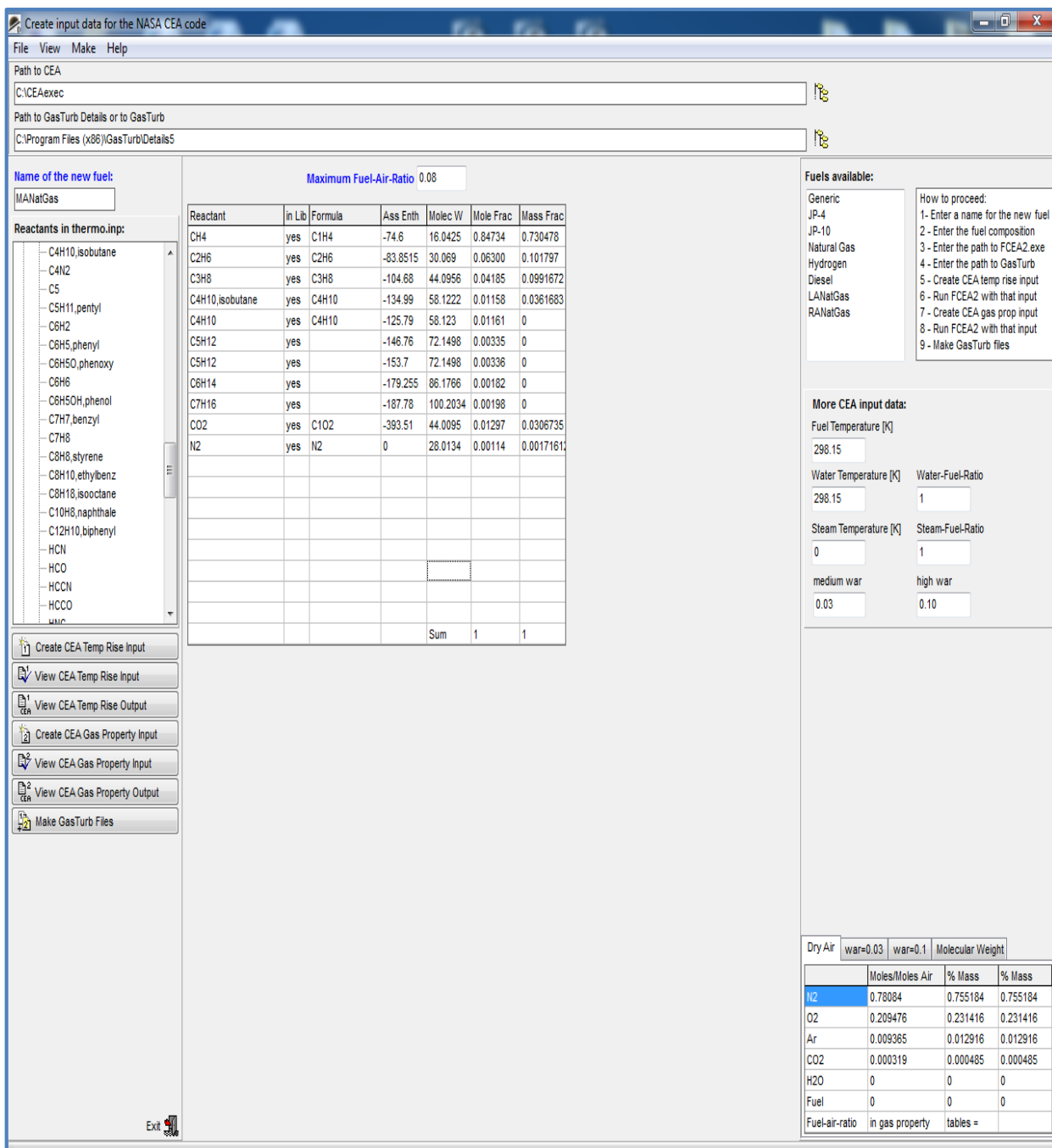
medium war: 0.03 | high war: 0.10

Dry Air: war=0.03 | war=0.1 | Molecular Weight

	Moles/Moles Air	% Mass	% Mass
N2	0.78084	0.755184	0.755184
O2	0.209476	0.231416	0.231416
Ar	0.009365	0.012816	0.012816
CO2	0.000319	0.000485	0.000485
H2O	0	0	0
Fuel	0	0	0
Fuel-air-ratio	in gas property	tables =	

Source of AG Composition: Nigeria Liquefied Natural Gas, 2012

## Appendix B.2 - Modelling of MANatGas



Source of AG Composition: Nigeria Liquefied Natural Gas, 2012

## Appendix B.3 - Modelling of RANatGas

Maximum Fuel-Air-Ratio: 0.08

Reactant	in Lib	Formula	Ass Enth	Molec W	Mole Frac	Mass Frac
CH4	yes	C1H4	-74.6	16.0425	0.82483	0.686434
C2H6	yes	C2H6	-83.8515	30.069	0.07026	0.109595
C3H8	yes	C3H8	-104.68	44.0956	0.04819	0.110234
C4H10	yes	C4H10	-125.79	58.1222	0.01332	0
C4H10.isobutane	yes	C4H10	-134.99	58.1222	0.01332	0.0401614
C5H12.npentane	no	C5H12	-146.76	72.1498	0.00405	0
C5H12.ipentane	no	C5H12	-153.7	72.1498	0.00405	0.0151584
C6H14	yes	C6H14	-179.255	86.1766	0.00224	0
C7H16	yes	C7H16	-187.78	86.1766	0.00233	0
CO2	yes	C1O2	-393.51	44.0095	0.01579	0.0360488
N2	yes	N2	0	28.0134	0.00163	0.0023687
Sum					1	1

Reactants in thermo.inp:

- H2
- HCHO, formaldehy
- HCOOH
- H2O
- H2O2
- H2S
- H2SO4
- NCO
- NH
- NH2
- NH3
- NH2OH
- NO
- NO2
- NO3
- N2
- NCN
- N2H2
- NH2NO2
- N2H4
- N2O

Fuels available:

- Generic
- JP-4
- JP-10
- Natural Gas
- Hydrogen
- Diesel
- LANatGas

How to proceed:

- 1- Enter a name for the new fuel
- 2 - Enter the fuel composition
- 3 - Enter the path to FCEA2.exe
- 4 - Enter the path to GasTurb
- 5 - Create CEA temp rise input
- 6 - Run FCEA2 with that input
- 7 - Create CEA gas prop input
- 8 - Run FCEA2 with that input
- 9 - Make GasTurb files

More CEA input data:

Fuel Temperature [K]: 298.15

Water Temperature [K]: 298.15 | Water-Fuel-Ratio: 1

Steam Temperature [K]: 0 | Steam-Fuel-Ratio: 1

medium war | high war

0.03 | 0.10

Dry Air: war=0.03, war=0.1 | Molecular Weight

C	12.011
H	1.0079
O	15.9994
N	14.0067
Ar	39.948
S	32.066

Source of AG Composition: Nigeria Liquefied Natural Gas, 2012

## Appendix C : Validation of Associated Gas Models

### Appendix C.1 - FHV for LANatGas from Aspen HYSIS

Allison's File.hsc - Aspen HYSYS V7.3 - aspenONE - [Material Stream: Lean Associated Gas]				
File Edit Simulation Flowsheet Tools Window Help				
<b>Worksheet</b>	Z Factor	0.9963	0.9963	
	Watson K	18.16	18.16	
Conditions	User Property	<empty>	<empty>	
Properties	Partial Pressure of H2S [bar]	0.0000	<empty>	
Composition	Cp/(Cp - R)	1.275	1.275	
Oil & Gas Feed	Cp/Cv	1.280	1.280	
Petroleum Assay	Heat of Vap. [kJ/kgmole]	1.424e+004	<empty>	
K Value	Kinematic Viscosity [cSt]	12.59	12.59	
User Variables	Liq. Mass Density (Std. Cond) [kg/m3]	0.8088	0.8088	
Notes	Liq. Vol. Flow (Std. Cond) [m3/h]	235.7	235.7	
Cost Parameters	Liquid Fraction	0.0000	0.0000	
Normalized Yield:	Molar Volume [m3/kgmole]	22.74	22.74	
	Mass Heat of Vap. [kJ/kg]	747.1	<empty>	
	Phase Fraction [Molar Basis]	1.0000	1.0000	
	Surface Tension [dyne/cm]	<empty>	<empty>	
	Thermal Conductivity [W/m-K]	2.868e-002	2.868e-002	
	Viscosity [cP]	1.055e-002	1.055e-002	
	Cv (Semi-Ideal) [kJ/kgmole-C]	30.25	30.25	
	Mass Cv (Semi-Ideal) [kJ/kg-C]	1.587	1.587	
	Cv [kJ/kgmole-C]	30.13	30.13	
	Mass Cv [kJ/kg-C]	1.581	1.581	
	Cv (Ent. Method) [kJ/kgmole-C]	<empty>	<empty>	
	Mass Cv (Ent. Method) [kJ/kg-C]	<empty>	<empty>	
	Cp/Cv (Ent. Method)	<empty>	<empty>	
	Reid VP at 37.8 C [bar]	<empty>	<empty>	
	True VP at 37.8 C [bar]	<empty>	<empty>	
	Liq. Vol. Flow - Sum(Std. Cond) [m3/h]	235.7	235.7	
	Viscosity Index	-3.074	<empty>	
	HHV Mass Basis[Gas] [kJ/kg]	5.191e+004	5.191e+004	
	HHV Molar Basis[Gas] [kJ/kgmole]	9.895e+005	9.895e+005	
	HHV Vol. Basis[Gas] [MJ/m3]	41.97	41.97	
	LHV Mass Basis[Gas] [kJ/kg]	4.694e+004	4.694e+004	
	LHV Molar Basis[Gas] [kJ/kgmole]	8.947e+005	8.947e+005	
	LHV Vol. Basis[Gas] [MJ/m3]	37.95	37.95	

## Appendix C.2 - FHV for MANatGas from Aspen HYSIS

Allison's File.hsc - Aspen HYSYS V7.3 - aspenONE - [Material Stream: Average Associated Gas]				
File Edit Simulation Flowsheet Tools Window Help				
<b>Worksheet</b>	Z Factor	0.9958	0.9958	
	Watson K	17.97	17.97	
Conditions	User Property	<empty>	<empty>	
Properties	Partial Pressure of H2S [bar]	0.0000	<empty>	
Composition	Cp/(Cp - R)	1.261	1.261	
Oil & Gas Feed	Cp/Cv	1.267	1.267	
Petroleum Assay	Heat of Vap. [kJ/kgmole]	1.498e+004	<empty>	
K Value	Kinematic Viscosity [cSt]	11.81	11.81	
User Variables	Liq. Mass Density (Std. Cond) [kg/m3]	0.8543	0.8543	
Notes	Liq. Vol. Flow (Std. Cond) [m3/h]	235.6	235.6	
Cost Parameters	Liquid Fraction	0.0000	0.0000	
Normalized Yield:	Molar Volume [m3/kgmole]	22.73	22.73	
	Mass Heat of Vap. [kJ/kg]	744.3	<empty>	
	Phase Fraction [Molar Basis]	1.0000	1.0000	
	Surface Tension [dyne/cm]	<empty>	<empty>	
	Thermal Conductivity [W/m-K]	2.797e-002	2.797e-002	
	Viscosity [cP]	1.045e-002	1.045e-002	
	Cv (Semi-Ideal) [kJ/kgmole-C]	31.84	31.84	
	Mass Cv (Semi-Ideal) [kJ/kg-C]	1.582	1.582	
	Cv [kJ/kgmole-C]	31.70	31.70	
	Mass Cv [kJ/kg-C]	1.575	1.575	
	Cv (Ent. Method) [kJ/kgmole-C]	<empty>	<empty>	
	Mass Cv (Ent. Method) [kJ/kg-C]	<empty>	<empty>	
	Cp/Cv (Ent. Method)	<empty>	<empty>	
	Reid VP at 37.8 C [bar]	<empty>	<empty>	
	True VP at 37.8 C [bar]	<empty>	<empty>	
	Liq. Vol. Flow - Sum(Std. Cond) [m3/h]	235.6	235.6	
	Viscosity Index	-3.494	<empty>	
	HHV Mass Basis[Gas] [kJ/kg]	5.240e+004	5.240e+004	
	HHV Molar Basis[Gas] [kJ/kgmole]	1.054e+006	1.054e+006	
	HHV Vol. Basis[Gas] [MJ/m3]	44.74	44.74	
	LHV Mass Basis[Gas] [kJ/kg]	4.746e+004	4.746e+004	
	LHV Molar Basis[Gas] [kJ/kgmole]	9.551e+005	9.551e+005	
	LHV Vol. Basis[Gas] [MJ/m3]	40.53	40.53	



### Appendix C.3 - FHV for RANatGas from Aspen HYSIS

Allison's File.hsc - Aspen HYSYS V7.3 - aspenONE - [Material Stream: Rich Associated Gas]			
File Edit Simulation Flowsheet Tools Window Help			
<b>Worksheet</b>	Z Factor	0.9956	0.9956
	Watson K	17.76	17.76
Conditions	User Property	<empty>	<empty>
Properties	Partial Pressure of H2S [bar]	0.0000	<empty>
Composition	Cp/(Cp - R)	1.255	1.255
Oil & Gas Feed	Cp/Cv	1.261	1.261
Petroleum Assay	Heat of Vap. [kJ/kgmole]	1.542e+004	<empty>
K Value	Kinematic Viscosity [cSt]	11.41	11.41
User Variables	Liq. Mass Density (Std. Cond) [kg/m3]	0.8820	0.8820
Notes	Liq. Vol. Flow (Std. Cond) [m3/h]	235.5	235.5
Cost Parameters	Liquid Fraction	0.0000	0.0000
Normalized Yield:	Molar Volume [m3/kgmole]	22.72	22.72
	Mass Heat of Vap. [kJ/kg]	742.3	<empty>
	Phase Fraction [Molar Basis]	1.0000	1.0000
	Surface Tension [dyne/cm]	<empty>	<empty>
	Thermal Conductivity [W/m-K]	2.755e-002	2.755e-002
	Viscosity [cP]	1.043e-002	1.043e-002
	Cv (Semi-Ideal) [kJ/kgmole-C]	32.58	32.58
	Mass Cv (Semi-Ideal) [kJ/kg-C]	1.568	1.568
	Cv [kJ/kgmole-C]	32.43	32.43
	Mass Cv [kJ/kg-C]	1.561	1.561
	Cv (Ent. Method) [kJ/kgmole-C]	<empty>	<empty>
	Mass Cv (Ent. Method) [kJ/kg-C]	<empty>	<empty>
	Cp/Cv (Ent. Method)	<empty>	<empty>
	Reid VP at 37.8 C [bar]	<empty>	<empty>
	True VP at 37.8 C [bar]	<empty>	<empty>
	Liq. Vol. Flow - Sum(Std. Cond) [m3/h]	235.5	235.5
	Viscosity Index	-3.785	<empty>
	HHV Mass Basis[Gas] [kJ/kg]	5.191e+004	5.191e+004
	HHV Molar Basis[Gas] [kJ/kgmole]	1.078e+006	1.078e+006
	HHV Vol. Basis[Gas] [MJ/m3]	45.76	45.76
	LHV Mass Basis[Gas] [kJ/kg]	4.705e+004	4.705e+004
	LHV Molar Basis[Gas] [kJ/kgmole]	9.773e+005	9.773e+005
	LHV Vol. Basis[Gas] [MJ/m3]	41.48	41.48

# Appendix D : Performance Simulations

## Appendix D.1 - GasTurb Simulation of SS9E with NG

Station	W kg/s	T K	P kPa	WRstd kg/s		
					PWSD	= 120187.3 kW
Amb		288.15	101.325			
1	379.272	288.15	101.325		PSFC	= 0.2236 kg/(kW*h)
2	379.272	288.15	101.325	380.000	Heat Rate=	11119.2 kJ/(kW*h)
3	379.272	634.13	1246.297	45.831	Therm Eff=	0.3238
31	337.552	634.13	1246.297		WF	= 7.46373 kg/s
4	345.016	1495.00	1208.909	66.518		
41	363.979	1454.88	1208.909	69.196	s NOx	= 0.29267
49	363.979	888.87	106.495		incidence=	0.00000 °
5	382.943	877.08	106.495	641.426	XM8	= 0.2111
6	382.943	877.08	104.365		A8	= 7.8229 m <sup>2</sup>
8	382.943	877.08	104.365	654.516	P8/Ps8	= 1.03000
Bleed	3.793	634.13	1246.290		WBld/W2	= 0.01000
-----					P2/P1	= 1.00000
Ps0-P2=	0.000	Ps8-Ps0=	0.000		Ps8	= 101.325 kPa
Efficiencies:	isent	polytr	RNI	P/P	W_NGV/W2	= 0.05000
Compressor	0.8500	0.8915	1.000	12.300	WCL/W2	= 0.05000
Burner	0.9999			0.970	Loading	= 100.00 %
Turbine	0.8900	0.8566	1.798	11.352	e45 th	= 0.87290
Generator	1.0000				PW_gen	= 120187.3 kW

## Appendix D.2 - GasTurb Simulation of SS9E with LANatGas

Station	W kg/s	T K	P kPa	WRstd kg/s		
					PWSD	= 120184.5 kW
Amb		288.15	101.325			
1	379.272	288.15	101.325		PSFC	= 0.2369 kg/(kW*h)
2	379.272	288.15	101.325	380.000	Heat Rate=	11122.1 kJ/(kW*h)
3	379.272	634.14	1246.297	45.831	Therm Eff=	0.3237
31	337.552	634.14	1246.297		WF	= 7.90989 kg/s
4	345.462	1495.00	1208.909	66.555		
41	364.426	1454.88	1208.909	69.233	s NOx	= 0.29267
49	364.426	888.74	106.495		incidence=	0.00000 °
5	383.389	876.96	106.495	641.706	XM8	= 0.2111
6	383.389	876.96	104.365		A8	= 7.8249 m <sup>2</sup>
8	383.389	876.96	104.365	654.802	P8/Ps8	= 1.03000
Bleed	3.793	634.13	1246.290		WBld/W2	= 0.01000
-----					P2/P1	= 1.00000
Ps0-P2=	0.000	Ps8-Ps0=	0.000		Ps8	= 101.325 kPa
Efficiencies:	isent	polytr	RNI	P/P	W_NGV/W2	= 0.05000
Compressor	0.8500	0.8915	1.000	12.300	WCL/W2	= 0.05000
Burner	0.9999			0.970	Loading	= 100.00 %
Turbine	0.8900	0.8566	1.798	11.352	e45 th	= 0.87288
Generator	1.0000				PW_gen	= 120184.5 kW

### Appendix D.3 - GasTurb Simulation of SS9E with MANatGas

Station	W kg/s	T K	P kPa	WRstd kg/s		
					PWSD	= 120003.3 kW
Amb		288.15	101.325			
1	379.272	288.15	101.325		PSFC	= 0.2339 kg/(kW*h)
2	379.272	288.15	101.325	380.000	Heat Rate=	11125.5 kJ/(kW*h)
3	379.272	634.14	1246.297	45.831	Therm Eff=	0.3236
31	337.552	634.14	1246.297		WF	= 7.79712 kg/s
4	345.349	1495.00	1208.909	66.520		
41	364.313	1454.83	1208.909	69.197	s NOx	= 0.29267
49	364.313	888.63	106.495		incidence=	0.00000 °
5	383.276	876.84	106.495	641.358	XM8	= 0.2111
6	383.276	876.84	104.365		A8	= 7.8208 m <sup>2</sup>
8	383.276	876.84	104.365	654.447	P8/Ps8	= 1.03000
Bleed	3.793	634.13	1246.290		WBld/W2	= 0.01000
-----					P2/P1	= 1.00000
Ps0-P2=	0.000	Ps8-Ps0=	0.000		Ps8	= 101.325 kPa
Efficiencies:	isent	polytr	RNI	P/P	W_NGV/W2	= 0.05000
Compressor	0.8500	0.8915	1.000	12.300	WCL/W2	= 0.05000
Burner	0.9999			0.970	Loading	= 100.00 %
Turbine	0.8900	0.8566	1.798	11.352	e45 th	= 0.87289
Generator	1.0000				PW_gen	= 120003.3 kW

## Appendix D.4 - GasTurb Simulation of SS9E with RANatGas

Station	W kg/s	T K	P kPa	WRstd kg/s		
					PWSD	= 119925.3 kW
Amb		288.15	101.325			
1	379.272	288.15	101.325		PSFC	= 0.2363 kg/(kW*h)
2	379.272	288.15	101.325	380.000	Heat Rate=	11130.9 kJ/(kW*h)
3	379.272	634.14	1246.297	45.831	Therm Eff=	0.3234
31	337.552	634.14	1246.297		WF	= 7.87030 kg/s
4	345.422	1495.00	1208.909	66.520		
41	364.386	1454.82	1208.909	69.198	s NOx	= 0.29268
49	364.386	888.67	106.495		incidence=	0.00000 °
5	383.350	876.87	106.495	641.373	XM8	= 0.2111
6	383.350	876.87	104.365		A8	= 7.8218 m <sup>2</sup>
8	383.350	876.87	104.365	654.463	P8/Ps8	= 1.03000
Bleed	3.793	634.14	1246.291		WBld/W2	= 0.01000
-----					P2/P1	= 1.00000
Ps0-P2=	0.000	Ps8-Ps0=	0.000		Ps8	= 101.325 kPa
Efficiencies:	isent	polytr	RNI	P/P	W_NGV/W2	= 0.05000
Compressor	0.8500	0.8915	1.000	12.300	WCL/W2	= 0.05000
Burner	0.9999			0.970	Loading	= 100.00 %
Turbine	0.8900	0.8566	1.798	11.352	e45 th	= 0.87286
Generator	1.0000				PW_gen	= 119925.3 kW

## Appendix D.5 - GasTurb Simulation of DS25 with NG

	W	T	P	WRstd	PWSD	=	25160.3 kW
Amb		288.15	101.325				
1	92.922	288.15	101.325		SFC	=	0.2051 kg/(kW*h)
2	92.922	288.15	101.325	93.100			
21	92.922	329.62	151.988	66.383			
24	92.922	361.54	202.650	52.142	P25/P24	=	0.98000
25	92.922	361.54	198.597	53.206	P3/P2	=	35.28
3	91.063	884.80	3574.746	4.532			
31	80.842	884.80	3574.746		Heat Rate=		10198.9 kJ/(kW*h)
4	82.275	1550.00	3467.504	5.622	WF	=	1.43314 kg/s
41	87.850	1511.23	3467.504	5.925	Loading	=	100.00 %
43	87.850	1041.35	541.025		s NOx	=	1.6198
44	91.567	1035.34	541.025		Therm Eff=		0.35298
45	91.567	1035.34	530.205	33.422	P45/P44	=	0.98000
49	91.567	730.20	106.495		P6/P5	=	0.98000
5	93.426	729.30	106.495	142.474			
6	93.426	729.30	104.365		A8	=	2.10980 m <sup>2</sup>
8	94.355	730.79	104.365	146.970	P8/Pamb	=	1.03000
Bleed	0.000	884.80	3574.740		WBld/W2	=	0.00000
-----					P2/P1	=	1.00000
Efficiencies:	isent	polytr	RNI	P/P			
LP Booster	0.8500	0.8583	1.000	1.500	driven by PT		
HP Booster	0.8800	0.8848	1.279	1.333			
Compressor	0.8300	0.8810	1.496	18.000	WHcl/W2	=	0.04000
Burner	0.9950			0.970	WLcl/W2	=	0.02000
HP Turbine	0.8800	0.8540	4.942	6.409	e444 th	=	0.86026
LP Turbine	0.8900	0.8678	1.164	4.979	eta t-s	=	0.68423
Generator	1.0000				PW_gen	=	25160.3 kW

## Appendix D.6 - GasTurb Simulation of DS25 with LANatGas

	W	T	P	WRstd	PWSD	=	25159.2 kW
Amb		288.15	101.325				
1	92.922	288.15	101.325		SFC	=	0.2173 kg/(kW*h)
2	92.922	288.15	101.325	93.100			
21	92.922	329.62	151.988	66.383			
24	92.922	361.54	202.650	52.142	P25/P24	=	0.98000
25	92.922	361.54	198.597	53.206	P3/P2	=	35.28
3	91.063	884.80	3574.746	4.532			
31	80.842	884.80	3574.746		Heat Rate=		10201.6 kJ/(kW*h)
4	82.361	1550.00	3467.504	5.625	WF	=	1.51880 kg/s
41	87.936	1511.21	3467.504	5.928	Loading	=	100.00 %
43	87.936	1041.26	541.093		s NOx	=	1.6198
44	91.653	1035.25	541.093		Therm Eff=		0.35289
45	91.653	1035.25	530.271	33.430	P45/P44	=	0.98000
49	91.653	730.09	106.495		P6/P5	=	0.98000
5	93.511	729.18	106.495	142.521			
6	93.511	729.18	104.365		A8	=	2.11019 m <sup>2</sup>
8	94.440	730.68	104.365	147.018	P8/Pamb	=	1.03000
Bleed	0.000	884.80	3574.740		WBld/W2	=	0.00000
-----					P2/P1	=	1.00000
Efficiencies:	isent	polytr	RNI	P/P			
LP Booster	0.8500	0.8583	1.000	1.500	driven by PT		
HP Booster	0.8800	0.8848	1.279	1.333			
Compressor	0.8300	0.8810	1.496	18.000	WHcl/W2	=	0.04000
Burner	0.9950			0.970	WLcl/W2	=	0.02000
HP Turbine	0.8800	0.8539	4.941	6.408	e444 th	=	0.86023
LP Turbine	0.8900	0.8678	1.165	4.979	eta t-s	=	0.68422
Generator	1.0000				PW_gen	=	25159.2 kW

## Appendix D.7 - GasTurb Simulation of SS9E with MANatGas

	W	T	P	WRstd	PWSD	=	25107.0 kW
Amb		288.15	101.325				
1	92.922	288.15	101.325		SFC	=	0.2147 kg/(kW*h)
2	92.922	288.15	101.325	93.100			
21	92.922	329.62	151.988	66.383			
24	92.922	361.54	202.650	52.142	P25/P24	=	0.98000
25	92.922	361.54	198.597	53.206	P3/P2	=	35.28
3	91.063	884.80	3574.746	4.532			
31	80.842	884.80	3574.746		Heat Rate=		10210.4 kJ/(kW*h)
4	82.339	1550.00	3467.504	5.622	WF	=	1.49714 kg/s
41	87.914	1511.19	3467.504	5.925	Loading	=	100.00 %
43	87.914	1040.87	540.261		s NOx	=	1.6198
44	91.631	1034.88	540.261		Therm Eff=		0.35258
45	91.631	1034.88	529.456	33.463	P45/P44	=	0.98000
49	91.631	730.02	106.495		P6/P5	=	0.98000
5	93.490	729.11	106.495	142.461			
6	93.490	729.11	104.365		A8	=	2.10939 m <sup>2</sup>
8	94.419	730.61	104.365	146.956	P8/Pamb	=	1.03000
Bleed	0.000	884.80	3574.740		WBld/W2	=	0.00000
-----					P2/P1	=	1.00000
Efficiencies:	isent	polytr	RNI	P/P			
LP Booster	0.8500	0.8583	1.000	1.500	driven by PT		
HP Booster	0.8800	0.8848	1.279	1.333			
Compressor	0.8300	0.8810	1.496	18.000	WHcl/W2	=	0.04000
Burner	0.9950			0.970	WLcl/W2	=	0.02000
HP Turbine	0.8800	0.8539	4.941	6.418	e444 th	=	0.86024
LP Turbine	0.8900	0.8678	1.163	4.972	eta t-s	=	0.68391
Generator	1.0000				PW_gen	=	25107.0 kW



## Appendix D.8 - GasTurb Simulation of SS9E with RANatGas

	W	T	P	WRstd	PWSD	=	25090.5 kW
Amb		288.15	101.325				
1	92.922	288.15	101.325		SFC	=	0.2168 kg/(kW*h)
2	92.922	288.15	101.325	93.100			
21	92.922	329.62	151.988	66.383			
24	92.922	361.54	202.650	52.142	P25/P24	=	0.98000
25	92.922	361.54	198.597	53.206	P3/P2	=	35.28
3	91.063	884.80	3574.746	4.532			
31	80.842	884.80	3574.746		Heat Rate=		10214.9 kJ/(kW*h)
4	82.353	1550.00	3467.504	5.622	WF	=	1.51110 kg/s
41	87.928	1511.19	3467.504	5.925	Loading	=	100.00 %
43	87.928	1040.80	540.020		s NOx	=	1.6198
44	91.645	1034.81	540.020		Therm Eff=		0.35243
45	91.645	1034.81	529.220	33.477	P45/P44	=	0.98000
49	91.645	730.06	106.495		P6/P5	=	0.98000
5	93.504	729.15	106.495	142.465			
6	93.504	729.15	104.365		A8	=	2.10953 m <sup>2</sup>
8	94.433	730.65	104.365	146.961	P8/Pamb	=	1.03000
Bleed	0.000	884.80	3574.740		WBld/W2	=	0.00000
-----					P2/P1	=	1.00000
Efficiencies:	isent	polytr	RNI	P/P			
LP Booster	0.8500	0.8583	1.000	1.500	driven by PT		
HP Booster	0.8800	0.8848	1.279	1.333			
Compressor	0.8300	0.8810	1.496	18.000	WHcl/W2	=	0.04000
Burner	0.9950			0.970	WLcl/W2	=	0.02000
HP Turbine	0.8800	0.8539	4.941	6.421	e444 th	=	0.86022
LP Turbine	0.8900	0.8679	1.163	4.969	eta t-s	=	0.68380
Generator	1.0000				PW_gen	=	25090.5 kW

## Appendix E : MATLAB Function for Fuel Required

```
function fuelRequired =  
calc_myfuelRequirements(currentConfig,SS94,SS9E,LM1H,LM6K,DS25)  
  
fuelRequired = currentConfig(1) * SS94.YearlyConsumption + ...  
    currentConfig(2) * SS9E.YearlyConsumption + ...  
    currentConfig(3) * LM1H.YearlyConsumption + ...  
    currentConfig(4) * LM6K.YearlyConsumption + ...  
    currentConfig(5) * DS25.YearlyConsumption;  
  
end
```

## Appendix F : MATLAB Script for Fitness with Divestment

```
% my_gaFitness4Divestment
% Script to specify the fitness function in the case of yearly
divestment
% Developed by Isaiah Allison, 02/07/2014
%
% Fitness Function is re-defined to cater for resource decline per
year for a particular plant configuration
% In the zeroth year, the "individuals" are defined as no1, no2, no3,
no4, no 5
% The aim is to divest the smaller engines depending on fuel
availability
% The Cost of each GT is worked in, Cost = purchase cost(currentConfig
or initialConfig)

function
[Fitness,currentConfig,divestedEngines,PowerOutput,PowerAverage,InitialCost,TotalCost,CoE] =
my_gaFitness4Divestment(no1,no2,no3,no4,no5,RangeMIN,RangeMAX,Discount
Rate,PlantLife,OperatingHours,fuelAvailable,fuelDecline,lowerLimit,upperLimit)

% Each group is solved separately with the implementation of the
denominator  $(1+r)^n$  of the
% maintenance, fuel and emissions cost; then the new Cost  $C = C +$ 
Summation/ $(1+r)^n$ 
% Fuel in the new year is then given by, fuel = 0.87 *fuel after
previous year's operations
% fuel  $(n+1) = k \cdot \text{fuel}(n)$ , where  $k = 0.87$ 
% The new cost will include maintenance cost, fuel cost, emission cost
for previous year
% Revenue from divestment is added to the the new Capital per year

% Variable definition for the whole power plant

SS94.PowerOut = 226.e3;
SS94.FuelC = 0.0;
SS94.MaintC = 29592440;
SS94.CapitalC = 219898000;
SS94.EmissionsC = 0.0;
SS94.YearlyConsumption = 448100241.; % kg

SS9E.PowerOut = 120.e3;
SS9E.FuelC = 0.0;
SS9E.MaintC = 15712800;
SS9E.CapitalC = 116760000;
SS9E.EmissionsC = 0.0;
SS9E.YearlyConsumption = 255451142.; % kg

LM1H.PowerOut = 100.e3;
LM1H.FuelC = 0.0;
LM1H.MaintC = 13094000;
LM1H.CapitalC = 97300000;
LM1H.EmissionsC = 0.0;
LM1H.YearlyConsumption = 157865639.; % kg
```

```

LM6K.PowerOut = 41.e3;
LM6K.FuelC = 0.0;
LM6K.MaintC = 5368540;
LM6K.CapitalC = 39893000;
LM6K.EmissionsC = 0.0;
LM6K.YearlyConsumption = 74394217.; % kg

DS25.PowerOut = 25.e3;
DS25.FuelC = 0.0;
DS25.MaintC = 3273500;
DS25.CapitalC = 24325000;
DS25.EmissionsC = 0.0;
DS25.YearlyConsumption = 47467952.; % kg

% Conversion from "genotype" variables to "phenotype" variables.
no1=round(lowerLimit(1)+no1*(upperLimit(1)-lowerLimit(1)));
no2=round(lowerLimit(2)+no2*(upperLimit(2)-lowerLimit(2)));
no3=round(lowerLimit(3)+no3*(upperLimit(3)-lowerLimit(3)));
no4=round(lowerLimit(4)+no4*(upperLimit(4)-lowerLimit(4)));
no5=round(lowerLimit(5)+no5*(upperLimit(5)-lowerLimit(5)));
initialConfig=[no1 no2 no3 no4 no5];
currentConfig=zeros(PlantLife+1,length(initialConfig));
divestedEngines=zeros(PlantLife+1,length(initialConfig));
currentConfig(1,:)=initialConfig;
divestedEngines(1,:)= [0 0 0 0 0];

%% ZEROTH YEAR
InitialCost = initialConfig(1) * SS94.CapitalC + ...
    initialConfig(2) * SS9E.CapitalC + ...
    initialConfig(3) * LM1H.CapitalC + ...
    initialConfig(4) * LM6K.CapitalC + ...
    initialConfig(5) * DS25.CapitalC;
TotalCost=InitialCost;

for year=1:PlantLife
    % check whether we need to divest any GT

    [divestedEngines(year+1,:),currentConfig(year+1,)] = my_ga4DivestmentSu
broutine(currentConfig(year,:), [0 0 0 0
0], fuelAvailable, SS94, SS9E, LM1H, LM6K, DS25);

    % costs/revenues for this year
    FuelCost = currentConfig(year+1,1) * SS94.FuelC + ...
        currentConfig(year+1,2) * SS9E.FuelC + ...
        currentConfig(year+1,3) * LM1H.FuelC + ...
        currentConfig(year+1,4) * LM6K.FuelC + ...
        currentConfig(year+1,5) * DS25.FuelC;
    FuelCost = FuelCost / (1 + DiscountRate)^year;

    MaintCost = currentConfig(year+1,1) * SS94.MaintC + ...
        currentConfig(year+1,2) * SS9E.MaintC + ...
        currentConfig(year+1,3) * LM1H.MaintC + ...
        currentConfig(year+1,4) * LM6K.MaintC + ...
        currentConfig(year+1,5) * DS25.MaintC;
    MaintCost = MaintCost / (1 + DiscountRate)^year;

    EmissionCost = currentConfig(year+1,1) * SS94.EmissionsC + ...

```

```

        currentConfig(year+1,2) * SS9E.EmissionsC + ...
        currentConfig(year+1,3) * LM1H.EmissionsC + ...
        currentConfig(year+1,4) * LM6K.EmissionsC + ...
        currentConfig(year+1,5) * DS25.EmissionsC;
    EmissionCost = EmissionCost / (1 + DiscountRate)^year;

    SecondHandPercentageRevenue = 0.6; % percentage of the capital
    cost that you would get back if you sold the GT on the zeroth year.
    DivestmentRevenue = divestedEngines(year+1,1) *
    SecondHandPercentageRevenue * SS94.CapitalC + ...
        divestedEngines(year+1,2) * SecondHandPercentageRevenue *
    SS9E.CapitalC + ...
        divestedEngines(year+1,3) * SecondHandPercentageRevenue *
    LM1H.CapitalC + ...
        divestedEngines(year+1,4) * SecondHandPercentageRevenue *
    LM6K.CapitalC + ...
        divestedEngines(year+1,5) * SecondHandPercentageRevenue *
    DS25.CapitalC;
    DivestmentRevenue = DivestmentRevenue / (1 + DiscountRate)^year;

    % add up to the total cost from previous years
    TotalCost = TotalCost + FuelCost + MaintCost + EmissionCost -
    DivestmentRevenue;

    % Update fuel available for the following year
    fuelAvailable = fuelAvailable * (1-fuelDecline);

end

% power output in the ZEROth YEAR
InitialTotalPower = initialConfig(1) * SS94.PowerOut + ...
    initialConfig(2) * SS9E.PowerOut + ...
    initialConfig(3) * LM1H.PowerOut + ...
    initialConfig(4) * LM6K.PowerOut + ...
    initialConfig(5) * DS25.PowerOut;
Penalization = my_ga4Penalization(InitialTotalPower, RangeMIN,
RangeMAX);

PowerOutput=zeros(PlantLife+1,1);
PowerOutput(1)=InitialTotalPower;
% power output in the LAST YEAR
for year=1:PlantLife
    PowerOutput(year+1) = currentConfig(year+1,1) * SS94.PowerOut +
    ...
        currentConfig(year+1,2) * SS9E.PowerOut + ...
        currentConfig(year+1,3) * LM1H.PowerOut + ...
        currentConfig(year+1,4) * LM6K.PowerOut + ...
        currentConfig(year+1,5) * DS25.PowerOut;
end

PowerAverage=sum(PowerOutput(2:end))/PlantLife;
% Cost of electricity and penalisation
CoE = TotalCost / (PowerAverage*OperatingHours);

% Fitness
Fitness = CoE * Penalization;
end

```

## Appendix G : MATLAB Script on Divestment Pattern

```
% My_DivestmentSubroutine.m
% Script to spell out divestment pattern
% Isaiah Allison, 02/07/2014
% Divestment subroutine works with fuel quantity in the current year
and the present engine configuration(fuel(i), CurrentConfig)
% The aim is to divest smaller GTs in the order no5(25MW),
no4(41MW),no3(100MW), no2(120MW), no1(226MW);
% Fuel declines over time from an initial fixed quantity, called
Ultimately Recoverable Reserve
function
[divestedEngines,currentConfig]=my_ga4DivestmentSubroutine(initialConf
ig,divestedEngines,fuelAvailable,SS94,SS9E,LM1H,LM6K,DS25)

currentConfig=initialConfig;
fuelRequired =
calc_myfuelRequirements(currentConfig,SS94,SS9E,LM1H,LM6K,DS25);

if fuelAvailable < fuelRequired

    if (currentConfig(5) >= 1)
        currentConfig(5) = currentConfig(5) - 1;
        divestedEngines(5) = divestedEngines(5) + 1;
        fuelRequired =
calc_myfuelRequirements(currentConfig,SS94,SS9E,LM1H,LM6K,DS25);

        if fuelAvailable < fuelRequired

[divestedEngines,currentConfig]=my_ga4DivestmentSubroutine(currentConf
ig,divestedEngines,fuelAvailable,SS94,SS9E,LM1H,LM6K,DS25);
            end

        elseif (currentConfig(4) >= 1)
            currentConfig(4) = currentConfig(4) - 1;
            divestedEngines(4) = divestedEngines(4) + 1;
            fuelRequired =
calc_myfuelRequirements(currentConfig,SS94,SS9E,LM1H,LM6K,DS25);

            if fuelAvailable < fuelRequired

[divestedEngines,currentConfig]=my_ga4DivestmentSubroutine(currentConf
ig,divestedEngines,fuelAvailable,SS94,SS9E,LM1H,LM6K,DS25);
                end

            elseif (currentConfig(3) >= 1)
                currentConfig(3) = currentConfig(3) - 1;
                divestedEngines(3) = divestedEngines(3) + 1;
                fuelRequired =
calc_myfuelRequirements(currentConfig,SS94,SS9E,LM1H,LM6K,DS25);

                if fuelAvailable < fuelRequired

[divestedEngines,currentConfig]=my_ga4DivestmentSubroutine(currentConf
ig,divestedEngines,fuelAvailable,SS94,SS9E,LM1H,LM6K,DS25);
                    end

                end

            end

        end

    end

end
```

```

elseif (currentConfig(2) >= 1)
    currentConfig(2) = currentConfig(2) - 1;
    divestedEngines(2) = divestedEngines(2) + 1;
    fuelRequired =
calc_myfuelRequirements(currentConfig,SS94,SS9E,LM1H,LM6K,DS25);

    if fuelAvailable < fuelRequired

[divestedEngines,currentConfig]=my_ga4DivestmentSubroutine(currentConf
ig,divestedEngines,fuelAvailable,SS94,SS9E,LM1H,LM6K,DS25);
    end

elseif (currentConfig(1) >= 1)
    currentConfig(1) = currentConfig(1) - 1;
    divestedEngines(1) = divestedEngines(1) + 1;
    fuelRequired =
calc_myfuelRequirements(currentConfig,SS94,SS9E,LM1H,LM6K,DS25);

    if fuelAvailable < fuelRequired

[divestedEngines,currentConfig]=my_ga4DivestmentSubroutine(currentConf
ig,divestedEngines,fuelAvailable,SS94,SS9E,LM1H,LM6K,DS25);
    end

end

end

end

```

## Appendix H : MATLAB Optimization Script

```
% my_gaOptimiser
% Script to minimize cost of electricity and select best plant
% Developed by Isaiah Allison, 27/05/2014
%
% Variable Dictionary
% SS94, Engine Type no1 with output of 226MW
% SS9E, Engine Type no2 with output of 120MW
% LM1H, Engine Type no3 with output of 100MW
% LM6K, Engine Type no4 with output of 41MW
% DS25, Engine Type no5 with output of 25MW
%
% Definition of Outputs
% Min CoE, NPV
% Best Power Plant: min CoE, max Power output
%
% % Constraints on Power Output Defined in Terms of Engine
Combinations
% Min and max number of each engine type
% SS94: 0 - 4; SS9E: 0 - 8; LM1H: 0 - 10; LM6K: 0 - 20; DS25: 0 - 38
%
% Solve the optimization problem
% Display the solution
% Syntax activating plot function, genealogy, etc

clear all;
clc;
% Control variables & domain boundaries
NoofControlVars=5;
% individual(1) = "no1"
% individual(2) = "no2"
% individual(3) = "no3"
% individual(4) = "no4"
% individual(5) = "no5"
bounds=[[0 4];...
        [0 8];...
        [0 10];...
        [0 20];...
        [0 38]];
lowerLimit = bounds(:,1)';
upperLimit = bounds(:,2)';
% Plots
selectedPlots={@gaplotbestf,@gaplotbestindiv,@gaplotdistance,@gaplotsc
ores};
% Options
options=gaoptimset('Display','iter',...
                  'PlotFcns',selectedPlots,...
                  'TolFun',0,...
                  'PopulationSize',10000,...
                  'Generations',500,...
                  'StallGenLimit',100,...
                  'CrossoverFraction',.5,...
                  'UseParallel','never',...
                  'Vectorized','off',...
                  'CrossoverFcn',@crossoverscattered,...
                  'MutationFcn',@mutationadaptfeasible,...
                  'CreationFcn',@gacreationlinearfeasible);
```



```

% Define parameters & optimize
RangeMIN=751.e3;
RangeMAX=950.e3;
DiscountRate=0.1;
PlantLife=20.;
OperatingHours=8000.;
fuelAvailable=1.e9;% Scenario1, insert figures for Scenario2 and
Scenario3 in subsequent runs
fuelDecline=0.13;%Giant oil field resource decline is typically at 13%
%
[bestConf,bestFitness,exitflag,output,population,scores]=...

ga(@(ind)my_gaFitness4Divestment(ind(1),ind(2),ind(3),ind(4),ind(5),Ra
ngeMIN,RangeMAX,DiscountRate,PlantLife,OperatingHours,fuelAvailable,fu
elDecline,lowerLimit,upperLimit),...
    NoofControlVars,...
% number of control variables
    [],[],...
% linear inequality constrains
    [],[],...
% linear equality constrains
    zeros(1,NoofControlVars),ones(1,NoofControlVars),...
% domain boundaries
    [],...
% nonlinear constrains (@functionHandle)
    options);
% options (defined with @gaoptimset)

%%
% Time to divest, a text file to reveal the history of divestment as
fuel declines
[Fitness,currentConfig,divestedEngines,PowerOutput,PowerAverage,Initia
lCost,TotalCost,CoE] =
my_gaFitness4Divestment(bestConf(1),bestConf(2),bestConf(3),bestConf(4
),bestConf(5),RangeMIN,RangeMAX,DiscountRate,PlantLife,OperatingHours,
fuelAvailable,fuelDecline,lowerLimit,upperLimit);

bestConf=round(lowerLimit+bestConf.*(upperLimit-lowerLimit));
for count=1:length(population)

population(count,:)=round(lowerLimit+population(count,:).*(upperLimit-
lowerLimit));
end

```

## Appendix I : MATLAB Script for Penalization

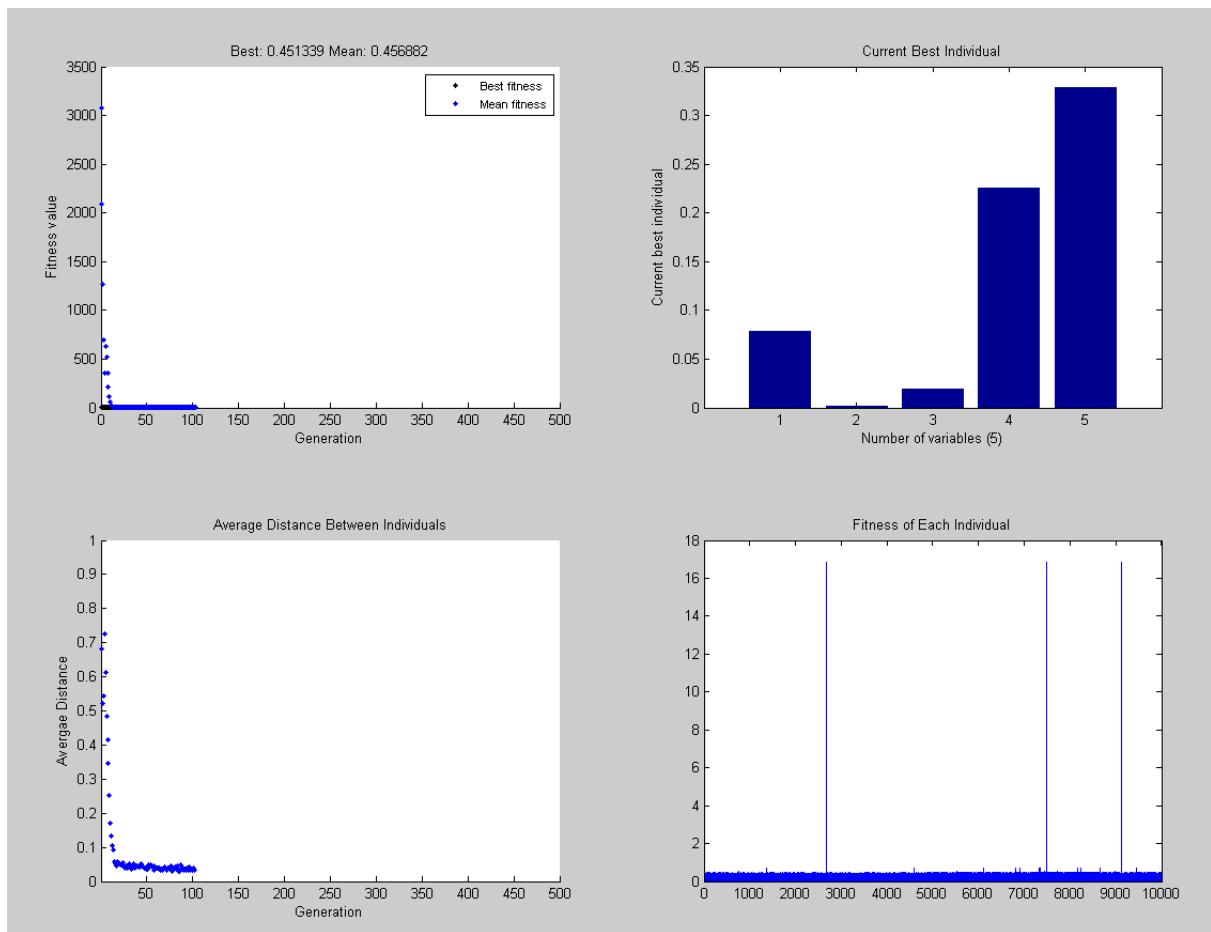
```
% My_ga4Penalization.m
% Script to spell out penalization
%
% Isaiah Allison, 27/05/2014
%
% Penalization Factor
function P = my_ga4Penalization(PowerOutPP, RangeMIN, RangeMAX)
% convert units
PowerOutPP = PowerOutPP/1000.; % from kW to MW
RangeMIN = RangeMIN/1000.; % from kW to MW
RangeMAX = RangeMAX/1000.; % from kW to MW
% penalisation function
if (PowerOutPP > RangeMAX)
P = 1. + (PowerOutPP - RangeMAX);
elseif (PowerOutPP < RangeMIN)
P = 1. + (RangeMIN - PowerOutPP);
else
P = 1.;
end
```

## Appendix J : 2<sup>nd</sup> Simulation for Optimization and Divestment

### Simulation at Discount Rate of 5%

- a. Range: 501-750MW
- b. Fuel: 1e9
- c. Decline: 13%
- d. Life: 20 Years
- e. Hours: 8000
- f. Population 10,000; Generation 500

### Best Individual, Fitness, Average Distance and Fitness of Each Individual



## Current Configuration and Divested Engines

Variables - currentConfig

currentConfig x divestedEngines x

21x5 double

	1	2	3	4	5	6	7	8	9	10
1	0	0	0	5	12					
2	0	0	0	5	12					
3	0	0	0	5	10					
4	0	0	0	5	8					
5	0	0	0	5	6					
6	0	0	0	5	4					
7	0	0	0	5	2					
8	0	0	0	5	1					
9	0	0	0	5	0					
10	0	0	0	4	0					
11	0	0	0	3	0					
12	0	0	0	3	0					
13	0	0	0	2	0					
14	0	0	0	2	0					
15	0	0	0	2	0					
16	0	0	0	1	0					
17	0	0	0	1	0					
18	0	0	0	1	0					
19	0	0	0	1	0					
20	0	0	0	1	0					
21	0	0	0	0	0					

Variables - divestedEngines

currentConfig x divestedEngines x

21x5 double

	1	2	3	4	5	6	7	8	9	10
1	0	0	0	0	0					
2	0	0	0	0	0					
3	0	0	0	0	2					
4	0	0	0	0	2					
5	0	0	0	0	2					
6	0	0	0	0	2					
7	0	0	0	0	2					
8	0	0	0	0	1					
9	0	0	0	0	1					
10	0	0	0	1	0					
11	0	0	0	1	0					
12	0	0	0	0	0					
13	0	0	0	1	0					
14	0	0	0	0	0					
15	0	0	0	0	0					
16	0	0	0	1	0					
17	0	0	0	0	0					
18	0	0	0	0	0					
19	0	0	0	0	0					
20	0	0	0	0	0					
21	0	0	0	1	0					

## The Best Configuration of Plant

For the 501-750MW power range, the best configuration of power plant is [0, 0, 0, 5, 12], that is 5 units of LM6K and 12 units of DS25.

## Divestment of Redundant Engines

Divestment begins in 2<sup>nd</sup> year of investment with 2 units of DS25, for 5 consecutive years; then 1 unit of DS25 divested in the 7<sup>th</sup> and 8<sup>th</sup> year ; thereafter, 1 unit each of LM6K divested in the 9<sup>th</sup> , 10<sup>th</sup> , 12<sup>th</sup>, 15<sup>th</sup> and 20<sup>th</sup> years.

## Power Output

The power churned out over the 20 year period is as shown by the matrix

The screenshot shows a software window titled "Variables - PowerOutput" with three tabs: "currentConfig", "divestedEngines", and "PowerOutput". The "PowerOutput" tab is active, displaying a 21x10 matrix of double values. The matrix shows a decreasing trend in power output over the 21-year period, starting at 505,000 in year 1 and ending at 0 in year 21. The values for each year are: 505000, 505000, 455000, 405000, 355000, 305000, 255000, 230000, 205000, 164000, 123000, 123000, 82000, 82000, 82000, 41000, 41000, 41000, 41000, 41000, and 0.

	1	2	3	4	5	6	7	8	9	10
1	505000									
2	505000									
3	455000									
4	405000									
5	355000									
6	305000									
7	255000									
8	230000									
9	205000									
10	164000									
11	123000									
12	123000									
13	82000									
14	82000									
15	82000									
16	41000									
17	41000									
18	41000									
19	41000									
20	41000									
21	0									

# Appendix K : 3<sup>rd</sup> Simulation for Optimization and Divestment

## Simulation at Discount Rate of 5%

Range: 751-950MW

Fuel: 1e9

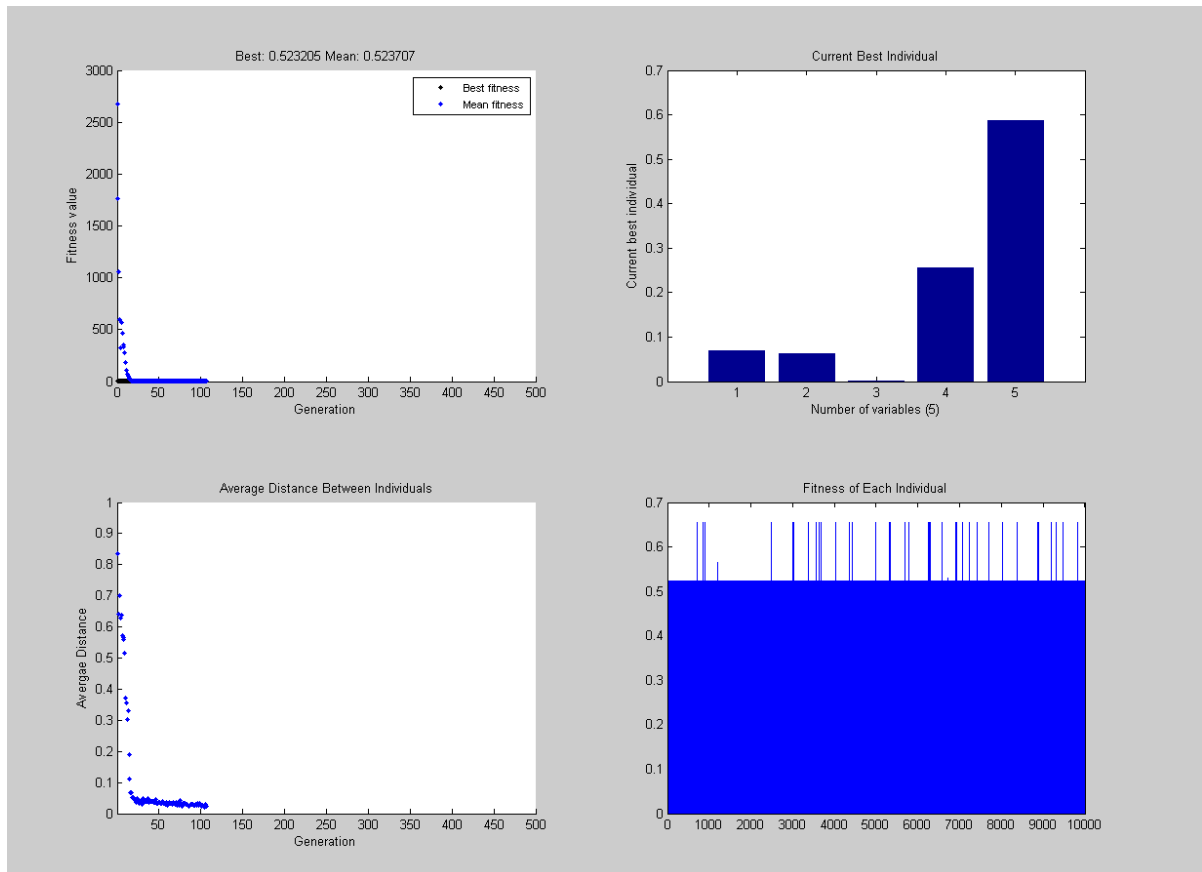
Decline: 13%

Life: 20 Years

Hours: 8000

Population 10,000; Generation 500

## Best Individual, Fitness, Average Distance and Fitness of Each Individual



## Current Configuration and Divested Engines

Variables - currentConfig

currentConfig x divestedEngines x PowerOutput x

21x5 double

	1	2	3	4	5	6	7	8	9	10
1	0	0	0	5	22					
2	0	0	0	5	13					
3	0	0	0	5	10					
4	0	0	0	5	8					
5	0	0	0	5	6					
6	0	0	0	5	4					
7	0	0	0	5	2					
8	0	0	0	5	1					
9	0	0	0	5	0					
10	0	0	0	4	0					
11	0	0	0	3	0					
12	0	0	0	3	0					
13	0	0	0	2	0					
14	0	0	0	2	0					
15	0	0	0	2	0					
16	0	0	0	1	0					
17	0	0	0	1	0					
18	0	0	0	1	0					
19	0	0	0	1	0					
20	0	0	0	1	0					
21	0	0	0	0	0					

Variables - divestedEngines

currentConfig x divestedEngines x PowerOutput x

21x5 double

	1	2	3	4	5	6	7	8	9	10
1	0	0	0	0	0					
2	0	0	0	0	9					
3	0	0	0	0	3					
4	0	0	0	0	2					
5	0	0	0	0	2					
6	0	0	0	0	2					
7	0	0	0	0	2					
8	0	0	0	0	1					
9	0	0	0	0	1					
10	0	0	0	1	0					
11	0	0	0	1	0					
12	0	0	0	0	0					
13	0	0	0	1	0					
14	0	0	0	0	0					
15	0	0	0	0	0					
16	0	0	0	1	0					
17	0	0	0	0	0					
18	0	0	0	0	0					
19	0	0	0	0	0					
20	0	0	0	0	0					
21	0	0	0	1	0					

## The Best Configuration of Plant

For the 751-950MW power range, the best configuration of power plant is [0, 0, 0, 5, 22], that is 5 units of LM6K and 22 units of DS25.

## Divestment of Redundant Engines

Divestment begins in the 1<sup>st</sup> year of operation with 9 units of DS25 and in the second year, 3 units of DS25 are divested. From the 3<sup>rd</sup> to 6<sup>th</sup> year, 2 units each of DS25 are divested every year. Then 1 unit of DS25 divested in the 7<sup>th</sup> and 8<sup>th</sup> year. Thereafter, 1 unit each of LM6K divested in the 9<sup>th</sup>, 10<sup>th</sup>, 12<sup>th</sup>, 15<sup>th</sup> and 20<sup>th</sup> years.

## Power Output

The power output over the 20 year period is as shown by the matrix

The screenshot shows a software window titled "Variables - PowerOutput" with three tabs: "currentConfig", "divestedEngines", and "PowerOutput". The "PowerOutput" tab is active, displaying a 21x10 matrix of double values. The matrix shows power output values for 21 years across 10 configurations. The values decrease over time for each configuration, with the first configuration starting at 755000 and the last configuration starting at 0.

	1	2	3	4	5	6	7	8	9	10
1	755000									
2	530000									
3	455000									
4	405000									
5	355000									
6	305000									
7	255000									
8	230000									
9	205000									
10	164000									
11	123000									
12	123000									
13	82000									
14	82000									
15	82000									
16	41000									
17	41000									
18	41000									
19	41000									
20	41000									
21	0									

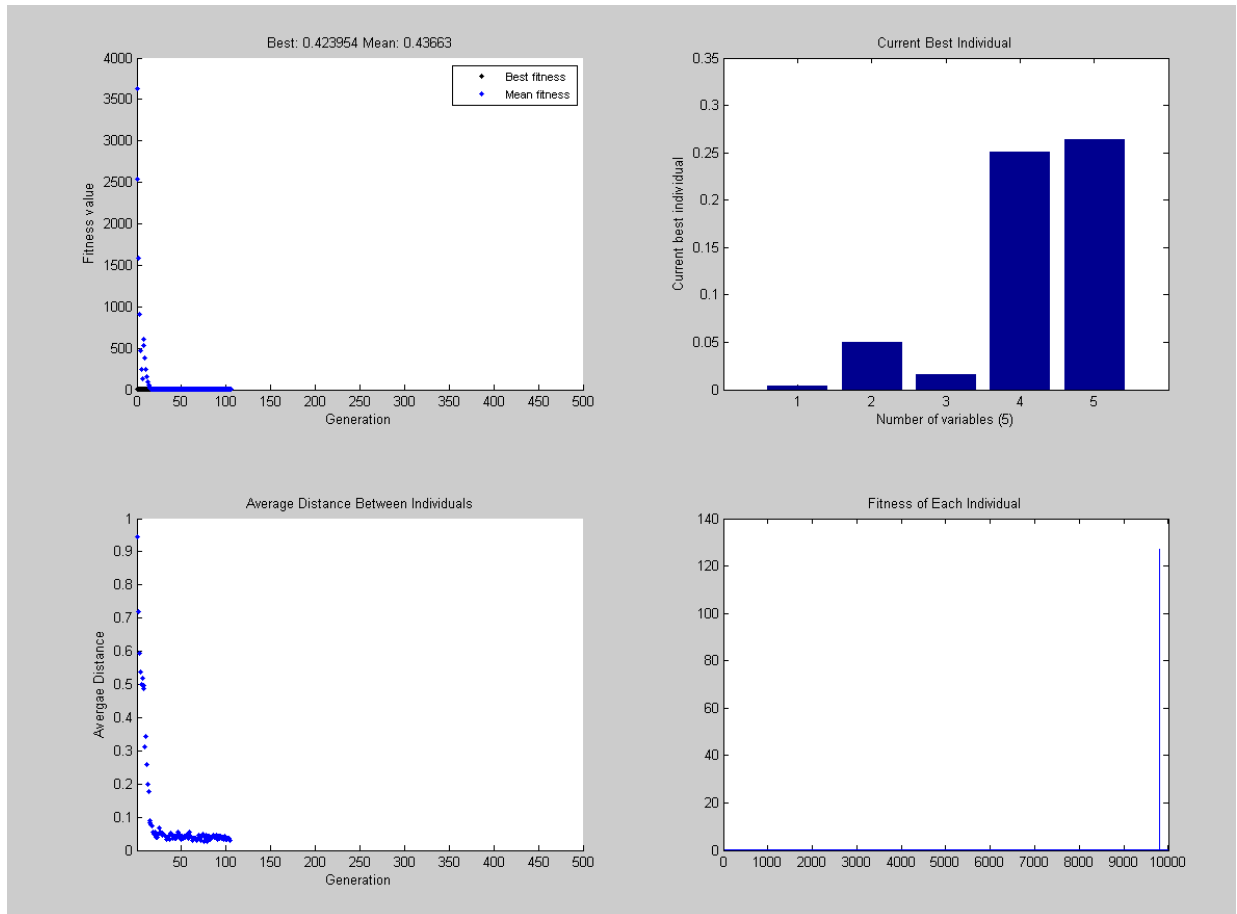


# Appendix L : 4<sup>th</sup> Simulation for Optimization and Divestment

## Simulation at Discount Rate of 10%

- Range: 450-500MW
- Fuel: 1e9
- Decline: 13%
- Life: 20 Years
- Hours: 8000
- Population 10,000; Generation 500

## Best Individual, Fitness, Average Distance and Fitness of Each Individual



## Current Configuration and Divested Engines

Variables - currentConfig

currentConfig x divestedEngines x PowerOutput x

21x5 double

	1	2	3	4	5	6	7	8	9	10
1	0	0	0	5	10					
2	0	0	0	5	10					
3	0	0	0	5	10					
4	0	0	0	5	8					
5	0	0	0	5	6					
6	0	0	0	5	4					
7	0	0	0	5	2					
8	0	0	0	5	1					
9	0	0	0	5	0					
10	0	0	0	4	0					
11	0	0	0	3	0					
12	0	0	0	3	0					
13	0	0	0	2	0					
14	0	0	0	2	0					
15	0	0	0	2	0					
16	0	0	0	1	0					
17	0	0	0	1	0					
18	0	0	0	1	0					
19	0	0	0	1	0					
20	0	0	0	1	0					
21	0	0	0	0	0					

Variables - divestedEngines

currentConfig x divestedEngines x PowerOutput x

21x5 double

	1	2	3	4	5	6	7	8	9	10
1	0	0	0	0	0					
2	0	0	0	0	0					
3	0	0	0	0	0					
4	0	0	0	0	2					
5	0	0	0	0	2					
6	0	0	0	0	2					
7	0	0	0	0	2					
8	0	0	0	0	1					
9	0	0	0	0	1					
10	0	0	0	1	0					
11	0	0	0	1	0					
12	0	0	0	0	0					
13	0	0	0	1	0					
14	0	0	0	0	0					
15	0	0	0	0	0					
16	0	0	0	1	0					
17	0	0	0	0	0					
18	0	0	0	0	0					
19	0	0	0	0	0					
20	0	0	0	0	0					
21	0	0	0	1	0					

## The Best Configuration of Plant

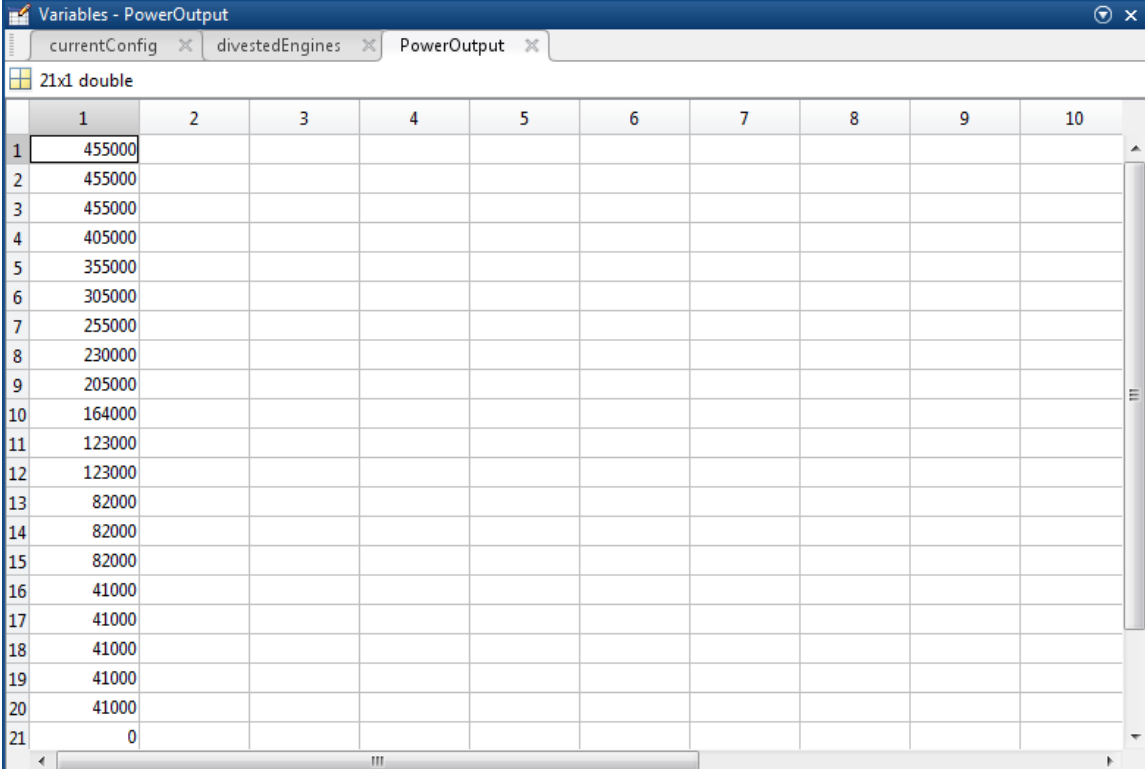
The best configuration of power plant is [0, 0, 0, 5, 10], that is 5 units of LM6K and 10 units of DS25. The same engine mix as was the case for a Discount Rate of 5%.

## Divestment of Redundant Engines

Divestment begins in 3<sup>rd</sup> year of investment with 2 units of DS25, for 4 consecutive years; then 1 unit of DS25 divested in the 7<sup>th</sup> and 8<sup>th</sup> year ; thereafter, 1 unit each of LM6K divested in the 9<sup>th</sup> , 10<sup>th</sup> , 12<sup>th</sup>, 15<sup>th</sup> and 20<sup>th</sup> years.

## Power Output

The power output over the 20 year period is as shown by the matrix.



The screenshot shows a software window titled "Variables - PowerOutput" with three tabs: "currentConfig", "divestedEngines", and "PowerOutput". The "PowerOutput" tab is active, displaying a 21x10 matrix of power output values. The matrix is labeled "21x1 double". The values are as follows:

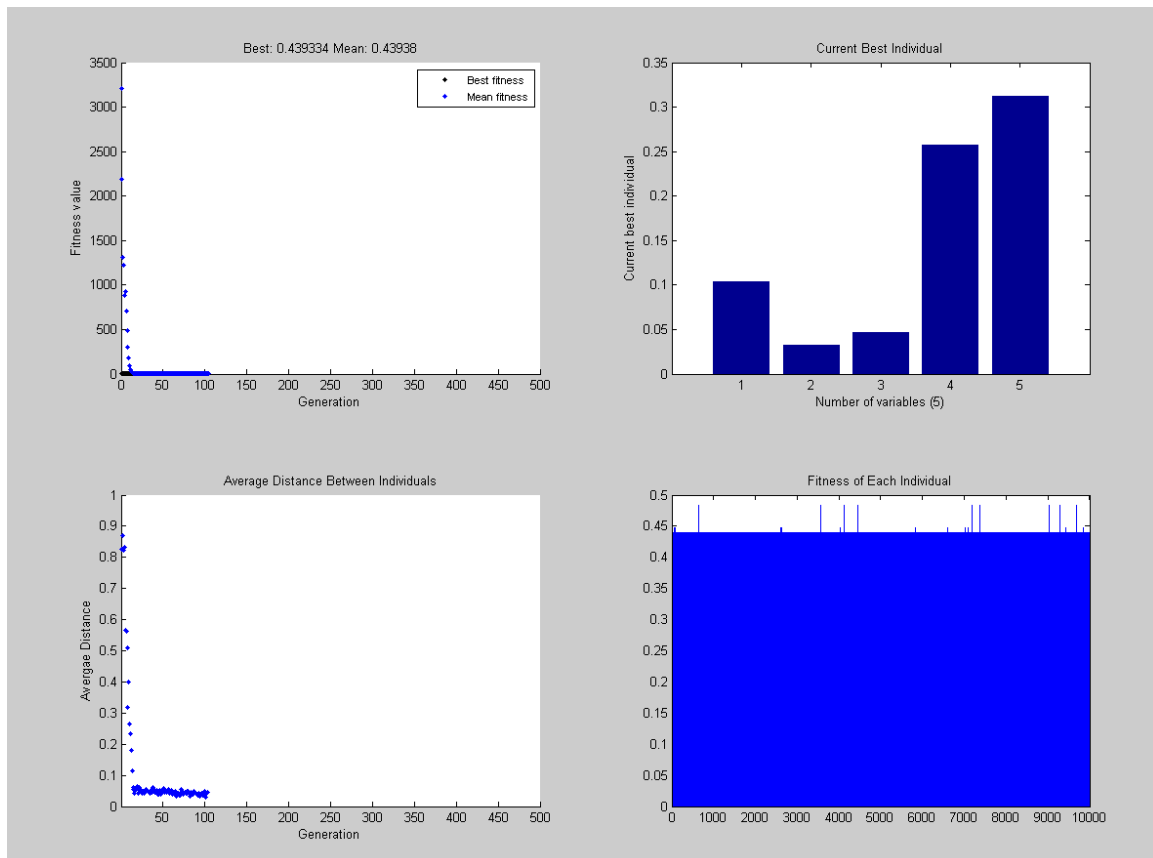
	1	2	3	4	5	6	7	8	9	10
1	455000									
2	455000									
3	455000									
4	405000									
5	355000									
6	305000									
7	255000									
8	230000									
9	205000									
10	164000									
11	123000									
12	123000									
13	82000									
14	82000									
15	82000									
16	41000									
17	41000									
18	41000									
19	41000									
20	41000									
21	0									

## Appendix M : 5<sup>th</sup> Simulation for Optimization and Divestment

### Simulation at Discount Rate of 10%

- Range: 501-750MW
- Fuel: 1e9
- Decline: 13%
- Life: 20 Years
- Hours: 8000
- Population 10,000; Generation 500

### Best Individual, Fitness, Average Distance and Fitness of Each Individual



## Current Configuration and Divested Engines

Variables - currentConfig

currentConfig x divestedEngines x PowerOutput x

21x5 double

	1	2	3	4	5	6	7	8	9	10
1	0	0	0	5	12					
2	0	0	0	5	12					
3	0	0	0	5	10					
4	0	0	0	5	8					
5	0	0	0	5	6					
6	0	0	0	5	4					
7	0	0	0	5	2					
8	0	0	0	5	1					
9	0	0	0	5	0					
10	0	0	0	4	0					
11	0	0	0	3	0					
12	0	0	0	3	0					
13	0	0	0	2	0					
14	0	0	0	2	0					
15	0	0	0	2	0					
16	0	0	0	1	0					
17	0	0	0	1	0					
18	0	0	0	1	0					
19	0	0	0	1	0					
20	0	0	0	1	0					
21	0	0	0	0	0					

Variables - divestedEngines

currentConfig x divestedEngines x PowerOutput x

21x5 double

	1	2	3	4	5	6	7	8	9	10
1	0	0	0	0	0					
2	0	0	0	0	0					
3	0	0	0	0	2					
4	0	0	0	0	2					
5	0	0	0	0	2					
6	0	0	0	0	2					
7	0	0	0	0	2					
8	0	0	0	0	1					
9	0	0	0	0	1					
10	0	0	0	1	0					
11	0	0	0	1	0					
12	0	0	0	0	0					
13	0	0	0	1	0					
14	0	0	0	0	0					
15	0	0	0	0	0					
16	0	0	0	1	0					
17	0	0	0	0	0					
18	0	0	0	0	0					
19	0	0	0	0	0					
20	0	0	0	0	0					
21	0	0	0	1	0					

## The Best Configuration of Plant

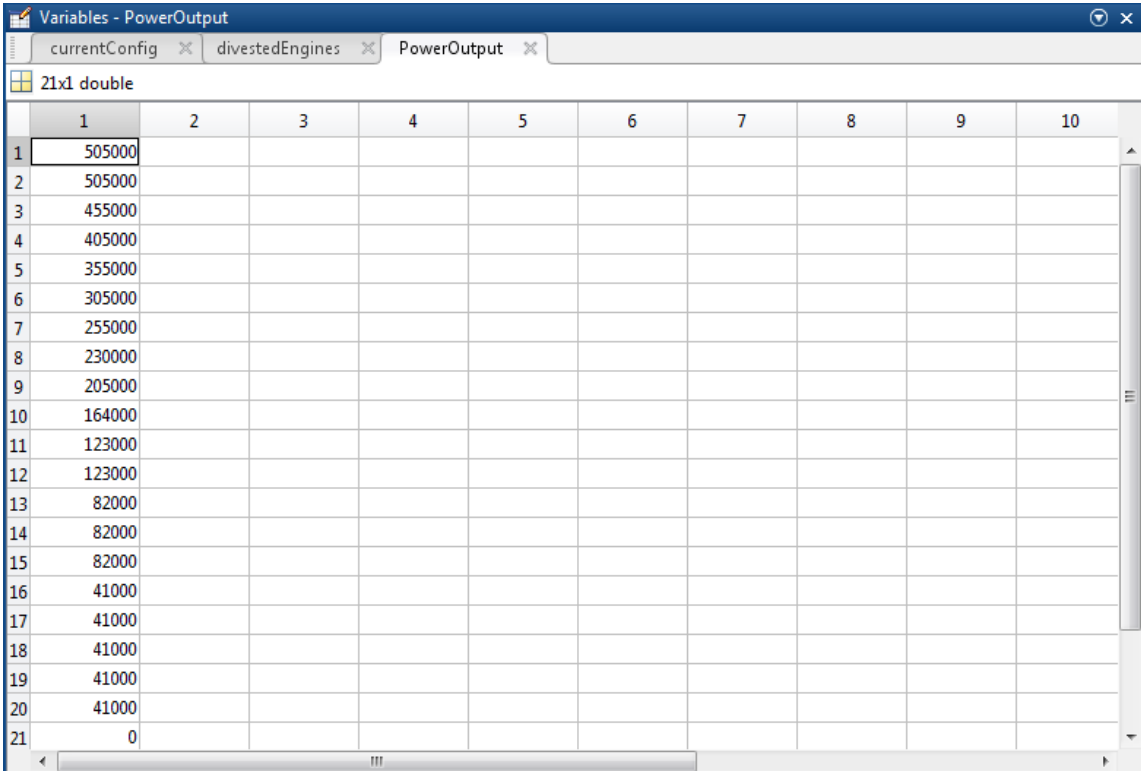
The best configuration of power plant is [0, 0, 0, 5, 12], that is 5 units of LM6K and 12 units of DS25.

## Divestment of Redundant Engines

Divestment begins in 2<sup>nd</sup> year of operation with 2 units of DS25, for 5 consecutive years; then 1 unit of DS25 divested in the 7<sup>th</sup> and 8<sup>th</sup> year ; thereafter, 1 unit each of LM6K divested in the 9<sup>th</sup> , 10<sup>th</sup> , 12<sup>th</sup>, 15<sup>th</sup> and 20<sup>th</sup> years.

## Power Output

The power output over the 20 year period is as shown by the matrix.



The screenshot shows a software window titled "Variables - PowerOutput" with three tabs: "currentConfig", "divestedEngines", and "PowerOutput". The "PowerOutput" tab is active, displaying a 21x10 matrix of double values. The matrix shows a decreasing trend in power output over the 20-year period, starting at 505,000 in year 1 and ending at 0 in year 21. The values are constant for each year from year 1 to year 20, with a final value of 0 in year 21.

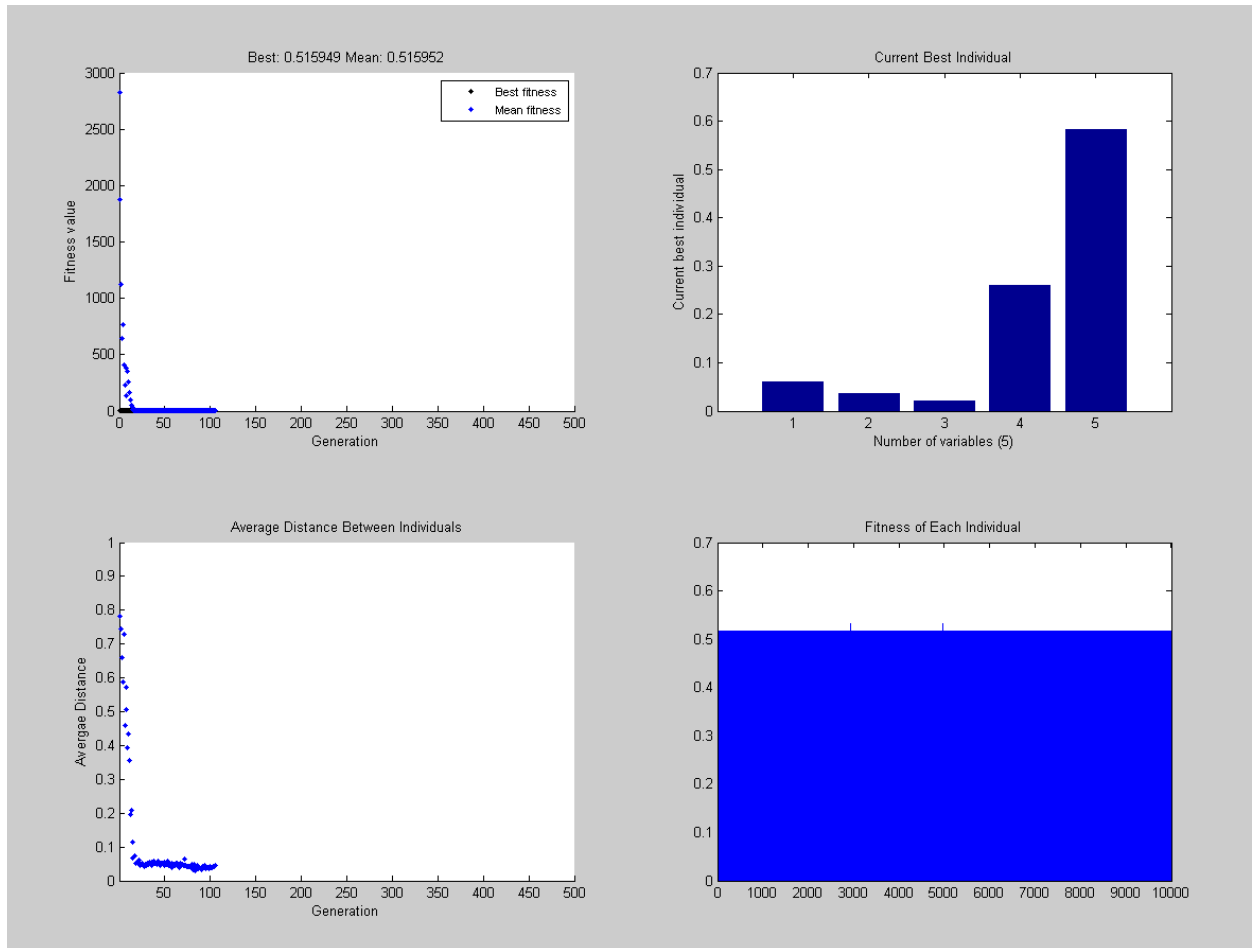
	1	2	3	4	5	6	7	8	9	10
1	505000									
2	505000									
3	455000									
4	405000									
5	355000									
6	305000									
7	255000									
8	230000									
9	205000									
10	164000									
11	123000									
12	123000									
13	82000									
14	82000									
15	82000									
16	41000									
17	41000									
18	41000									
19	41000									
20	41000									
21	0									

# Appendix N : 6<sup>th</sup> Simulation for Optimization and Divestment

## Simulation at Discount Rate of 10%

- Range: 751-950MW
- Fuel: 1e9
- Decline: 13%
- Life: 20 Years
- Hours: 8000
- Population 10,000; Generation 500

## Best Individual, Fitness, Average Distance and Fitness of Each Individual



## Current Configuration and Divested Engines

Variables - currentConfig

currentConfig | divestedEngines | PowerOutput

21x5 double

	1	2	3	4	5	6	7	8	9	10
1	0	0	0	5	22					
2	0	0	0	5	13					
3	0	0	0	5	10					
4	0	0	0	5	8					
5	0	0	0	5	6					
6	0	0	0	5	4					
7	0	0	0	5	2					
8	0	0	0	5	1					
9	0	0	0	5	0					
10	0	0	0	4	0					
11	0	0	0	3	0					
12	0	0	0	3	0					
13	0	0	0	2	0					
14	0	0	0	2	0					
15	0	0	0	2	0					
16	0	0	0	1	0					
17	0	0	0	1	0					
18	0	0	0	1	0					
19	0	0	0	1	0					
20	0	0	0	1	0					
21	0	0	0	0	0					

Variables - divestedEngines

currentConfig | divestedEngines | PowerOutput

21x5 double

	1	2	3	4	5	6	7	8	9	10
1	0	0	0	0	0					
2	0	0	0	0	9					
3	0	0	0	0	3					
4	0	0	0	0	2					
5	0	0	0	0	2					
6	0	0	0	0	2					
7	0	0	0	0	2					
8	0	0	0	0	1					
9	0	0	0	0	1					
10	0	0	0	1	0					
11	0	0	0	1	0					
12	0	0	0	0	0					
13	0	0	0	1	0					
14	0	0	0	0	0					
15	0	0	0	0	0					
16	0	0	0	1	0					
17	0	0	0	0	0					
18	0	0	0	0	0					
19	0	0	0	0	0					
20	0	0	0	0	0					
21	0	0	0	1	0					



## The Best Configuration of Plant

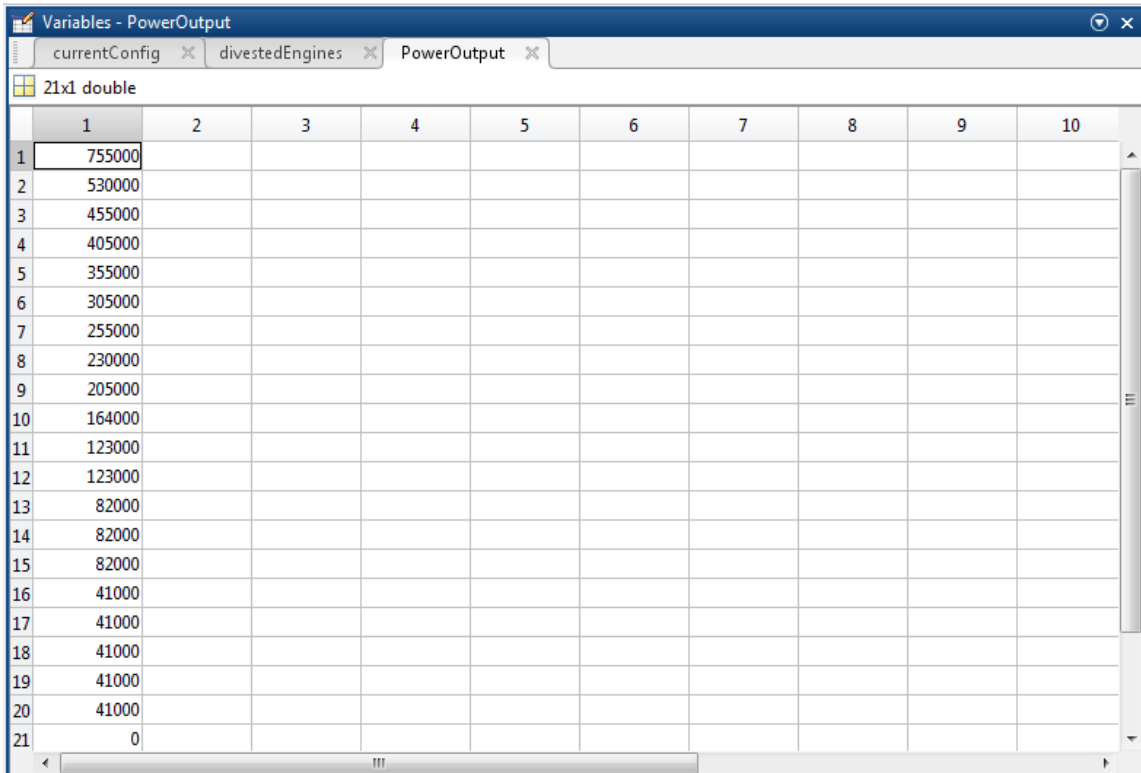
The best configuration of power plant is [0, 0, 0, 5, 22], that is 5 units of LM6K and 22 units of DS25.

## Divestment of Redundant Engines

Divestment begins in first year of investment with 9 units of DS25 and in the second year, 3 units of DS25 are divested. From the 3<sup>rd</sup> to 6<sup>th</sup> year, 2 units each are divested every year. Then 1 unit of DS25 divested in the 7<sup>th</sup> and 8<sup>th</sup> year . Thereafter, 1 unit each of LM6K divested in the 9<sup>th</sup>, 10<sup>th</sup>, 12<sup>th</sup>, 15<sup>th</sup> and 20<sup>th</sup> years.

## Power Output

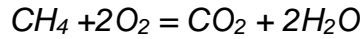
The power output over the 20 year period is as shown by the matrix



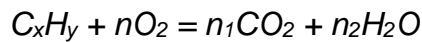
	1	2	3	4	5	6	7	8	9	10
1	755000									
2	530000									
3	455000									
4	405000									
5	355000									
6	305000									
7	255000									
8	230000									
9	205000									
10	164000									
11	123000									
12	123000									
13	82000									
14	82000									
15	82000									
16	41000									
17	41000									
18	41000									
19	41000									
20	41000									
21	0									

## Appendix P : CO<sub>2</sub> Emissions by Hand Calculation

CO<sub>2</sub> can be worked out by hand using the stoichiometric equation which assumes complete or near complete combustion



The emission produced by each engine has to be predicted for comparison purposes. Engine emissions are regulated and taxed, hence it is a vital element of the economic model. This becomes obvious because an engine with good performance that falls short of the emissions regulations could turn out to be less profitable as a result of the emission tax levied. Equation 1 emphasizes the consumption of CH<sub>4</sub> to produce CO<sub>2</sub> and H<sub>2</sub>O; CH<sub>4</sub> is a very potent greenhouse gas, 21 times more potent than CO<sub>2</sub>. The generic equation governing the formation of CO<sub>2</sub> during combustion of hydrocarbon fuels (Razak, 2007) is given by,



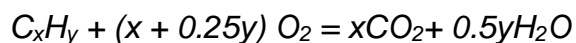
Performing a molar balance gives,

$$n_1 = x$$

$$n_2 = 0.5y$$

$$n = n_1 + 0.5n_2 = x + 0.25y$$

Substituting n, n<sub>1</sub> and n<sub>2</sub> into Equation 2 gives,



Hence, 1 mole of fuel will produce x g of CO<sub>2</sub>

But 1 kilo mole of fuel weighs (x \*12 + y\*1) kg

1 kilo mole of CO<sub>2</sub> will weigh 44kg

That is, 1 kg of fuel = 44/(12 +x/y)kg of CO<sub>2</sub>

If 1kg of methane CH<sub>4</sub> whose x/y ratio is 0.25 is burnt, then 2.75kg of CO<sub>2</sub> will be emitted. That is, 2.75kgCO<sub>2</sub> will be emitted per kg of Methane based hydrocarbon fuel burnt. Therefore, the Emission Index (EI) for CO<sub>2</sub> = 2.75.

# Appendix Q : TERA of the Study Engines

## Appendix Q.1: DS25 Economic Analysis at Design Point

Economic Model for DS25 [Compatibility Mode] - Excel

Isaiah Allison

FILE HOME INSERT PAGE LAYOUT FORMULAS DATA REVIEW VIEW @RISK

Define Add Insert Define Distribution Model Distributions Output Function Correlations Fitting Window Iterations: 5000 Simulations: 1 Start Simulation Excel Reports Results Summary Define Filters Advanced Analyses Optimizer Time Library Color Cells Utilities Help

G40 : =RiskOutput("NPVclean25")+J33-D6

DS25 Economic Analysis at Design Point												
10% Discount Rate (r)			0.1	Gas Collection Cost (\$/kWh)		0.045	Electricity Tariff from Grid (\$/kWh)		0.1			Loan Details
Capital Cost (\$/Kw)			973	Gas Consumed/year (kg)		451037964	Electricity Consumed/year (kWh)		1611840000			Amount (\$)
Initial Cash Flow (F <sub>0</sub> , \$)			243250000	Excess Electricity Sold to Grid/year (kWh)		241776000	Grid Electricity/year (kWh)		140160000			Interest rate (%)
Conversion			1000	Emission/year (kg)		358974933	Electricity Export Tariff to Grid (\$/kWh)		0.09			Loan Duration (years)
Emission Tax (\$/kg)			0.005	Number of GT Engines		10	Fixed O&M Cost (\$)		1000000			Repayment Holiday
				Nominal Capacity at DP (MW)		25	Variable O&M Cost (\$/kWh)		0.02			
				Hours of Operation		8059	Major Maintenance Cost (\$)		1112169.6			
				Power Generated from 10xGTs		1.854E+09						
Year (n)	O&M Cost (3% Annual Increase, \$)	Gas Collection Cost (5% Annual Increase, \$)	Grid Electricity Cost (5% Annual Increase During Outages, \$)	Emission Tax, (3% Annual Increase, \$)	Saved Electricity Cost (5% Annual Increase, \$)	Revenue on Excess Electricity Sold to Grid (5% Annual Increase, \$)	Annual Loan Repayment, \$)	Annual Net Cash Flow, \$)	Present Value (10% Discount Rate, \$) F <sub>n</sub> /(1 + r) <sup>n</sup>	Internal Rate of Return (IRR % Discount Rate, %)	Cost of Electricity (1% Annual Increase)	
1	39184490	83412720	14016000	1794874.663	161184000	21759840	0	44535755.74	40487050.67	37863250.68	0.061007564	
2	40360024	87583356	14716800	1848720.903	169243200	22847832	0	47582130.81	39324075.05	34392363.9	0.06161764	
3	41570825	91962523.8	15452640	1904182.53	177705360	23990223.6	31501988	19303424.39	14502948.45	11862099.7	0.062233816	
4	42817950	96560649.99	16225272	1961308.006	186590628	25189734.78	31501988	22713195.16	15513417.91	11866277.87	0.062856155	
5	44102488	101388682.5	17036535.6	2020147.247	195920159.4	26449221.52	31501988	26319539.46	16342363.27	11690245.66	0.063484716	
6	45425563	106458116.6	17888362.38	2080751.664	205716167.4	27771682.59	31501988	30133068.54	17009331.62	11378834.52	0.064119563	
7	46788330	111781022.4	18782780.5	2143174.214	216001975.7	29160266.72	31501988	34164947.65	17532020.25	10968424.56	0.064760759	
8	48191980	117370073.6	19721919.52	2207469.44	226802074.5	30618280.06	31501988	38426924.51	17926443.88	10488374.61	0.065408367	

DP Case1 Case2 Case3 Summary

# Appendix Q.2: DS25 Economic Analysis for Slow Degradation

Economic Model for DS25 [Compatibility Mode] - Excel

FILE HOME INSERT PAGE LAYOUT FORMULAS DATA REVIEW VIEW @RISK

Define Add Insert Define Distribution Model Iterations: 5000 Start Simulation

Distributions Output Function Correlations Fitting Window Simulations: 1 Simulation

Excel Reports Results Define Filters Results

Advanced Analyses RISK Optimizer Time Series Library Tools

Color Cells Utilities Help

G40 :  $=RiskOutput("NPVslowDeg25")+J33-D6$

Year (n)	O&M Cost (3% Annual Increase, \$)	Gas Collection Cost (5% Annual Increase, \$)	Grid Electricity Cost (5% Annual Increase During Outages, \$)	Emission Tax (3% Annual Increase, \$)	Saved Electricity Cost (5% Annual Increase, \$)	Revenue on Excess Electricity Sold to Grid (5% Annual Increase, \$)	Annual Loan Repayment, \$)	Annual Net Cash Flow (\$)	Present Value (10% Discount Rate, \$)	Internal Rate of Return (IRR % Discount Rate, \$)	Cost of Electricity (1% Annual Increase)
1	39671010	83122443.73	14016000	1772752.126	161184000	21179287.47	0	43781081.17	39800983	37319379	0.067436938
2	40861141	87278565.92	14716800	1825934.69	169243200	22238251.84	0	46799010.47	38676868	34004197	
3	42086975	91642494.22	15452640	1880712.731	177705360	23350164.43	31501987.86	18490714.65	13892348	11452425	
4	43349584	96224618.93	16225272	1937134.113	186590628	24517672.66	31501987.86	21869703.53	14937302	11546081	
5	44650072	101035849.9	17036536	1995248.136	195920159.4	25743556.29	31501987.86	25444022.46	15798736	11450525	
6	46090674	106087642.4	17888362	2066106.68	206716167.4	27030734.4	31501987.86	28224220.38	16496316	11210646	

READY

# Appendix Q.3: DS25 Economic Analysis for Medium Degradation

Economic Model for DS25 [Compatibility Mode] - Excel

Isaiah Allison

FILE HOME INSERT PAGE LAYOUT FORMULAS DATA REVIEW VIEW @RISK

Define Add Insert Define Distribution Model  
Distributions Output Function Correlations Fitting Window

Iterations: 5000  
Simulations: 1  
Settings: [Icons]  
Start Simulation

Excel Reports Browse Results Summary Define Filters

Advanced Analyses RISK Optimizer Time Series Library

Color Cells Utilities Help

G40 :  $\text{=RiskOutput("NPVmedDeg25")+J33-D6}$

DS25 Economic Analysis for Medium Degradation												
4	10% Discount Rate (r)	0.1	Gas Collection Costs (\$/kWh)	0.045	Electricity Tariff From Grid (\$/kWh)	0.1	Loan Details					
5	Engine Capital Cost (\$/Kw)	973	Fuel Consumed (kg/year)	456782561.3	Electricity Consumed/year (kWh)	1611840000	Amount (\$)					
6	Initial Cash flow (F <sub>0</sub> , \$)	243250000	Excess Electricity Sold to Grid/year (kWh)	226947072	Grid Electricity/year (kWh)	140160000	Interest rate (%)					
7	Conversion	1000	Emissions/year (kg)	359565401.9	Electricity Tariff to Grid (\$/kWh)	0.09	Loan Duration (year)					
8			Number of GTs	10	Fixed O&M Cost (\$)	992000	Repayment Holiday					
9	Emission Tax (\$/kg)	0.005	Nominal Capacity at DP (MW)	24.8	Variable O&M cost (\$/kWh)	0.02						
10			Hours of Operation	8059	Major Maintenance Cost (\$)	2063407.55						
11			Power Generated from 10xGTs	1838787072								
12	Year (n)	O&M Cost (3% Annual Increase, \$)	Gas Collection Cost (5% Annual Increase, \$)	Grid Electricity Cost (5% Annual Increase During Outages (\$))	Emission Tax (3% Annual Increase, \$)	Saved Electricity Cost (5% Annual Increase, \$)	Revenue on Electricity Sold to Grid (5% Annual Increase, \$)	Annual Loan Repayment (\$)	Annual Net Cash Flow (\$)	Present Value (10% Discount Rate, \$) $F_n/(1+r)^n$	Internal Rate of Return (IRR % Discount Rate, \$) $F_n/(1+IRR)^n$	Cost of Electricity (1% Annual Increase)
13	1	39831149	82745418.24	14016000	1797827.009	161184000	20425236.48	0	43218842.24	39289856.58	36914727.88	0.0676399
14	2	41026083	86882689.15	14716800	1851761.82	169243200	21446498.3	0	46212363.87	38192036.26	33714076.63	
15	3	42256866	91226823.61	15452640	1907314.674	177705360	22518823.22	31501987.86	17878551.11	13432420.07	11140686.37	
16	4	43524572	95788164.79	16225272	1964534.114	186590628	23644764.38	31501987.86	21230861.67	14500964.19	11299878.96	
17	5	44830309	100577573	17036535.6	2023470.138	195920159.4	24827002.6	31501987.86	24777286.27	15384745.37	11263839.46	
18	6	46175218	105606451.7	17888362.38	2084174.242	205716167.4	26068352.73	31501987.86	28528325.56	16103496.05	11077341.33	
19	7	47560475	110886774.3	18782780.5	2146699.469	216001975.7	27371770.37	31501987.86	32495029.08	16675087.98	10777120.25	
20	8	48987289	116431113	19721919.52	2211100.453	226802074.5	28740358.88	31501987.86	36689023.42	17115700.2	10393181.06	
21	9	50456908	122252668.6	20708015.5	2277433.467	238142178.3	30177376.83	31501987.86	41122541.78	17439972.03	9949902.714	

READY

# Appendix Q.4: DS25 Economic Analysis for Fast Degradation

Economic Model for DS25 [Compatibility Mode] - Excel

FILE HOME INSERT PAGE LAYOUT FORMULAS DATA REVIEW VIEW @RISK

Define Add Insert Define Distribution Model Iterations: 5000 Simulations: 1 Start Simulation Excel Reports Browse Results Summary Define Filters Advanced Analyses Optimizer Time Series Library Color Cells Utilities Help

G40 :  $=RiskOutput("NPVfastDeg25")+J33-D6$

1	A	B	C	D	E	F	G	H	I	J	K	L	M	N
2	DS25 Economic Analysis for Fast Degradation													
4	10% Discount Rate (r)		0.1	Gas Collection Cost (\$/kWh)			0.045	Electricity Tariff From Grid (\$/kWh)		0.1	Loan De			
5	Capital Cost (\$/Kw)		973	Fuel Consumed/year (kg)		470331688.3	Electricity Consumed/year (kWh)		1611840000	Amount				
6	Initial Cash flow (F <sub>0</sub> , \$)		243250000	Excess Electricity Sold to Grid/year (kWh)		257568808.3	Grid Electricity/year (kWh)		140160000	Interest				
7	Conversion		1000	Emission/year (kg)		353627679.4	Electricity Tariff to Grid (\$/kWh)		0.09	Loan Du				
8	Emission Tax (\$/kg)		0.005	Number of GTs		10	Fixed O&M Cost (\$)		1008520	Repaym				
9				Nominal Capacity at DP (MW)		24.8	Variable O&M Cost (\$/kWh)		0.02					
10				Hours of Operation		8059	Major Maintenance Cost (\$)		5227310.655					
11				Power Generated from 10xGTs		1869408808								
12	Year (n)	O&M Cost (3% Annual Increase, \$)	Gas Collection Cost (5% Annual Increase, \$)	Grid Electricity Cost (5% Annual Increase During Outages, \$)	Emission Tax (3% Annual Increase, \$)	Saved Electricity Cost (5% Annual Increase, \$)	Revenue From Excess Electricity Sold to Grid (5% Annual Increase, \$)	Annual Loan Repayment (\$)	Annual Net Cash Flow (\$)	Present Value (10% Discount Rate, \$) $F_n/(1+r)^n$	Internal Rate of Return (IRR % Discount Rate, \$) $F_n/(1+IRR)^n$	Cost of Electricity (1% Annual Increase)		
13	1	43624007	84123396.37	14016000	1768138.397	161184000	23181192.75	0	40833651.16	37121501.1	35136755.16	0.069282071		
14	2	44932727	88329566.19	14716800	1821182.549	169243200	24340252.39	0	43783176.62	36184443.5	32418591.66			
15	3	46280709	92746044.5	15452640	1875818.025	177705360	25557265.01	31501987.86	15405425.78	11574324.4	9815309.994			
16	4	47669130	97383346.73	16225272	1932092.566	186590628	26835128.26	31501987.86	18713927	12781863.9	10259795.01			
17	5	49099204	102252514.1	17036536	1990055.343	195920159.4	28176884.67	31501987.86	22216747.2	13794852.1	10480877.95			
18	6	50572180	107365139.8	17888362	2049757.003	205716167.4	29585728.9	31501987.86	25924469.14	14633687	10523749.47			

... Burner Turbines Nozzles Mass Flow Pressure Temperature Creep Life Power Demand DP Case1 Case2 Case3 Summary

READY 100%

# Appendix Q.5: LM6K Economic Analysis at Design Point

Economic Model for LM6K [Compatibility Mode] - Excel

Isaiah Allison

FILE HOME INSERT PAGE LAYOUT FORMULAS DATA REVIEW VIEW @RISK

From Access From Web From Text From Other Sources Existing Connections Refresh All Connections Sort Filter Clear Reapply Advanced Text to Columns Flash Fill Remove Duplicates Data Validation Consolidate What-If Analysis Relationships Group Ungroup Subtotal Outline

K40 : =K33-D6

LM6K Economic Analysis at Design Point													
4	10% Discount Rate (r)		0.1	Gas Collection Cost (\$/kWh)		0.045	Electricity Tariff From Grid (\$/kWh)		0.1	Loan Details			
5	Capital Cost (\$/Kw)		973	Fuel Consumed/years (kg)		342166230.7	Electricity Consumed/year (kWh)		805920000	Amount (\$)			
6	Initial Cash Flow (F <sub>0</sub> , \$)		198127125	Excess Electricity Sold to Grid/year (kWh)		703850232	Grid Electricity/year (kWh)		70080000	Interest Rate (%)			
7	Conversion		1000	Emissions/year (kg)		279903801.7	Electricity Selling Tariff to Grid (\$/kWh)		0.09	Loan Duration (year)			
8				Number of GTs		5	Fixed O&M Cost (\$)		814500	Repayment Holiday			
9	Emissions Tax (\$/kg)		0.005	Nominal Capacity at DP (MW)		40.725	Variable O&M Cost (\$/kWh)		0.02				
10				Hours of Operation		8059	Major Maintenance Cost (\$)		2264655.348				
11				Power Generated from 5xGT		1509770232							
12	Year (n)	O&M cost (3% Annual Increase, \$)	Fuel Cost (5% Annual Increase, \$)	Grid Electricity Cost (5% Annual Increase During Outages, \$)	Emissions Tax (3% Annual Increase, \$)	Saved Electricity Cost (5% Annual Increase, \$)	Revenue From Excess Electricity Sold to Grid (5% Annual Increase, \$)	Annual Loan Repayment, \$)	F <sub>n</sub> (Annual Net Cash Flow, \$)	Present Value (10% Discount Rate, \$) F <sub>n</sub> /(1 + r) <sup>n</sup>	Internal Rate of Return (IRR % Discount Rate, \$) F <sub>n</sub> /(1 + IRR) <sup>n</sup>	Cost of Electricity (1% Annual Increase)	
13	1	33274560	67939660.44	7008000	1399519.009	80592000	63346520.88	0	34316781.44	31197074.04	27422380.53	0.061788278	
14	2	34272797	71336643.46	7358400	1441504.579	84621600	66513846.92	0	36726102.1	30352150.49	23451576.66	0.06240616	
15	3	35300981	74903475.64	7726320	1484749.716	88852680	69839539.27	25658369.11	13618324.12	10231648.47	6948954.679	0.063030222	
16	4	36360010	78648649.42	8112636	1529292.208	93295314	73331516.23	25658369.11	16317873.38	11145327.08	6653619.732	0.063660524	
17	5	37450810	82581081.89	8518267.8	1575170.974	97960079.7	76998092.05	25658369.11	19174471.56	11905838.25	6247646.167	0.064297129	
18	6	38574335	86710135.98	8944181.19	1622426.103	102858083.7	80847996.65	25658369.11	22196633.22	12529420.79	5779346.48	0.064940101	
19	7	39731565	91045642.78	9391390.249	1671098.886	108000987.9	84890396.48	25658369.11	25393318.55	13030787.56	5283353.764	0.065589502	
20	8	40923512	95597924.92	9860959.762	1721231.853	113401037.3	89134916.3	25658369.11	28773956.21	13423262.93	4783969.62	0.066245397	

... Turbines | Nozzles | Mass Flow | Pressure | Temperature | Creep Life | Power Demand | DP | Case1 | Case2 | Case3 | Summary

READY

# Appendix Q.6: LM6K Economic Analysis for Slow Degradation

Economic Model for LM6K [Compatibility Mode] - Excel

Isaiah Allison

FILE HOME INSERT PAGE LAYOUT FORMULAS DATA REVIEW VIEW @RISK

Define Add Insert Define Distribution Model  
Distributions Output Function Correlations Fitting Window

Iterations: 5000  
Simulations: 1  
Settings: Start Simulation

Excel Reports Browse Results Summary Define Filters

Advanced Analyses RISK Optimizer Time Series Library

Color Cells Utilities Help

G40 :  $=RiskOutput("NPVslowDeg6k")+J33-D6$

LM6K Economic Analysis for Slow Degradation														
4	10% Discount Rate (r)	0.1	Gas Collection Cost (\$/kWh)	0.045	Electricity Tariff From Grid (\$/kWh)	0.1	Loan Details							
5	Engine Capital Cost (\$/Kw)	973	Fuel Consumed/year (kg)	355048056	Electricity Consumed/year (kWh)	805920000	Amount (\$)	1.9						
6	Initial Cash flow (F <sub>0</sub> )\$	198127125	Excess Electricity Sold to Grid/year (kWh)	745334158.1	Grid Electricity/year (kWh)	70080000	Interest Rate (%)							
7	Conversion	1000	Emissions/year (kg)	269560740	Electricity Selling Tariff to Grid (\$/kWh)	0.09	Loan Duration (years)							
8			Number of GT Engines	5	Fixed O&M cost (\$)	836880	Repayment Holiday	2 ye						
9	Emissions Tax (\$/kg)	0.005	Nominal Capacity at DP (MW)	41.844	Variable O&M Cost (\$/kWh)	0.02								
10			Hours of Operation	8059	Major Maintenance Cost (\$)	3994326.412								
11			Power Generated from 5xGT	1551254158										
12	Year (n)	O&M Cost (3% Annual Increase, \$)	GT Fuel Cost (5% Annual Increase, \$)	Grid Electricity Cost (5% Annual Increase) During Outages (\$)	Emissions Tax (3% Annual Increase, \$)	Saved Electricity Cost (5% Annual Increase)	Revenue From Excess Electricity Sold to Grid (5% Annual Increase, \$)	Annual Loan repayment (\$)	Annual Net Cash Flow (\$)	Present Value (10% Discount Rate) (\$)	Internal Rate of Return (IRR % Discount Rate) (\$)	Cost of Electricity (1% Annual Increase)		
13	1	35856290	69806437.11	7008000	1347803.7	80592000	67080074.23	0	33653543.84	30594131	28902366.36	0.068983862		
14	2	36931978	73296758.97	7358400	1388237.811	84621600	70434077.94	0	36080302.9	29818432	26611868.63			
15	3	38039938	76961596.92	7726320	1429884.945	88852680	73955781.84	25658369.11	12992353.25	9761347	8229920.011			
16	4	39181136	80809676.76	8112636	1472781.494	93295314	77653570.93	25658369.11	15714285.82	10733069	8548797.702			
17	5	40356570	84850160.6	8518267.8	1516964.938	97960079.7	81536249.47	25658369.11	18595996.91	11546651	8688252.928			
18	6	41567267	89092668.63	8944181.2	1562473.886	102858083.7	85613061.95	25658369.11	21646185.91	12218708	8685542.947			

Case1 Case2 Case3 Summary

READY 100%



# Appendix Q.7: LM6K Economic Analysis for Medium Degradation

Economic Model for LM6K [Compatibility Mode] - Excel

FILE HOME INSERT PAGE LAYOUT FORMULAS DATA REVIEW VIEW @RISK

Define Add Insert Define Distribution Model  
Distributions Output Function Correlations Fitting Window

Iterations: 5000  
Simulations: 1  
Settings

Start Simulation

Excel Reports Browse Results

Summary Define Filters

Advanced Analyses Risk Optimizer Time Series Library

Color Cells Utilities Help

Isaiah Allison

K40 : X ✓ fx =K33-D6

	A	B	C	D	E	F	G	H	I	J	K	L	M	N	O
1															
2	<b>LM6K Economic Analysis for Medium Degradation</b>														
3															
4	10% Discount Rate (r)			0.1	Gas Collection Cost (\$/kWh)			0.045	Electricity Tariff From Grid (\$/kWh)			0.1	Loan Details		
5	Capital Cost (\$/Kw)			973	Fuel Consumed/year (kg)			360691107.8	Electricity Consumed/year (kWh)			805920000	Amount (\$)		
6	Initial Cash Flow (F <sub>0</sub> )\$			198127125	Excess Electricity Sold to Grid/year (kWh)			763388377.9	Grid Electricity/year (kWh)			70080000	Interest Rate (%)		
7	Conversion			1000	Emission/year kg			284154027.8	Electricity Export Tariff to Grid (\$/kWh)			0.09	Loan Duration (years)		
8					Number of GT Engines			5	Fixed O&M Cost (\$)			846620	Repayment Holiday		
9	Emission Tax (\$/kg)			0.005	Nominal Capacity at DP (MW)			42.331	Variable O&M Cost (\$/kWh)			0.02			
10					Hours of Operation			8059	Major Maintenance Cost (\$)			5037656.97			
11					Power Generated from 5xGTs			1569308378							
12	Year (n)	O&M cost (3% Annual Increase Rate, \$)	Fuel Cost, (5% Annual Increase, \$)	Grid Electricity Cost (5% Annual Increase During Outages, \$)	Emissions Tax (3% Annual Increase, \$)	Saved Electricity Cost (5% Annual Increase, \$)	Revenue on Excess Electricity Sold to Grid (5% Annual Increase, \$)	Annual Loan Repayment (\$)	Annual Net Cash Flow (\$)	Present Value (10% Discount Rate) (\$)	Internal Rate of Return (IRR % Discount Rate) (\$)	Cost of Electricity (1% Annual Increase)			
13	1	37270445	70618877.01	7008000	1420770.139	80592000	68704954.01	0	32978862.34	29980783.94	28389637.44	0.06965557			
14	2	38388558	74149820.86	7358400	1463393.243	84621600	72140201.71	0	35401629.75	29257545.25	26234428.54				
15	3	39540215	77857311.9	7726320	1507295.04	88852680	75747211.8	25658369.11	12310381.15	9248971.559	7853152.457				
16	4	40726421	81750177.49	8112636	1552513.892	93295314	79534572.39	25658369.11	15029768.85	10265534.36	8253706.229				
17	5	41948214	85837686.37	8518267.8	1599089.308	97960079.7	83511301.01	25658369.11	17909754.45	11120548.43	8466628.684				
18	6	43206660	90129570.69	8944181.19	1647061.988	102858083.7	87686866.06	25658369.11	20959106.69	11830869.32	8529387.136				
19	7	44502860	94636049.22	9391390.249	1696473.847	108000987.9	92071209.36	25658369.11	24187054.92	12411783.59	8473293.027				
20	8	45837946	99367851.68	9860959.762	1747368.063	113401037.3	96674769.83	25658369.11	27603312.79	12877149.14	8324432.155				
21	9	47213084	104336244.3	10354007.75	1799789.104	119071089.1	101508508.3	25658369.11	31218103.16	13239523.2	8104460.301				

READY

Turbines Nozzles Mass Flow Pressure Temperature Creep Life Power Demand DP Case1 Case2 Case3 Summary

100%

# Appendix Q.8: LM6K Economic Analysis for Fast Degradation

Economic Model for LM6K [Compatibility Mode] - Excel

FILE HOME INSERT PAGE LAYOUT FORMULAS DATA REVIEW VIEW @RISK

Clipboard Font Alignment Number Styles Cells Editing

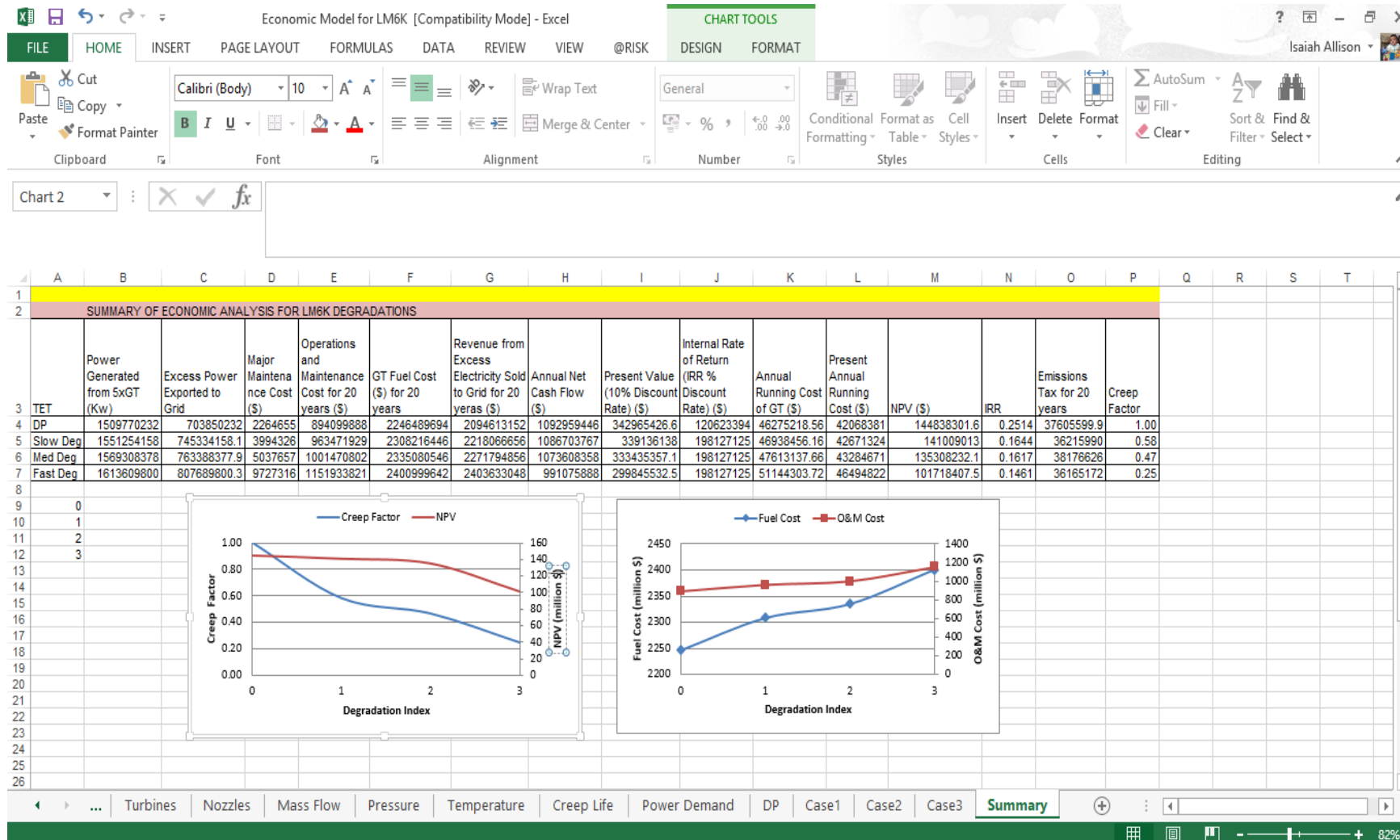
P18

12	Year (n)	O&M Cost(3% Annual Increase, \$)	Gas Collection Cost (5% Annual Increase, \$)	Grid Electricity Cost (5% Annual Increase During Outages, \$)	Emissions Tax (3% Annual Increase, \$)	Saved Electricity Cost (5% Annual Increase, \$)	Revenue on Excess Electricity Sold to Grid (5% Annual Increase, \$)	Annual Loan Repayment (\$)	Annual Net Cash Flow (\$)	Present Value (10% Discount Rate) (\$)	Internal Rate of Return (IRR % Discount Rate) (\$)	Cost of Electricity (1% Annual Increase)
13	1	42870032	72612441.01	7008000	1345912.462	80592000	72692082.03	0	29447696.28	26770633	25693432.3	0.072402485
14	2	44156133	76243063.07	7358400	1386289.835	84621600	76326686.13	0	31804399.99	26284628.1	24211896.25	
15	3	45480817	80055216.22	7726320	1427878.53	88852680	80143020.44	25658369.11	8647099.339	6496693.72	5743582.249	
16	4	46845242	84057977.03	8112636	1470714.886	93295314	84150171.46	25658369.11	11300546.68	7718425.43	6549115.484	
17	5	48250599	88260875.88	8518267.8	1514836.333	97960079.7	88357680.03	25658369.11	14114811.6	8764187.49	7137219.932	
18	6	49698117	92673919.67	8944181.2	1560281.423	102858083.7	92775564.03	25658369.11	17098779.34	9651815.17	7543795.39	

Turbines Nozzles Mass Flow Pressure Temperature Creep Life Power Demand DP Case1 Case2 Case3 Summary

READY 98%

# Appendix R : Summary of TERA on LM6K



## Appendix S : Creep Life Consumption for DS25 and LM6K

DS25 Creep Life Calculations				Minimum Creep Life			
Location		Stress (MPa)	Temp (Kelvin)	C/Life (Hours)			
Life Calculations with Cycle1		Cycle1	Cycle1	Cycle1		Cycle1	
	Root	187.4651	1096.569	809115.215		53010.85	
Max Stres	Max Tep	25%Root	149.0739	1137.84	211607.15	Cycle2	
Cycle1	Cycle1	Mid	110.6828	1202.533	53010.848	33937.44	Creep Life
189.8296	1100.187	75%Root	60.66681	1247.536	61421.3077	Cycle3	Creep Factor
151.1011	1139.413	Tip	10.6508	1096.569	2088779148	54250.13	%Life Loss
112.3726	1201.849	Cycle2	Cycle2	Cycle2	Cycle2	Cycle4	
61.51169	1246.319	Root	187.2447	1103.489	558978.95	28344.08	
10.6508	1100	25%Root	148.885	1145.827	141506.041	Cycle5	
Cycle2	Cycle2	Mid	110.5253	1212.113	33937.4364	57066.78	
178.0147	1075.247	75%Root	60.58807	1258.127	37990.2347	Cycle6	
141.7248	1113.019	Tip	10.6508	1103.489	1364374209	11374.75	

LM6K Creep Life Calculations				Minimum Creep Life			
Location		Stress (MPa)	Temp (Kelvin)	C/Life (Hours)			
Cycle1		Cycle1	Cycle1	Cycle1		Cycle1	
	Root	219.97881	1128.052	44537.08		44537.0757	
	25%Root	176.04696	1149.704	68660.51		Cycle2	
	Mid	132.11511	1181.266	47737.92		25944.9217	Creep Life
	75%Root	71.828958	1200.803	344180.6		Cycle3	Creep Factor
	Tip	11.542808	1128.052	3E+08		44530.4053	%Life Loss
	Cycle2	Cycle2	Cycle2	Cycle2		Cycle4	
	Root	219.4234	1138.408	27140.58		20810.9861	
	25%Root	175.56958	1161.183	39305.82		Cycle5	
	Mid	131.71576	1194.35	25944.92		45187.659	
	75%Root	71.629282	1214.84	175240.1		Cycle6	
	Tip	11.542808	1138.408	1.65E+08		11082.0076	

